

# **High Precision Dynamic Power System Frequency Estimation Algorithm Based on Phasor Approach**

Xuan Zhang

Thesis submitted to the Faculty of the  
Virginia Polytechnic Institute and State University  
in partial fulfillment of the requirement for the degree of

MASTER OF SCIENCE  
in  
Electrical Engineering

Yilu Liu, Chair  
Charles W Bostian  
Virgilio A Centeno

January 16, 2004  
Blacksburg, Virginia

Keywords: DFT, phase-shift, averaging, moving-averaging

Copyright 2004, Xuan Zhang

# **High Precision Dynamic Power System Frequency Estimation Algorithm Based on Phasor Approach**

Xuan Zhang

## **(ABSTRACT)**

An internet-based, real-time, Global Positioning System (GPS) ---synchronized relative to the wide-area frequency-monitoring network (FNET) ---has been developed at Virginia Tech. In this FNET system, an algorithm that employs the relationship between phasor angles and deviated frequency [13] is used to calculate both frequency and its rate of change. Tests of the algorithm disclose that, for non-pure sinusoidal input (as compared to pure sinusoidal input), significant errors in the output frequency will result. Three approaches for increasing the accuracy of the output frequency were compared. The first---increasing the number of samples per cycle  $N$ ---proved ineffective. The second---using the average of the first estimated frequencies rather than the instant first estimated frequency as the resampling frequency---produces a moderate increase in accuracy of the frequency estimation. The third---multiple resampling---significantly increased accuracy. But both the second and the third become ineffective to the extent the input is not pure sinusoidal.

From a practical standpoint, attention needs to be paid toward eliminating noise in the input data from the power grid so as to make it more purely sinusoidal. Therefore, it will be worthwhile to test more sophisticated digital filters for processing the input data before feeding it to the algorithm.

## **Acknowledgments**

I would like to express my sincere gratitude and appreciation to my advisor, Dr. Yilu Liu for her professional guidance and constant encouragement. Her intellectual and financial support was indispensable for the completion of this thesis. My committee members, Dr. Virgilio A Centeno and Dr. Charles W Bostian have provided valuable insights on my research project. I thank them for their interest and concern. I am greatly thankful to the graduate students in the Power Systems Laboratory for their help and friendship.

I would also like to express my personal thanks to my parents who always provide love, understanding and support. Finally, I especially thank Dr. F.Donald Bloss and his wife Louise for their invaluable help throughout my study at Virginia Tech and their sincerest love and support.

# Table of Contents

<b>Chapter 1 Introduction</b> .....	1
<b>Chapter 2 Review of the Techniques for Power System Frequency Estimation</b> .....	4
2.1 Overview.....	4
2.2 Review of DFT-based frequency measurement techniques.....	4
2.2.1 Technique Using Leakage Effect.....	4
2.2.2 Variable N DFT .....	6
2.3 The Algorithm used in our FNET System.....	8
2.3.1 Overview.....	8
2.3.2 The fundamental theory of the algorithm .....	9
2.3.3 Technique Details of the algorithm.....	11
2.4 Conclusion of DFT-based frequency estimation techniques .....	18
2.5 Techniques that are not based on DFT .....	19
<b>Chapter 3 Performance of the algorithm with non pure sinusoidal input</b> .....	21
3.1 Overview.....	21
3.2 Effect of Harmonic Components .....	22
3.3 Tests with Variable Frequency Waveform .....	24
3.3.1 Ramp case.....	24
3.3.2 Sinusoidal case.....	32
<b>Chapter 4 Analysis of the Practical Problems</b> .....	40
4.1 Overview.....	40
4.2 Averaging and moving averaging.....	41
4.3 One missing point .....	43
4.4 Phase & amplitude shift.....	47
4.4.1 Phase shift.....	47
4.4.2 Amplitude shift .....	57
<b>Chapter 5 Approaches to improve the frequency estimation accuracy of our algorithm</b> .....	68
5.1 Overview.....	68
5.2 Larger N approach .....	68
5.3 Averaging first estimated frequencies approach.....	70
5.3.1 test with pure sinusoidal input waveform.....	70
5.3.2 Test with input that contains harmonic noise .....	72
5.3.3 Test with input that has a variable frequency .....	74

5.3.3.1 Test with input of which frequency changes as a ramp function .....	74
5.3.3.2 Test with input of which frequency changes as a sinusoidal .....	83
5.4 Multi-resampling approach .....	91
5.4.1 Results with pure sinusoidal input .....	93
5.4.2 Test with input that contains harmonic noise .....	98
5.4.3 Test with input that has a variable frequency .....	100
5.4.3.1 Test with input for which frequency changes as a ramp function .....	100
5.4.3.2 Test with input for which frequency changes as a sinusoidal .....	114
<b>Chapter 6 Computation Time Study</b> .....	125
<b>Chapter 7 Summary and Future Work</b> .....	130
<b>References</b> .....	134
<b>Vita</b> .....	137

## List of Tables

Table 2-1 .....	8
Table 3-1 .....	22
Table 3-2 .....	23
Table 3-3 .....	23
Table 3-4 .....	25
Table 3-5 .....	25
Table 3-6 .....	32
Table 3-7 .....	33
Table 3-8 .....	33
Table 3-9 .....	34
Table 3-10 .....	39
Table 3-11 .....	39
Table 4-1 .....	57
Table 4-2 .....	67
Table 5-1 .....	69
Table 5-2 .....	72
Table 5-3 .....	73
Table 5-4 .....	74
Table 5-5 .....	93
Table 5-6 .....	96
Table 5-7 .....	96
Table 5-8 .....	98
Table 5-9 .....	99
Table 5-10 .....	99
Table 7-1 .....	132

## List of Figures

Figure 2-1.....	14
Figure 2-2.....	17
Figure 2-3.....	18
Figure 3-1.....	24
Figure 3-2.....	26
Figure 3-3.....	27
Figure 3-4.....	27
Figure 3-5.....	28
Figure 3-6.....	28
Figure 3-7.....	29
Figure 3-8.....	29
Figure 3-9.....	30
Figure 3-10.....	30
Figure 3-11.....	31
Figure 3-12.....	31
Figure 3-13.....	32
Figure 3-14.....	34
Figure 3-15.....	35
Figure 3-16.....	35
Figure 3-17.....	36
Figure 3-18.....	36
Figure 3-19.....	37
Figure 3-20.....	37
Figure 3-21.....	38
Figure 3-22.....	38
Figure 3-23.....	39
Figure 4-1.....	40
Figure 4-2.....	41
Figure 4-3.....	42
Figure 4-4.....	42
Figure 4-5.....	43
Figure 4-6.....	44
Figure 4-7.....	45
Figure 4-8.....	45
Figure 4-9.....	46
Figure 4-10.....	46
Figure 4-11.....	47
Figure 4-12.....	48
Figure 4-13.....	48
Figure 4-14.....	49
Figure 4-15.....	49
Figure 4-16.....	50
Figure 4-17.....	50
Figure 4-18.....	51

Figure 4-19.....	51
Figure 4-20.....	52
Figure 4-21.....	52
Figure 4-22.....	53
Figure 4-23.....	53
Figure 4-24.....	54
Figure 4-25.....	54
Figure 4-26.....	55
Figure 4-27.....	55
Figure 4-28.....	56
Figure 4-29.....	56
Figure 4-30.....	58
Figure 4-31.....	58
Figure 4-32.....	59
Figure 4-33.....	59
Figure 4-34.....	60
Figure 4-35.....	60
Figure 4-36.....	61
Figure 4-37.....	61
Figure 4-38.....	62
Figure 4-39.....	62
Figure 4-40.....	63
Figure 4-41.....	63
Figure 4-42.....	64
Figure 4-43.....	64
Figure 4-44.....	65
Figure 4-45.....	65
Figure 4-46.....	66
Figure 4-47.....	66
Figure 5-1.....	69
Figure 5-2.....	70
Figure 5-3.....	71
Figure 5-4.....	71
Figure 5-5.....	73
Figure 5-6.....	74
Figure 5-7.....	75
Figure 5-8.....	75
Figure 5-9.....	76
Figure 5-10.....	76
Figure 5-11.....	77
Figure 5-12.....	77
Figure 5-13.....	78
Figure 5-14.....	78
Figure 5-15.....	79
Figure 5-16.....	79
Figure 5-17.....	80

Figure 5-18.....	80
Figure 5-19.....	81
Figure 5-20.....	81
Figure 5-21.....	82
Figure 5-22.....	82
Figure 5-23.....	83
Figure 5-24.....	83
Figure 5-25.....	84
Figure 5-26.....	84
Figure 5-27.....	85
Figure 5-28.....	85
Figure 5-29.....	86
Figure 5-30.....	86
Figure 5-31.....	87
Figure 5-32.....	87
Figure 5-33.....	88
Figure 5-34.....	88
Figure 5-35.....	89
Figure 5-36.....	89
Figure 5-37.....	90
Figure 5-38.....	90
Figure 5-39.....	91
Figure 5-40.....	97
Figure 5-41.....	97
Figure 5-42.....	98
Figure 5-43.....	99
Figure 5-44.....	100
Figure 5-45.....	101
Figure 5-46.....	101
Figure 5-47.....	102
Figure 5-48.....	102
Figure 5-49.....	103
Figure 5-50.....	103
Figure 5-51.....	104
Figure 5-52.....	105
Figure 5-53.....	105
Figure 5-54.....	106
Figure 5-55.....	106
Figure 5-56.....	107
Figure 5-57.....	108
Figure 5-58.....	108
Figure 5-59.....	109
Figure 5-60.....	109
Figure 5-61.....	110
Figure 5-62.....	110
Figure 5-63.....	111

Figure 5-64.....	111
Figure 5-65.....	112
Figure 5-66.....	112
Figure 5-67.....	113
Figure 5-68.....	113
Figure 5-69.....	114
Figure 5-70.....	115
Figure 5-71.....	115
Figure 5-72.....	116
Figure 5-73.....	116
Figure 5-74.....	117
Figure 5-75.....	117
Figure 5-76.....	118
Figure 5-77.....	118
Figure 5-78.....	119
Figure 5-79.....	119
Figure 5-80.....	120
Figure 5-81.....	120
Figure 5-82.....	121
Figure 5-83.....	121
Figure 5-84.....	122
Figure 5-85.....	122
Figure 5-86.....	123
Figure 5-87.....	123
Figure 5-88.....	124
Figure 6-1.....	126
Figure 6-2.....	126
Figure 6-3.....	127
Figure 6-4.....	127
Figure 6-5.....	128
Figure 6-6.....	128
Figure 6-7.....	129
Figure 6-8.....	129

# Chapter One

## Introduction

System frequency is one of the most important parameters of a power system. Area frequency can vary over a small range due to generation-load mismatches. When the power consumed by loads and losses is greater than the generated power, the system operating frequency will decrease, resulting in a situation classified as ‘the underfrequency condition’. This can happen when there is a loss of one or more generators, or when there is an increase in power demand during certain peak period of the day. When loads are suddenly lost in a system, input power will be greater than the consumed power. The extra power generated will be absorbed by the rest of the loads and the generator inertia, resulting in an increase in the operating frequency. This is classified as ‘the overfrequency condition’. In either case, a change in frequency can jeopardize the efficiency and safety of the power system and may cause it to collapse.

As mentioned above, load unbalance is always faithfully portrayed by a change in the operating frequency. Consequently, many power-system protection-and-control applications [1] [2] require accurate and fast estimation of area system frequency. Frequency information has also been used routinely in the control and management of generation [3]. Fast and accurate real time measurement of frequency is an important component in the operation of the transmission system. Moreover, if the rate of change of frequency is known, more accurate adjustments can be made to quickly restore the system back to its normal operation point [4].

In the past forty years, various techniques have been developed to measure power system frequency. Recently, more sophisticated and accurate algorithms are being developed to take advantage of the powerful computing capability of digital computers.

Whereas, the market economy is likely to force power systems to operate much closer to their limits [5], it is impossible using offline studies to predict the behavior of the system under a sequence of faults outside the design criteria. Unfortunately, online simulation has not reached the required level of speed or the detail of modeling accuracy necessary for online dynamic security assessment. The alternative solution is to rely on continuous real-time monitoring of the system dynamics [6]. Several projects have been launched for wide-area measurement systems in the past 10 years [7] [8] [9]. The results of all earlier efforts clearly point to the need of a real time,

continuous, comprehensive and uniform-measurement system.

The internet is proposed as a solution to the difficulty of providing the wide-area frequency monitoring system. It allows electric utility companies to interconnect directly to external organizations such as customers, generators and distributors, brokers, and strategic partners. Also internet makes the wide area information communication and exchange easy and cost-effective.

An internet-based real-time Global Positioning System (GPS) synchronized wide-area frequency monitoring network (FNET) [10] [11] has been developed at Virginia Tech. This FNET system consists of two major components: (1)the Frequency Record Unit (FRU), which performs GPS synchronized frequency data measurement and network interface, and (2) the information management system (IMS) server which provides the data management, analysis, and user interface [12]. Internet provides the integrated wide area communication network between FRU and IMS server.

In the FNET system, an algorithm that employs the relationship between phasor angles and deviated frequency [13] calculates both frequency and its rate of change. The accuracy is  $\pm 0.001$  Hz which is already very acceptable, but precise frequency estimation in a wider range is desired. And some practical problems which affect the output estimated frequency have occurred within the system that has been set up and running at Virginia Tech. Part of my goal was to improve the accuracy of the frequency estimation algorithm used in the FNET system. An additional goal was to analyze the problems that have occurred to the system and arrive at some solutions. All my study has been done off line on a PC with the tool Visual C++ and Matlab.

This thesis presents my conclusions. More specifically, Chapter 2 reviews several DFT-based frequency measurement techniques and takes a close look at our algorithm, then summarizes the advantages of this algorithm over other options. It also reviews briefly other several other techniques that are not based on DFT and explains why they are rejected. Chapter 3 discusses the validity of the algorithm when the input is not a pure sinusoid. Three cases are discussed: input with harmonic noise, input frequency changes at a constant rate as a ramp function and input whose frequency changes as a sinusoidal function. Chapter 4 analyzes two practical problems that affect the output estimated frequency of our FNET system. The first--an observed spike every 29 or 30 seconds in the output frequency of our FNET system was confirmed to be caused by one point missing in the output data of the ADC in our FNET system. The second concerns the phase or amplitude shift of the

input voltage that usually results from the load change. I attribute such large deviation from the normal output frequency range to phase or amplitude shifts in the input voltage; the bigger the shift is, the larger the deviation will be. Three approaches improving the frequency estimation accuracy of our algorithm will be discussed in Chapter 5. The first, to increase  $N$  the number of samples per cycle, proves ineffective. The second, to use as the resampling frequency the average of the first estimated frequencies instead of the instantaneous first estimated frequency (as the original algorithm does) moderately improved the frequency estimation accuracy. The third, to do the resampling multiple times instead of just once as the original algorithm does, made a significant difference. However, it shows no effect on the frequency estimation accuracy when the input is not a pure sinusoidal, nor does the second approach. Chapter 6 presents the study results of the computation time of different versions of the algorithm. Chapter 7 summarizes the thesis and suggests possible directions for future work.

In Chapter 4 the version of the algorithm that outputs 10 frequencies per second is used to test the case of missing one point. In Chapter 6 different versions of the algorithm are tested for the computation time study. All other cases in the thesis are studied using the algorithm that outputs 1440 frequencies per second.

## Chapter Two

### Review of the Techniques for Power System Frequency Estimation

#### 2.1 Overview

Throughout the past forty years, various techniques for measuring power system frequency have been developed. Most are based on DFT, as does the frequency estimation algorithm used in our FNET system. This chapter reviews several DFT-based frequency measurement techniques, takes a close look at our algorithm, and then summarizes the advantages of this algorithm over other options. It ends with a very brief review of several other techniques, not based on DFT, and explains why we rejected them.

#### 2.2 Review of DFT-based Frequency Estimation Techniques

##### 2.2.1 Technique Using Leakage Effect [14]

The fast Fourier transform (FFT), which is an efficient method for computing the discrete Fourier transform (DFT), has been used as an analysis tool in many diverse areas. Its major pitfall is leakage. However, in [14] the fact that leakage can occur in the FFT is used advantageously for detecting fluctuations in the fundamental frequency of a power system.

Leakage arises if a time sequence is so truncated that a fraction of a cycle exists in the waveform subjected to the FFT. To illustrate how the leakage occurs in FFT, suppose a unity amplitude 60Hz sinusoidal waveform is sampled 32 times in a window-length of 1/60 sec. The sampling frequency ( $f_s$ ) in this case would be the number of points ( $N$ ) times the fundamental frequency component, or  $32 \cdot 60\text{Hz}$ . The FFT result shows only a non-zero magnitude value at 60Hz and zero at all other frequency components. In other words, no leakage has occurred. This is true since one cycle of the waveform exists in the window length. Now suppose unity amplitude 55Hz sinusoidal waveform is sampled 32 times in the same window length and the same sampling frequency  $f_s$ . The FFT result shows non-zero magnitude values at frequency components other than 55Hz instead of just at 55Hz. Leakage now occurs since the 55Hz waveform does not have an integral number of cycles in the window length specified.

As stated previously, leakage in the FFT can be used advantageously to detect fluctuations in the fundamental frequency of a power system. The method is based on the leakage coefficient, defined

as

$$\eta = \frac{\sum_{k=0}^{N-1} |X(k)| - |X(1)|}{|X(1)|} \quad (2-1)$$

Where  $X(k)$  is the Discrete Fourier Transform term, and  $X(1)$  corresponds to the fundamental component.

It is found [14] that for a small frequency deviation ( $\pm 5\text{Hz}$ ), the relationship between the leakage coefficient,  $\eta$  and the frequency deviation,  $\Delta f$  for a *sinusoidal* waveform, is linear. In fact, the equation governing the relationship is

$$|\Delta f| = \frac{\eta}{0.095584345} \quad (2-2)$$

Close examination of Eq. (2-1) reveals that the leakage coefficient will always be positive regardless of whether the frequency has increased or decreased. Therefore,  $\eta$  will give only the magnitude of the frequency deviation. To determine whether the fundamental component has increased or decreased the real part of  $X(1)$  must be examined. If  $\text{Re}(X(1))$  is positive, then the fundamental component has increased, i.e.  $\Delta f > 0$ . A negative  $\text{Re}(X(1))$  indicates a decrease in fundamental component, i.e.  $\Delta f < 0$ .

Eq. (2-2) holds true only if the waveform is purely sinusoidal, that is, the waveform has only one frequency component---fundamental frequency---present. However, a real power voltage waveform contains many frequency components in addition to the fundamental component. The presence of non-fundamental frequency components will definitely impair the technique's performance.

For a cosinusoidal waveform, the above relationship will not hold because the cosinusoidal waveform will yield a nonlinear  $\eta$  versus  $\Delta f$  curve. Hence, a zero-crossing detector must be employed to detect positive going zero-crossing to yield the sinusoidal waveform. Since no zero-crossing-detector is perfect, a time error  $\Delta t$  will always be introduced. This implies that the

sine wave being used will possess a phase delay. Hence, the Fourier transform will not be a Fourier transform of a perfect sine wave. As the whole algorithm is based on the assumption that a perfect sine wave is being analyzed, this will definitely introduce an error in the computed frequency deviation.

### 2.2.2 Variable N DFT [15] [16] [17] [18]

Frequency tracking and estimation using the DFT is examined using two methods. Considering the use of an N point DFT with sampling interval  $\Delta T$ , the methods are:

Method 1: estimate the frequency and adjust the sampling interval  $\Delta T$  online such that an integer number of samples is maintained. Thus, N maintains constant and  $\Delta T$  is varied. The algorithm used in our FNET system to estimate the frequency employs this method by adjusting the sampling frequency based on the initial estimated frequency. It will be discussed thoroughly in section 2.3. [13] [19]

Method 2: estimate the frequency and adjust the DFT window length N. Thus,  $\Delta T$  remains constant, and N is varied. The frequency estimation technique I will discuss in this section is based on method2 [15] [16] [17] [18].

Consider a signal given by:

$$s(t) = B \cos(\omega_1 t + \gamma) \quad (2-3)$$

Defining  $\omega_1$  as  $2\pi(f + \Delta f)$ . The sampling frequency can be determined as  $f_s = (N * f)$ . Applying the DFT equation results in:

$$\begin{aligned} S(1) &= \frac{2}{N} \sum_{k=0}^{N-1} s_k e^{-j(k\psi)} \\ &= B e^{j(\gamma)} \frac{\sin(\frac{\pi\Delta f}{f})}{N \sin(\frac{\pi\Delta f}{fN})} e^{j(\frac{\pi\Delta f}{f} - \frac{\pi\Delta f}{fN})} + B e^{-j(\gamma)} \frac{\sin(\frac{-\pi\Delta f}{f})}{N \sin(-\frac{\pi\Delta f}{fN} - \frac{2\pi}{N})} e^{j(-\frac{\pi\Delta f}{f} + \frac{\pi\Delta f}{fN} + \frac{2\pi}{N})} \end{aligned} \quad (2-4)$$

Where S (1) is the fundamental component of DFT,  $\psi = \frac{2\pi}{N}$  f is the fundamental frequency (60Hz).

From equation (2-4), it is easy to determine that if  $\Delta f$  is zero the equation simplifies to the usual DFT. Note  $\gamma$  is the offset angle and will vary depending on when the DFT estimate begins. If  $\Delta f$  is

small, the equation simplifies to

$$S(1) = Be^{j(\gamma)} e^{j\left(\frac{\pi\Delta f}{f} - \frac{\pi\Delta f}{fN}\right)} \quad (2-5)$$

In the above equation, the values of N and f are known.  $\Delta f$  is an unknown which must be determined to calculate the actual system frequency.

Using the previous cycle of data, the DFT is computed according to equation (2-4). A new sample is acquired at instant  $t_{k+1}$  when the waveform has a new offset angle  $\beta$ . The offset angle between two consecutive samples is given by

$$\beta = \frac{2\pi(f + \Delta f)}{fN} \quad (2-6)$$

Thus, the ratio of two consecutive DFT estimates is given by

$$\frac{DFT(t_{k+1})}{DFT(t_k)} = \frac{Be^{j(\gamma)} e^{j\left(\frac{\pi\Delta f}{f} - \frac{\pi\Delta f}{fN}\right)} e^{j\left(\frac{2\pi(f+\Delta f)}{fN}\right)}}{Be^{j(\gamma)} e^{j\left(\frac{\pi\Delta f}{f} - \frac{\pi\Delta f}{fN}\right)}}$$

Ignoring the magnitude and examining the argument yields:

$$\arg\left(\frac{DFT(t_{k+1})}{DFT(t_k)}\right) = \beta = \frac{2\pi(f + \Delta f)}{fN} \quad (2-7)$$

By determining the DFT at different points in time, the angle difference from the two DFT estimates can be used to compute the actual frequency given by  $f + \Delta f$ .

This method tracks the frequency and uses the frequency estimate to vary the DFT window by changing N. For example, for a fixed  $\Delta T = [1/60\text{secs}]/32$ , one cycle at 60Hz will entail 32 samples, but one cycle at 40Hz will require 48 samples. Thus, the DFT at 60Hz will use a 32 sample window, but will use a 48 sample window at 40Hz. Since the sampling period is fixed, the possible fundamental frequencies are discrete, i.e., the fundamental frequency must have a period that is an integer value of the sampling period. However, this is not always true, which will definitely bring about error. For a sampling period of  $\Delta T$ , the possible frequencies are  $1/(N\Delta T)$  where N is the numbers of samples per cycle. For the case of  $\Delta T = (1/60)/32$  (32 samples per cycle at 60Hz), the possible frequencies are shown in Table 2-1. While the variable window is able to cover a large frequency range, the window length can be very large for real time computations (96 samples).

N samples per Cycle	Frequency
22	87.2727
23	83.4783
24	80.0000
25	76.8000
26	73.8462
27	71.1111
28	68.5714
29	66.2069
30	64.0000
31	61.9355
32	60.0000
...	...
94	20.4255
95	20.2105
96	20.0000

Table 2-1 the possible frequencies for  $\Delta T = (1/60)/32$

This algorithm involves adjusting the DFT window by changing N as close to 1 cycle of the input signal as possible. However, since the DFT window may not include exactly one cycle because of harmonics, error will occur to the frequency estimate and the phasor computations.

## 2.3 The Algorithm Used in Our FNET System

### 2.3.1 Overview

Like the technique described in section 2.2.2, the frequency estimation algorithm used in our FNET system also employs the relationship between phasor (usual DFT) angles and deviated frequency. The difference is that our algorithm adjusts the sampling frequency (i.e. sampling interval  $\Delta T$ ) so that an integral number of samples per cycle are maintained. Whereas the technique described in section 2.2.2 estimates the frequency and adjusts the DFT window length N, but keeps the sampling interval  $\Delta T$  constant. Our algorithm involves three major steps. First, rough frequency estimation for a data window is computed using a second-order least error square approximation on the phasor angles of the input waveform. Next, a resampling based on the rough frequency estimation is carried out, and this is then followed by another second order least square error approximation to obtain the final results. In the following two sections I will look into the

frequency measurement technique theory based on the relationship between phasor angles and deviated frequency and then talk about the implementation details of the algorithm used in our FNET system.

### 2.3.2 The Fundamental Theory of the Algorithm

In this section, frequency measurement technique proposed by Phadke [20] using the voltage phasor angles will be briefly described.

A pure sinusoidal waveform can be expressed as

$$x(t) = \sqrt{2}X \sin(\omega t + \phi) \quad (2-8)$$

After sampling Eq. (2-8) with a sampling frequency N times per cycle, Eq.(2-8) can be rewritten into

$$x_k = \sqrt{2}X \sin\left(\frac{2\pi}{N}k + \phi\right) \quad (2-9)$$

The Discrete Fourier Transform (DFT) of Eq. (2-9) is given by

$$\bar{X} = \frac{1}{\sqrt{2}}(X_c + jX_s) \quad (2-10)$$

where  $X_c = \frac{2}{N} \sum_0^{N-1} X_k \cos \frac{2\pi}{N}k$  and

$$X_s = -\frac{2}{N} \sum_0^{N-1} X_k \sin \frac{2\pi}{N}k$$

Next, the recursive phasor computation technique is used to obtain the  $r$ th phasor, which is given below

$$\bar{X}^{(r)} = \bar{X}^{(r-1)} + j \frac{1}{\sqrt{2}} \frac{2}{N} (x_{N+r} - x_r) \exp\left(-j \frac{2\pi}{N}(r-1)\right) \quad (2-11)$$

From Eq. (2-11), the phasor of a sinusoidal wave at a frequency  $f = f_0 + \Delta f$  can be found to be:

$$\begin{aligned}
\bar{X}_{f_0+\Delta f}^{(r)} &= \bar{X}_{f_0}^{(0)} \frac{\sin\left(\frac{N\Delta\omega\Delta t}{2}\right)}{N \sin\left(\frac{\Delta\omega\Delta t}{2}\right)} \exp(jr\Delta\omega\Delta t) \exp\left(j(N-1)\frac{\Delta\omega\Delta t}{2}\right) \\
&+ \bar{X}_{f_0}^{*(0)} \frac{\sin\left(\frac{N(\omega+\omega_0)\Delta t}{2}\right)}{N \sin\left(\frac{(\omega+\omega_0)\Delta t}{2}\right)} \exp\left(-j\frac{(N-1)(\omega+\omega_0)\Delta t}{2}\right) \exp(-jr(\omega+\omega_0)\Delta t)
\end{aligned}
\tag{2-12}$$

where  $\bar{X}_{f_0}^{(0)}$  is the initial computation of the phasor at  $f_0$  and

$\Delta t$  is time interval between sampled data

For small values of  $\Delta f$ , the following simplifications are introduced [19]

$$\frac{\sin\left(\frac{N\Delta\omega\Delta t}{2}\right)}{N \sin\left(\frac{\Delta\omega\Delta t}{2}\right)} \cong 1
\tag{2-13}$$

and

$$\frac{\sin\left(\frac{N(\omega+\omega_0)\Delta t}{2}\right)}{N \sin\left(\frac{(\omega+\omega_0)\Delta t}{2}\right)} \cong 0
\tag{2-14}$$

So that (2-12) reduces to

$$\bar{X}_{f_0+\Delta f}^{(r)} = \bar{X}_{f_0}^{(0)} \exp(jr\Delta\omega\Delta t) \exp\left((N-1)\frac{\Delta\omega\Delta t}{2}\right)
\tag{2-15}$$

By denoting the angle of the new phasor as  $\psi_r$  and the angle of the previous phasor as  $\psi_{r-1}$ , one can approximate the new phasor angle as

$$\psi_r = \frac{\Delta f}{f_0} \frac{2\pi}{N} + \psi_{r-1}
\tag{2-16}$$

Now, using the definition of derivatives,

$$\frac{d\psi}{dt} = \lim_{t \rightarrow 0} \frac{\psi_r - \psi_{r-1}}{t}$$

$$\begin{aligned} &\approx \frac{\psi_r - \psi_{r-1}}{1/Nf_0} \\ &= 2\pi\Delta f \end{aligned} \tag{2-17}$$

The system frequency can now be computed with

$$\begin{aligned} f &= f_0 + \Delta f \\ &= f_0 + \frac{1}{2\pi} \frac{d\psi}{dt} \end{aligned} \tag{2-18}$$

And the rate of change of frequency is

$$\frac{df}{dt} = \frac{1}{2\pi} \frac{d^2\psi}{dt^2} \tag{2-19}$$

By computing the phasor, the harmonic noise can be partially eliminated. With the help of a low-pass filter, the high frequency noise will not interfere with the frequency computation. With the help of least error square computation on redundant number of phasor angles, the accuracy of frequency computation and the rate of change of frequency computation will be greatly improved. Since the technique is based on sampled phasor data and because most microcomputer-based power-system devices installed already have the ability to compute phasors, the method can be added for low incremental cost to microcomputer-based devices that are performing other functions, without additional hardware.

It is seen that the simplifications of Eq. (2-13) and Eq. (2-14) are made to obtain the relationship between phasor angle and deviated frequency. This approximation will inadvertently introduce some error in the estimation. One way to alleviate the above approximation error is to use the positive sequence voltage waveform as the input instead of the phase voltage waveform since computing the positive sequence quantities will introduce an automatic filtering effect.

### 2.3.3 Technique Details of the Algorithm [13], [21]

The first step in this proposed technique is to compute the phasor. Let the sampling rate be  $N$  samples per cycle, the first phasor is computed using

$$\bar{X} = \frac{1}{\sqrt{2}} \left( \frac{2}{N} \sum_{k=1}^N x_k \cos\left(\frac{2\pi}{N} k\right) - j \frac{2}{N} \sum_{k=1}^N x_k \sin\left(\frac{2\pi}{N} k\right) \right) \quad (2-20)$$

Denoting  $\frac{2}{N} \sum_{k=1}^N x_k \cos\left(\frac{2\pi}{N} k\right)$  by  $X_c$  and  $-\frac{2}{N} \sum_{k=1}^N x_k \sin\left(\frac{2\pi}{N} k\right)$  by  $X_s$  and using the recursive

formula derived in [14], each successive phasor can be computed with

$$\begin{aligned} X_c^{(k+1)} &= X_c^{(k)} + \frac{2}{N} (x_{k+1} - x_{k+1-N}) \cos\left(\frac{2\pi}{N} k\right) \\ X_s^{(k+1)} &= X_s^{(k)} - \frac{2}{N} (x_{k+1} - x_{k+1-N}) \sin\left(\frac{2\pi}{N} k\right) \end{aligned} \quad (2-21)$$

Hence, a new phasor is available for every incoming sample after initialization. The angle of the  $k$ th phasor is given by

$$\phi(k) = \tan^{-1} \frac{-X_s^{(k)}}{X_c^{(k)}} \quad (2-22)$$

Assuming that voltage phasor angles vary as a quadratic function with respect to the sample number,

$$\phi(k) = a_0 + a_1 k + a_2 k^2 \quad (2-23)$$

Let a computation window of  $M$  phasor angles be used to estimate the value of coefficients  $a_0$ ,  $a_1$  and  $a_2$ ,

$$\begin{aligned} \phi(1) &= a_0 + a_1 + a_2 1^2 \\ \phi(2) &= a_0 + a_1 2 + a_2 2^2 \\ &\dots\dots\dots \\ \phi(M) &= a_0 + a_1 M + a_2 M^2 \end{aligned} \quad (2-24)$$

Putting Eq.(2-24) in the form of matrices,

$$\begin{bmatrix} \phi_1 \\ \phi_2 \\ \vdots \\ \phi_M \end{bmatrix} = \begin{bmatrix} 1 & 1 & 1 \\ 1 & 2 & 2^2 \\ \vdots & \vdots & \vdots \\ 1 & M & M^2 \end{bmatrix} \begin{bmatrix} a_0 \\ a_1 \\ a_2 \end{bmatrix} \text{ or} \quad (2-25)$$

$$\boldsymbol{\phi} = \mathbf{X}\mathbf{a}$$

The unknown matrix  $\mathbf{a}$  can be solved using the least error square solution

$$\mathbf{a} = [\mathbf{X}^T \mathbf{X}]^{-1} \mathbf{X}^T \boldsymbol{\phi} \quad (2-26)$$

Here, the pseudo-inverse matrix  $[\mathbf{X}^T \mathbf{X}]^{-1} \mathbf{X}^T$  is known as the gain matrix and can be computed off-line. Since the least error square approximation is actually doing a curve fit, all the phasor angles,  $\phi$ s, must be made monotonic, i.e., there should not be any wrap-around of angles. This can be easily done by appropriately adding  $\pm 2\pi$ . Also, it is best to subtract  $\phi_1$  from all the angles so that the angles always begin at 0. This keeps the curve fitting uniform in all intervals and the arithmetic errors at a minimum.

Once the values of  $a_1$  and  $a_2$  are known, one can proceed to compute the frequency and the rate of change of frequency.

Taking the derivative of Eq. (2-23) with respect to  $k$

$$\frac{d\phi}{dk} = a_1 + 2a_2k \quad (2-27)$$

The relationship between sample number and time can be expressed as

$$k = Nf_0t \quad \text{and} \quad \frac{dk}{dt} = Nf_0 \quad (2-28)$$

where  $N$  is the number of phasor angles used in the computation per cycle

$f_0$  is the nominal frequency.

Using chain rule,

$$\Delta f = \frac{1}{2\pi} \frac{d\phi}{dt} = \frac{1}{2\pi} \frac{dk}{dt} \frac{d\phi}{dk} = \frac{1}{2\pi} Nf_0 \frac{d\phi}{dk} = \frac{1}{2\pi} Nf_0 (a_1 + 2a_2k) \quad (2-29)$$

$$\frac{d\Delta\omega}{dt} = 2\pi \frac{d\Delta f}{dt} = 2\pi \frac{df}{dt} \approx \frac{d^2\phi}{dt^2} = \frac{d}{dt} (Nf_0 a_1 + 2(Nf_0)^2 a_2 t) = 2(Nf_0)^2 a_2 \Rightarrow$$

$$\frac{df}{dt} \approx \frac{1}{2\pi} 2(Nf_0)^2 a_2 \quad (2-30)$$

Eq. (2-29) and Eq. (2-30) are the main formulas used for calculating the frequency and the rate of change of frequency. It is seen from Eq. (2-30) that the rate of change of frequency is assumed to be constant within the computation window. The frequency and the rate of change of frequency estimations obtained above are already rather accurate. However, since more precise frequency estimation is needed, one more step is required.

The simplifications of Eq. (2-13) and Eq. (2-14) are made to obtain the relationship between

phasor angle and deviated frequency. This approximation will inadvertently introduce some error in the estimation. However, the smaller  $\Delta f$  is, the more accurate the simplifications of Eq. (2-13) and Eq. (2-14) will be, and hence the more accurate the estimation will be. In other words, the frequency estimation will be more accurate when the actual frequency approaches the frequency established for the sampling rate. Hence, resampling the waveform with the estimated frequency obtained and using the new phasor to perform final correction estimation will be a rather attractive solution to achieve precise measurement.

To explain the idea of resampling in detail, assume the nominal frequency is 60 Hz and the sampling rate is 1440 samples per second, which corresponds to  $\frac{1440}{60} = 24$  samples per cycle. When the frequency has changed to 55 Hz, each cycle will now have  $\frac{1440}{55} = 26.18$  samples. By re-normalizing through resampling, one attempts a mathematical interpolation such that there will always be 24 samples per cycle regardless of the waveform frequency.

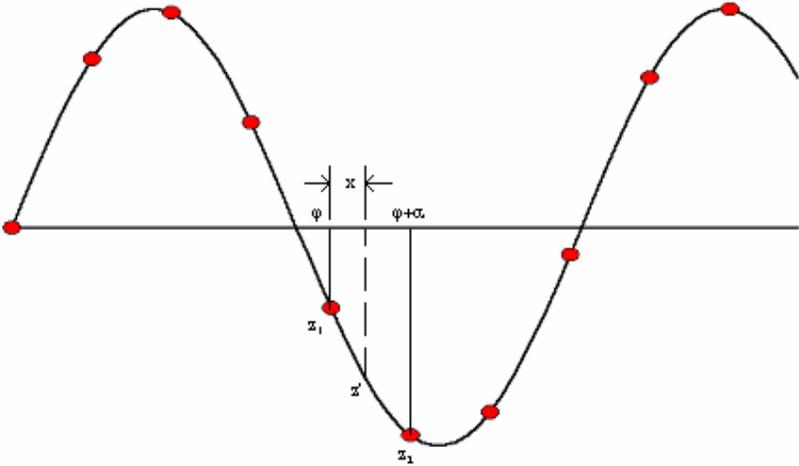


Figure 2-1 Illustration of Resampling Technique

In Figure 2-1 which illustrates the resampling algorithm, the values of  $z_1$  and  $z_2$  can be

represented by the following two equations

$$z_1 = Z_m \sin(\varphi) \quad (2-31)$$

$$z_2 = Z_m \sin(\varphi + \alpha) = Z_m \sin \varphi \cos \alpha + Z_m \cos \varphi \sin \alpha \quad (2-32)$$

where  $Z_m$  is the amplitude of the waveform

$\varphi$  is a sample instant and is an arbitrary known value

$\alpha$  is the interval between two samples at the new frequency and is

$$2\pi f_{new} / (Nf_0)$$

Combining Eq. (2-31) and Eq. (2-32) results in

$$Z_m \cos \varphi = \frac{(z_2 - z_1 \cos \alpha)}{\sin \alpha} \quad (2-34)$$

Let  $x$  be the fractional distance between  $z_1$  and  $z_2$ , the resampled point  $z'$  is then given by

$$\begin{aligned} z' &= Z_m \sin(\varphi + x\alpha) \\ &= Z_m \sin \varphi \cos x\alpha + Z_m \cos \varphi \sin x\alpha \\ &= z_1 \cos x\alpha + (z_2 - z_1 \cos \alpha) \frac{\sin x\alpha}{\sin \alpha} \end{aligned} \quad (2-35)$$

After resampling points have been found, the phasor angles of the new sampled data are computed and another estimation using Eq.(2-26), Eq. (2-29) and Eq. (2-30) is made to obtain the correction frequency,  $\Delta f'$ , and the final rate of change of frequency measurements.

The rate of change of frequency computed here is the final estimation of the rate. The final frequency estimation is computed using

$$f_{final} = f_0 + \Delta f + \Delta f' \quad (2-36)$$

Two major assumptions have been made on the input waveform when performing resampling:

- The input waveform is a pure sinusoidal waveform (i.e., the input waveform is free from any major distortions)

- The input waveform is a single frequency waveform (i.e., frequency deviation within the resampling window is small)

The algorithm basically consists of three major steps:

- computes rough frequency estimation using raw voltage phasors from sampled data
- resamples the waveform with the first estimated frequency
- computes the correction frequency using the new voltage phasors of the resampled waveform and obtains the final results.

The number of cycles used to compute a frequency estimate is assumed to be 6 nominal cycles. Number of samples per cycle used to compute a phasor is 24. Hence, after initialization, each new phasor will be obtained in every  $\frac{1}{24 \times 60} = 0.6944$  millisecond. The whole estimation proceeds recursively. The sliding window is 8 cycles long with 6 cycles for estimating frequency. The reason to use an 8 cycle sliding window is:

1) It takes one cycle of sampled data to compute the first phasor value.

2) When frequency is less than 60 Hz, we need more data to fulfill the 6 cycle criterion for resampling. For example, let us say that  $f = 55$  Hz. Number of samples needed to compute the frequency will now be  $24 \times 6 \times \frac{60}{55} \approx 158$  samples. Hence, the number of 60 Hz periods that is needed will be  $\frac{158}{24} \approx 7$  cycles.

The complete flowcharts of the algorithm are shown in Figure 2-2 and Figure 2-3.

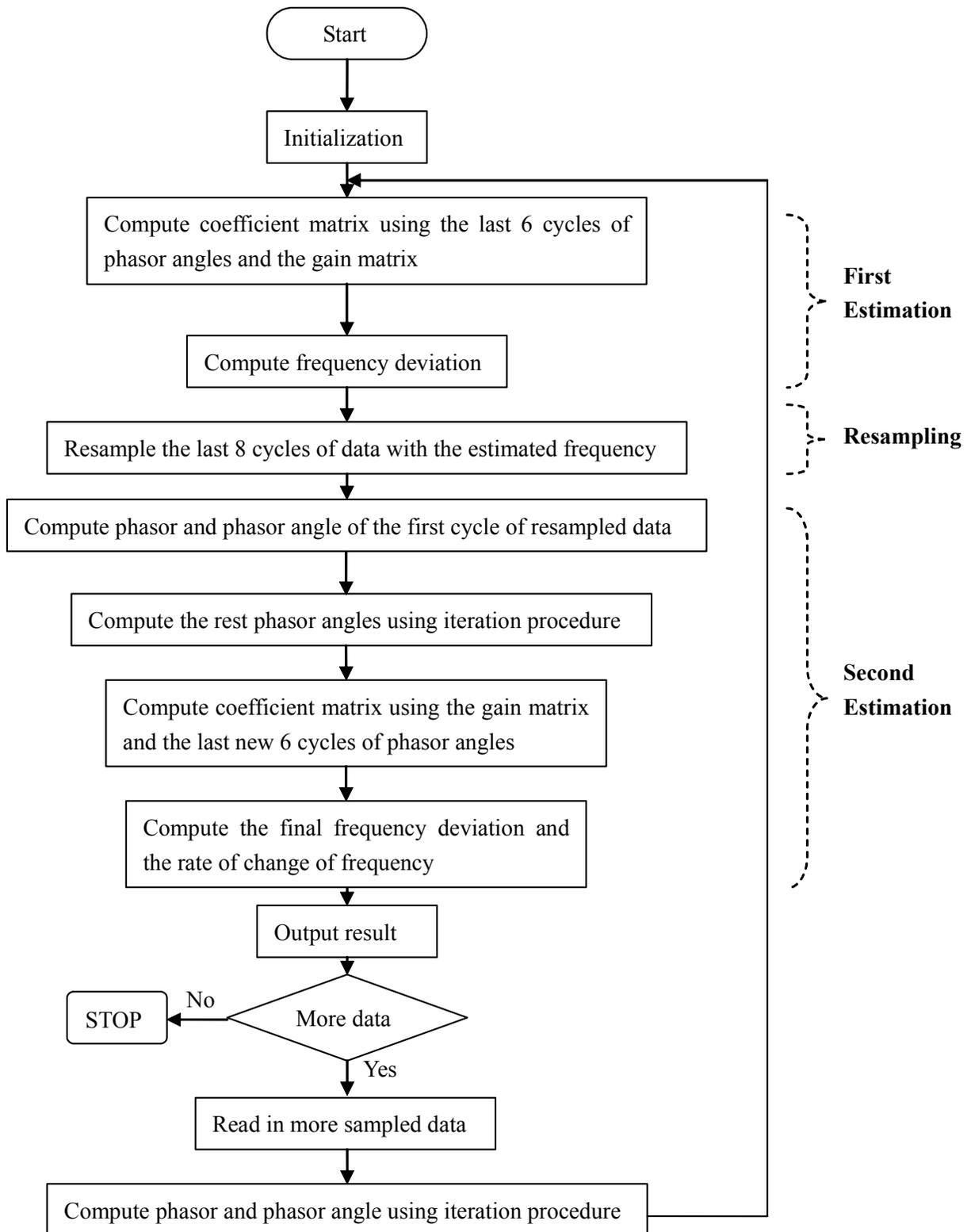


Figure 2-2 flow chart of the algorithm (main body)

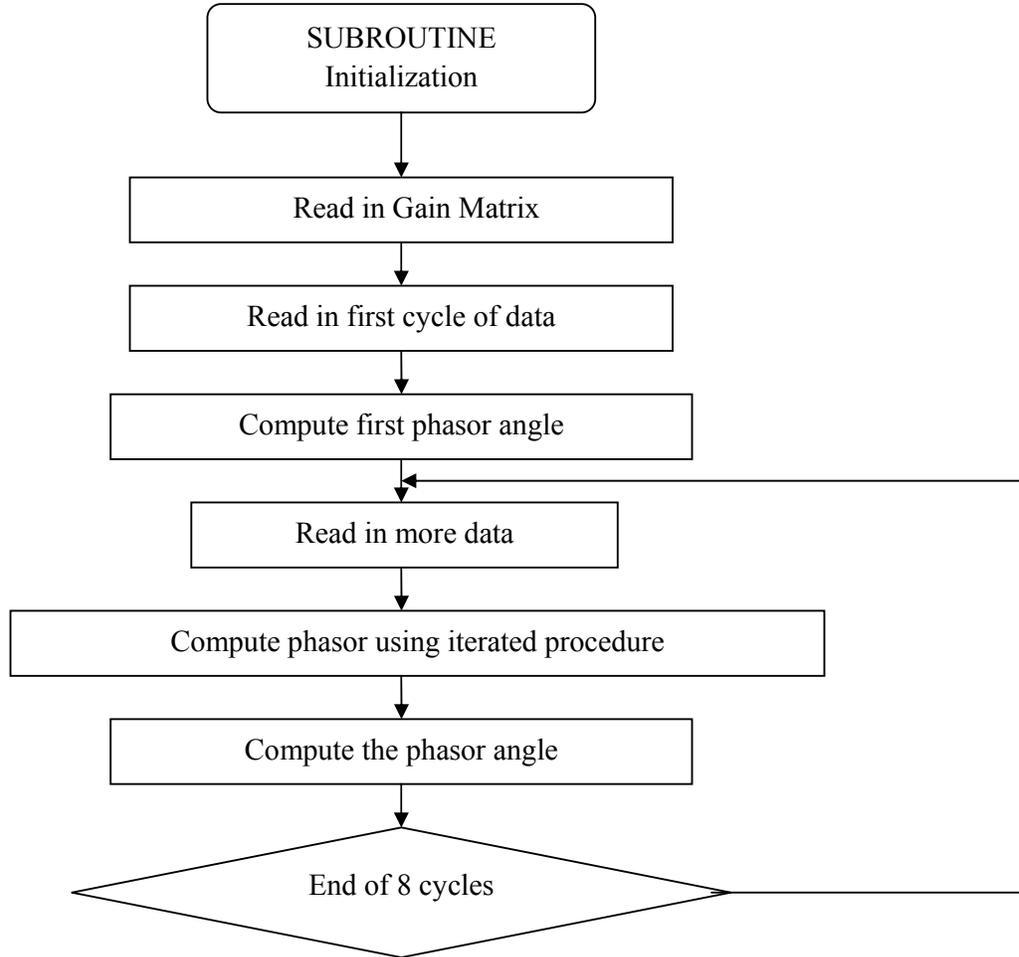


Figure 2-3 Flow chart of the algorithm (Initialization)

## 2.4 Conclusion of DFT-based Frequency Estimation Techniques

In this chapter three frequency measurement techniques based on DFT are discussed. The reasons the last one was chosen instead of its peers can be concluded in the following aspects.

- The frequency range for which the algorithm can make an accurate estimation is large. By contrast, the technique using leakage effect works well only when the frequency deviation is not beyond  $\pm 5\text{Hz}$ , because the linear relationship between the leakage coefficient,  $\eta$ , and the frequency deviation,  $\Delta f$  holds only when the frequency deviation is within  $\pm 5\text{Hz}$ .
- Our algorithm works well with a cosinusoidal waveform or a sinusoidal waveform; this means it is not dependent upon zero-crossing detection of a waveform. Whereas, a

zero-crossing detector must be employed to detect positive going zero-crossing to yield a sinusoidal waveform for the technique using leakage effect. Since no zero-crossing-detector is perfect, a time error  $\Delta t$  will always be introduced. This implies that the sine wave being used will possess a phase delay. Thus the use of a zero-crossing-detector will definitely introduce an error in the computed frequency deviation.

- For the method using variable N DFT, since the sampling period is fixed, the possible fundamental frequencies are discrete, i.e., the fundamental frequency must have a period that is an integer value of the sampling period. While our algorithm does not have this restriction, the frequencies for which it can make accurate estimates are continuous.
- Although the variable window for the method using variable N DFT is able to cover a large frequency range as shown in Table 2-1, the window length can be very large for real time computations. By contrast, our algorithm does not have this problem.

## **2.5 Techniques that Are Not Based on DFT**

Three other frequency estimation techniques require brief discussion. They are Zero Crossing Techniques, the Least Error Square Approximation, and the Kalman Filter Technique [13]. Skipping their details, we focus, as follows, on their disadvantages compared to the algorithm used in our FNET system.

- Zero Crossing Technique is based on rather simple and straight forward mathematics. Hence, the computation is not really a burden. However, Zero Crossing Technique has three big problems for which we reject it. First, Zero Crossing Technique needs a zero-crossing detector which as shown in section 2.2.1 will definitely introduce error. Second, only two or three points in each voltage cycle are used to compute the frequency, i.e., very little signal information is being used. Third, a new frequency can only be obtained at every cycle. Level Crossing Technique [22], one of the variations of Zero Crossing Technique, measures frequency at every incoming sample instead of measuring frequency at only the zero-crossings of a signal. However, even so, since the Level Crossing Technique does a linear interpolation between every two samples, over and under-estimation will inadvertently be introduced.
- Least Error Square Approximation [23] technique involves the least error square

approximation as its name shows. One may see intuitively that when more data is used in a least error square approximation, the error of the estimation will be reduced. In other words the longer the data window used, the smaller the effect of noise on the output. However, this is only partially true, because the foundation of this algorithm is not the least error square approximation, but the approximation of the input waveform with the Taylor series expansion. The least error square approximation only builds upon the results of the Taylor Series Expansion. Hence, error is being introduced from the start. When a larger window is used, more expansion terms will be required to give an accurate approximation of the longer waveform. Thus, increasing the data window size alone will not increase the accuracy. More Taylor series expansion terms also imply more unknowns and a bigger pseudo-inverse matrix. These all add up to a heavier computation burden. Also, when approximating the sinusoidal waveform with Taylor series expansion, an assumption is made that the frequency within the data window is constant. This may not be true. If the window size is increased when the waveform frequency is not constant, the frequency deviation within the data window will be even larger. This will introduce additional errors.

- Kalman Filter Technique [24]: The most significant advantage of the Kalman filter technique is its ability to filter out variable covariance noise. In fact, the Kalman filter technique produces results that are least affected by noise than any of other algorithms discussed in this chapter. However, the Kalman filter technique has one major drawback: the whole technique is based on the assumption that the probability density functions of the state vectors are known. However, this is not always true. For example, during or immediately after a transient has occurred, the state vectors may not have a pure Gaussian probability density function. This will definitely affect the accuracy of the estimation. Moreover, since the purpose of the relay is to detect abnormality, the moment right after transient is usually the most crucial moment. Also, in order to minimize the effect of noise on the measurement, high values for the variance of the measurement noise need to be used. At the same time, high variance will introduce unnecessary delay in obtaining the estimates, i.e., the response time will be even longer.

## **Chapter Three**

### **Performance of the algorithm with non pure sinusoidal input**

#### **3.1 Overview**

In Chapter two, two major assumptions were made relative to the input waveform when performing the resampling needed to enhance the accuracy of the algorithm:

- The input waveform is a pure sinusoidal waveform (i.e., the input waveform is free from any major distortions)
- The input waveform is a single frequency waveform (i.e., frequency deviation within the resampling window is small).

However, for the practical FNET system the input voltage from the real power grid is not always pure sinusoidal because small changes in frequency usually occurs in a power system during quasi steady state. This suggests the need to study the performance of the algorithm with non pure sinusoidal input as done in the two sections that follow. The first discusses the effect of harmonic components on the accuracy of the algorithm and the second presents the test results for a variable frequency waveform. It is instructive to compare these results for non pure sinusoidal input with the accuracy the algorithm yields (Table 3-1) from a pure sinusoidal input.

Frequency (Hz)	Absolute estimation error (Hz)
56	7.0E-05
57	8.2E-05
57.5	7.1E-05
58	5.0E-05
58.5	2.8E-05
59	1.4E-05
59.5	4.0E-06
60	0.0
60.5	5.0E-06
61	1.6E-05
61.5	3.0E-05
62	4.7E-05
62.5	5.6E-05
63	5.9E-05
64	3.9E-05

Table 3-1 the frequency estimation error for pure sinusoidal input whose frequency is between 56Hz and 64Hz

### 3.2 Effect of Harmonic Components

As outlined in [18], power system noise can be viewed as composed of white noise, spike noise and harmonic noise. Both spike noise and white noise can be filtered by analog filters. Harmonic noise, however, has been a major challenge to most power system measurements. Low order harmonics can not be filtered by analog filters and thus are usually present in the waveform entering the measuring device. In this section, simulations are performed on waveforms containing harmonic distortions while maintaining a constant frequency. The harmonic components tested were chosen based on the results of the FFT performed on the input voltage from the power grid (Table 3-2.)

A FFT performed on the input signal from the power grid disclosed a very high frequency (20 kHz) component in addition to the low order harmonic components. It is interesting that the high frequency component has worse effect on the estimation accuracy than do the lower order harmonics.

Harmonic No.	DC	3	5	7	9	20k
Percentage (%)	10	10	5	5	5	2

Table 3-2 major harmonic components of the FFT results with the input voltage directly from power grid

In order to compare the effect of the different harmonics with the same percentage, I also tested 5% DC and 5% No. 3 harmonic.

Since the actual power-grid frequency normally swings in a very narrow range around the nominal frequency of 60 Hz, I studied three base operating frequencies which are 59.5Hz, 60 Hz and 60.5 Hz to see how much the harmonic noise affects the accuracy. The results are displayed in Table 3-3 and Figure 3-1:

Base frequency (Hz) \ Harmonic No.(percentage)	59.5	60	60.5
DC(10%)	3.05E-04(Hz)	0	3.15E-04(Hz)
DC(5%)	1.54E-04(Hz)	0	1.58E-04(Hz)
3(10%)	3.44E-04(Hz)	0	3.35E-04(Hz)
3(5%)	1.72E-04(Hz)	0	1.67E-04(Hz)
5(5%)	1.61E-04(Hz)	0	1.55E-04(Hz)
7(5%)	1.42E-04(Hz)	0	1.66E-04(Hz)
9(5%)	1.24E-04(Hz)	0	1.89E-04(Hz)
20kHz(2%)	2.887E-03(Hz)	1.338E-03(Hz)	2.357E-03(Hz)

Table 3-3 the estimation error of the algorithm with harmonic components existing

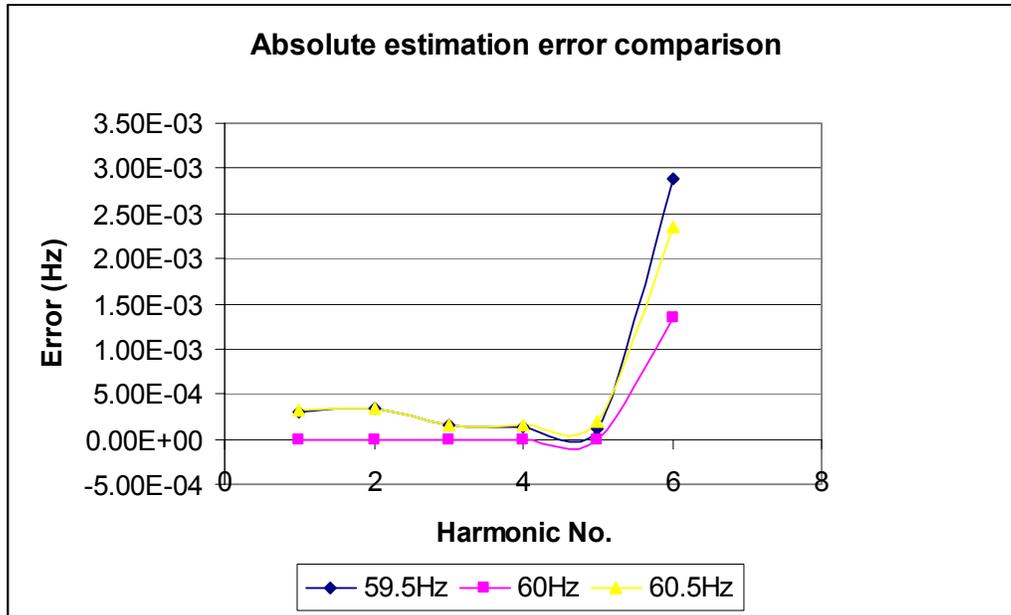


Figure 3-1 the comparison of the frequency estimation error of the algorithm for input with different base frequency and varied harmonic components (The x-axis corresponds to the harmonic No. in Table 3-2)

From Table 3-3 and Figure 3-1, we can draw the following conclusion:

- High frequency components more adversely affect the estimation accuracy than do the low order harmonics.
- Low order harmonics have no effect on the estimation accuracy when the base frequency is 60Hz. But the high frequency component does.
- For low order harmonics, the higher the harmonic order, the less it affects the estimation accuracy. And, particularly, DC has less effect than the No. 3 harmonic does.

### 3.3 Tests with Variable Frequency Waveform

In this section, two cases will be discussed. In the first, the frequency of the input waveform changes at a constant rate like a ramp function. In the second, the frequency of the input waveform changes as a sinusoidal function.

#### 3.3.1 Ramp Case

Table 3-4 shows the Matlab code used to create the ramp function input file where  $t_1$  is the starting time and  $t_2$  is the ending time.  $1/m$  is the rate of change of frequency. The time  $t_1$  can not be zero because I tried starting from 0s but the resultant frequency in the first several seconds was unreasonable. Thus the first few seconds were omitted.

```

inc=1/1440;
t=t1:inc:t2;
f=50+t./m;
wave=169.7.*sin(2.*pi.*f.*t);
wklwrite('input.xls', transpose(wave));

```

Table 3-4 the Matlab code to create the ramp function input file

To obtain the desired results, the output frequency needed modification because of the extra factor of 2 in the slope of the estimated frequency. The modification used the following formula:

$$f(i)=f^*(i)+[f(0)+((408/1440)/m)-f^*(i)]/2 \quad (3-1)$$

where  $f(i)$  is the output data that we will see on the following graphs (Figure 3-1 to Figure 3-23),  $f^*(i)$  is the output data directly from the algorithm,  $f(0)$  is the frequency that the ramp starts at, and  $1/m$  is the rate of change in Hz/s of the ramp function. The  $(408/1440)/m$  term was added to compensate for the omission of a certain number of data points at the beginning. Table 3-5 displays the program coded in Matlab.

```

[t]=transpose(out);
n=1;
for i=5:1:28609
frequency(n)=55.248118+[i-1]*(1/1440)+(408/1440);
new(n)=t(i)+(55.248118+((408/1440))-t(i))/2;
time(n)=(i-1)/1440;
n=n+1;
end
plot(time,new,'.');
hold on
xlabel('time, t, s')
ylabel('frequency, Hz')
title('Time Versus Frequency')
plot(time, frequency, 'r');
legend('Approximation', 'Exact');

```

Table 3-5 the Matlab code for displaying the test results for the input waveform with the frequency changing at a constant rate like a ramp function

To change the data range, simply change the values for  $i$  on line 3. The output frequency data from the algorithm is stored in a file named out.m. In order to change the rate of change, change the value of  $m$ .

Why I dealt with the output frequency for display had to do with the fact that the model for the input did not take into consideration that when the frequency is varying, it cannot be represented as  $w=2\pi f$ . Instead, another function is used. Simply modifying the output produces the desired

effect.

Next, Figure 3-2 to Figure 3-13 display the resultant frequencies. They were sorted into four groups according to the different ramp rates tested which are 0.04Hz/s, 0.1Hz/s, 0.5Hz/s and 1Hz/s. Each group has three Figures---Figure 3-2, 3-3, and 3-4 for the 0.04Hz/sec results; Figure 3-5 to Figure 3-7 for 0.1Hz/sec; Figure 3-8 to Figure 3-10 for 0.5 Hz/sec; Figure 3-11 to Figure 3-13 for 1Hz/sec---the first depicts the resultant frequency during the whole time period denoted as Approximation as well as the theoretical frequency according to the mathematic formula denoted as Exact. The second is a zoomed-in part of the first figure. The third represents the error between the actual and the theoretical frequency. In the first two figures, the continuous line shows the output frequency from the algorithm while the dotted one displays the theoretical frequency according to formula (Eq. 3-1.)

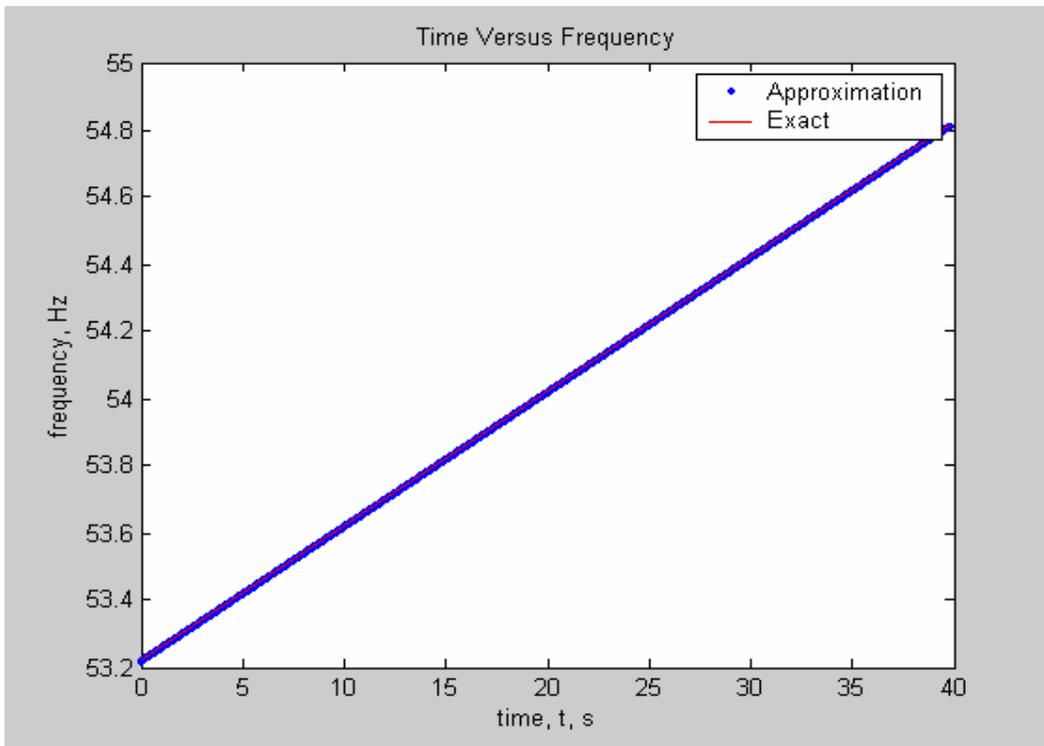


Figure 3-2 the estimated frequency for an input waveform with frequency changing as a ramp function at the rate of .04 Hz/sec, for frequencies within the range from 53. 2Hz to 54.8Hz compared to the exact frequency calculated from the formula (Eq. 3-1.)

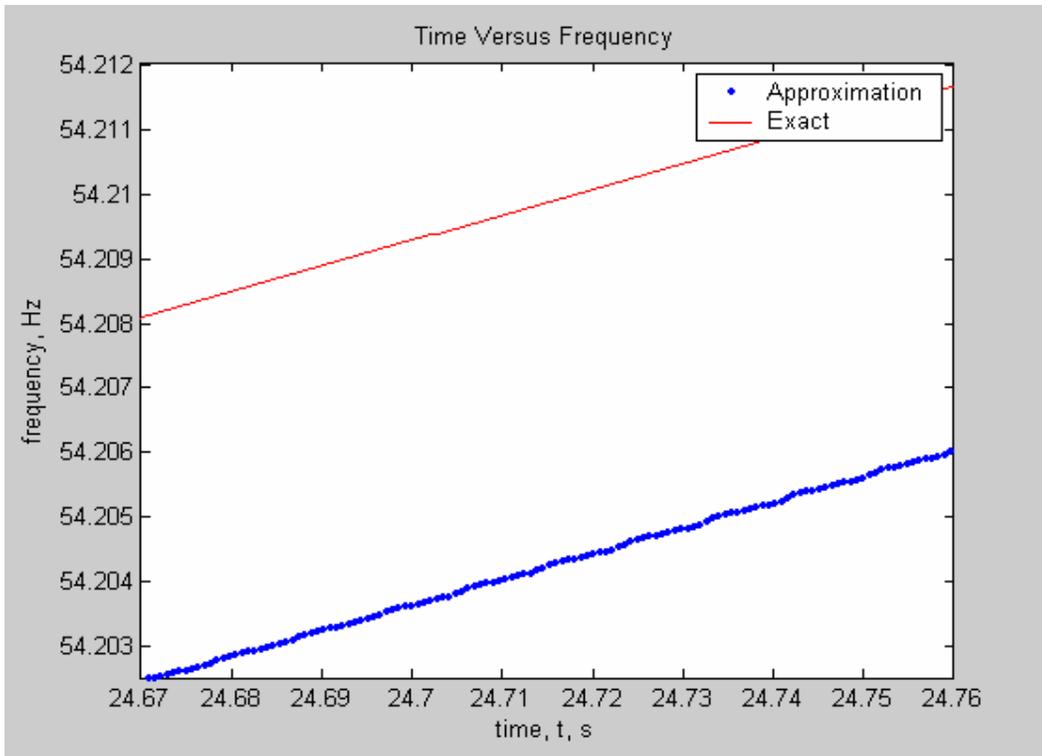


Figure 3-3 a zoomed-in part of Figure 3-2

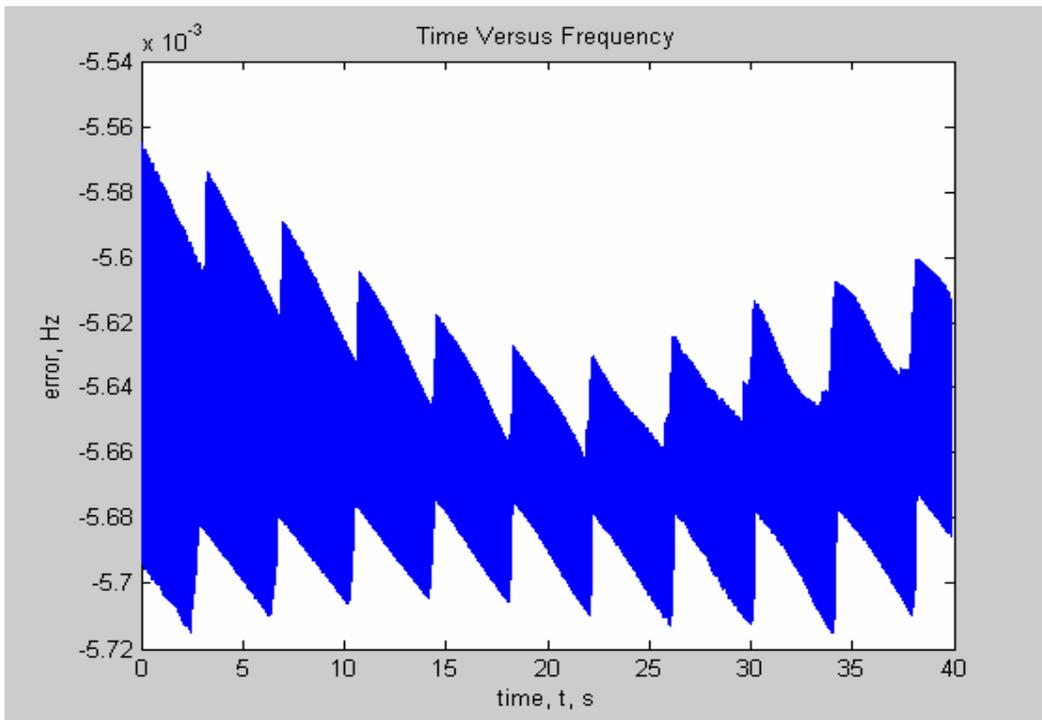


Figure 3-4 the error between the estimated frequency for input waveform with frequency changing as a ramp function with a rate of .04 Hz/sec, for frequencies within the range from 53. 2Hz to 54.8Hz and the exact frequency calculated from the formula(Eq. 3-1.)

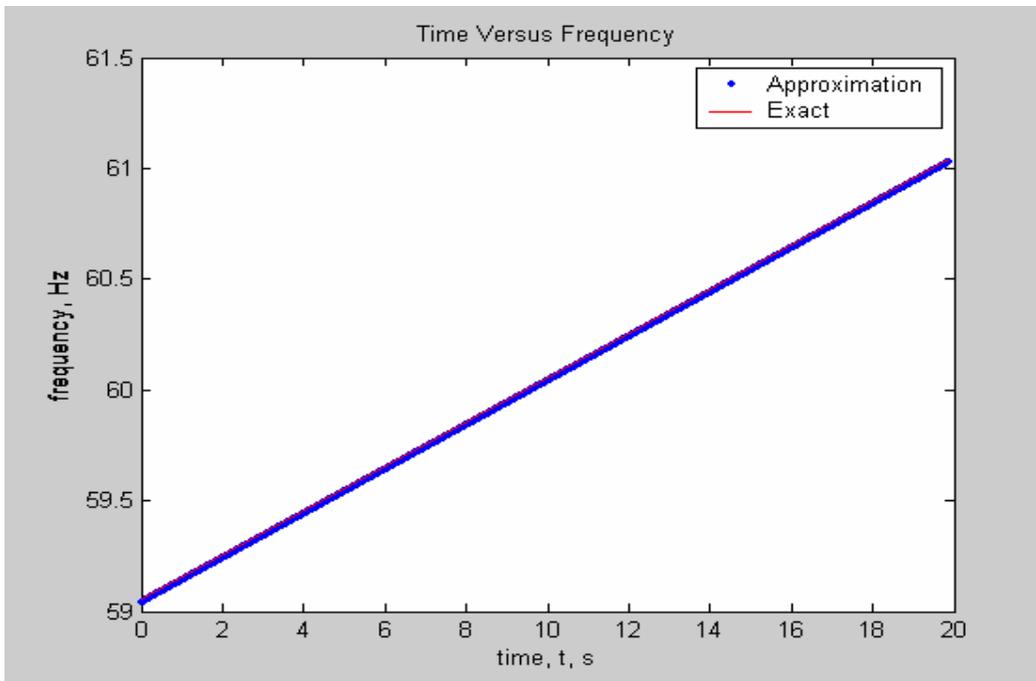


Figure 3-5 the estimated frequency for input waveform with frequency changing as a ramp function with a rate of .1 Hz/sec, for frequencies within the range from 59 Hz to 61Hz and the exact frequency calculated from the formula (Eq. 3-1.)

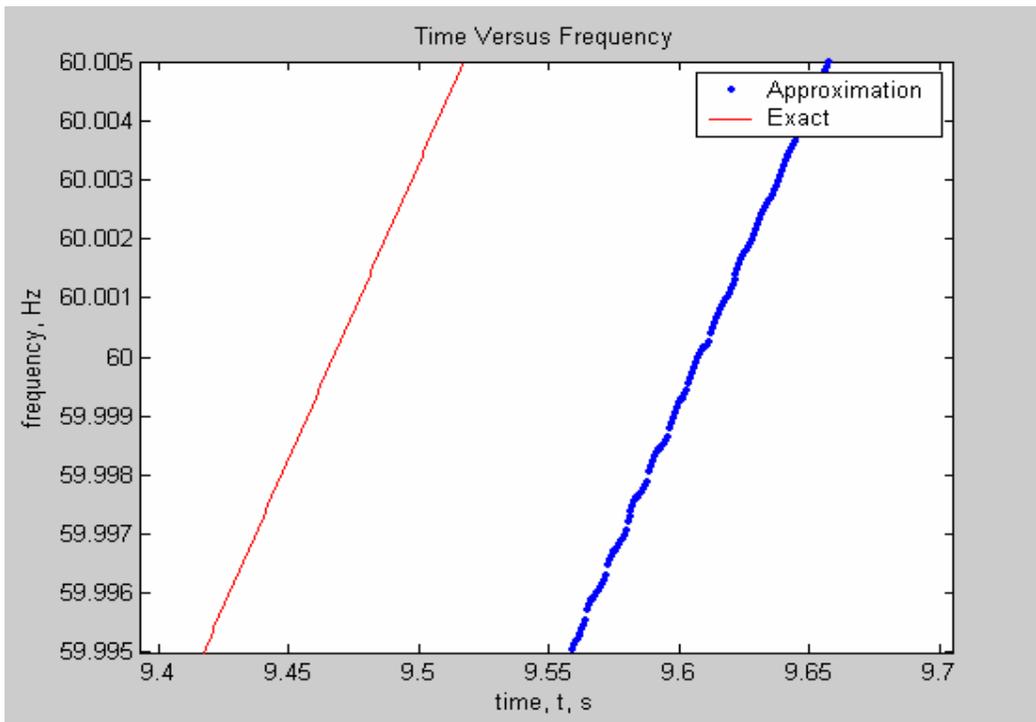


Figure 3-6 a zoomed-in part of Figure 3-5

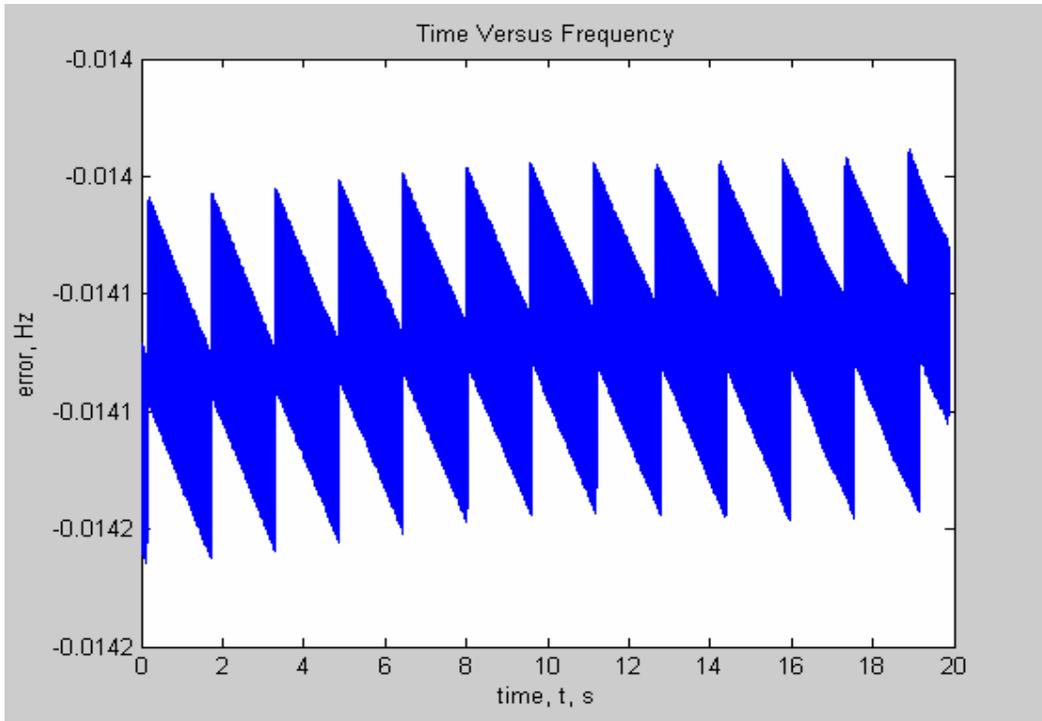


Figure 3-7 the difference between the estimated frequency for input waveform with frequency changing as a ramp function with a rate of .1 Hz/sec, for frequencies within the range from 59 Hz to 61Hz and the exact frequency calculated from the formula (Eq. 3-1.)

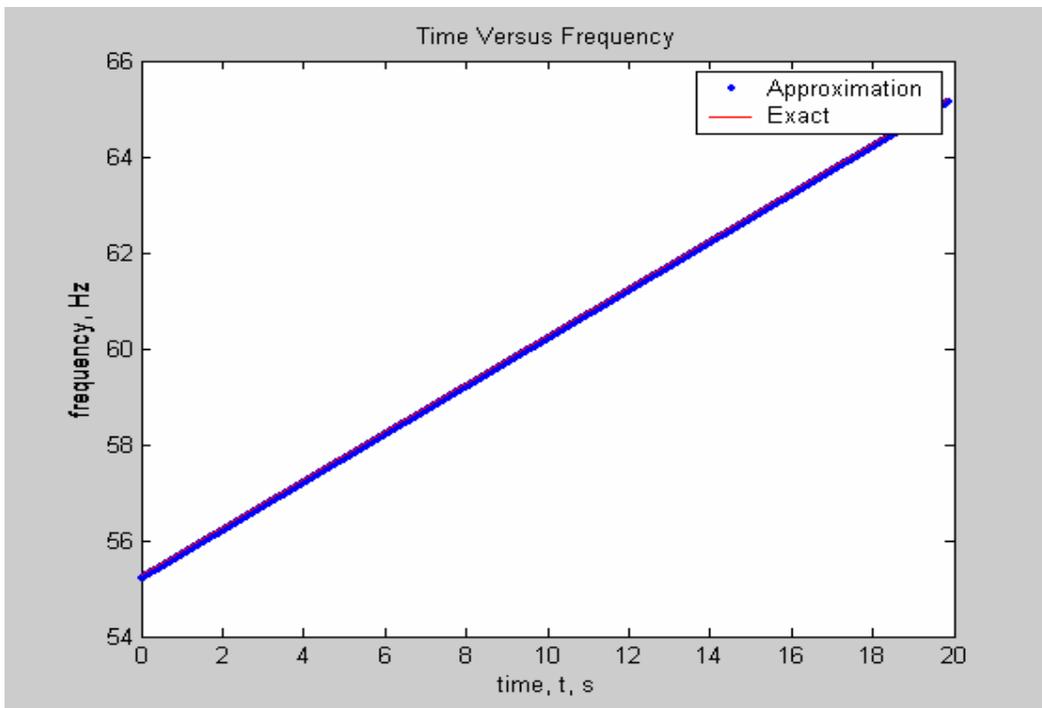


Figure 3-8 the estimated frequency for input waveform with frequency changing as a ramp function with a rate of .5 Hz/sec, for frequencies within the range from 55 Hz to 65Hz and the exact frequency calculated from the formula (Eq. 3-1.)

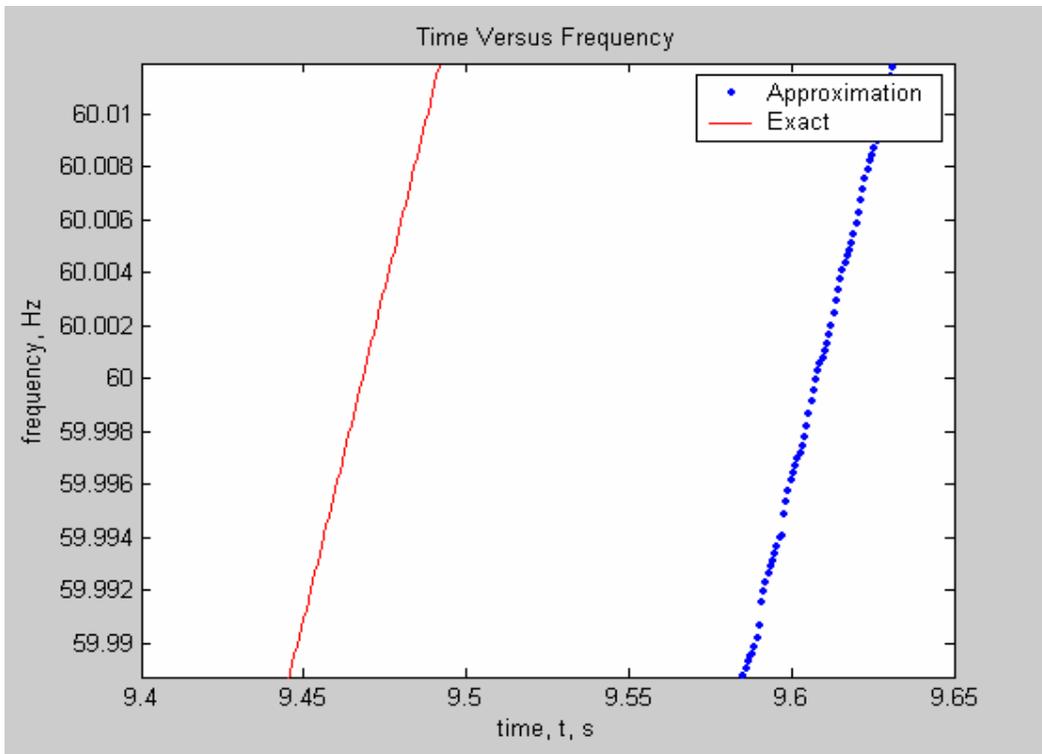


Figure 3-9 a zoomed-in part of Figure 3-8

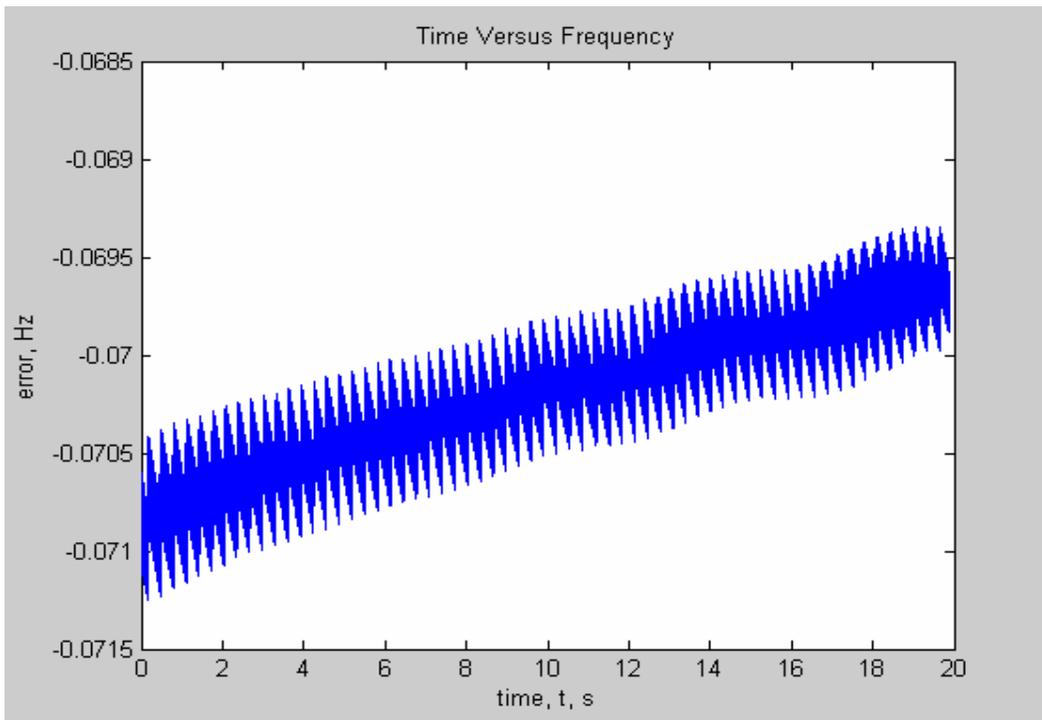


Figure 3-10 the difference between the estimated frequency for input waveform with frequency changing as a ramp function with a rate of .5 Hz/sec, for frequencies within the range from 55 Hz to 65Hz and the exact frequency calculated from the formula(Eq. 3-1.)

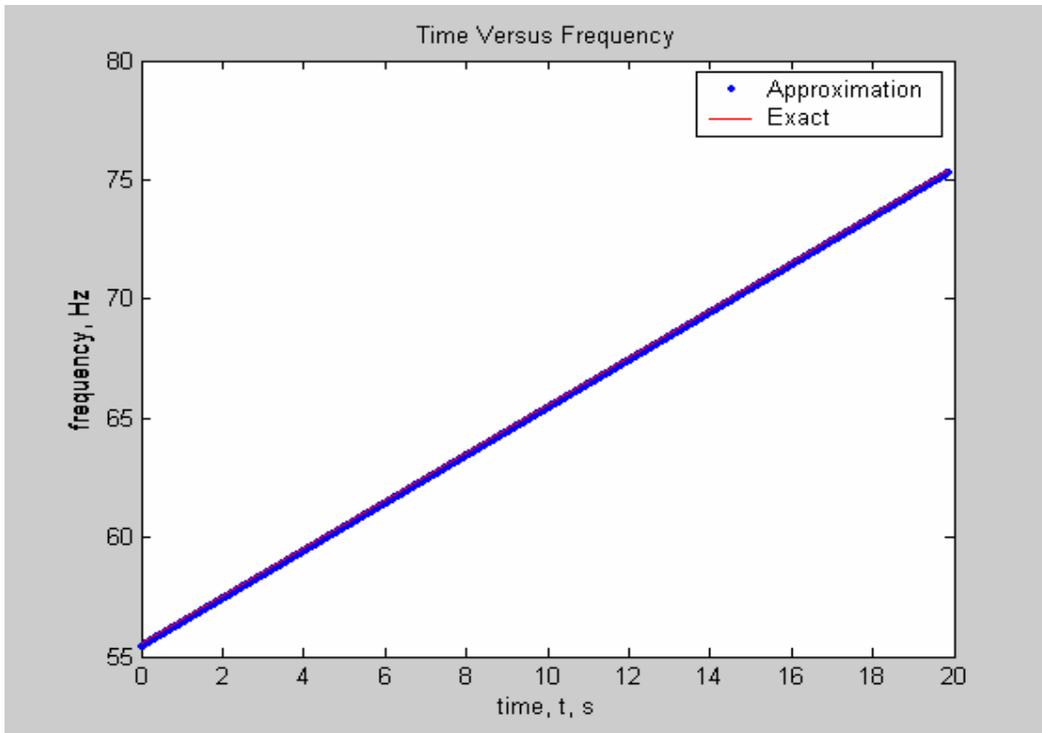


Figure 3-11 the estimated frequency for input waveform with frequency changing as a ramp function with a rate of 1 Hz/sec, for frequencies within the range from 55 Hz to 75Hz and the exact frequency calculated from the formula (Eq. 3-1.)

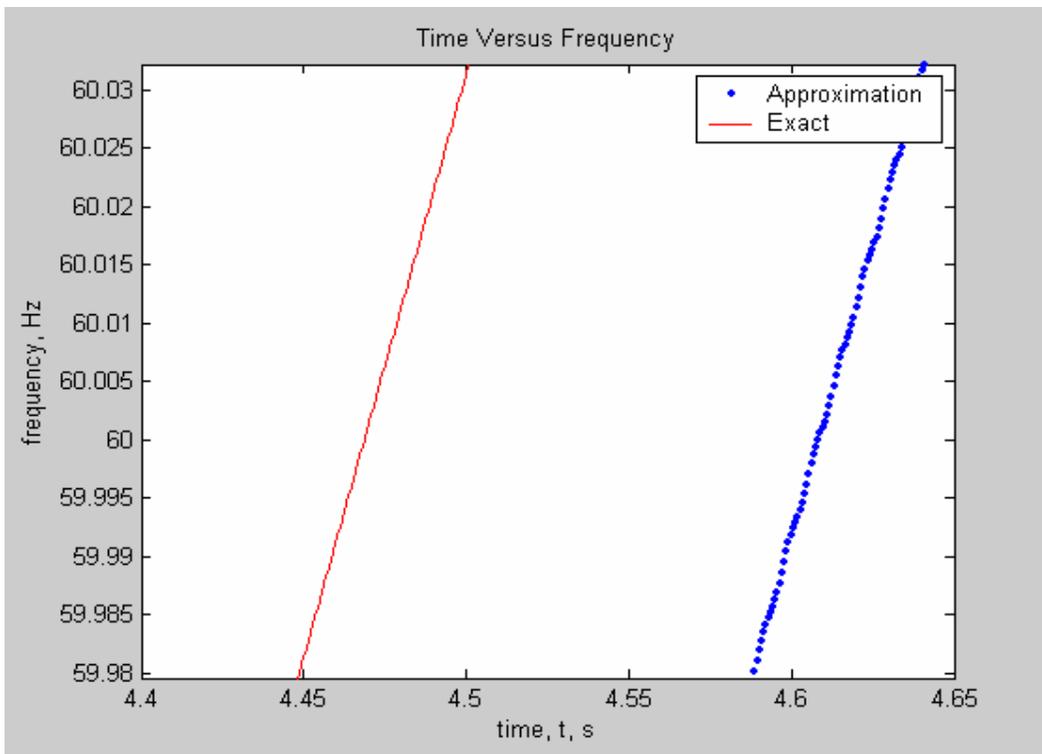


Figure 3-12 a zoomed-in part of Figure 3-11

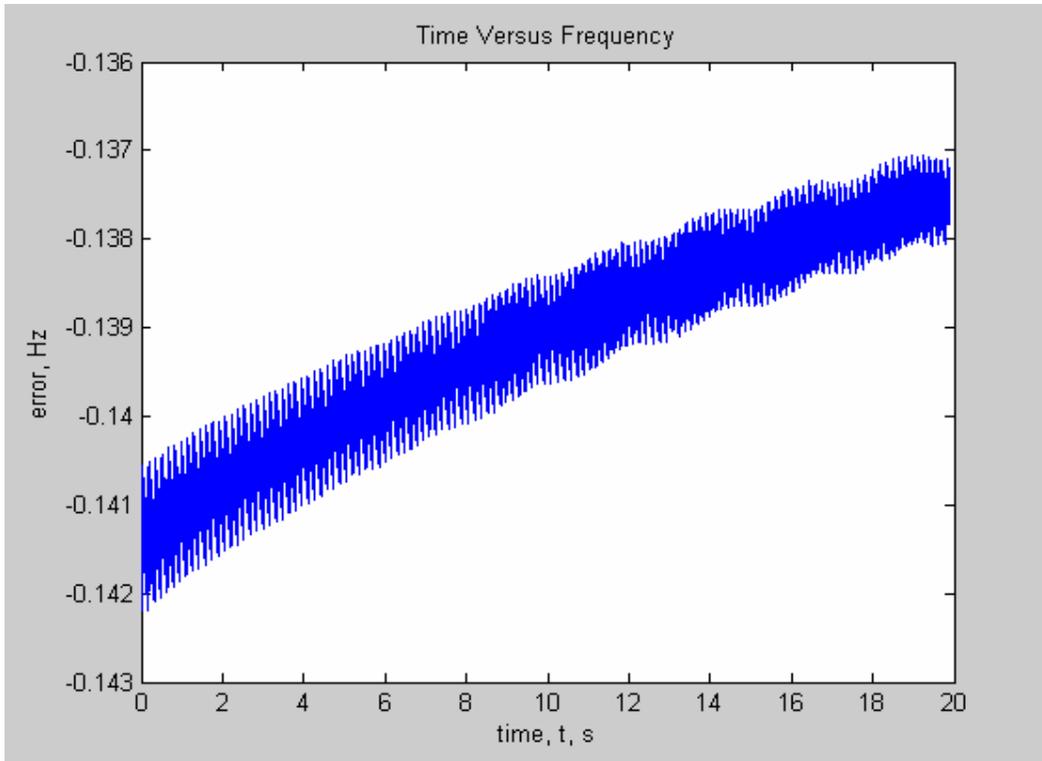


Figure 3-13 the difference between the estimated frequency for input waveform with frequency changing as a ramp function with a rate of 1Hz/sec, for frequencies within the range from 55 Hz to 75Hz and the exact frequency calculated from the formula (Eq. 3-1.)

Figures 3-2 to 3-13 disclose that the higher the rate of the ramp function, the lower will be the frequency estimation accuracy (Table 3-6.)

Rate of ramp(Hz/s)	0.04	0.1	0.5	1
Error range (Hz)	-5.72E-3~-5.575E-3	-0.0142~-0.014	-0.0713~-0.0697	-0.142~-0.137

Table 3-6 Differences between the estimated frequency and the exact frequency for the input as frequency changes at different constant rates as a ramp function

### 3.3.2 Sinusoidal Case

For the sinusoidal case, the following equations are necessary to create the input waveform for the algorithm.

$$\omega = \omega_0 + A \sin(\omega_1 t) \quad (3-2)$$

$$\varphi = \int [\omega_0 + A \sin(\omega_1 t)] dt = \omega_0 t - \frac{A}{\omega_1} \cos(\omega_1 t) \quad (3-3)$$

where  $\omega_0$  is the base line frequency (in our situation  $60 \cdot 2\pi$  rad/s),  $A$  is the amplitude of the sinusoid multiplied by  $2\pi$  and  $\omega_1$  is the frequency of the sinusoid.

Table 3-7 shows the Matlab used to created an input signal with a sinusoidal frequency that has a frequency of 0.5 Hz and an amplitude of 3 added to a base line frequency of 60 Hz.

```
inc=1/1440;
t=0:inc:10;
w2=.5*2*pi;
phase=120*pi*t-(3*2*pi/w2)*cos(w2*t);
wk1 write('sinramp.xls', transpose(sin(phase)));
```

Table 3-7 The Matlab code used to create an input signal with a sinusoidal frequency that has a frequency of 0.5 Hz and an amplitude of 3 added to a base line frequency of 60 Hz

The program mult\_freq\_wave.m as shown in Table 3-8 was to create the graphs (Figure 3-14 to Figure 3-23.)

```

                                sampling_rate = 1440;
end_time = 9+1248/1440; %change depending on how long running. This is for when it runs 10s.

                                % time vector
                                time = [0:20/sampling_rate:end_time];
                                time_for_freq_var = [191/1440:20/1440:end_time+1/sampling_rate+190/1440];
                                %above factor of 191/1440 added to account for data points cut off by algorithm
                                %**IMPORTANT**: Change increment 20/1440 to 1/1440 when plotting exact and
                                %approximate plots.
                                %frequency variation
                                freq_hz = .0333; % the frequency variation rate of voltage waveform frequency
                                freq_var_amp = 3; % the variation amplitude of the frequency variation
                                offset_freq = 60; % the baseline frequency, e.g. 60 Hz
                                var = freq_var_amp*sin(2*pi*freq_hz*time_for_freq_var)+offset_freq; %the frequency vary betw
                                60+-freq_var_amp

                                %60*ones(1,length(time_for_freq_var)); % base line

                                %plot(time, freq_var); %uncomment this line to plot approximate and exact graph

                                %hold on
                                e(['Waveform's frequency varying with ',num2str(freq_hz),' Hz, amplitude of ',num2str(freq_var_amp)
                                sinusoid'])
                                xlabel('Time (sec)')
                                hold on
                                [p]=transpose(sineramp); %define data
                                n=1;
                                for i=1:20:14209
                                    new(n)=p(i); %data from algorithm
                                    second(n)=(i-1)/1440; %time in seconds
                                    n=n+1; %increment by 1
                                end

                                %plot(second,new,'r'); %uncomment this line to plot approximate and exact graph
                                plot(second,new-freq_var) %plots error graph. Comment out this line to plot app and exact graphs
                                %hold on
                                ylabel('Error') %Comment out this line to plot app and exact graphs
                                %ylabel('Frequency, Hz') %uncomment this line to plot approximate and exact graph
                                %legend('Exact', 'Approximation') %uncomment this line to plot approximate and exact graph

```

Table 3-8 program mult\_freq\_wave.m coded in Matlab (The algorithm output frequency data is placed in sineramp.m)

Table 3-9 shows the five combinations of frequency and amplitude being tested.

Freq.(Hz)	0.1	0.1	0.1	0.5	0.0333
Amp. (V)	1	2	3	3	3

Table 3-9 the parameters of the sinusoidal functions as which the frequency changes

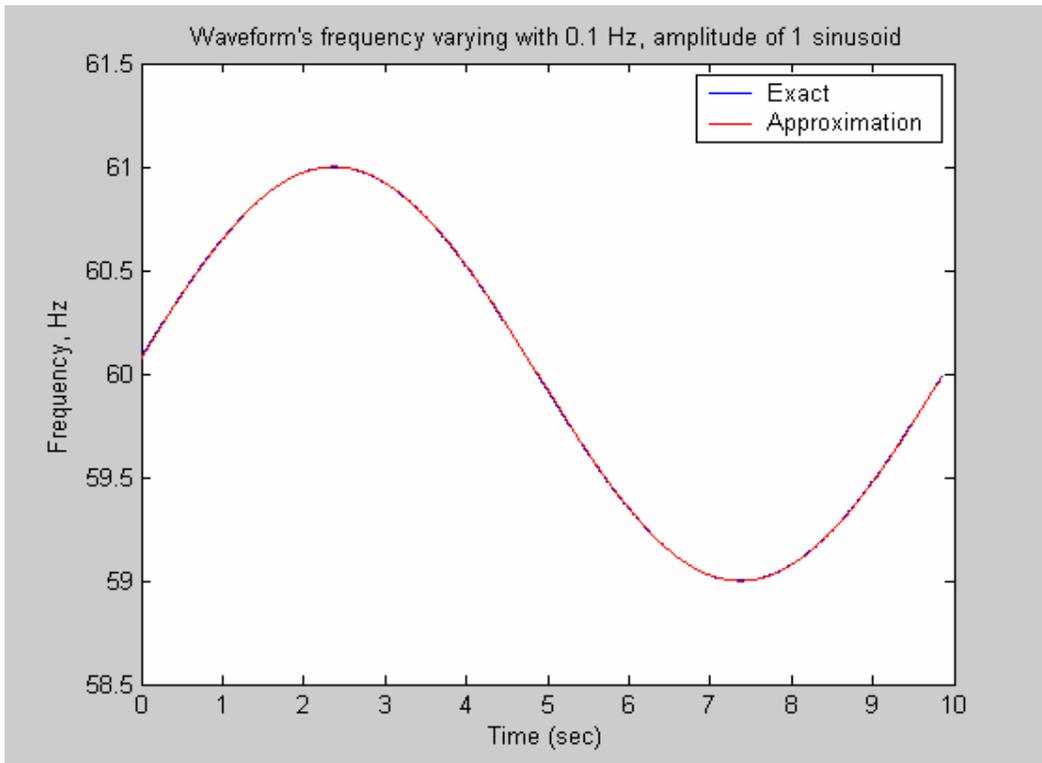


Figure 3-14 the estimated frequency for input waveform with  $f=0.1\text{Hz}$ ,  $\text{Amp}=1$  sinusoidal changing frequency (between 59Hz and 61Hz) compared to the exact frequency

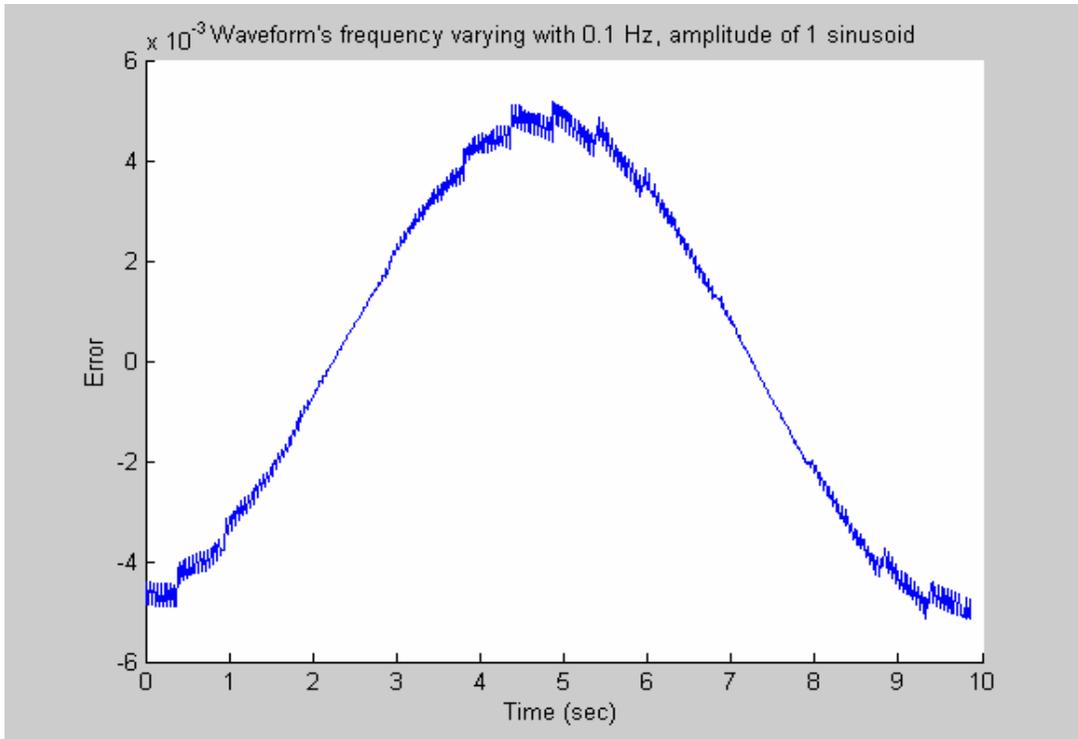


Figure 3-15 Difference between the estimated frequency and the exact one for an input waveform with  $f=0.1\text{Hz}$ , Amp=1 sinusoidal changing frequency (between 59Hz and 61Hz) (the unit of Y-axis is Hz)

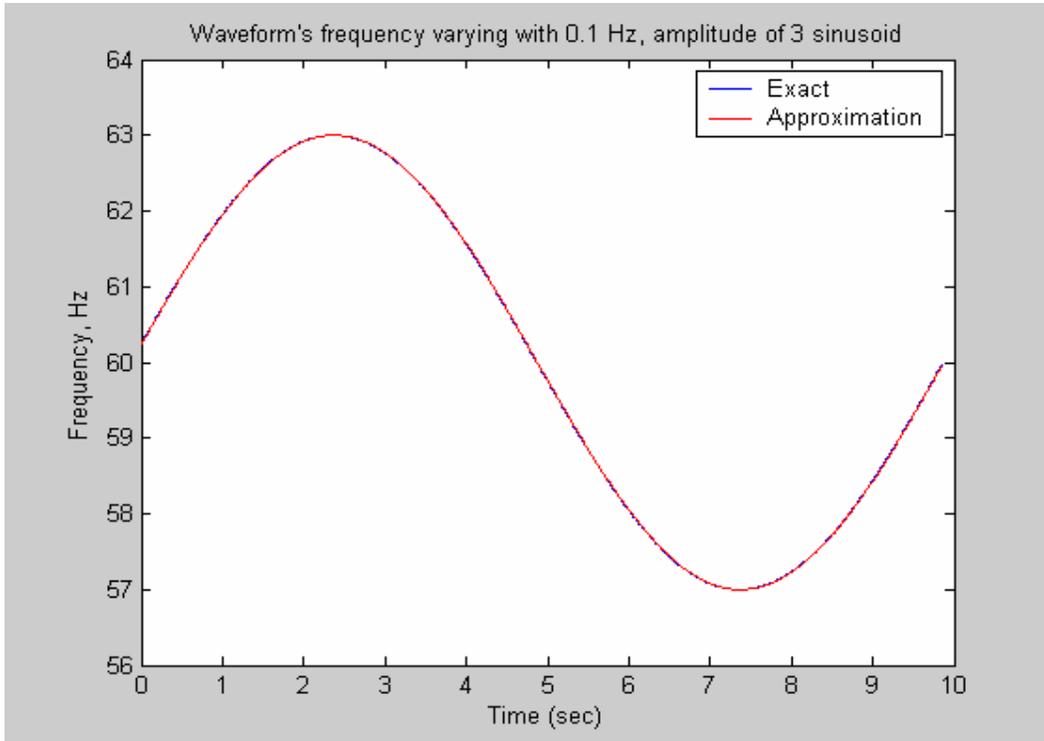


Figure 3-16 the estimated frequency for input waveform with  $f=0.1\text{Hz}$ , Amp=3 sinusoidal changing frequency (between 57Hz and 63Hz) and the exact frequency

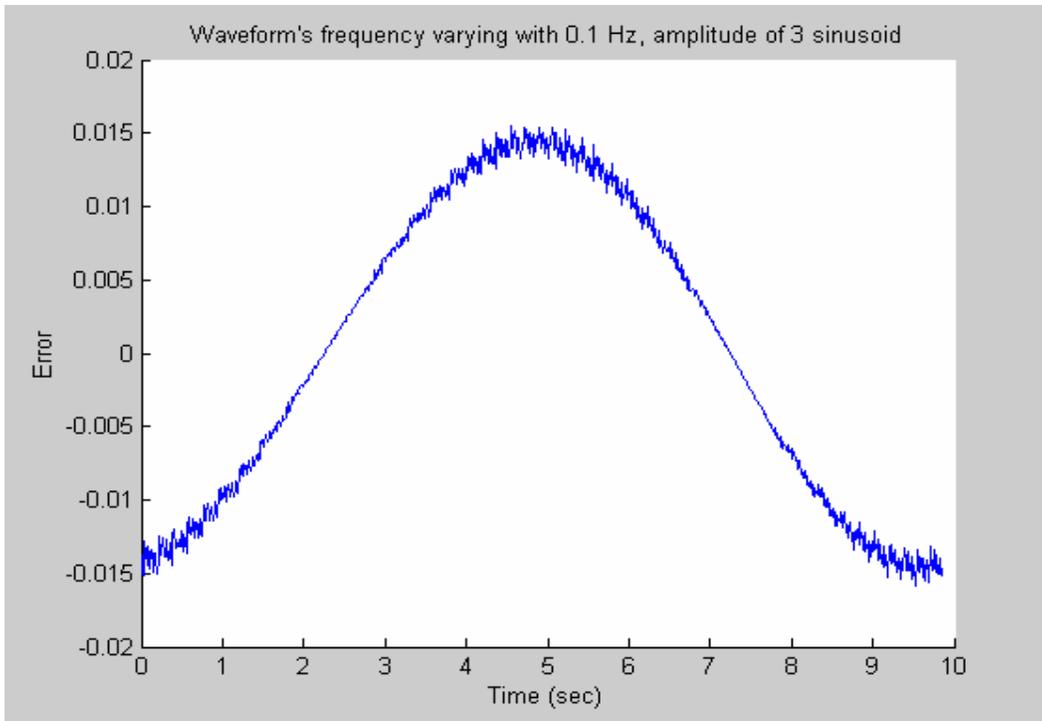


Figure 3-17 the difference between the estimated frequency and the exact one for input waveform with  $f=0.1\text{Hz}$ ,  $\text{Amp}=3$  sinusoidal changing frequency (between 57Hz and 63Hz) (the unit of Y-axis is Hz)

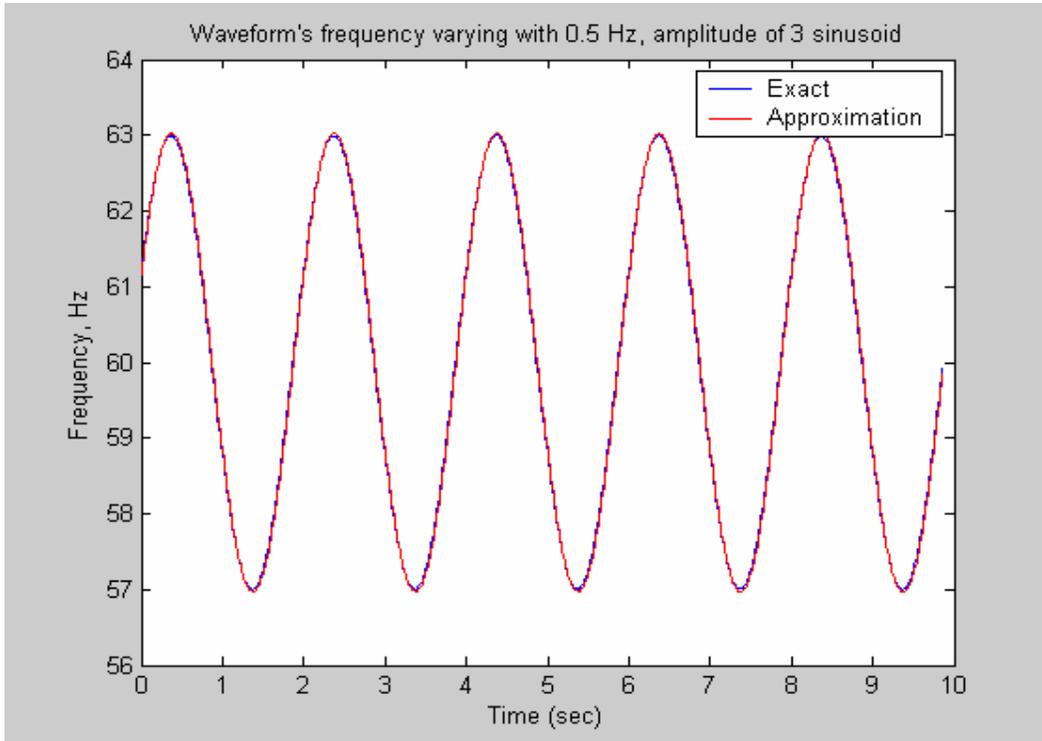


Figure 3-18 the estimated frequency for input waveform with  $f=0.5\text{Hz}$ ,  $\text{Amp}=3$  sinusoidal changing frequency (between 57Hz and 63Hz) and the exact frequency

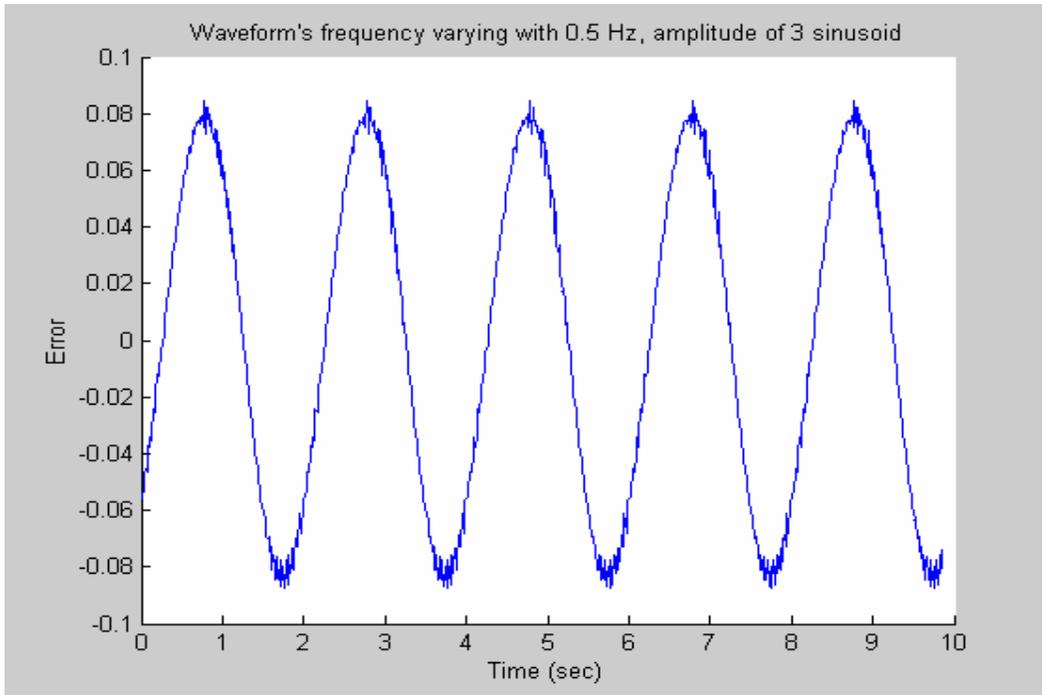


Figure 3-19 the error between the estimated frequency and the exact one for input waveform with  $f=0.5\text{Hz}$ ,  $\text{Amp}=3$  sinusoidal changing frequency (between 57Hz and 63Hz) (the unit of Y-axis is Hz)

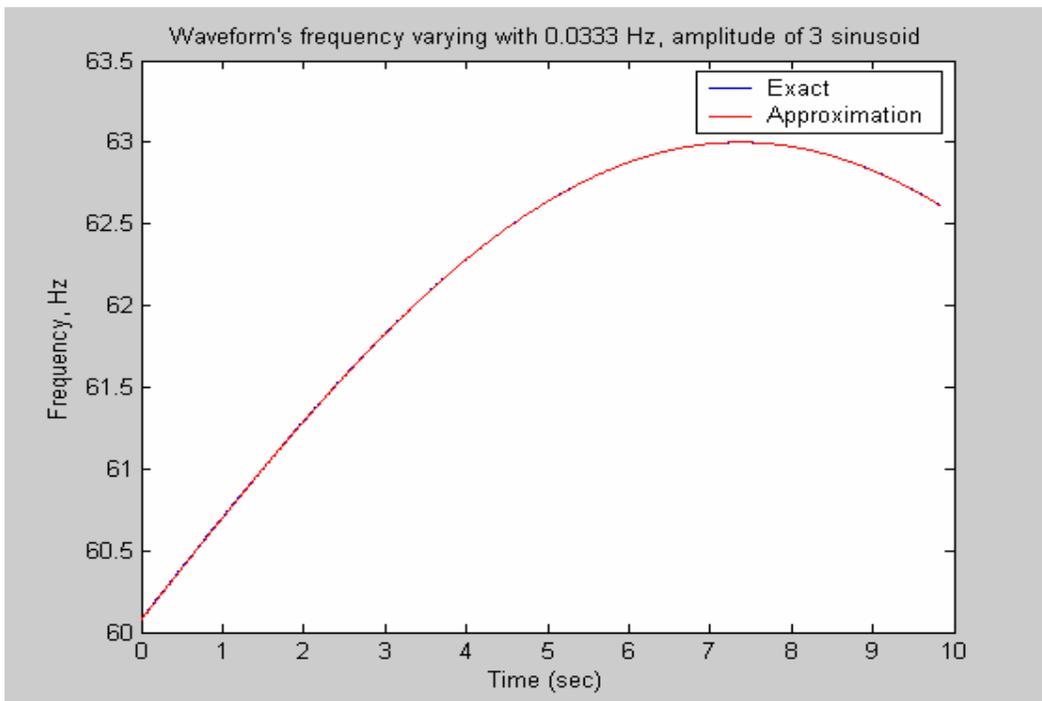


Figure 3-20 the estimated frequency for input waveform with  $f=0.0333\text{Hz}$ ,  $\text{Amp}=3$  sinusoidal changing frequency ( between 57Hz and 63Hz, only a part of a cycle is shown in this Figure which is why you just see a part of the frequency above 60Hz) and the exact frequency

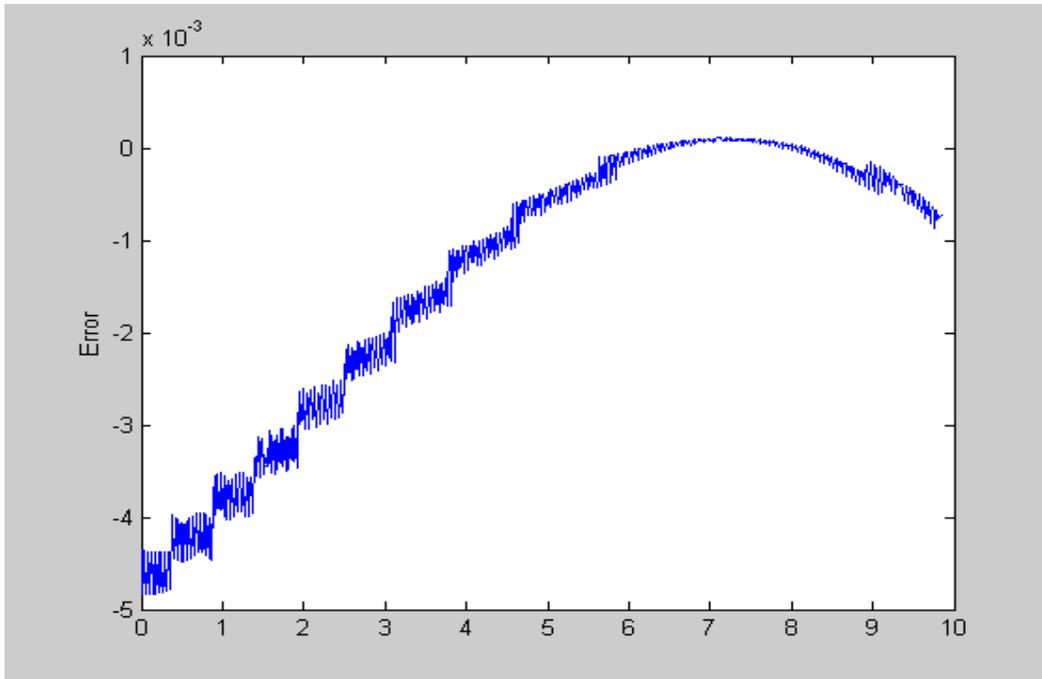


Figure 3-21 the difference between the estimated frequency and the exact one for input waveform with  $f=0.0333\text{Hz}$ ,  $\text{Amp}=3$  sinusoidal changing frequency (between 57Hz and 63Hz) (the unit of Y-axis is Hz)

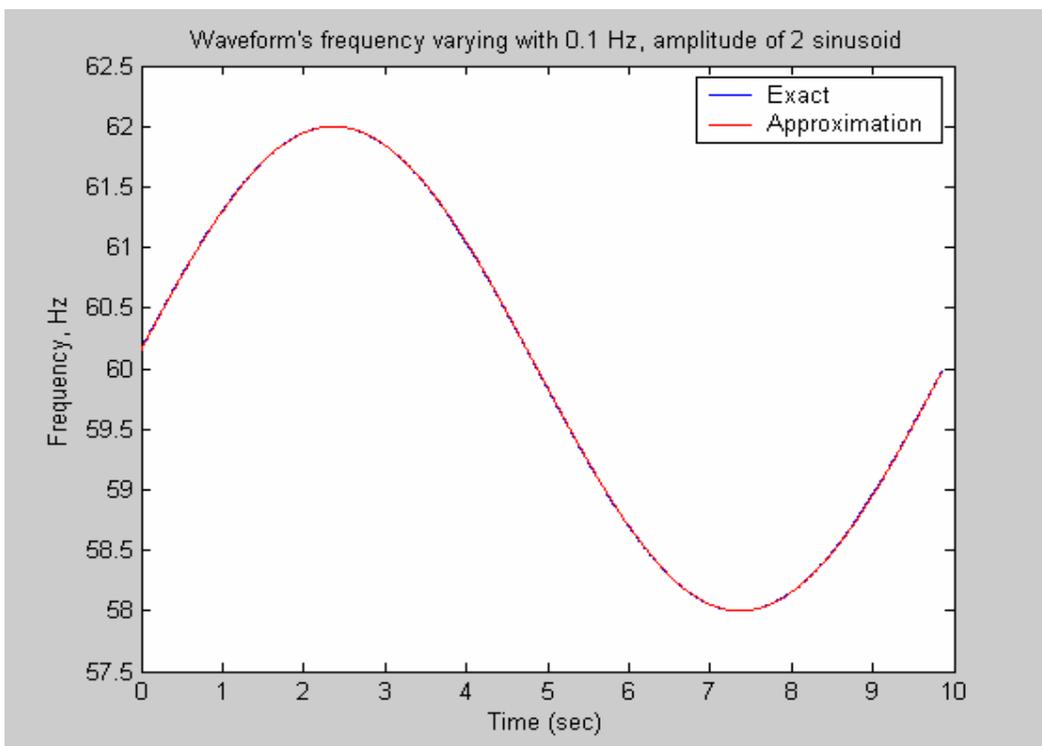


Figure 3-22 the estimated frequency for input waveform with  $f=0.1\text{Hz}$ ,  $\text{Amp}=2$  sinusoidal changing frequency (between 58Hz and 62Hz) and the exact frequency

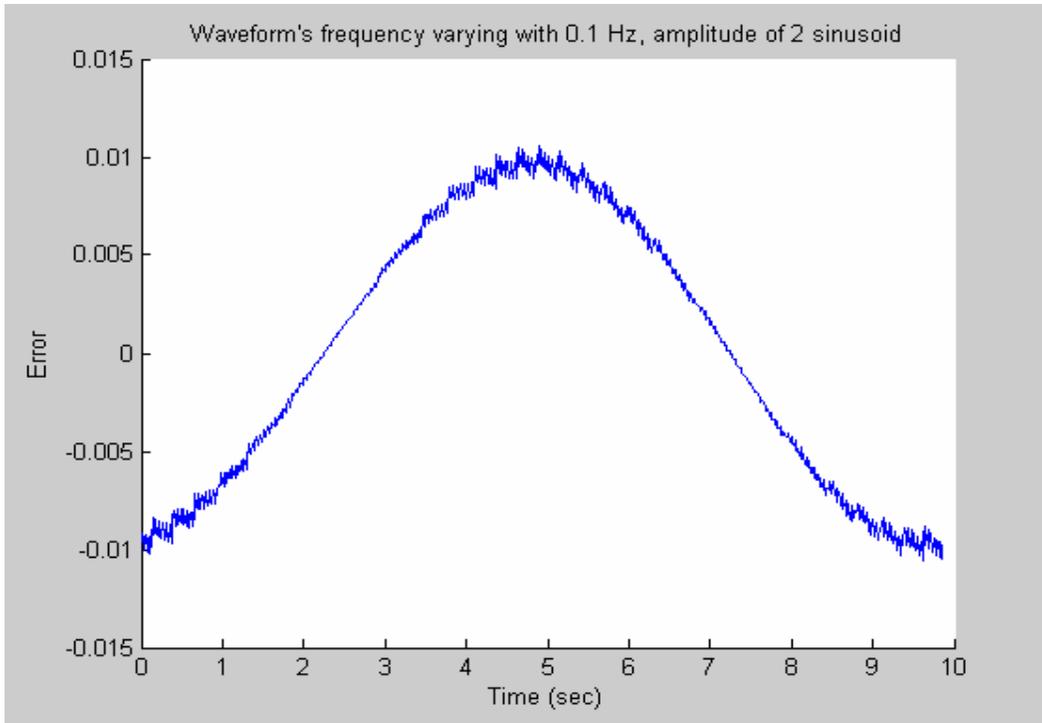


Figure 3-23 the difference between the estimated frequency and the exact one for input waveform with  $f=0.1\text{Hz}$ ,  $\text{Amp}=2$  sinusoidal changing frequency (between 58Hz and 62Hz) (the unit of Y-axis is Hz)

The error range for sinusoidal changing frequency with different frequency and amplitude is summarized in the following two tables. The sinusoids in Table 3-10 have the same frequency of 0.1Hz and varied amplitudes. Whereas, those in Table 3-11 have the same amplitude of 3 and different frequencies.

Parameters	F=0.1 Hz Amp=1	F=0.1 Hz Amp=2	F=0.1 Hz Amp=3
Error range (Hz)	-5E-3~5E-3	-0.01~0.01	-0.015~0.015

Table 3-10 the error range for sinusoidal changing frequency with the same frequency

Parameters	F=0.0333Hz Amp=3	F=0.1 Hz Amp=3	F=0.5Hz Amp=3
Error range (Hz)	-4.9E-3~0	-0.015~0.015	-0.084~0.083

Table 3-11 the error range for sinusoidal changing frequency with the same amplitude

It is clearly seen that the higher the sinusoidal frequency and the larger the amplitude, the bigger will be the estimation error.

## Chapter Four

### Analysis of the Practical Problems

#### 4.1 Overview

Two practical problems that arise when estimating frequency using the FNET system are discussed. Next, two methods are suggested for improving the accuracy when calculating frequency using inputs directly from the power grid. Finally, two problems inherent to the input waveform and their effect on the accuracy of the estimated frequency are described.

#### 4.2 Averaging and Moving Averaging

Data from the power grid with the sampling frequency of 100,000Hz was down sampled to 1440Hz by interpolation before being entered into the algorithm to yield the following output (Figure 4-1.)

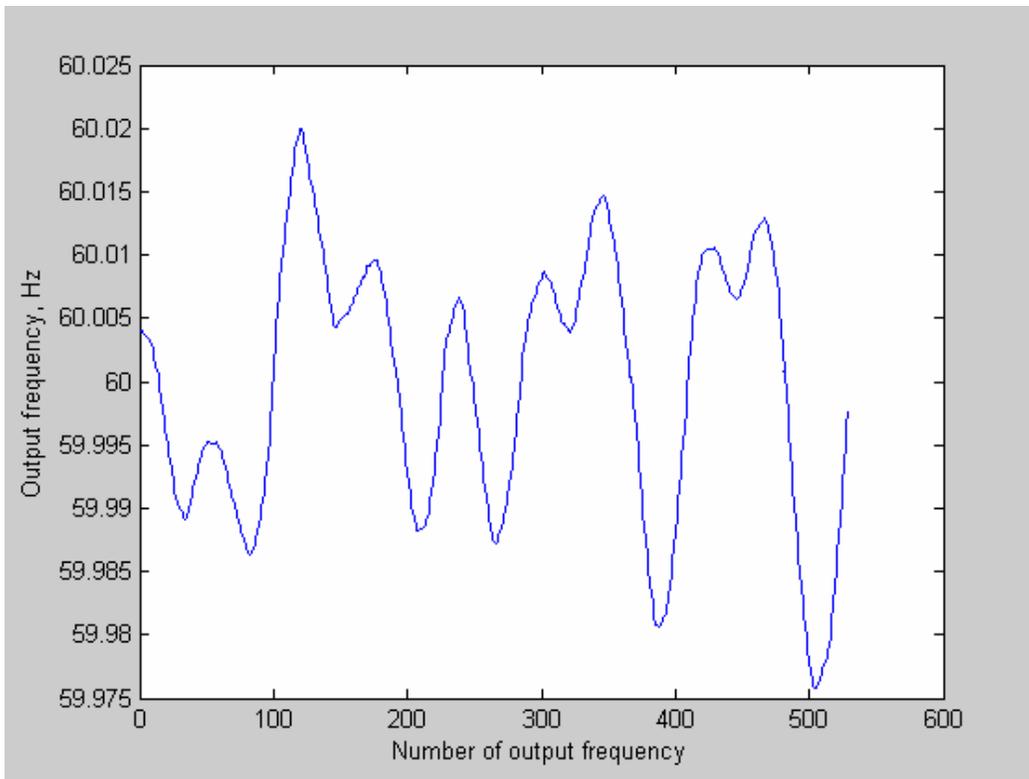


Figure 4-1 Output frequency after interpolation but before averaging

The result proved unacceptable because the input signal directly from the power grid contains too much noise whereas our algorithm works very well only if the input signal has no big

deviation from pure sinusoidal. Thus it is necessary to process the data before feeding it to the algorithm. Some simple analog filters in our practical system helped, but left more to be desired. Consequently, digital signal processing was introduced, chiefly, averaging and moving averaging.

The number of points used to do the averaging is 64. The averaging of 64 points is actually equivalent to down sampling the data by 64. The original data directly from power grid was sampled at the rate of 100,000Hz. Therefore, in order to obtain the final desired sampling rate of 1440Hz, which fits the algorithm, one must down sample it to  $64 \times 1440\text{Hz}$  before averaging the 64 points. The resultant output frequency is shown in Figure 4-2.

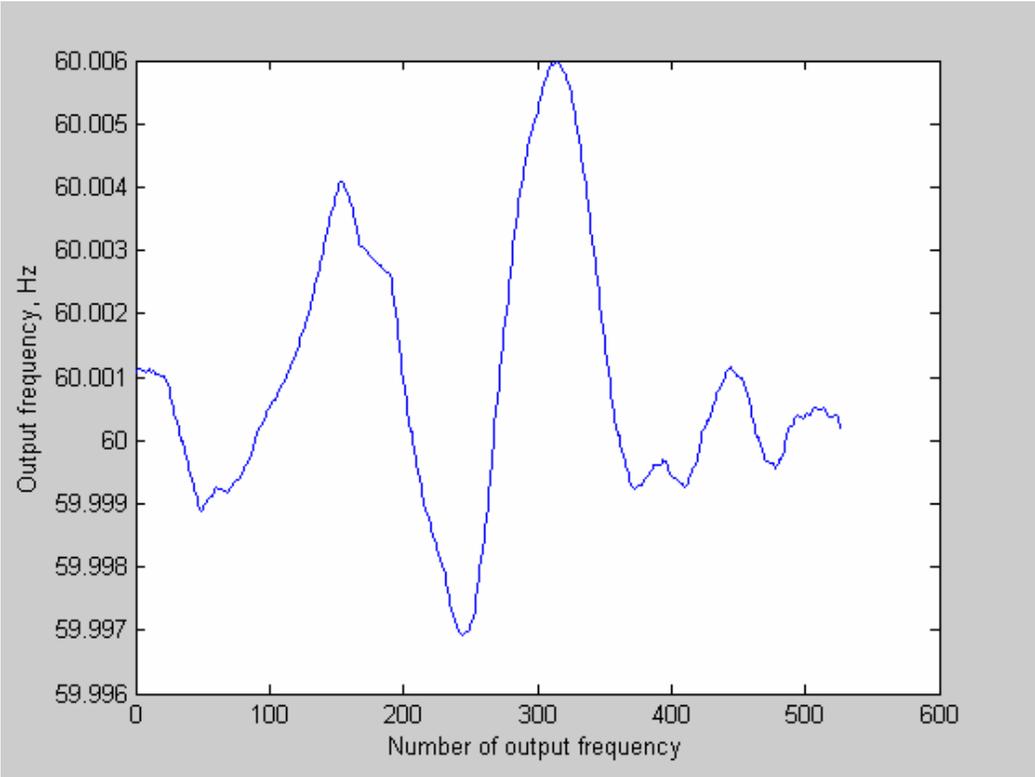


Figure 4-2 Output frequency after averaging of 64 points being used

The data processed by moving averaging retains the original sampling rate. Thus, the moving averaging was performed before down sampling the raw data directly from power grid to the rate of 1440Hz. The moving averaging of 3 (Figure 4-3), 5 (Figure 4-4) and 64 (Figure 4-5) points were performed and only the 64 –point moving averaging proved useful.

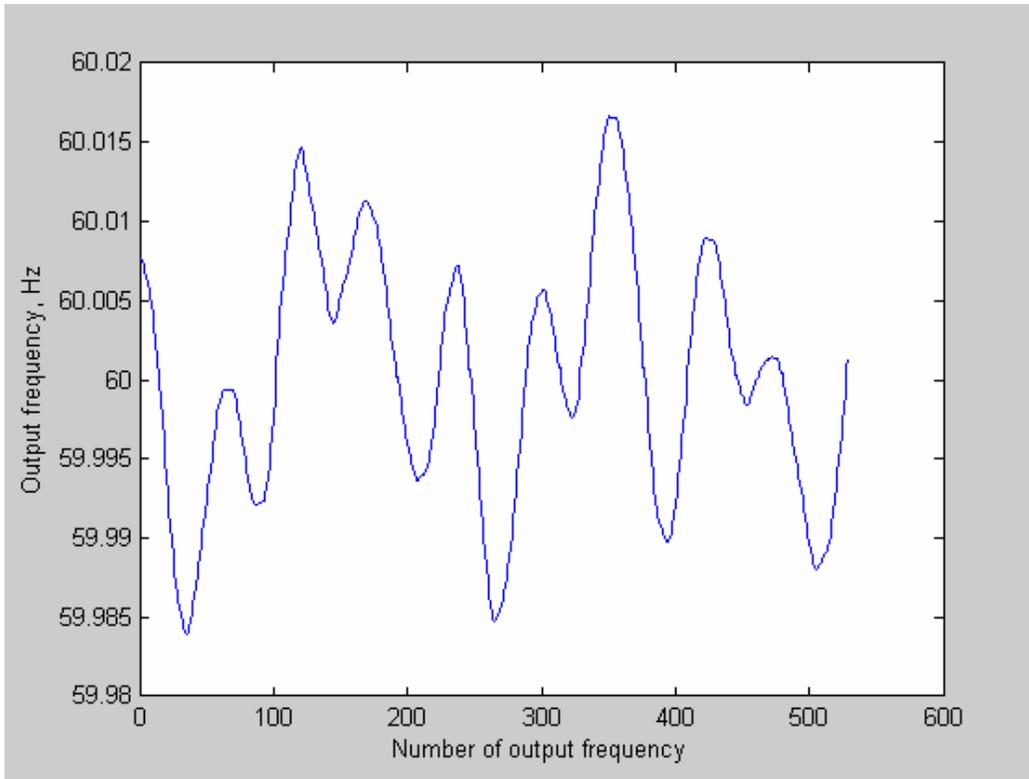


Figure 4-3 Output frequency of moving averaging of 3 points

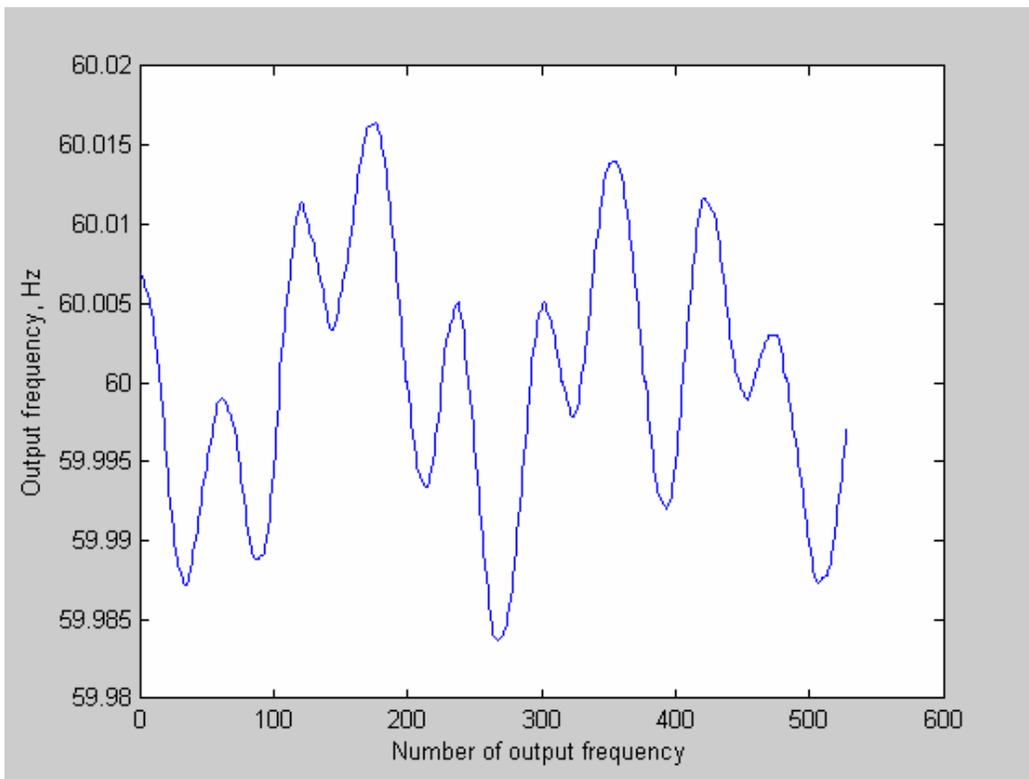


Figure 4-4 Output frequency of moving averaging of 5 points

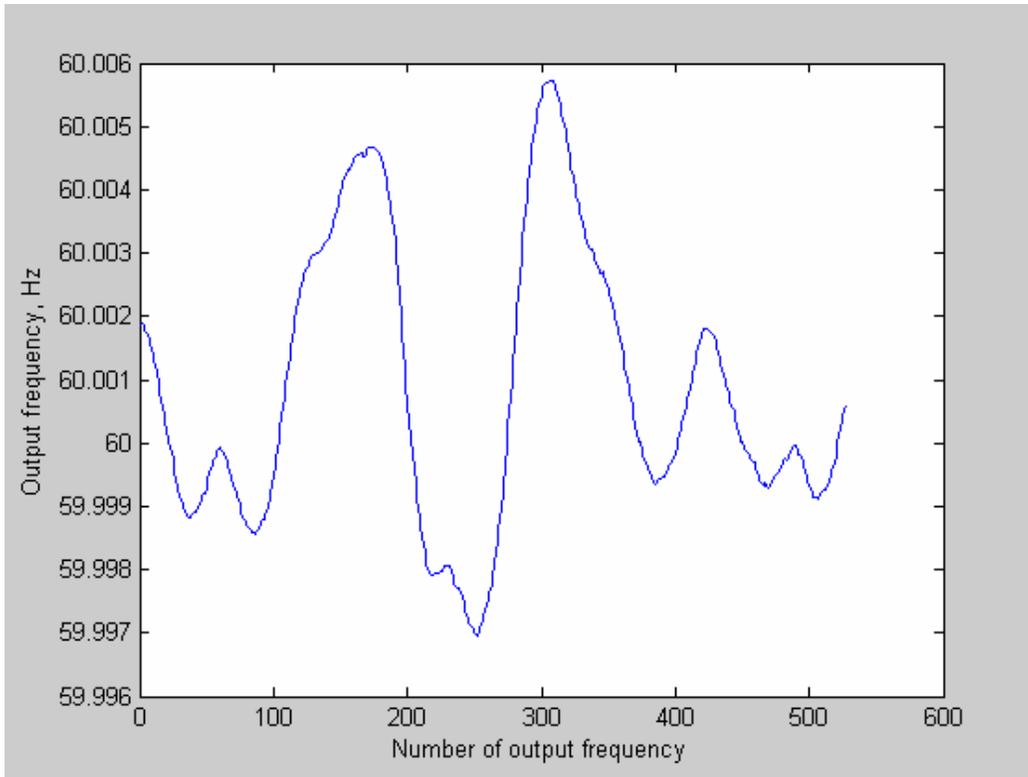


Figure 4-5 Output frequency of moving averaging of 64 points

Figure 4-1, Figure 4-2 and Figure 4-5 permit the following conclusion:

- Both the averaging of 64 points and moving averaging of 64 points significantly improve the frequency estimation accuracy using input data directly from the power grid.
- The effect of the averaging of 64 points and moving averaging of 64 points on the frequency estimation accuracy shows no big difference

### 4.3 One Missing Point

During the development process, the output frequency showed a spike every 29 or 30 seconds. This proved to be caused by a missing data point. To confirm this, the following tests were performed:

- 1) Generate several cycles of discrete pure sinusoidal data with the sampling frequency of 1440 (24\*60).
- 2) Omit one point at various locations in one waveform-cycle to generate different sinusoidal waveform, each with one point missing from one cycle. (Figure 4-6 shows the various locations chosen for the one missing point)

- 3) Generate the input signal by repeating one point missing at a long enough constant interval (20 cycles) of normal pure sinusoidal without points missing.
- 4) Feed the generated signal to a version of the algorithm on PC which had been modified to estimate and output 10 frequencies per second just as the practical system does. (That is why you do not see as long a space as you might suppose to see between the two consecutive spikes since only 10 frequencies were estimated and output per second. )

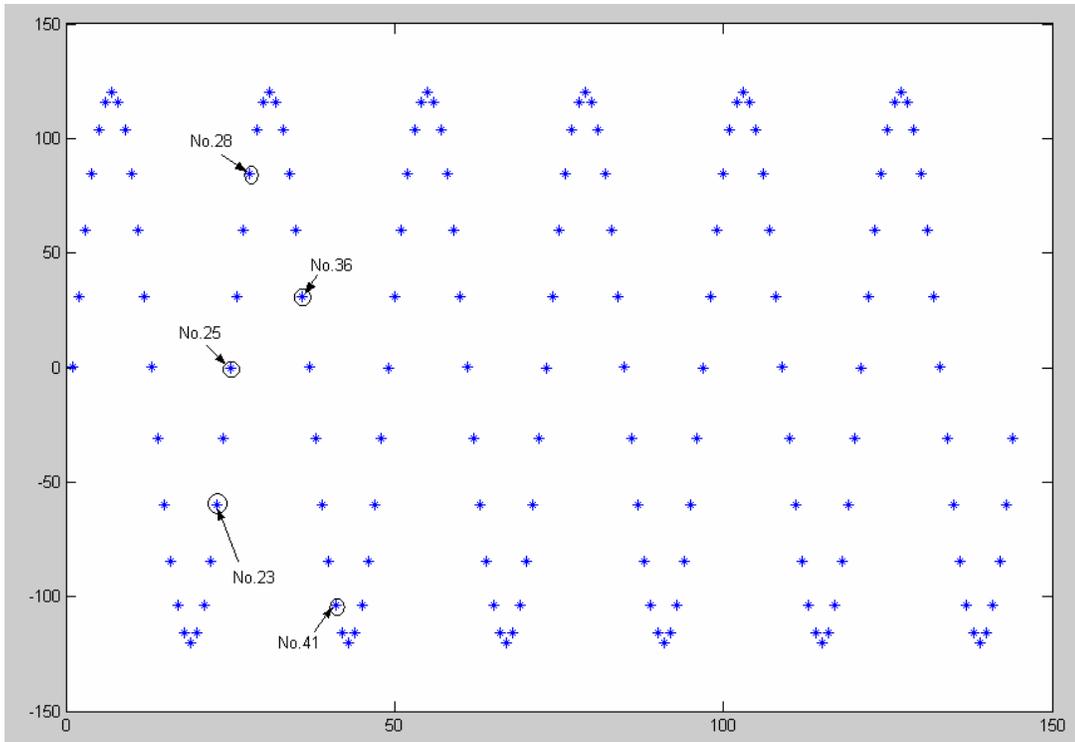


Figure 4-6 different locations of the missing one point during one cycle

The results are displayed in the Figure 4-7 to Figure 4-11.

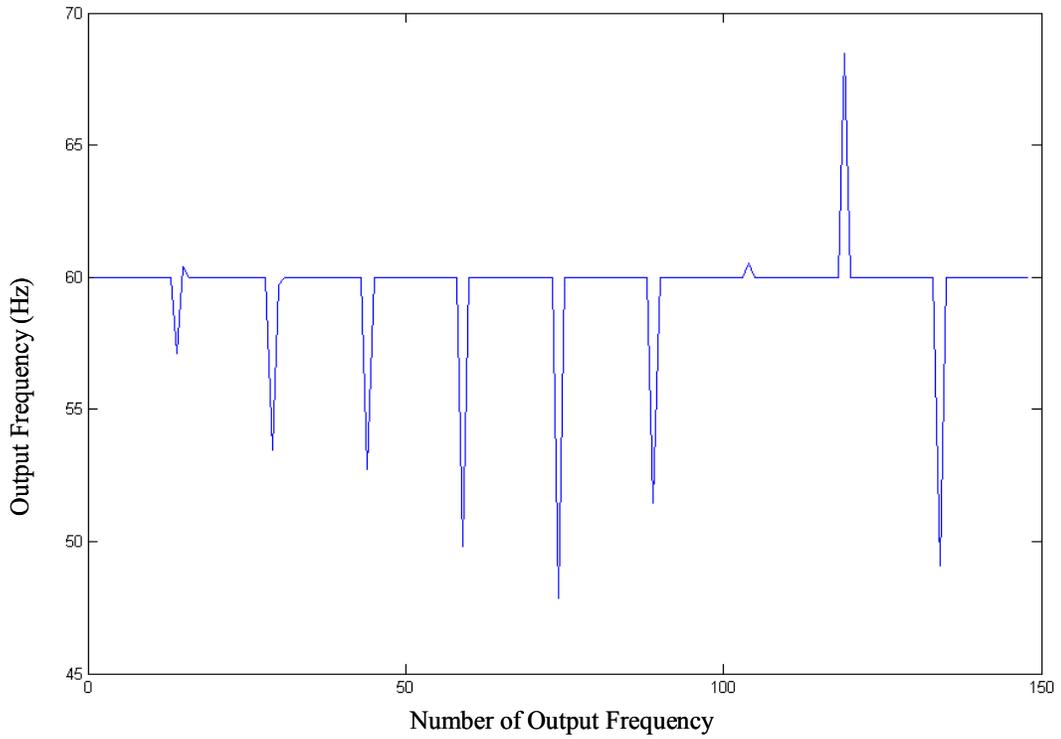


Figure 4-7 output frequency for input with point No.23 missing

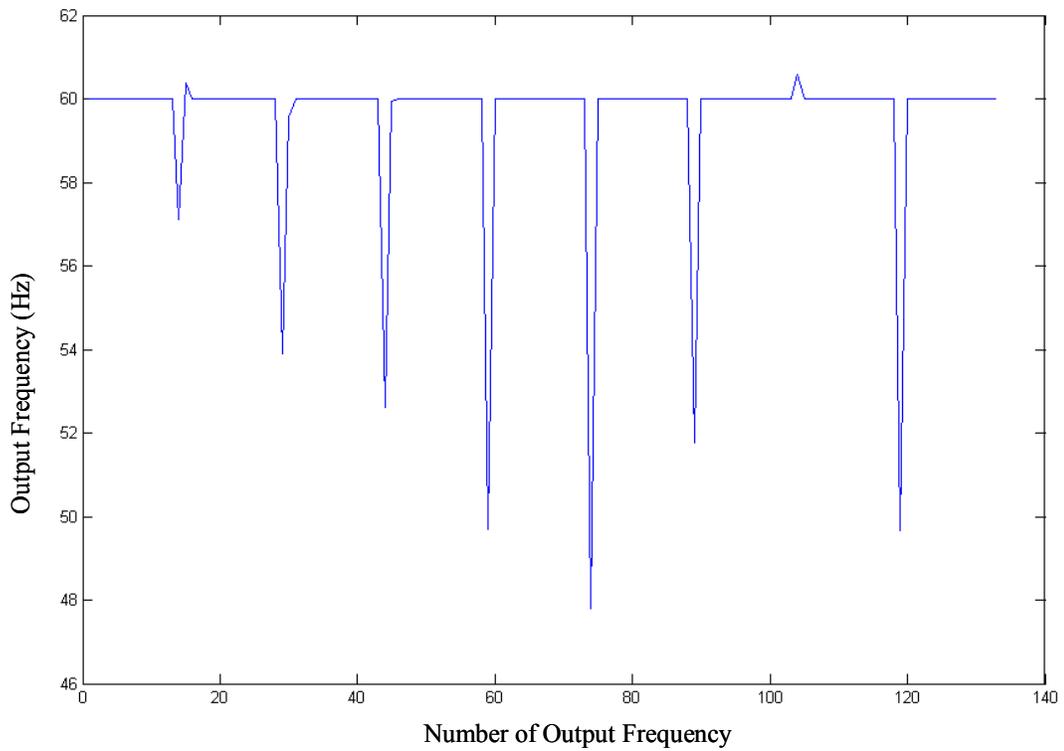


Figure 4-8 output frequency for input with point No.25 missing

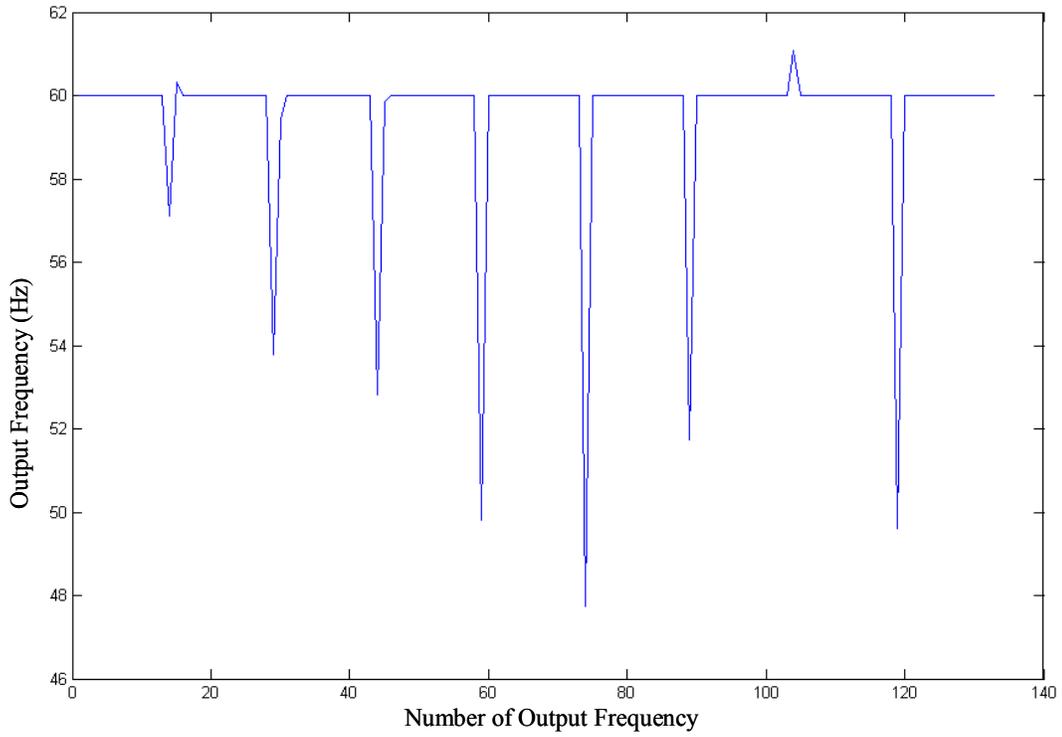


Figure 4-9 output frequency for input with point No.28 missing

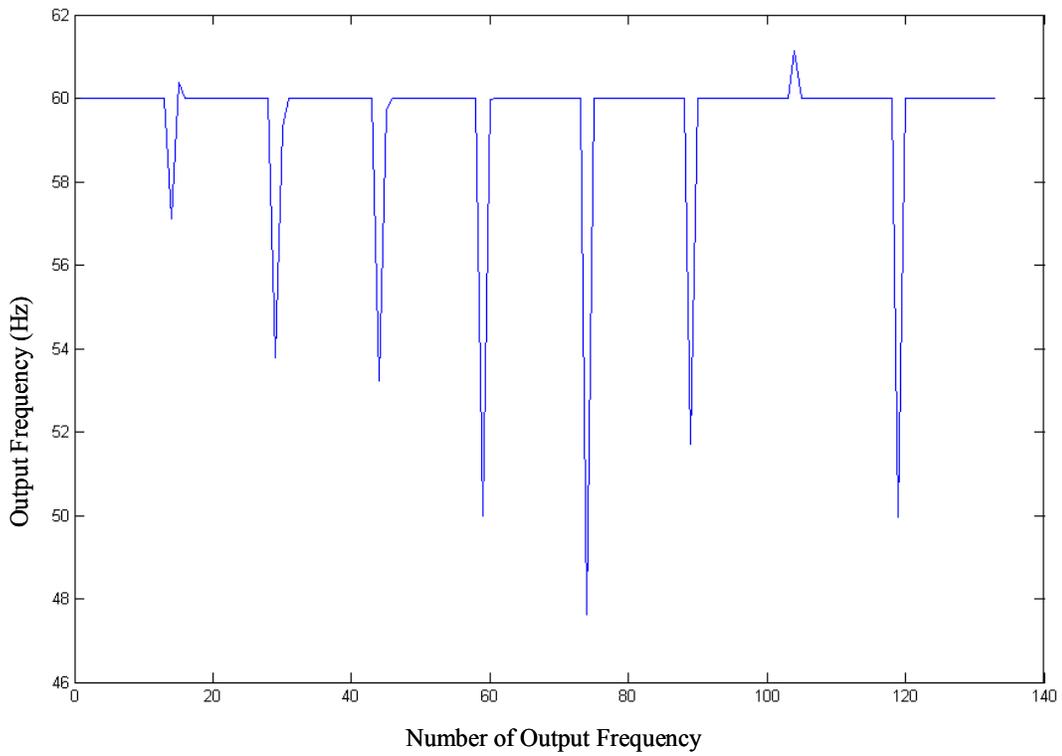


Figure 4-10 output frequency for input with point No.36 missing

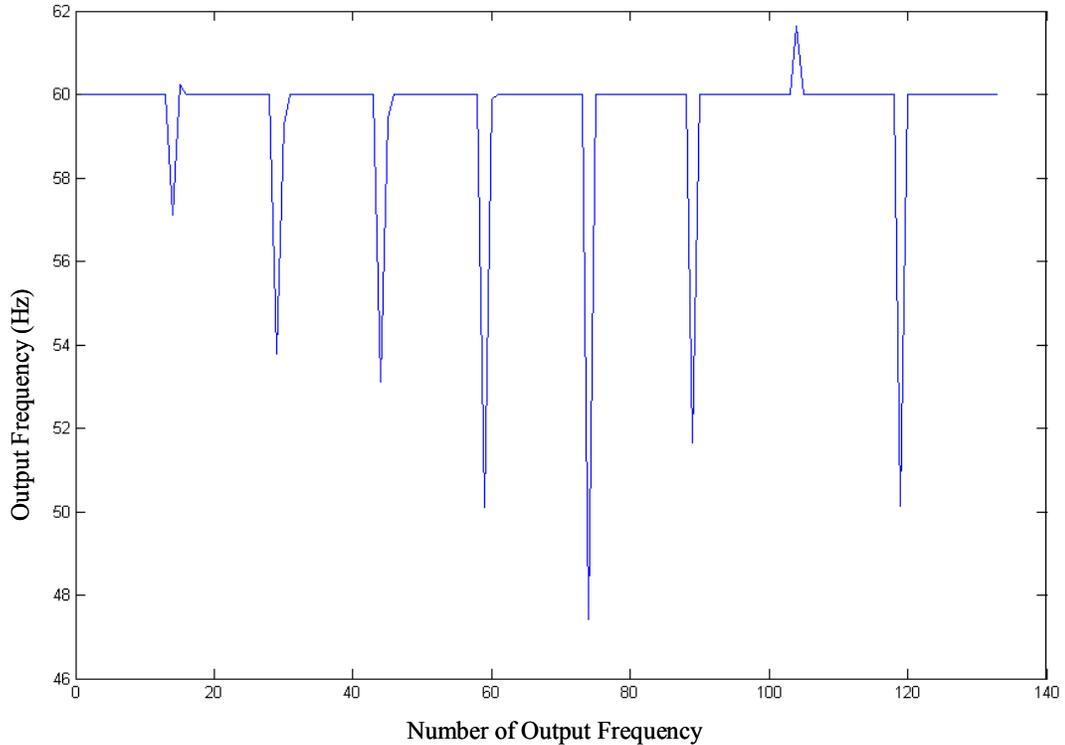


Figure 4-11 output frequency for input with point No.41 missing

From the above figures the following conclusions can be drawn:

- Significant deviation occurs whenever the one point is missing. And the deviations are almost in the same direction, that is, below the nominal frequency.
- It does not matter where the one point missing occurs during one pure sinusoidal cycle. A similar pattern and magnitude of the deviation results for input signals with different locations of the one missing point with the exception of missing point No. 23 (Figure 4-7.)

#### 4.4 Phase & Amplitude Shift

Sometimes the amplitude and phase of the power grid voltage will shift (change) because of the change of load; this will influence the estimation accuracy as discussed next.

##### 4.4.1 Phase Shift

Positive phase shifts of 3, 1, 0.5, 0.1, 0.01 and 0.001 degree occurring around 1/3 of the whole test period were tested for base frequencies of 59Hz, 60Hz and 61Hz. For 59Hz the shift occurs at around 254.75 degree. For 60Hz the shift occurs at around 15 degree; 61Hz at around

135.25 degree. Because the error for the 0.001 degree case is so small, its error figure (Figure 4-12) is displayed instead of the output frequency figure.

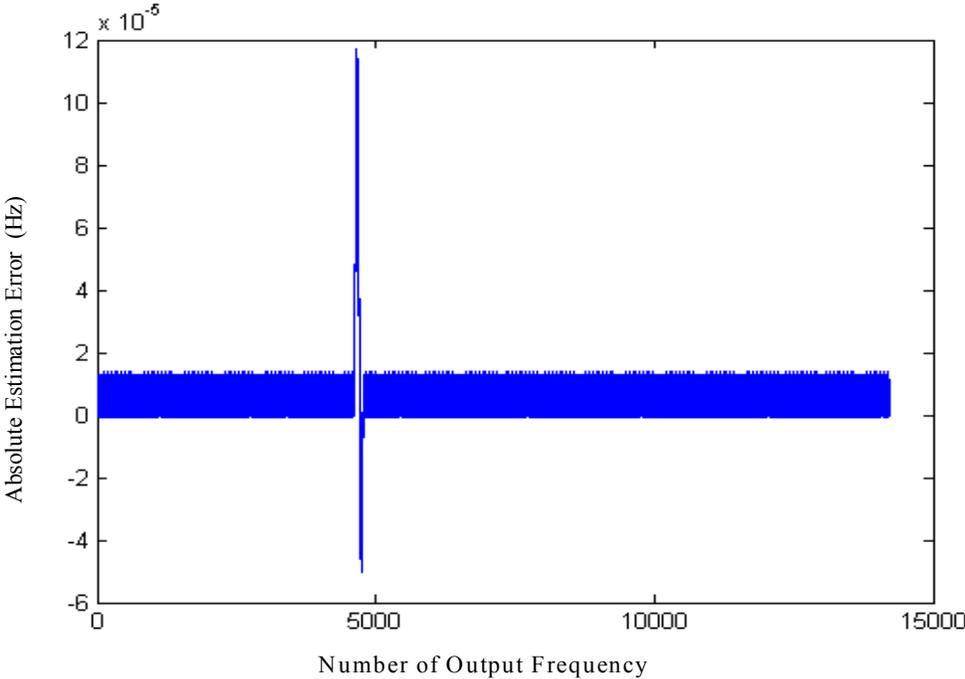


Figure 4-12 the frequency estimation error for input with the frequency of 59Hz and 0.001 degree phase shift that occurs around 1/3 of the whole test period

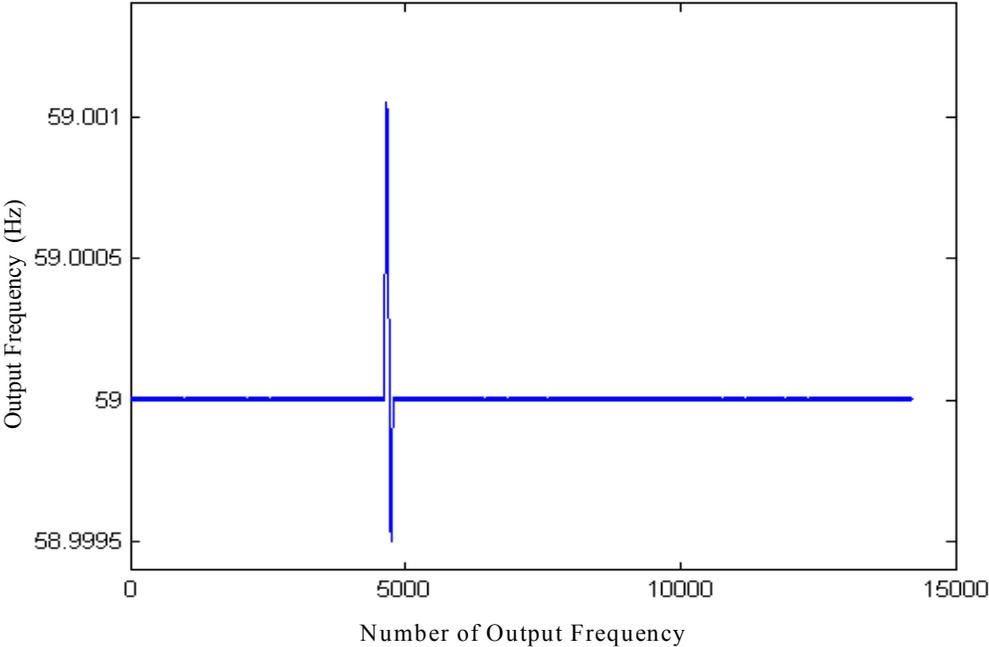


Figure 4-13 the output frequency for input with the frequency of 59Hz and 0.01 degree phase shift that occurs around 1/3 of the whole test period

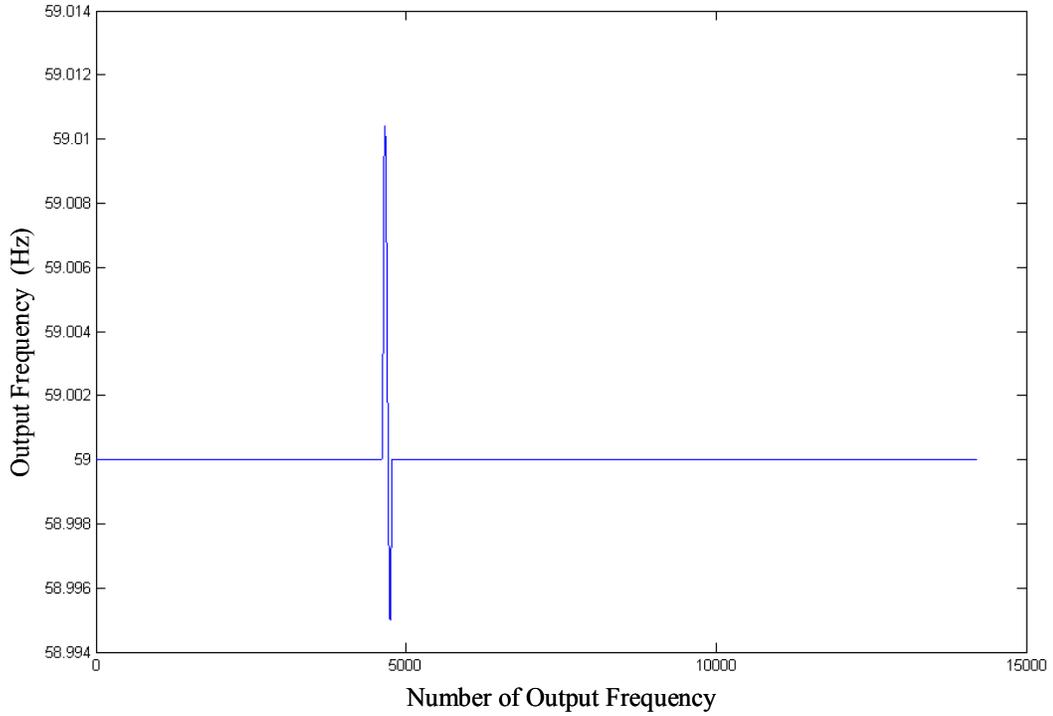


Figure 4-14 the output frequency for input with the frequency of 59Hz and 0.1 degree phase shift that occurs around 1/3 of the whole test period

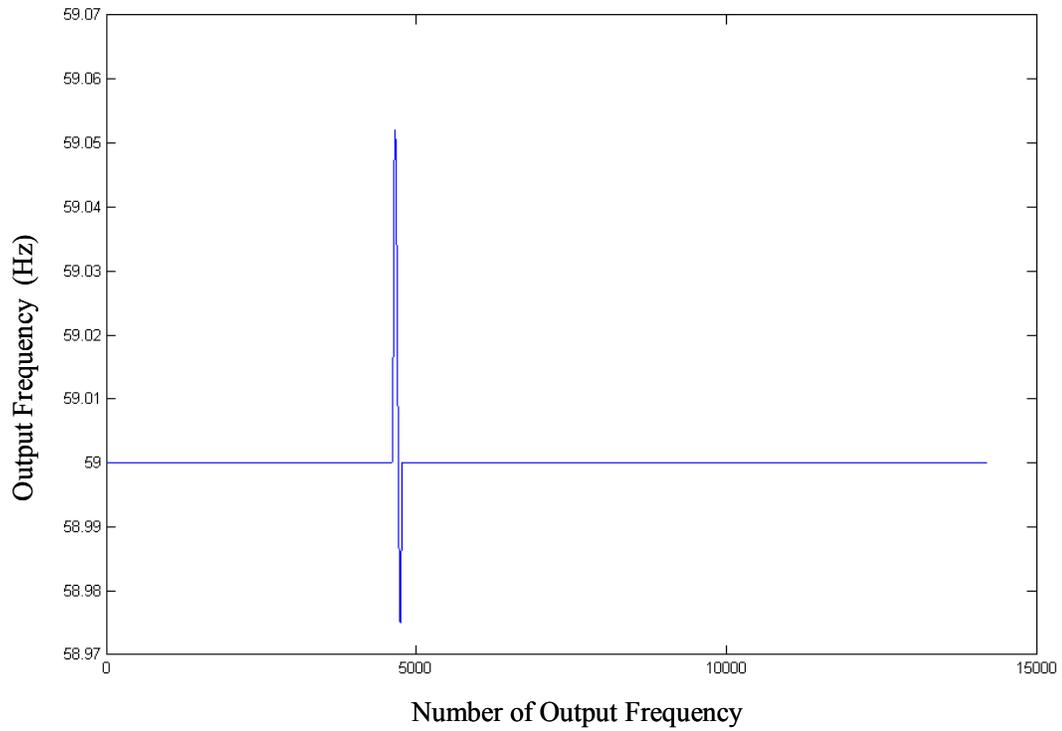


Figure 4-15 the output frequency for input with the frequency of 59Hz and 0.5 degree phase shift that occurs around 1/3 of the whole test period

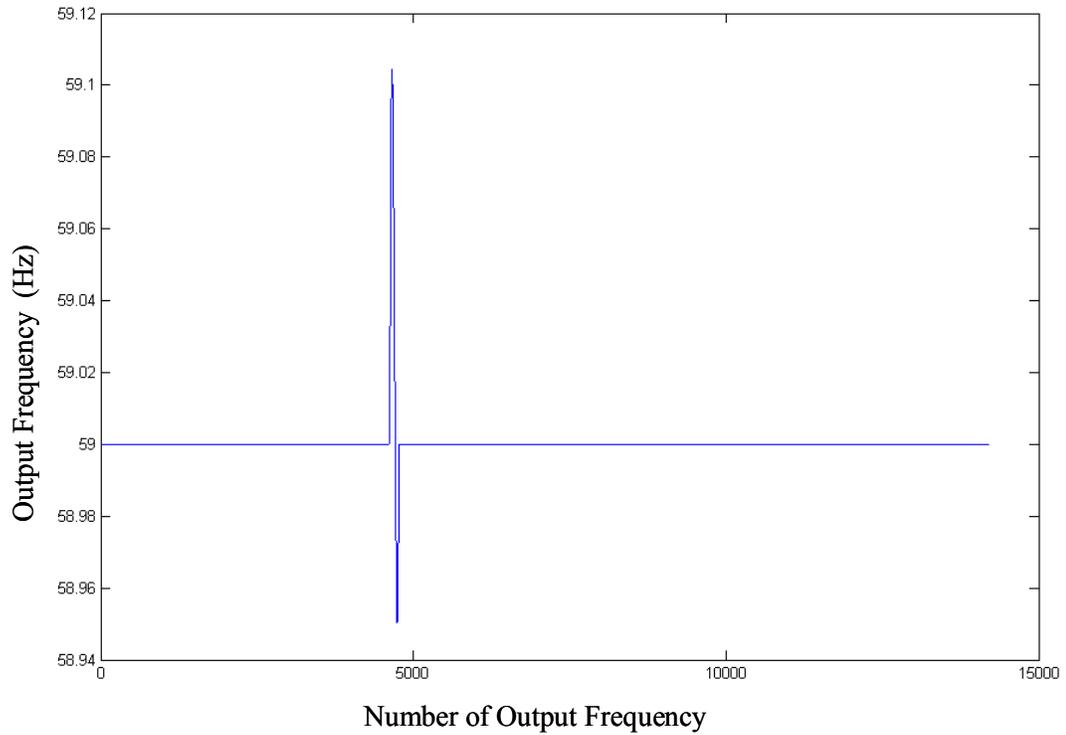


Figure 4-16 the output frequency for input with the frequency of 59Hz and 1 degree phase shift that occurs around 1/3 of the whole test period

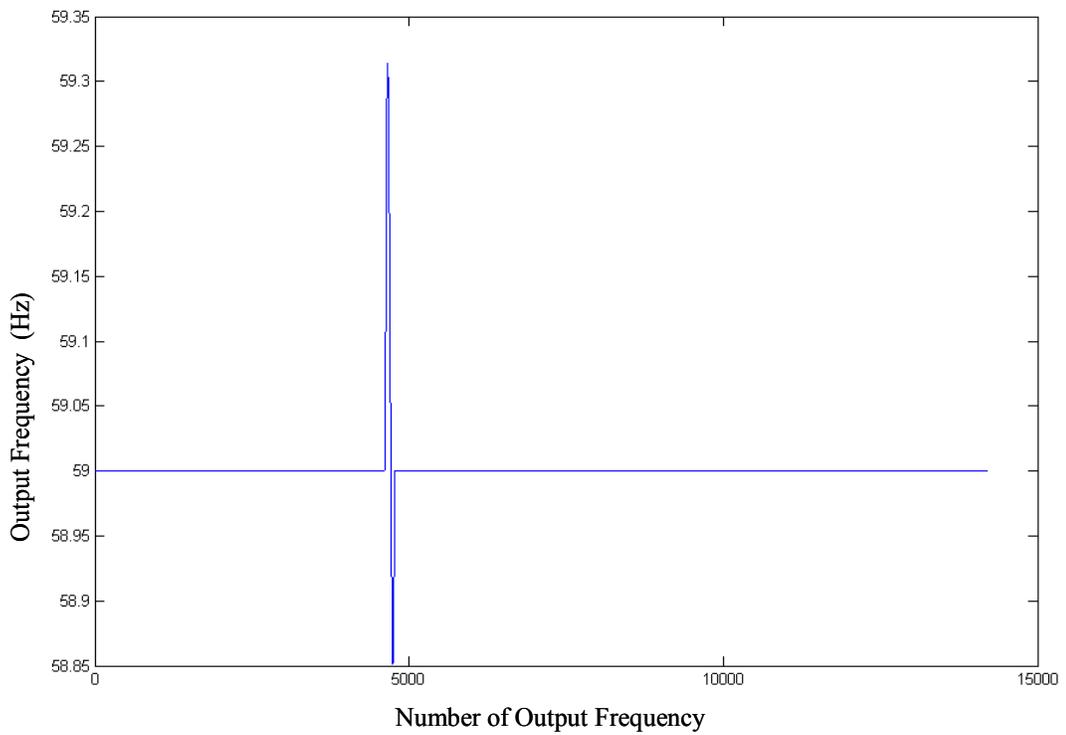


Figure 4-17 the output frequency for input with the frequency of 59Hz and 3 degree phase shift that occurs around 1/3 of the whole test period

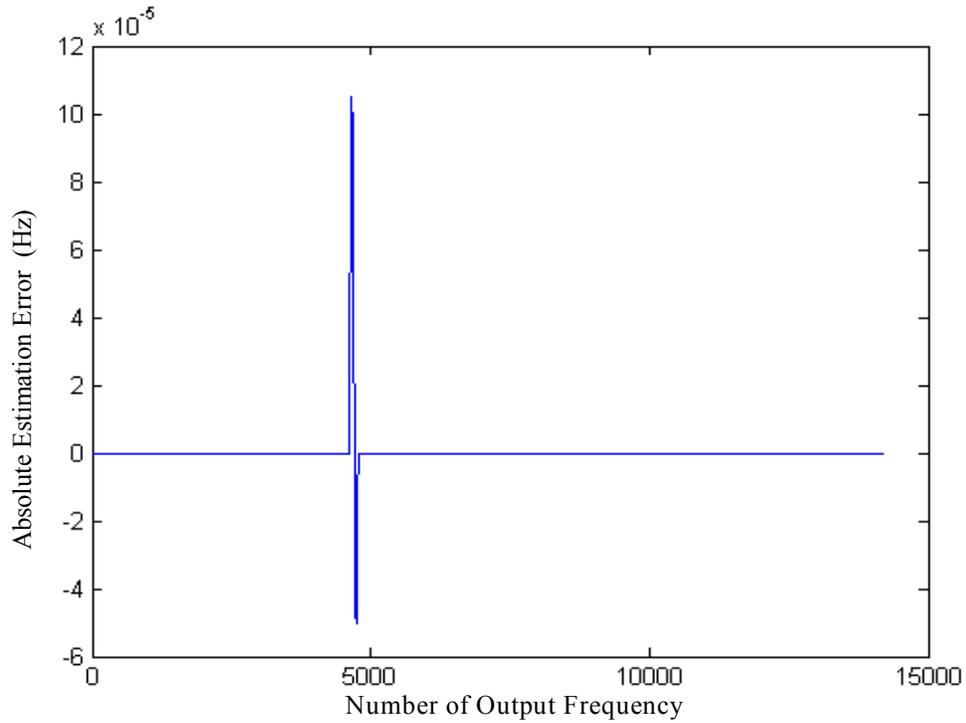


Figure 4-18 the frequency estimation error for input with the frequency of 60Hz and 0.001 degree phase shift that occurs around 1/3 of the whole test period

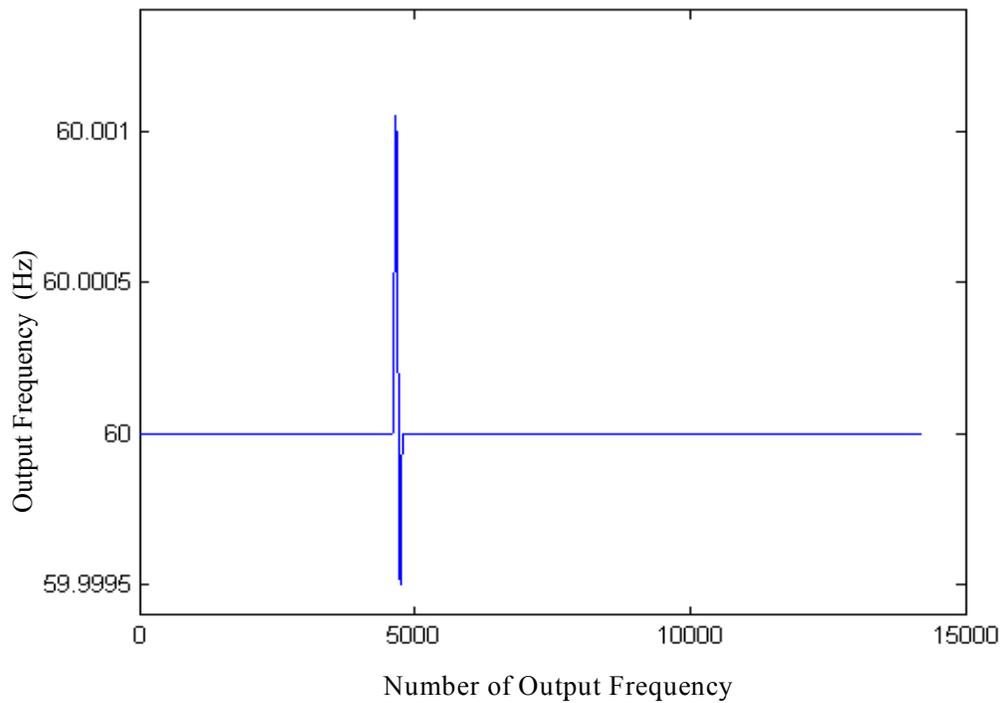


Figure 4-19 the output frequency for input with the frequency of 60Hz and 0.01 degree phase shift that occurs around 1/3 of the whole test period

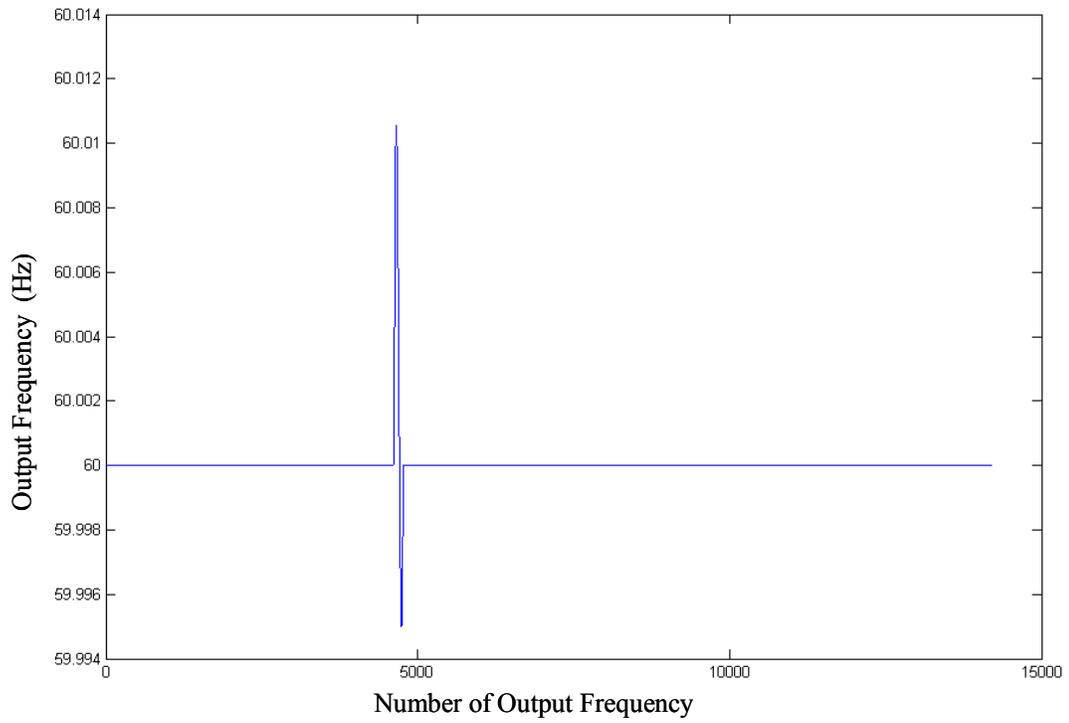


Figure 4-20 the output frequency for input with the frequency of 60Hz and 0.1 degree phase shift that occurs around 1/3 of the whole test period

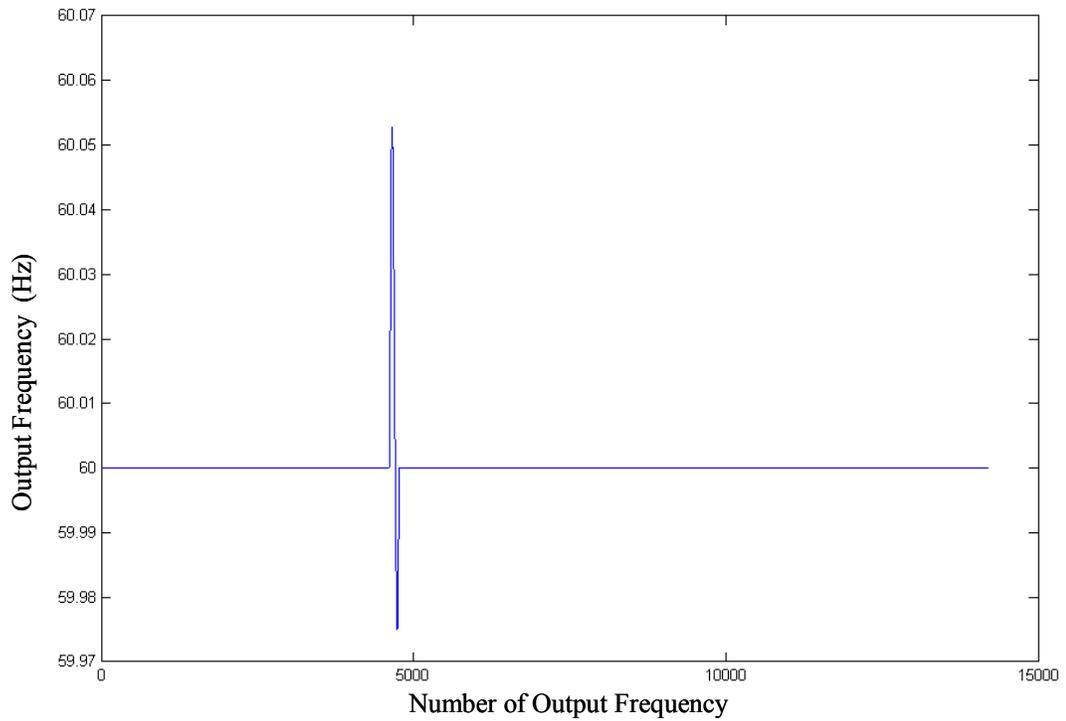


Figure 4-21 the output frequency for input with the frequency of 60Hz and 0.5 degree phase shift that occurs around 1/3 of the whole test period

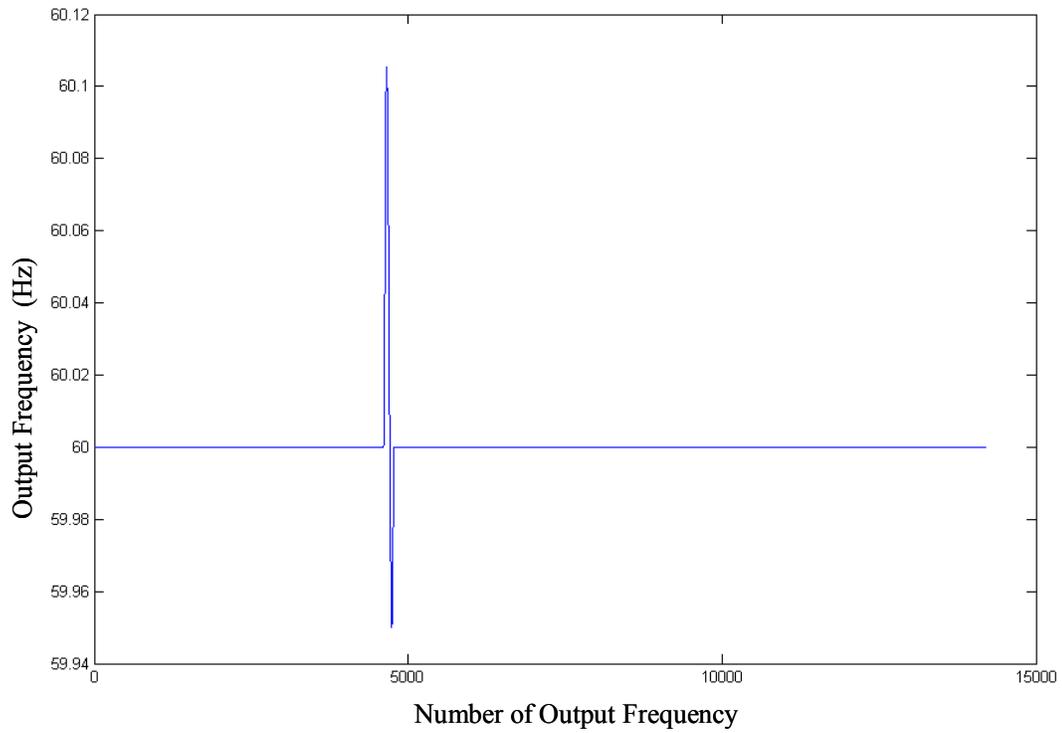


Figure 4-22 the output frequency for input with the frequency of 60Hz and 1 degree phase shift that occurs around 1/3 of the whole test period

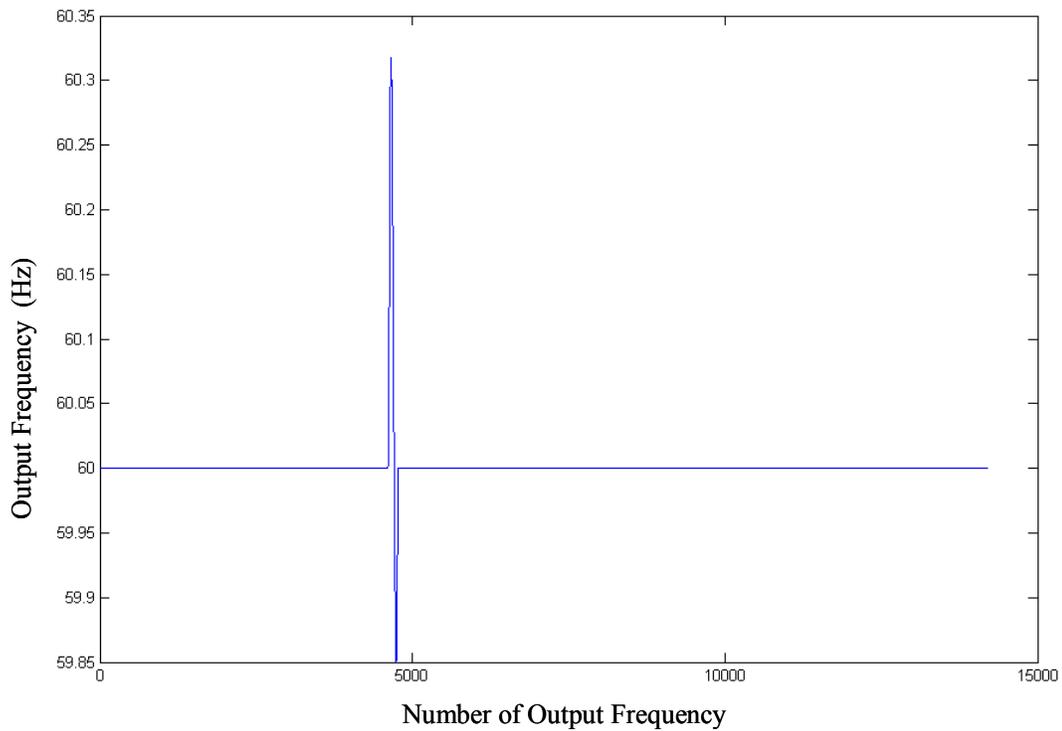


Figure 4-23 the output frequency for input with the frequency of 60Hz and 3 degree phase shift that occurs around 1/3 of the whole test period

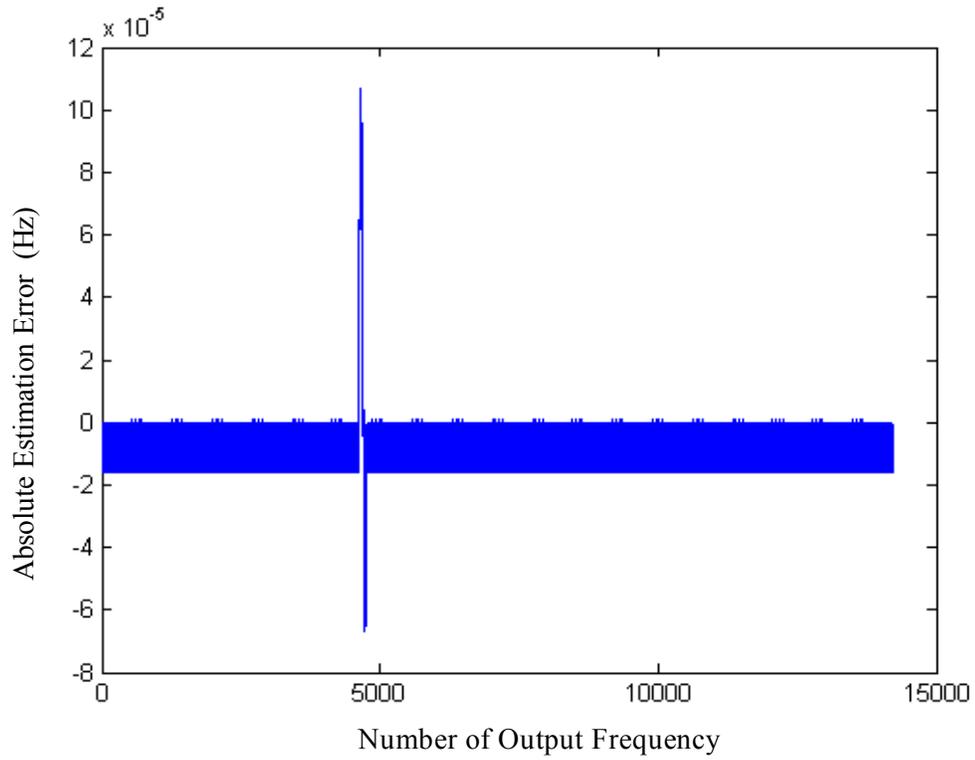


Figure 4-24 the frequency estimation error for input with the frequency of 61Hz and 0.001 degree phase shift that occurs around 1/3 of the whole test period

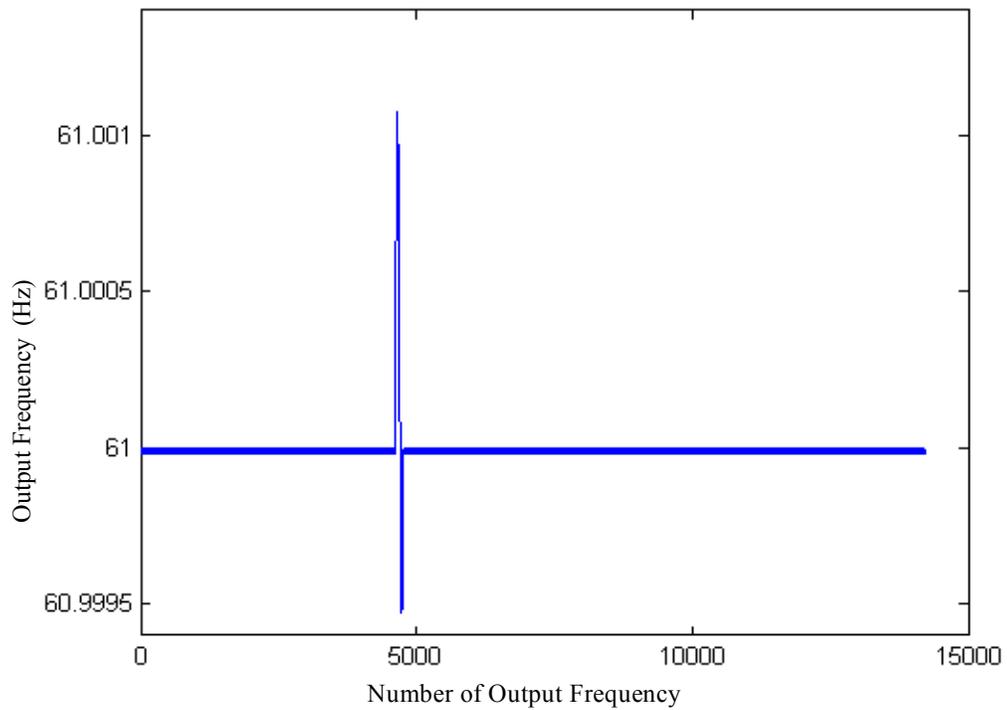


Figure 4-25 the output frequency for input with the frequency of 61Hz and 0.01 degree phase shift that occurs around 1/3 of the whole test period

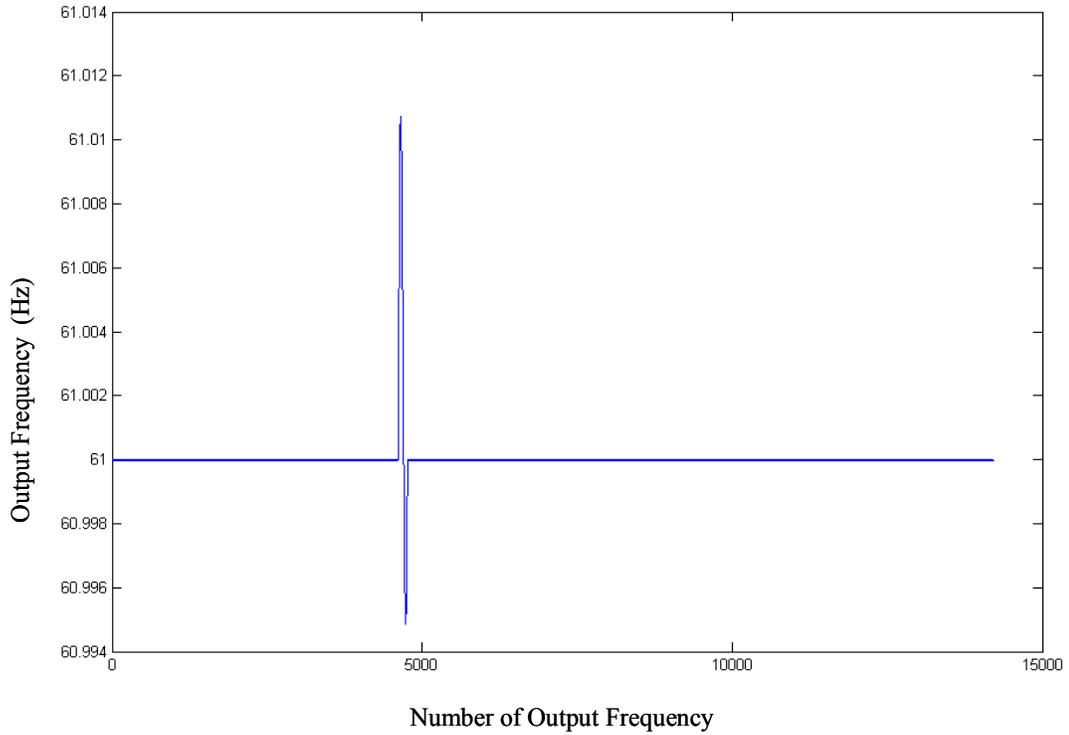


Figure 4-26 the output frequency for input with the frequency of 61Hz and 0.1 degree phase shift that occurs around 1/3 of the whole test period

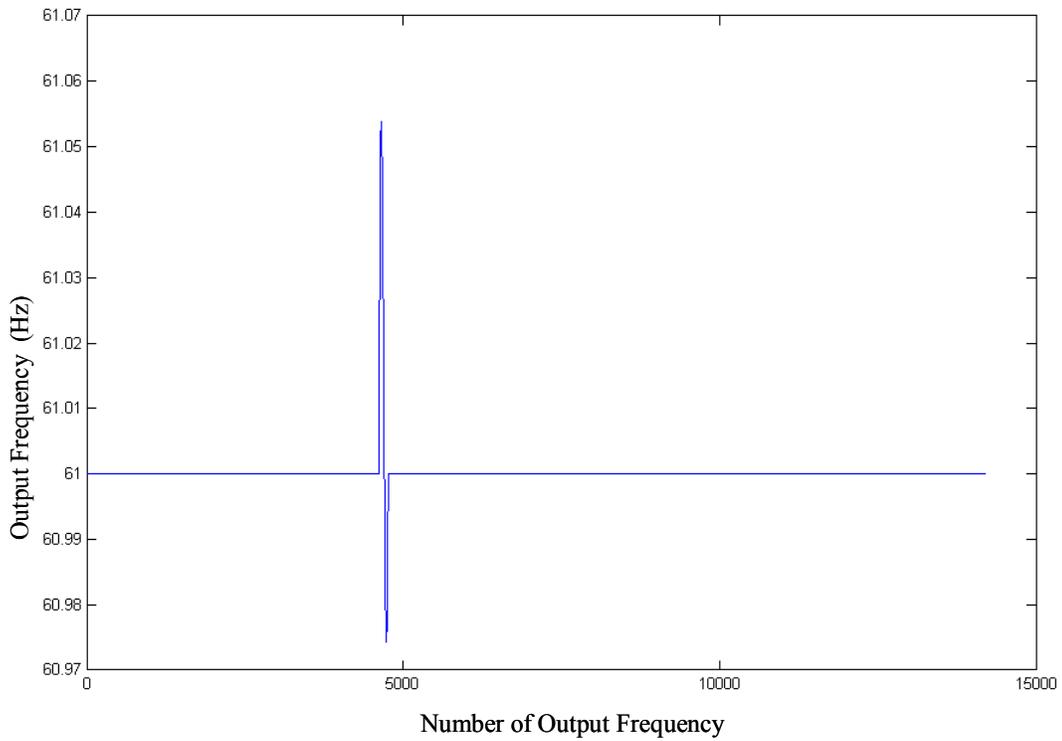


Figure 4-27 the output frequency for input with the frequency of 61Hz and 0.5 degree phase shift that occurs around 1/3 of the whole test period

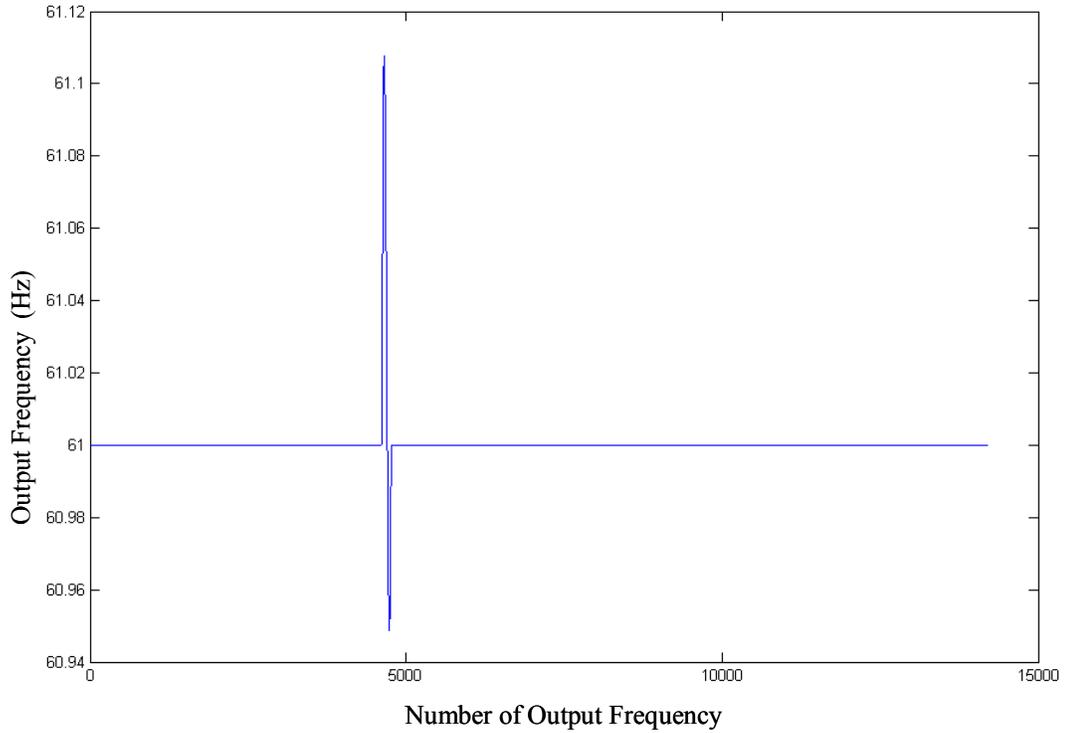


Figure 4-28 the output frequency for input with the frequency of 61Hz and 1 degree phase shift that occurs around 1/3 of the whole test period

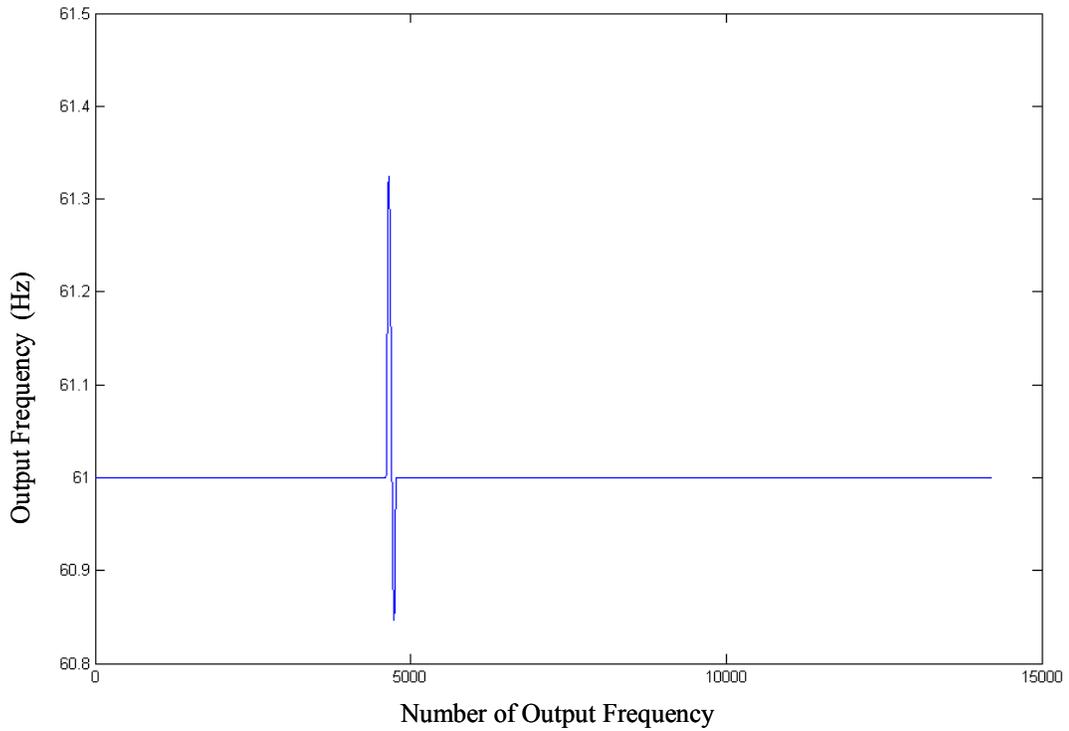


Figure 4-29 the output frequency for input with the frequency of 61Hz and 3 degree phase shift that occurs around 1/3 of the whole test period

Figures 4-12 to 4-29 permit the following conclusions:

- 1) Significant deviation from the base frequency occurs whenever the phase shift occurs, and then is followed by a comparatively smaller (yet still big) deviation in the opposite direction before the estimation error goes back to its original range. And apparently, the bigger the shifted phase, the larger the deviation.
- 2) The accuracy during the rest of the whole test period is the same as that obtained from input without a phase shift.
- 3) The magnitude of the deviation keeps almost constant with the same shifted phase as the base frequency changes.

Table 4-1 shows the range of output points during which the deviation occurs for different combinations of base frequencies and shifted phase.

Shifted Phase (degree)	Base Frequency =59Hz			Base Frequency =60Hz			Base Frequency =61Hz		
	Start No.	End No.	Total number	Start No.	End No.	Total number	Start No.	End No.	Total number
0.001	4619	4775	156	4609	4776	167	4614	4768	154
0.01	4613	4775	162	4609	4776	167	4610	4768	158
0.1	4613	4781	168	4609	4776	167	4609	4774	165
0.5	4612	4780	168	4609	4774	165	4609	4774	165
1	4612	4780	168	4609	4776	167	4609	4774	165
3	4610	4780	170	4609	4776	167	4609	4774	165

Table 4-1 the range of output points during which the deviation occurs for different combinations of base frequencies and shifted phase

#### 4.4.2 Amplitude Shift

Consider next how the change of the amplitude will affect the estimation accuracy. The input signal used experiences a negative amplitude change that occurs around 1/3 of the whole test period. The change is 10%, 5%, 2%, 1%, 0.1% and 0.01% of the original amplitude and the base frequencies are 59Hz, 60Hz and 61Hz. For 59Hz, the shift occurs at around 254.75 degrees. For 60Hz, the shift occurs at around 15 degree and for 61Hz at around 135.25 degree. Again, since the error for the 0.01% case is so small, its error figure is displayed instead of the output frequency figure (This was also done for the 0.1% and 61Hz case.)

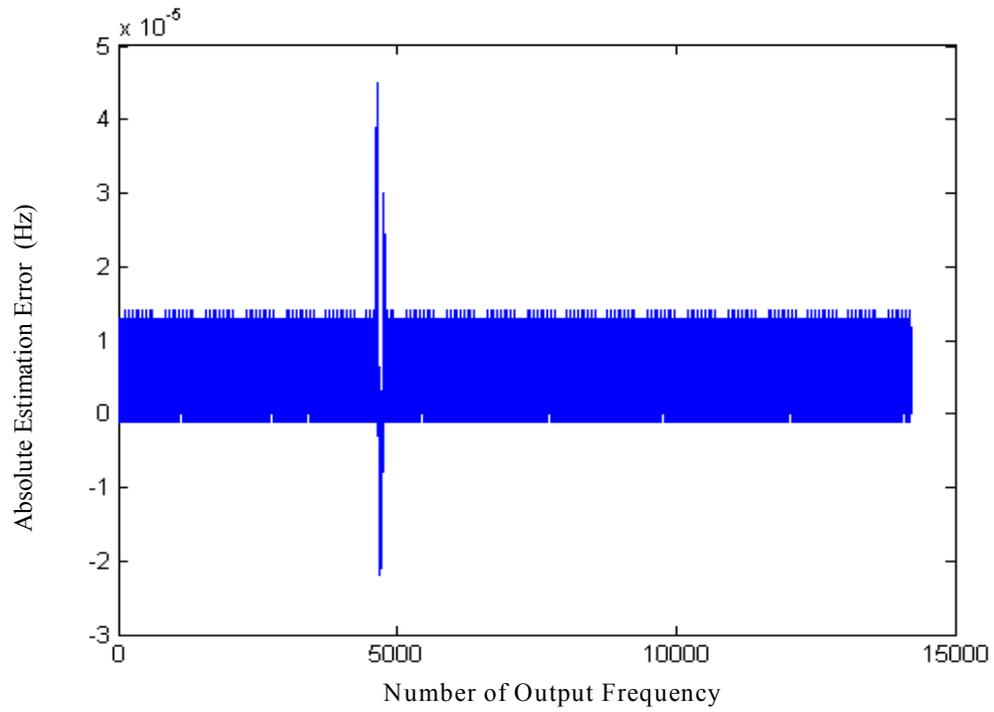


Figure 4-30 the frequency estimation error for input with the frequency of 59Hz and 0.01% amplitude change that occurs around 1/3 of the whole test period

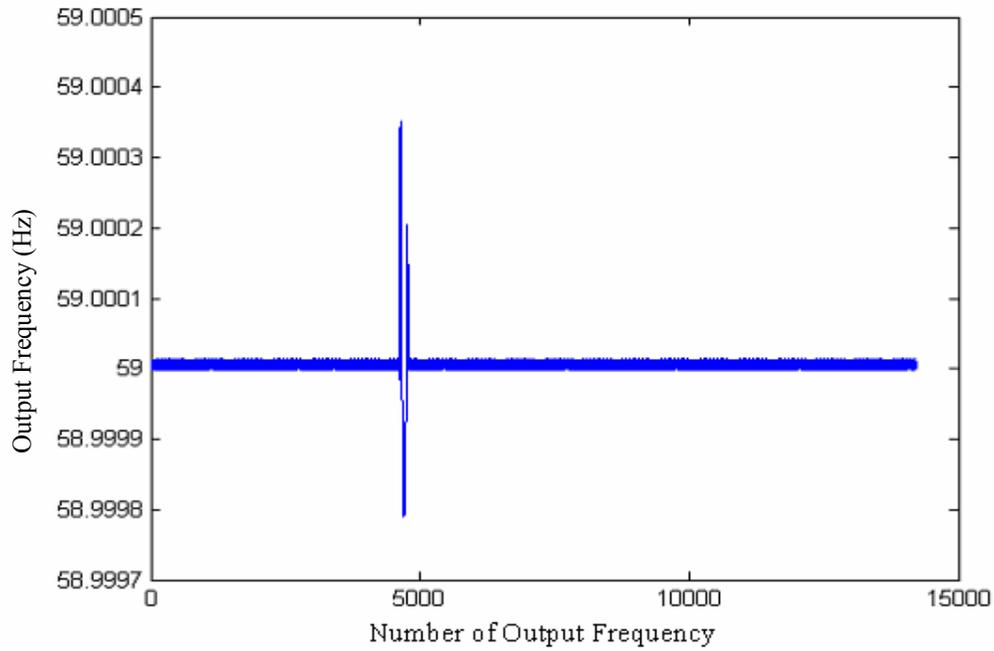


Figure 4-31 the output frequency for input with the frequency of 59Hz and 0.1% amplitude change that occurs around 1/3 of the whole test period

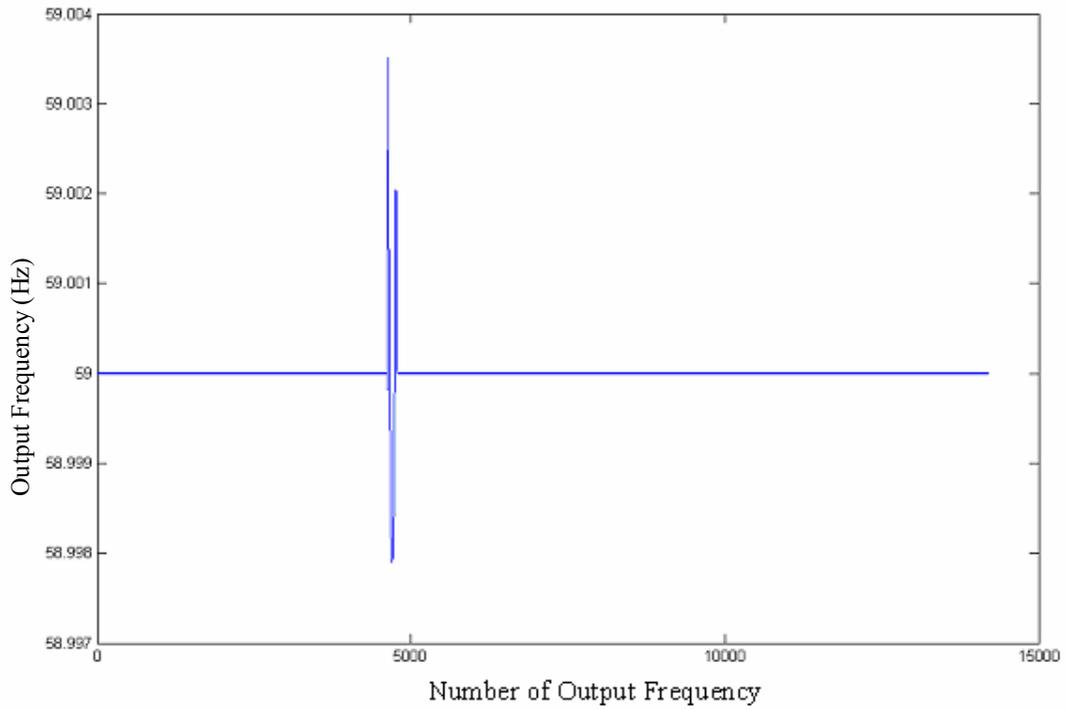


Figure 4-32 the output frequency for input with the frequency of 59Hz and 1% amplitude change that occurs around 1/3 of the whole test period

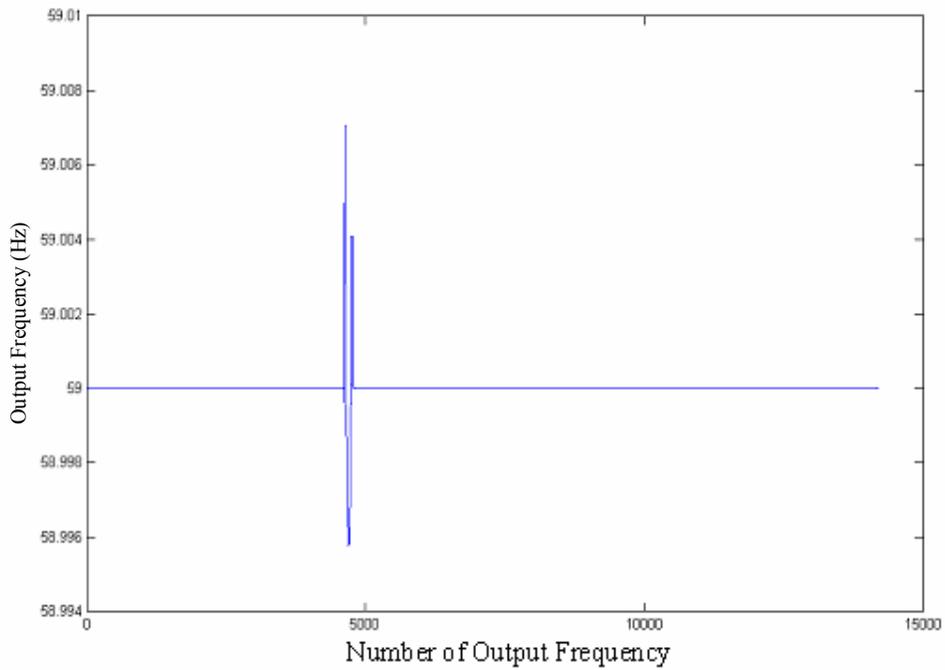


Figure 4-33 the output frequency for input with the frequency of 59Hz and 2% amplitude change that occurs around 1/3 of the whole test period

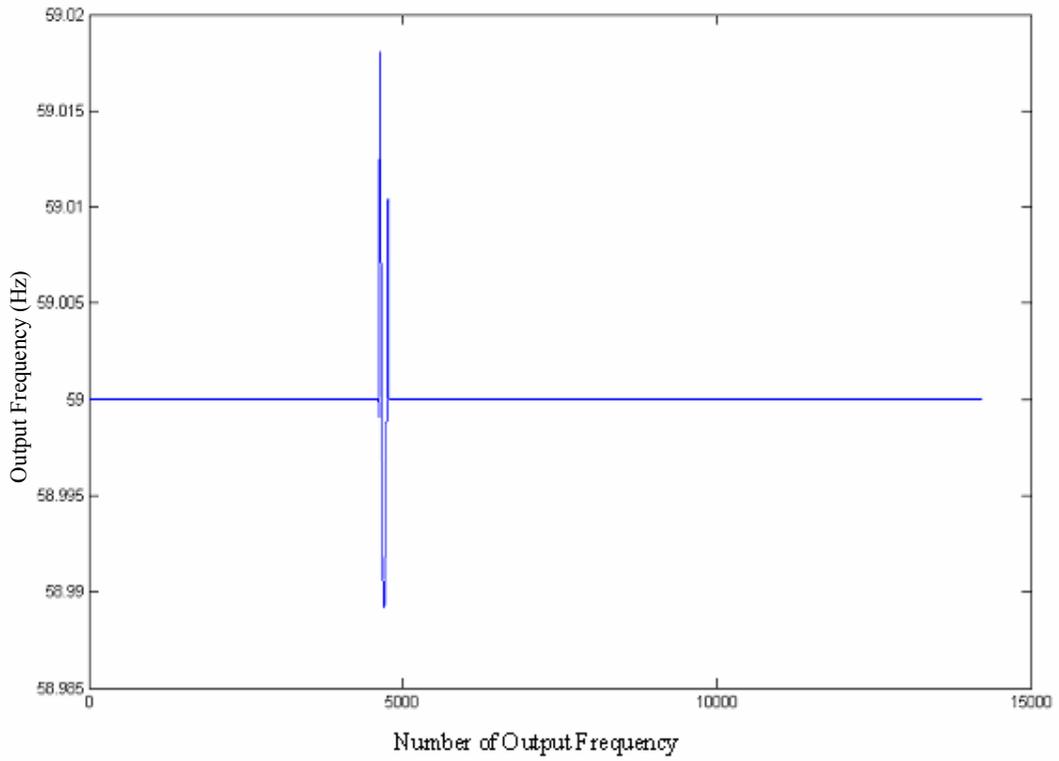


Figure 4-34 the output frequency for input with the frequency of 59Hz and 5% amplitude change that occurs around 1/3 of the whole test period

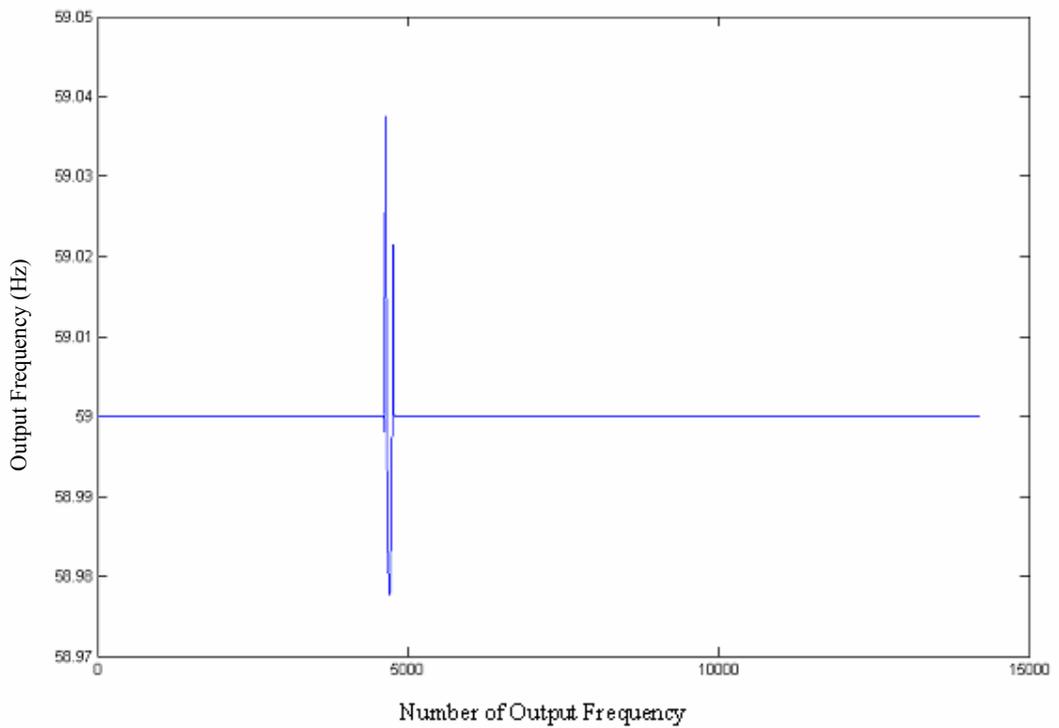


Figure 4-35 the output frequency for input with the frequency of 59Hz and 10% amplitude change that occurs around 1/3 of the whole test period

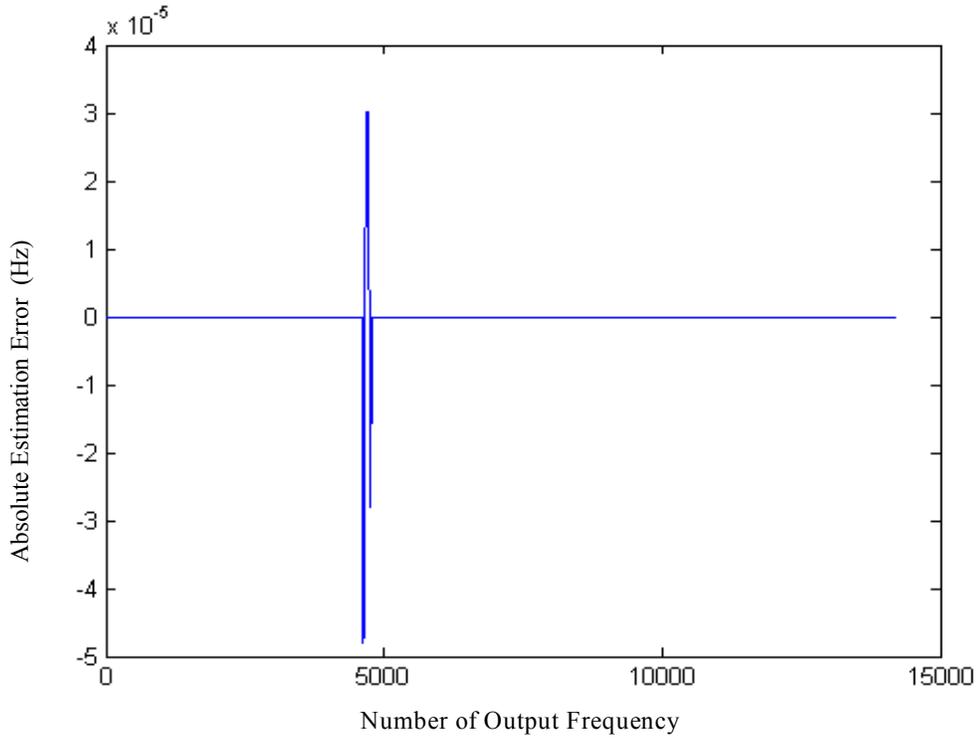


Figure 4-36 the frequency estimation error for input with the frequency of 60Hz and 0.01% amplitude change that occurs around 1/3 of the whole test period

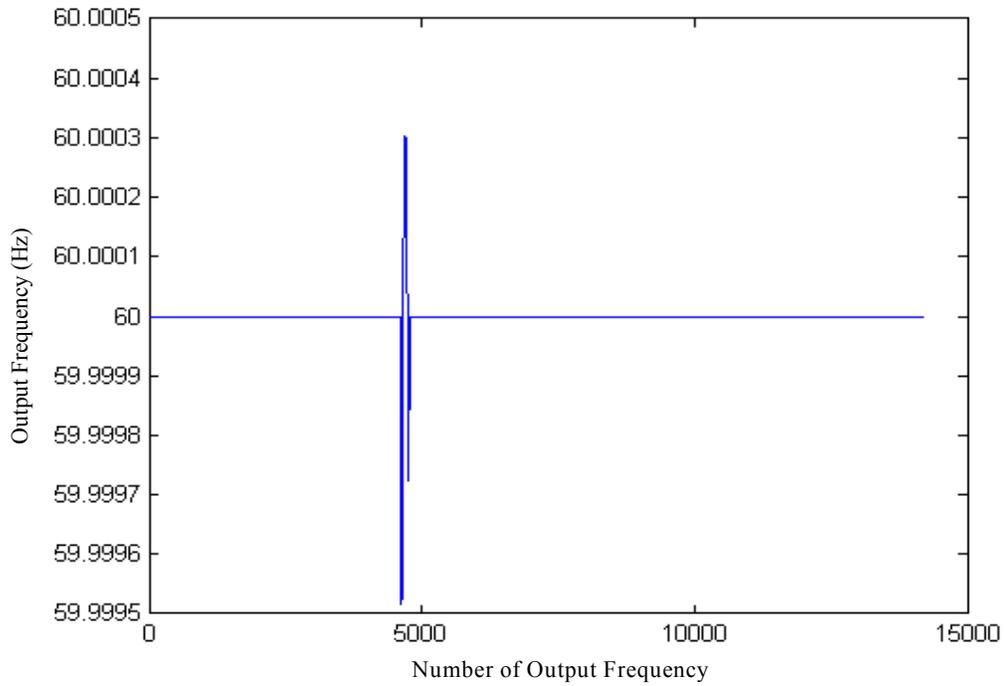


Figure 4-37 the output frequency for input with the frequency of 60Hz and 0.1% amplitude change that occurs around 1/3 of the whole test period

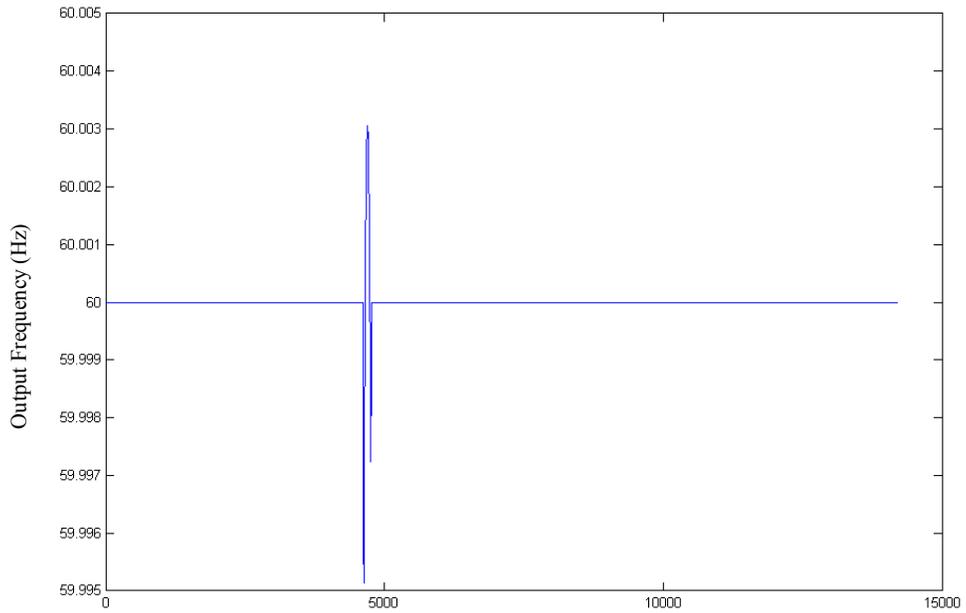


Figure 4-38 the output frequency for input with the frequency of 60Hz and 1% amplitude change that occurs around 1/3 of the whole test period

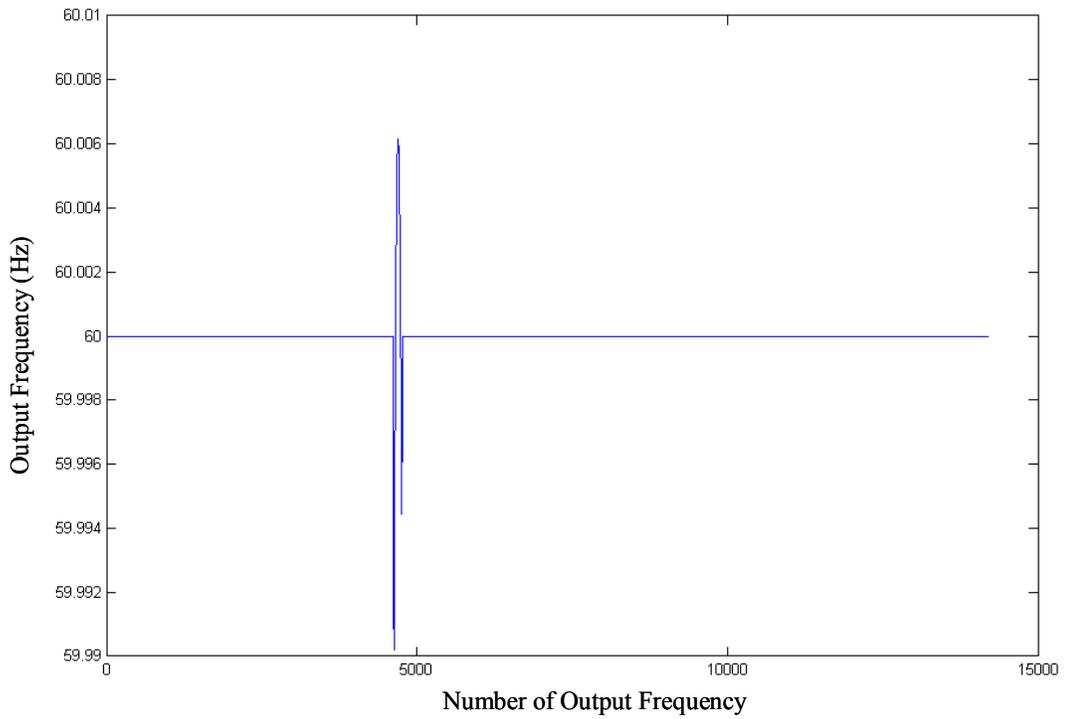


Figure 4-39 the output frequency for input with the frequency of 60Hz and 2% amplitude change that occurs around 1/3 of the whole test period

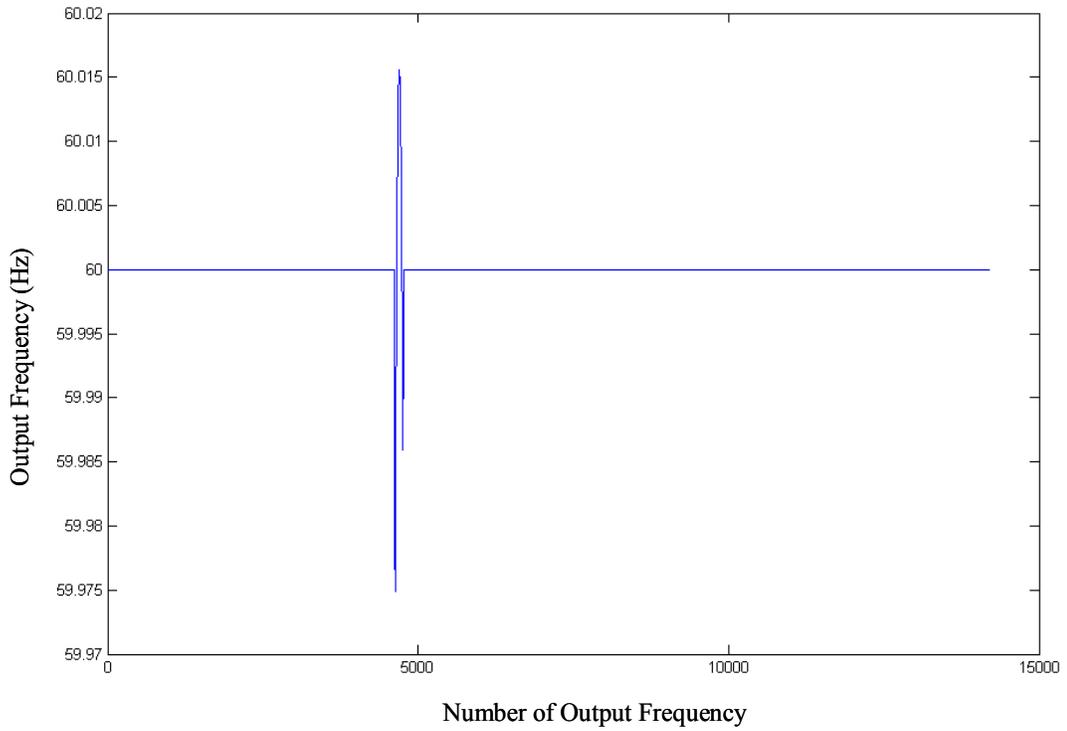


Figure 4-40 the output frequency for input with the frequency of 60Hz and 5% amplitude change that occurs around 1/3 of the whole test period

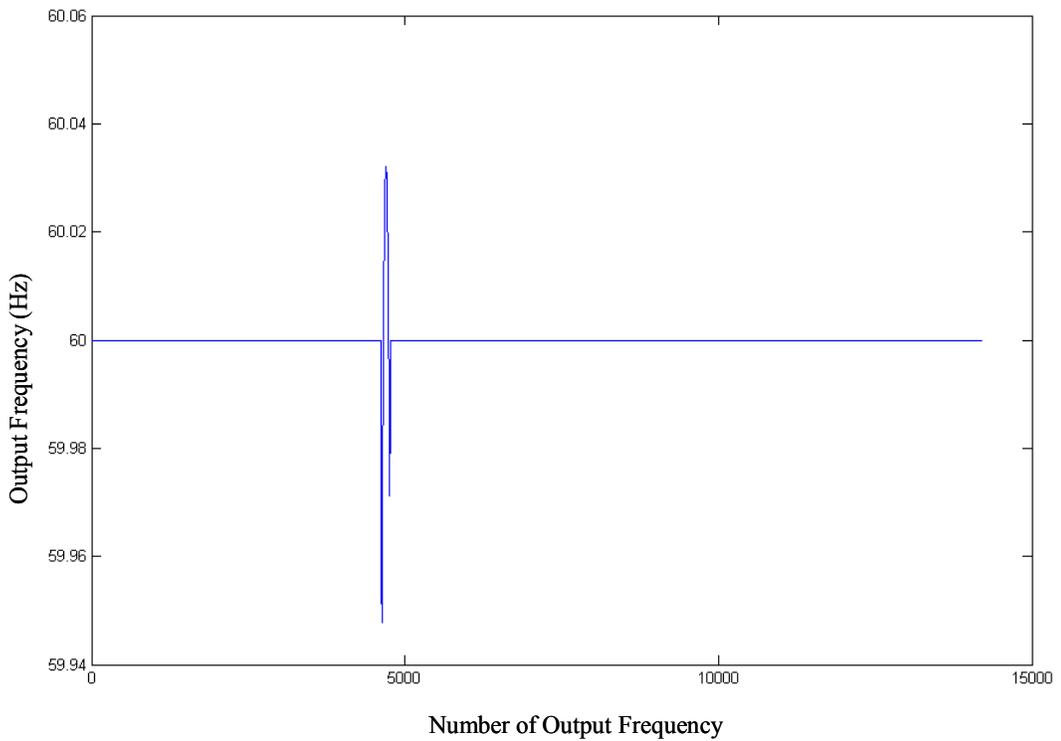


Figure 4-41 the output frequency for input with the frequency of 60Hz and 10% amplitude change that occurs around 1/3 of the whole test period

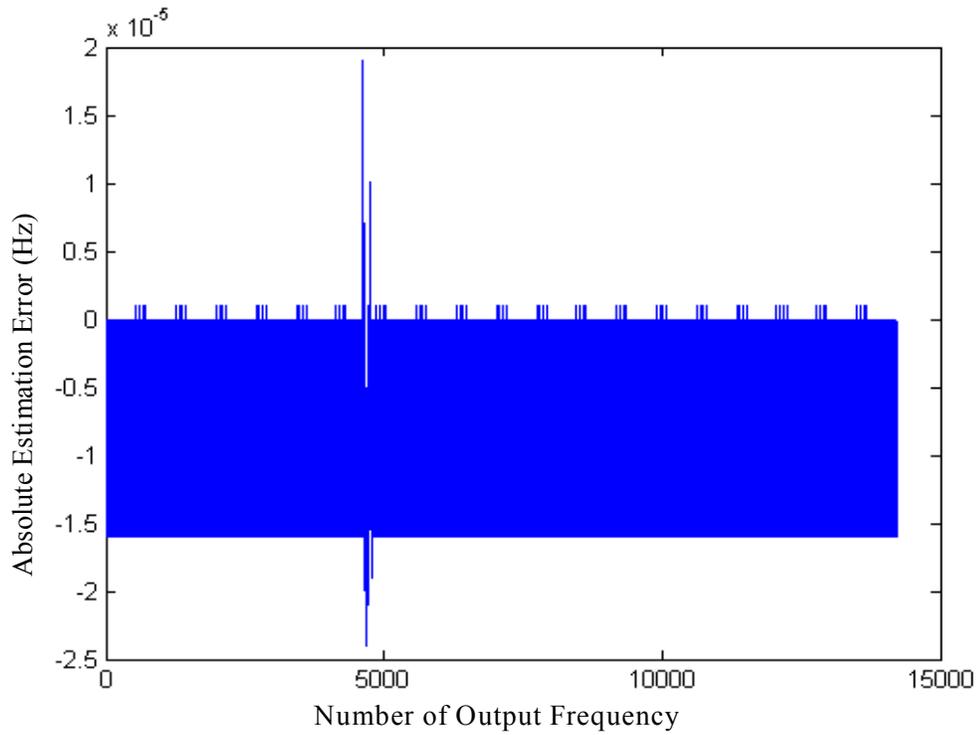


Figure 4-42 the frequency estimation error for input with the frequency of 61Hz and 0.01% amplitude change that occurs around 1/3 of the whole test period

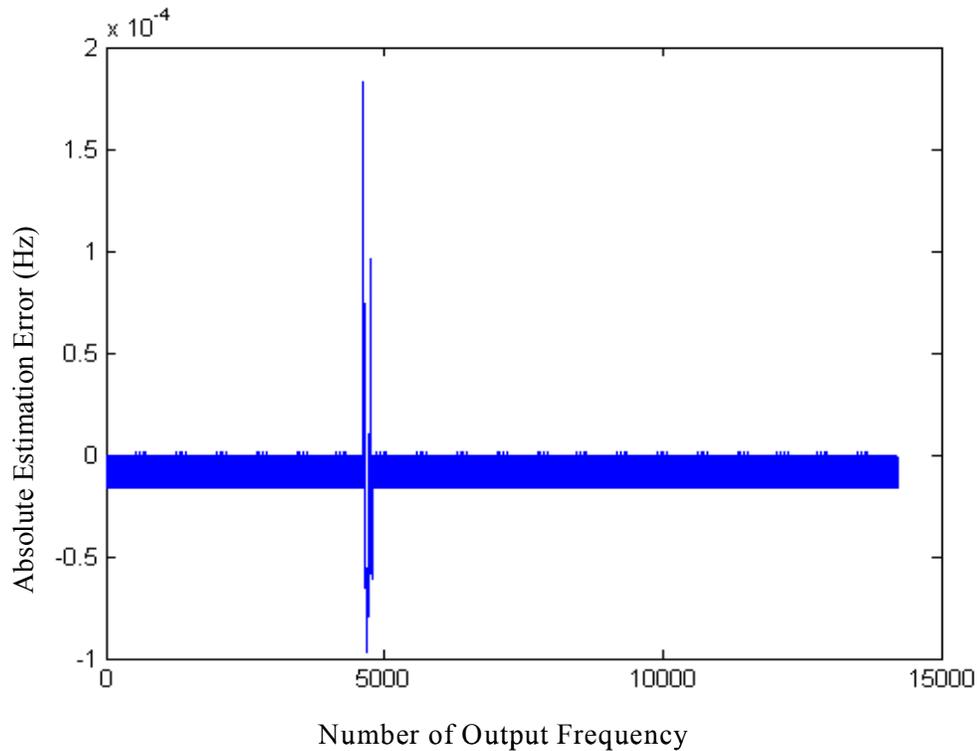


Figure 4-43 the frequency estimation error for input with the frequency of 61Hz and 0.1% amplitude change that occurs around 1/3 of the whole test period

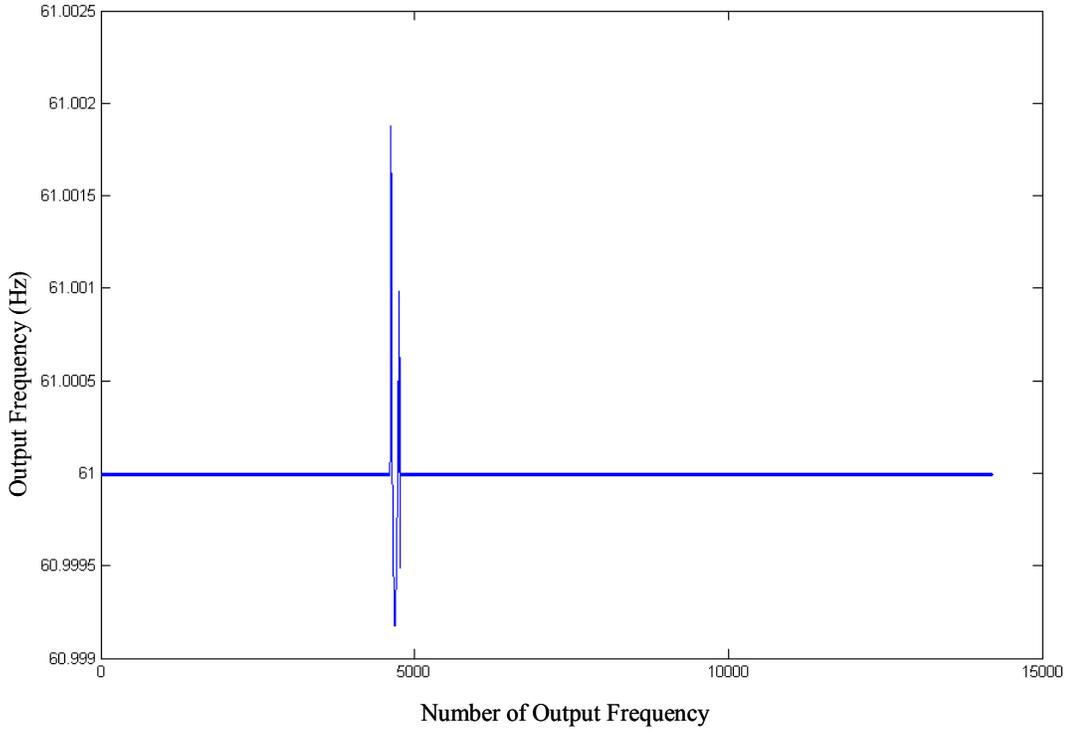


Figure 4-44 the output frequency for input with the frequency of 61Hz and 1% amplitude change that occurs around 1/3 of the whole test period

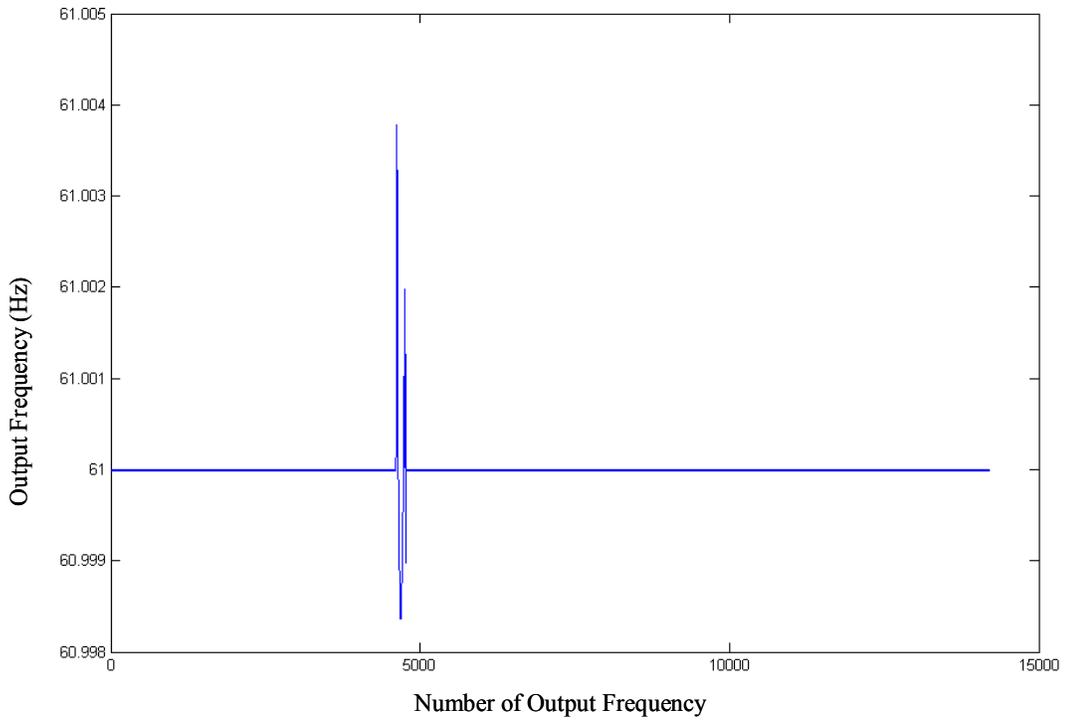


Figure 4-45 the output frequency for input with the frequency of 61Hz and 2% amplitude change that occurs around 1/3 of the whole test period

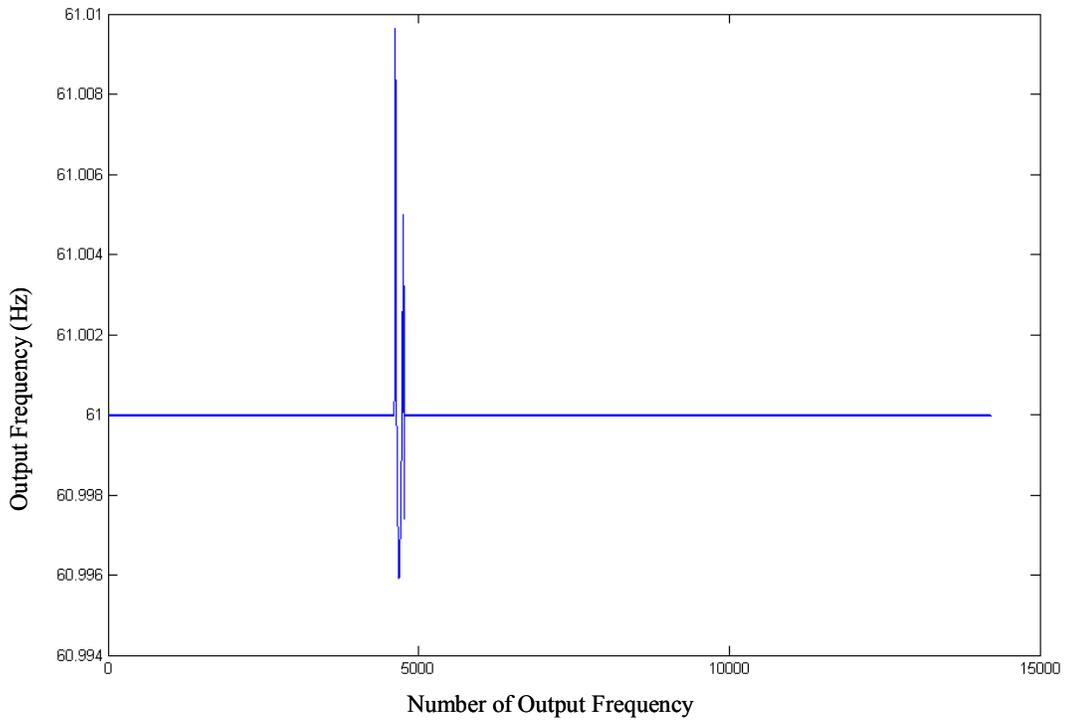


Figure 4-46 the output frequency for input with the frequency of 61Hz and 5% amplitude change that occurs around 1/3 of the whole test period

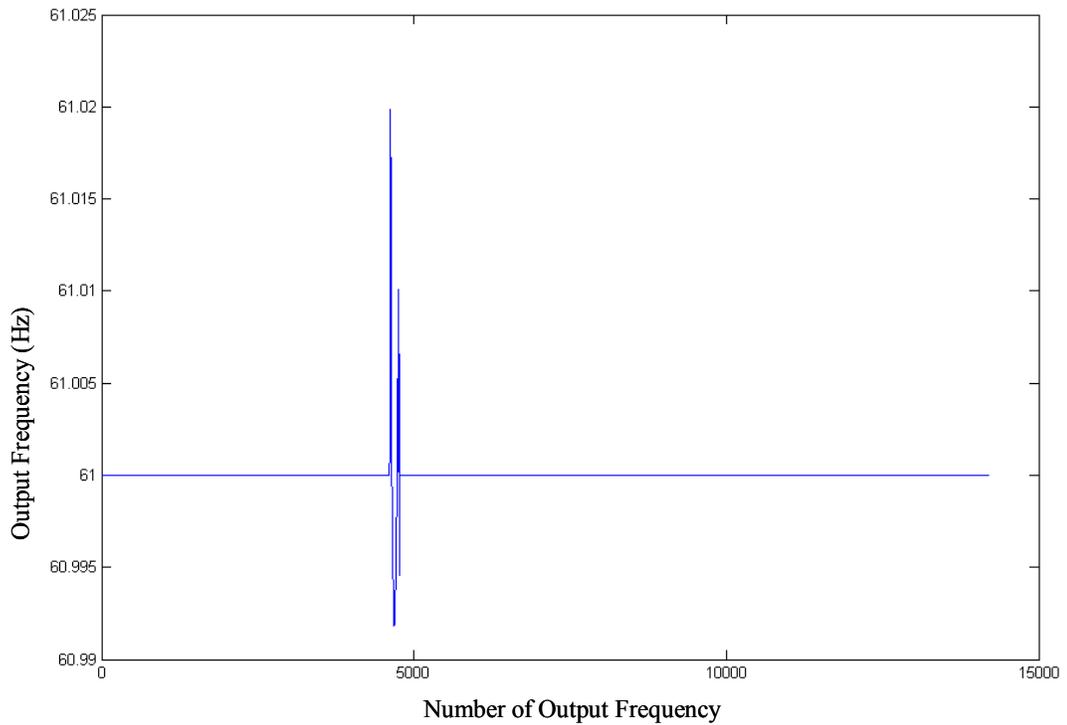


Figure 4-47 the output frequency for input with the frequency of 61Hz and 10% amplitude change that occurs around 1/3 of the whole test period

Figures 4-30 to 4-47 allow the following conclusions to be drawn:

- 1) Large deviations occur when the amplitude changes but the trend differs for different base frequencies. Specifically, at 60Hz (Figure 4-36 to Figure 4-41), the deviation first goes below 60Hz, then jumps above 60Hz but drops below again before the error returns within its original normal range---a down, up, down trend. By contrast, at 59Hz (Figure 4-30 to Figure 4-45) and 61Hz (Figure 4-42 to Figure 4-47) the trend is totally opposite, namely, up,down and up.
- 2) The bigger the amplitude change, the larger the deviation will be.
- 3) The accuracy during the rest of the whole test period is the same as the one obtained from input that does not experience amplitude change.

Table 4-2 shows the range of output points during which the deviation occurs for different combinations of base frequencies and shifted amplitude percentages.

Shifted Amp. Per.(%)	Base Frequency =59Hz			Base Frequency =60Hz			Base Frequency =61Hz		
	Start No.	End No.	Total number	Start No.	End No.	Total number	Start No.	End No.	Total number
0.01	4613	4780	167	4610	4776	166	4609	4774	165
0.1	4610	4780	170	4610	4776	166	4609	4774	165
1	4609	4780	171	4610	4776	166	4609	4774	165
2	4609	4780	171	4610	4776	166	4609	4774	165
5	4609	4780	171	4609	4776	167	4609	4774	165
10	4609	4780	171	4610	4776	166	4609	4774	165

Table 4-2 the range of output points during which the deviation occurs for different combinations of base frequencies and shifted amplitude percentages

## **Chapter Five**

# **Approaches to Improve the Frequency Estimation Accuracy of Our Algorithm**

### **5.1 Overview**

In this chapter, three approaches to improve the frequency estimation accuracy of our algorithm will be discussed. The first---increase  $N$  the number of samples per cycle---proves ineffective. The second---to use as the resampling frequency the average of the first estimated frequencies instead of the instantaneous first estimated frequency (as the original algorithm in the thesis does) ---moderately improves the frequency estimation accuracy. The last---to do the resampling multiple times instead of just once as the original algorithm does--- makes a significant difference.

Since the two approaches last mentioned improve the frequency estimation accuracy with the pure sinusoidal input waveform, it is intuitive to wonder if they will also make a difference when the input is not a pure sinusoidal. Updated versions of the algorithm were thus tested using the two approaches, respectively, for two different kinds of non pure sinusoidal input: one contains harmonic components and the other has a variable frequency. The results, as shown in the following sections, indicate clearly that neither of the two approaches helps to improve the frequency estimation accuracy for non-pure sinusoidal input.

### **5.2 Larger $N$ Approach**

It seems reasonable to assume that, if  $N$  equals the number of samples per cycle, larger values of  $N$  should yield higher accuracy. Such is not the case. When  $N$  was increased from 24 to 96, no significant improvement in accuracy is discerned (Figure 5-1 and Table 5-1.)

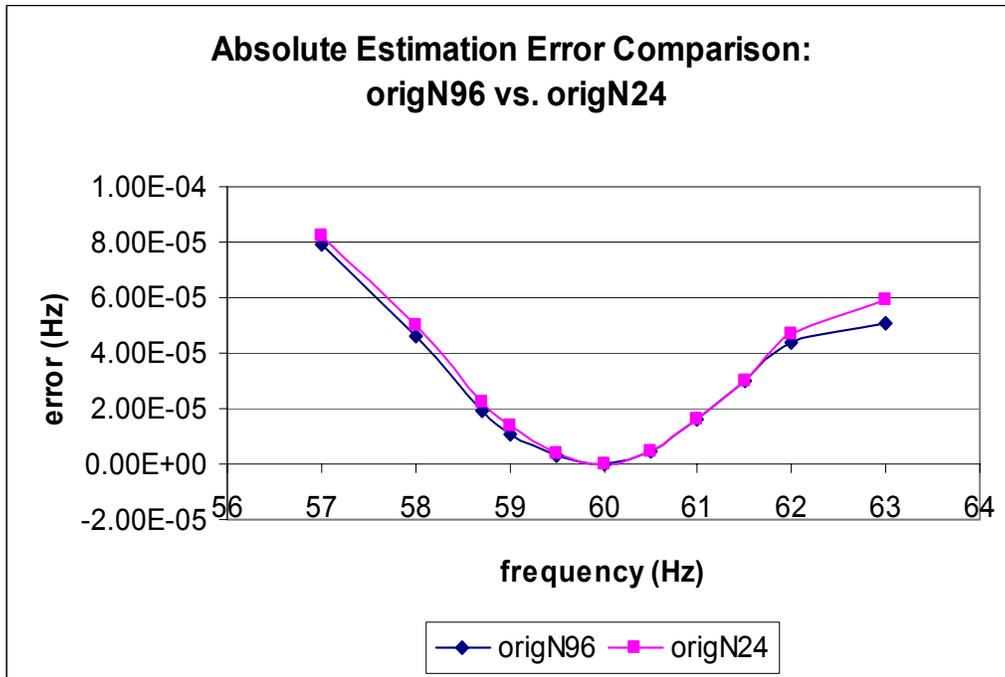


Figure 5-1 the comparison of the frequency estimation errors for the algorithm with N of 24 and the algorithm with N equal to 96

Frequency(Hz)	N=96error (Hz)	N=24error (Hz)
57	7.90E-05	8.20E-05
58	4.60E-05	5.00E-05
58.7	1.90E-05	2.20E-05
59	1.10E-05	1.40E-05
59.5	3.00E-06	4.00E-06
60	0.00E+00	0.00E+00
60.5	5.00E-06	5.00E-06
61	1.60E-05	1.60E-05
61.5	3.00E-05	3.00E-05
62	4.40E-05	4.70E-05
63	5.10E-05	5.90E-05

Table 5-1 the frequency estimation errors for the algorithm with N of 24 and the algorithm with N equal to 96

## 5.3 Averaging First Estimated Frequencies Approach

### 5.3.1 Testing with Pure Sinusoidal Input Waveform

Another attempt to improve the frequency estimation accuracy consisted of using as the resampling frequency the average of the first estimated frequencies instead of the instantaneous first estimated frequency (as the original algorithm does). For this approach one variable that may make a difference is the number of the first estimated frequencies that are averaged to generate the resampling frequency. I tried two possibilities: 24 and 144 (referenced later as 24-average and 144-average respectively). Figure 5-2 and Figure 5-3 show that both increased the accuracy greatly compared to the original algorithm. Firstly, the original algorithm has 100 percent accuracy (zero error) only at 60Hz. While, both 24-average and 144-average show a range of frequencies with zero estimation error. Secondly, for the original algorithm, the error is below  $1.00E-5$  only within the frequency range from 59.5 Hz to 60.7 Hz. On the contrary, for both 24-average and 144-average the estimation error is far below  $1.00E-5$  (not over  $3.00E-6$ ) within the whole range between 56Hz and 64Hz.

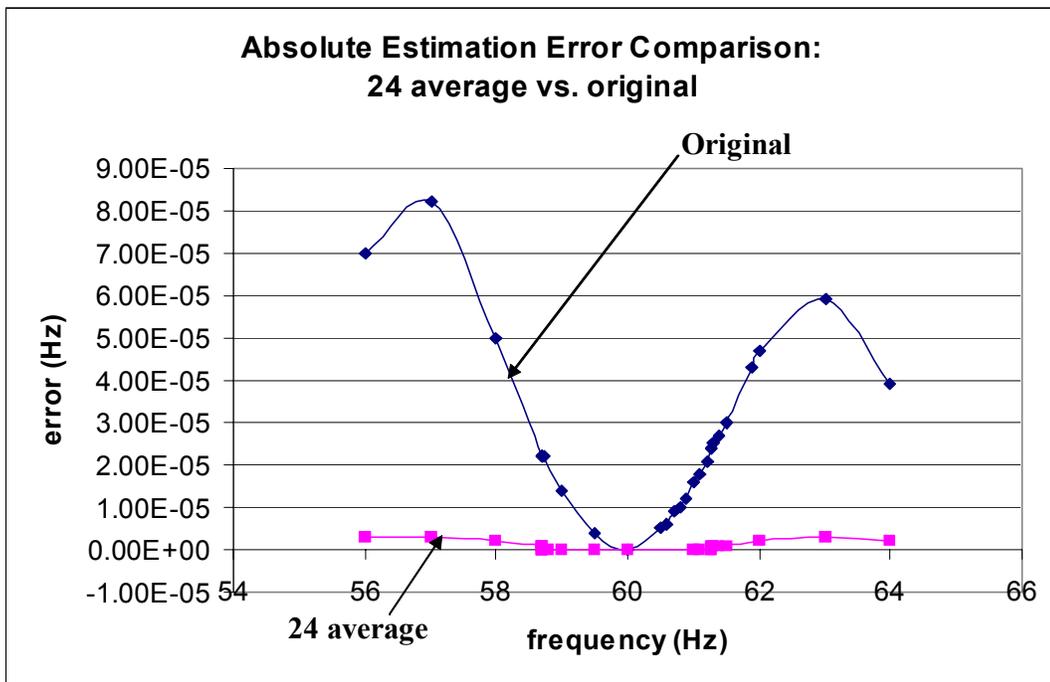


Figure 5-2 the comparison of the frequency estimation error: updated algorithm with 24-average vs. original algorithm

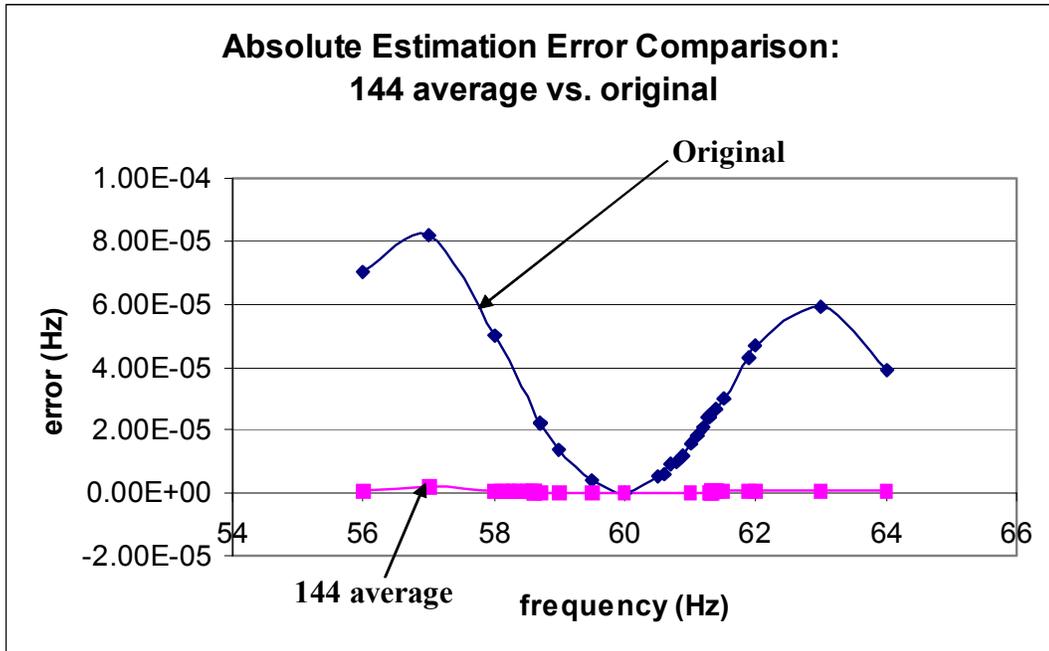


Figure 5-3 the comparison of the frequency estimation error: updated algorithm with 144-average vs. original algorithm

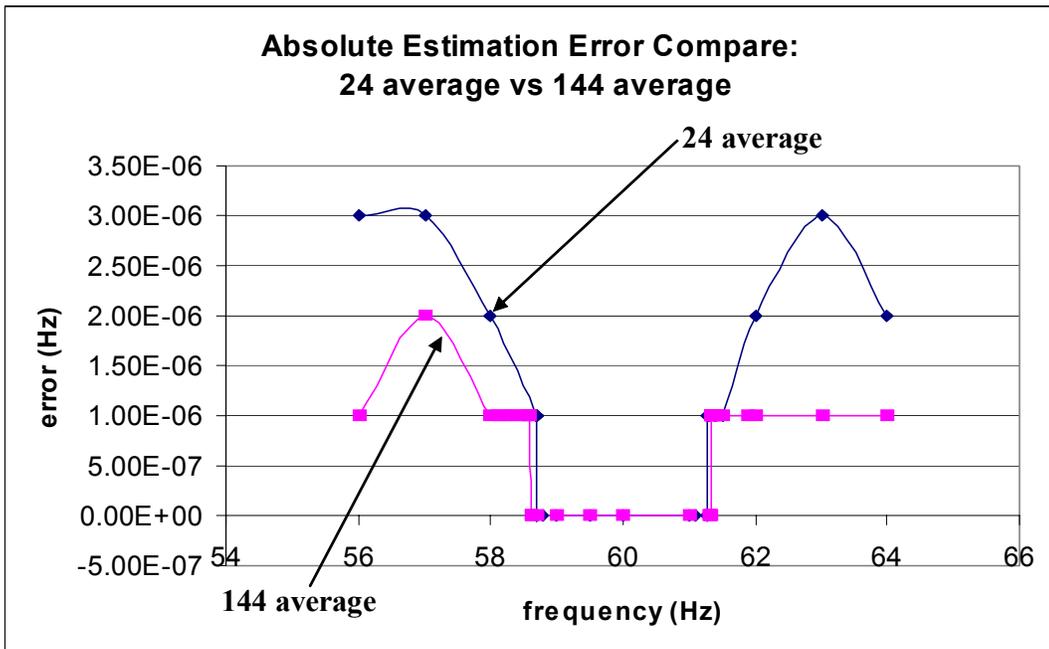


Figure 5-4 the comparison of the frequency estimation error: updated algorithm with 24-average vs. updated algorithm with 144-average

Figure 5-4 compares the accuracy from the 24-average to that from the 144-average. Results are better for the 144-average. First, for the 24-average the range of the frequencies with zero

estimation error is between 58.706Hz and 61.279Hz. Comparatively, the range of the frequencies with zero estimation error for 144-average expands to between 58.597 and 61.336. Second, for frequencies outside this range that have non-zero estimation error, the 144-average has higher accuracy than the 24-average. Actually for the 144-average, the estimation error for the frequencies between 56Hz and 64Hz is either zero or 1.00E-6 with the exception of 2.00E-6 for the frequency of 57Hz. While, for the 24-average, the error is 2.00E-6 for the frequency of 58Hz, 62Hz, 64Hz and jumps to 3.00E-6 for the frequency of 56Hz, 57Hz and 63Hz.

**5.3.2 Testing with Input That Contains Harmonic Noise**

Since the averaging approach discussed above helps to improve the frequency estimation accuracy for pure sinusoidal input waveform, it is possible it may also make a difference if the input is not pure sinusoidal waveform. In this section the results from input that contains harmonic noise are presented, from which no big difference can be seen. The results from an input with a variable frequency will be displayed in the next section.

For comparison, the base frequencies, the harmonic components and their percentages used to do the test are the same as those used to test the original algorithm (the results are shown in Chapter Three).

Harm No.(percentage)	Original (Hz)	24 average (Hz)	144 average (Hz)
DC(10%)	3.05000E-04	3.09000E-04	3.09000E-04
3(10%)	3.44000E-04	3.47000E-04	3.47000E-04
5(5%)	1.61000E-04	1.62000E-04	1.62000E-04
7(5%)	1.42000E-04	1.57000E-04	1.57000E-04
9(5%)	1.24000E-04	1.45000E-04	1.45000E-04
20kHz (2%)	2.88700E-03	2.89500E-03	2.89500E-03

Table 5-2 the frequency estimation error comparison with different harmonics present at the base frequency of 59.5Hz: updated algorithm with 24-average, updated algorithm with 144-average and original algorithm

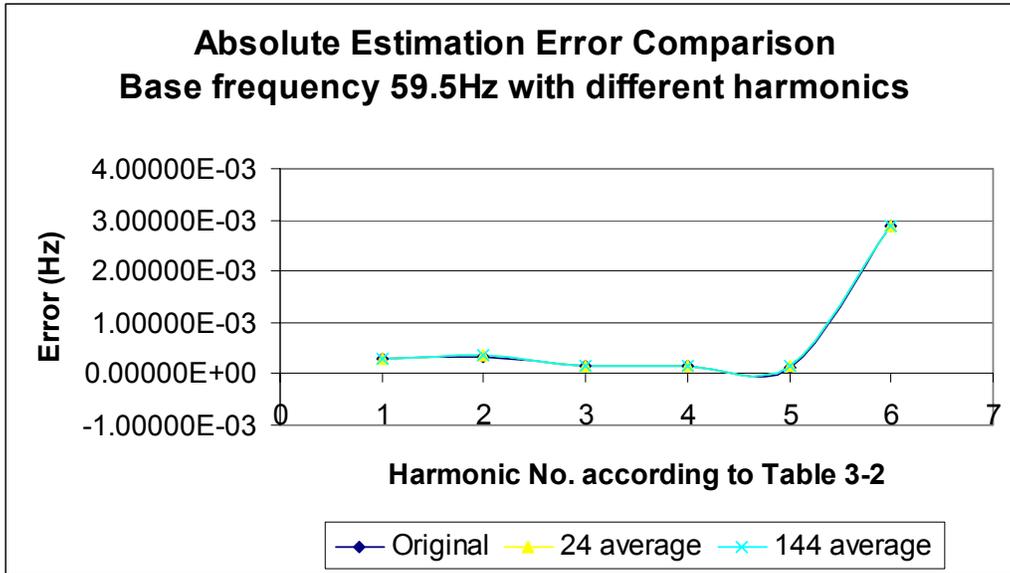


Figure 5-5 the frequency estimation error comparison with different harmonics present at the base frequency of 59.5Hz: updated algorithm with 24-average, updated algorithm with 144-average and original algorithm

Harm No.(percentage)	Original (Hz)	24 average (Hz)	144 average (Hz)
DC(10%)	0	0.00000E+00	0.00000E+00
3(10%)	0	0.00000E+00	0.00000E+00
5(5%)	0	0.00000E+00	0.00000E+00
7(5%)	0	0.00000E+00	0.00000E+00
9(5%)	0	0.00000E+00	0.00000E+00
20kHz (2%)	1.33800E-03	1.33700E-03	1.33900E-03

Table 5-3 the frequency estimation error comparison with different harmonics present at the base frequency of 60 Hz: updated algorithm with 24-average, updated algorithm with 144-average and original algorithm

Harm No.(percentage)	Original (Hz)	24 average (Hz)	144 average (Hz)
DC (10%)	3.15000E-04	3.16000E-04	3.16000E-04
3(10%)	3.35000E-04	3.54000E-04	3.54000E-04
5(5%)	1.55000E-04	1.70000E-04	1.70000E-04
7(5%)	1.66000E-04	1.78000E-04	1.78000E-04
9(5%)	1.89000E-04	1.96000E-04	1.96000E-04
20kHz (2%)	2.35700E-03	2.35800E-03	2.35800E-03

Table 5-4 the frequency estimation error comparison with different harmonics present at the base frequency of 60.5 Hz: updated algorithm with 24-average, updated algorithm with 144-average and original algorithm

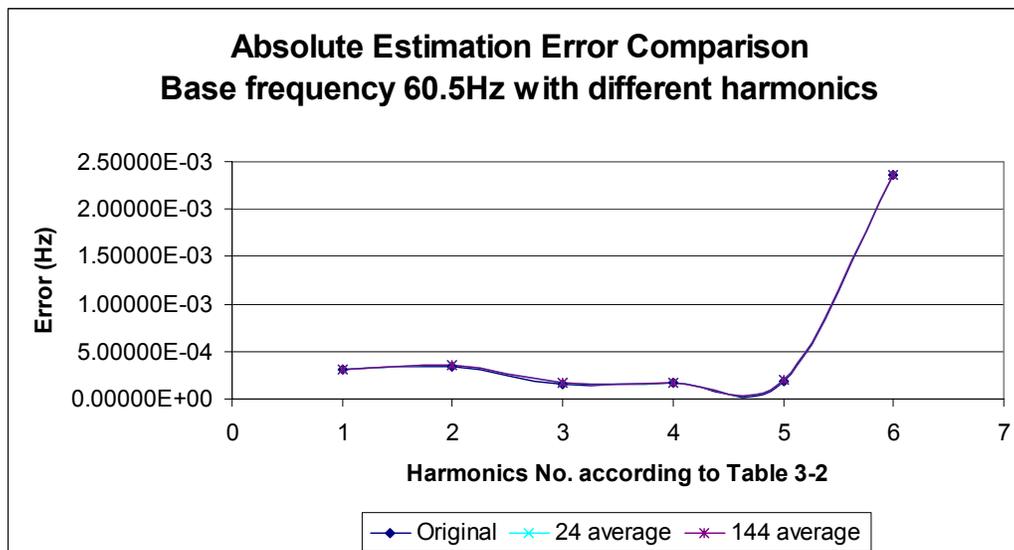


Figure 5-6 the frequency estimation error comparison with different harmonics present at the base frequency of 60.5 Hz: updated algorithm with 24-average, updated algorithm with 144-average and original algorithm

### 5.3.3 Testing with Input That Has a Variable Frequency

This section considers the sensitivity of the updated algorithm with averaging first estimated frequencies approach to the change of frequency. For comparison, consider the same two cases of the changing frequency input as used with the original algorithm in Chapter Three. For the ramp case, the 24-average approach was studied whereas for the sinusoidal case the 144-average approach was studied.

#### 5.3.3.1 Test with Input of Which Frequency Changes as a Ramp Function

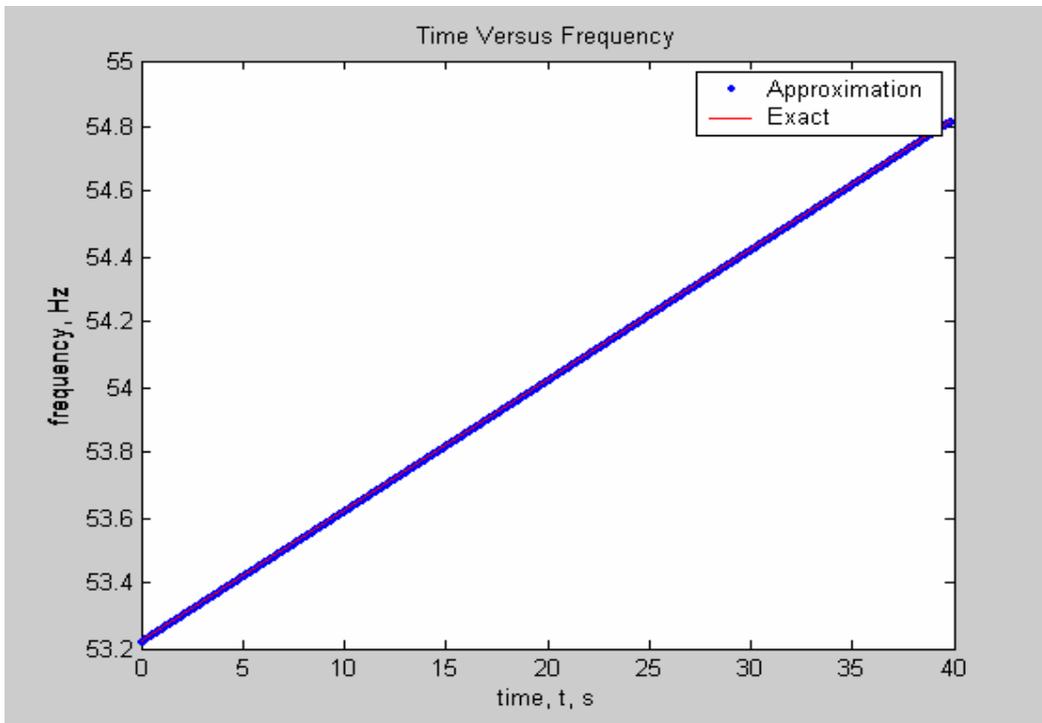


Figure 5-7 the estimated frequency for input waveform with frequency changing as a Ramp function with a rate of .04 Hz/sec (53.2Hz~54.8Hz) and the exact frequency resulted from the formula (the updated algorithm with 24-average approach)

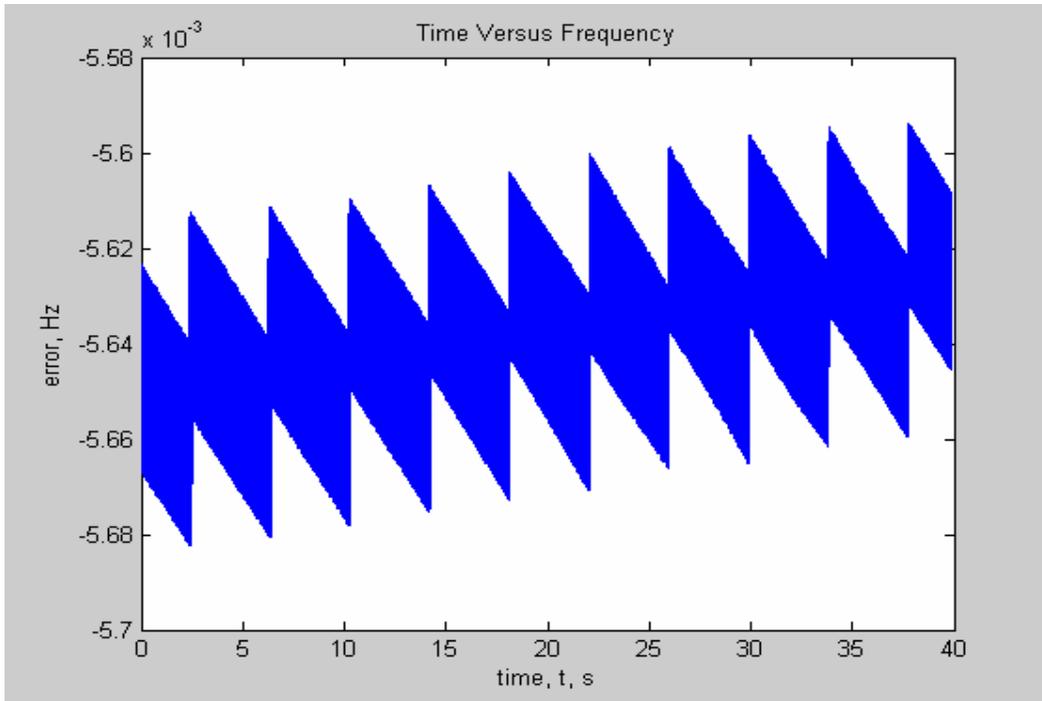


Figure 5-8 the error between the estimated frequency for input waveform with frequency changing as a Ramp function with a rate of .04 Hz/sec and the exact frequency resulted from the formula (the updated algorithm with 24-average approach)

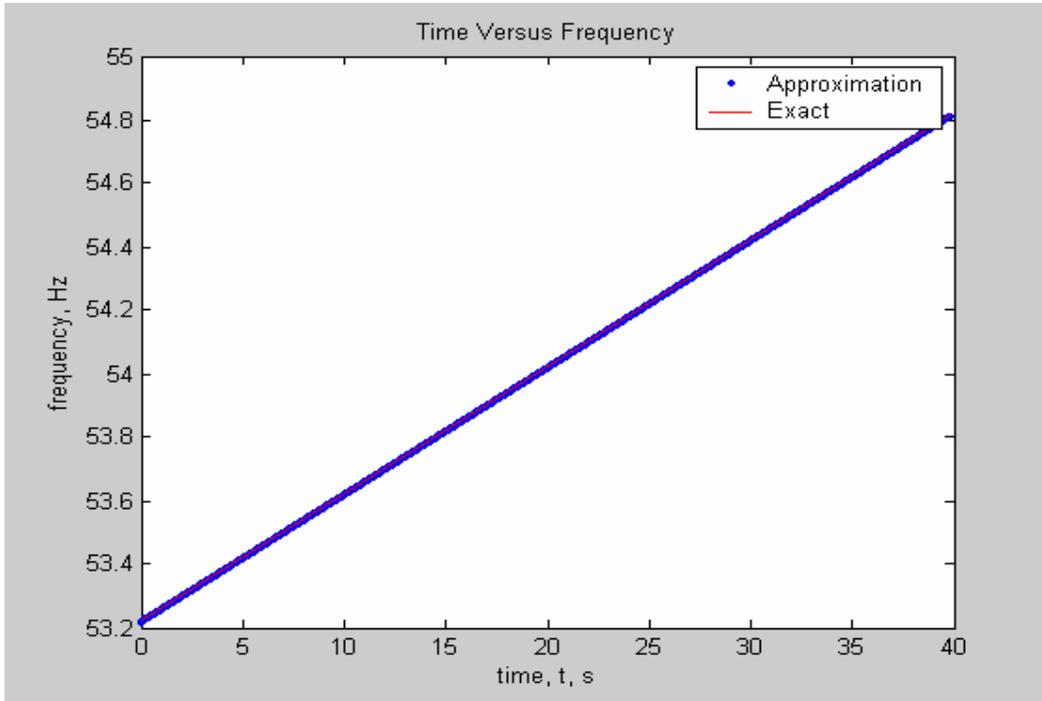


Figure 5-9 the estimated frequency for input waveform with frequency changing as a Ramp function with a rate of .04 Hz/sec (53.2Hz~54.8Hz) and the exact frequency resulted from the formula (original algorithm)

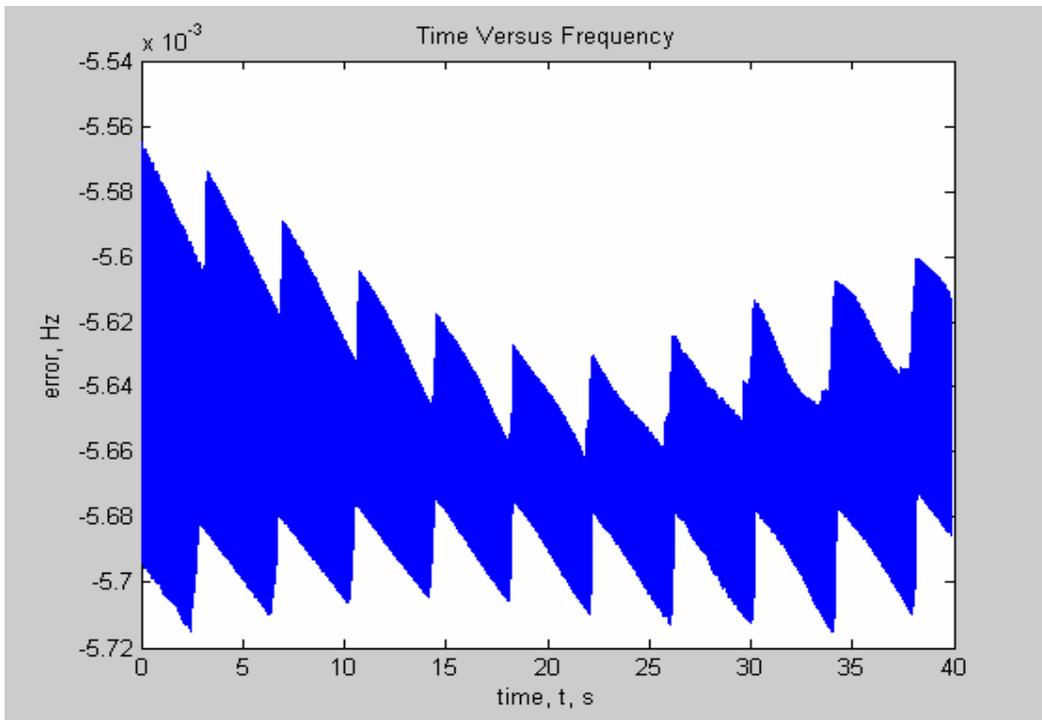


Figure 5-10 the error between the estimated frequency for input waveform with frequency changing as a Ramp function with a rate of .04 Hz/sec and the exact frequency resulted from the formula (original algorithm)

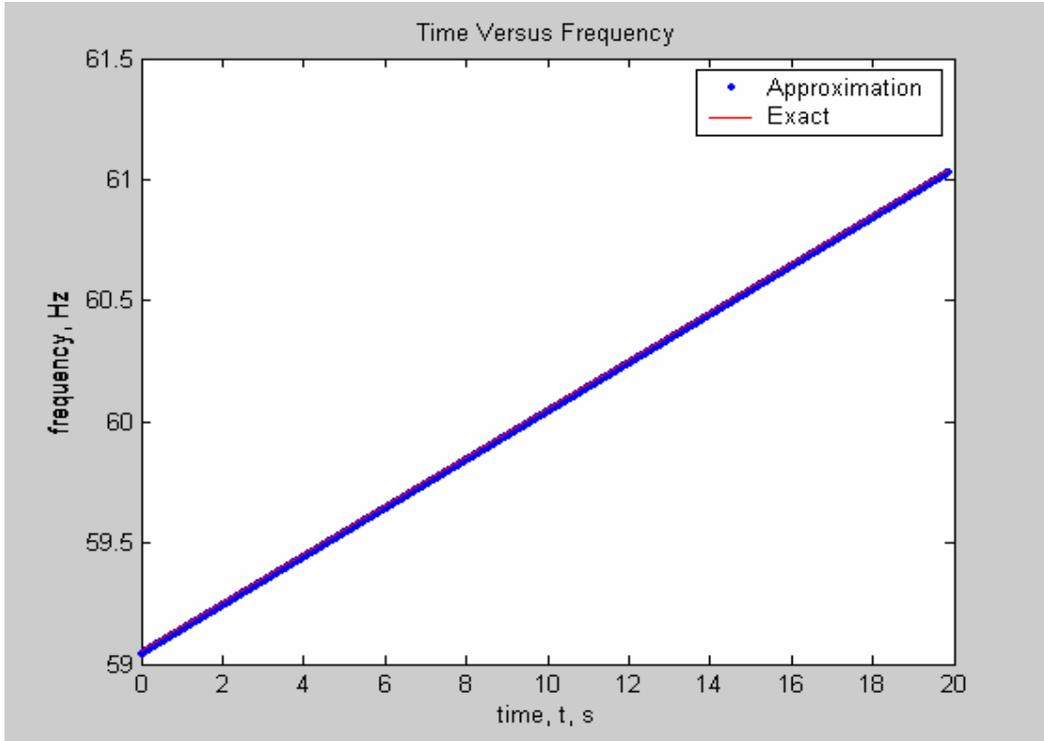


Figure 5-11 the estimated frequency for input waveform with frequency changing as a Ramp function with a rate of .1 Hz/sec (59Hz~61Hz) and the exact frequency resulted from the formula (the updated algorithm with 24-average approach)

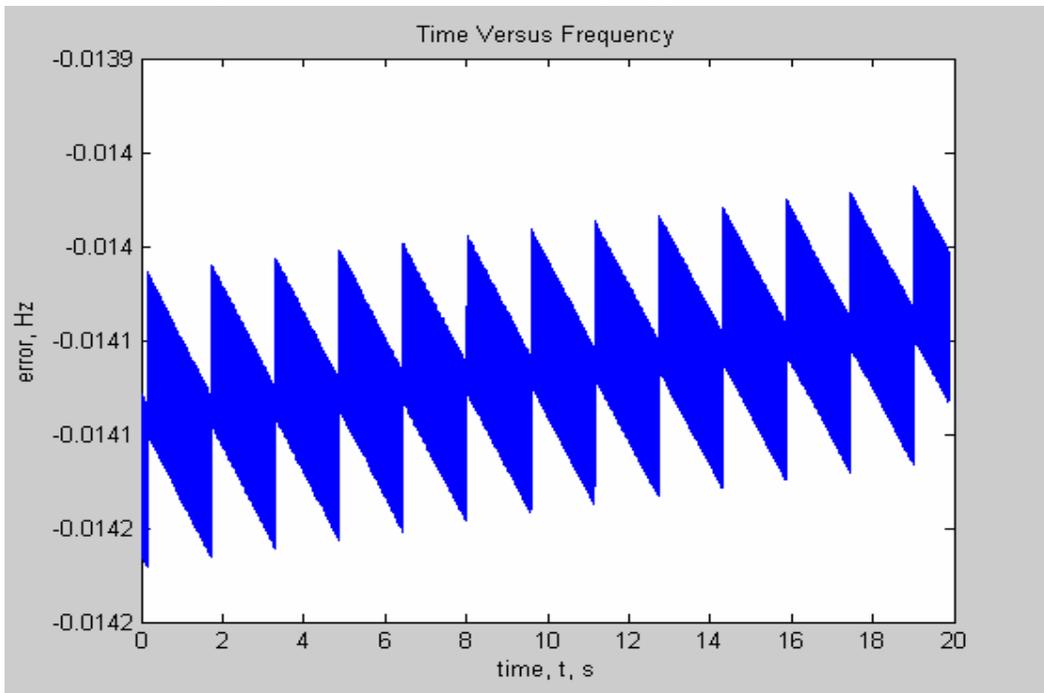


Figure 5-12 the error between the estimated frequency for input waveform with frequency changing as a Ramp function with a rate of .1 Hz/sec and the exact frequency resulted from the formula (the updated algorithm with 24-average approach)

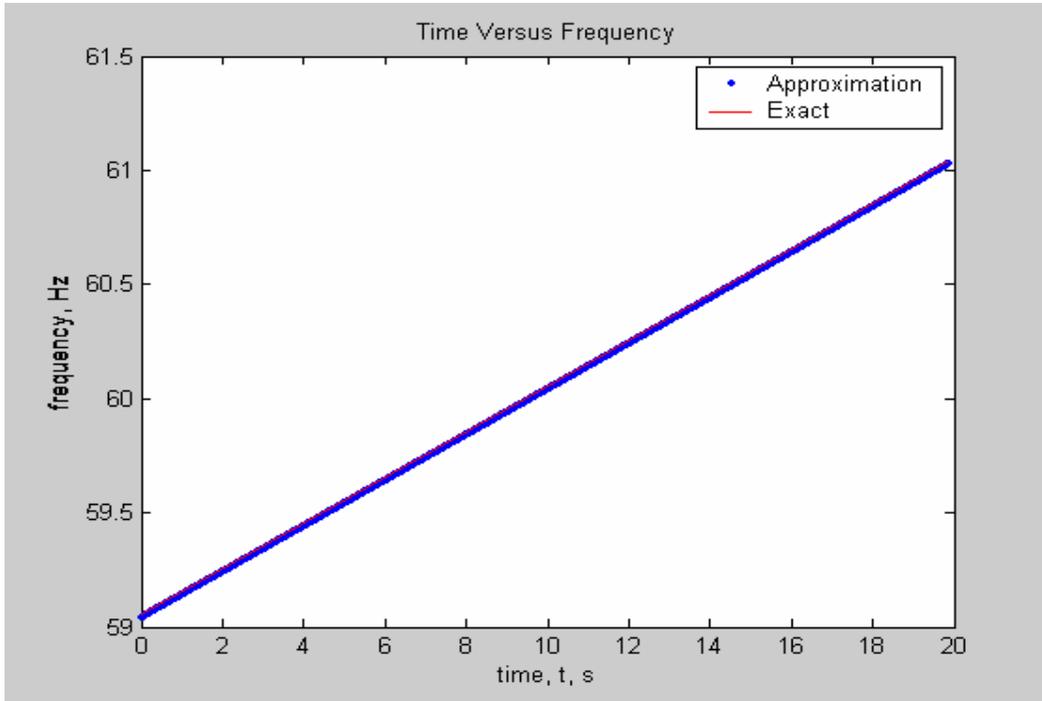


Figure 5-13 the estimated frequency for input waveform with frequency changing as a Ramp function with a rate of .1 Hz/sec (59Hz~61Hz) and the exact frequency resulted from the formula (original algorithm)

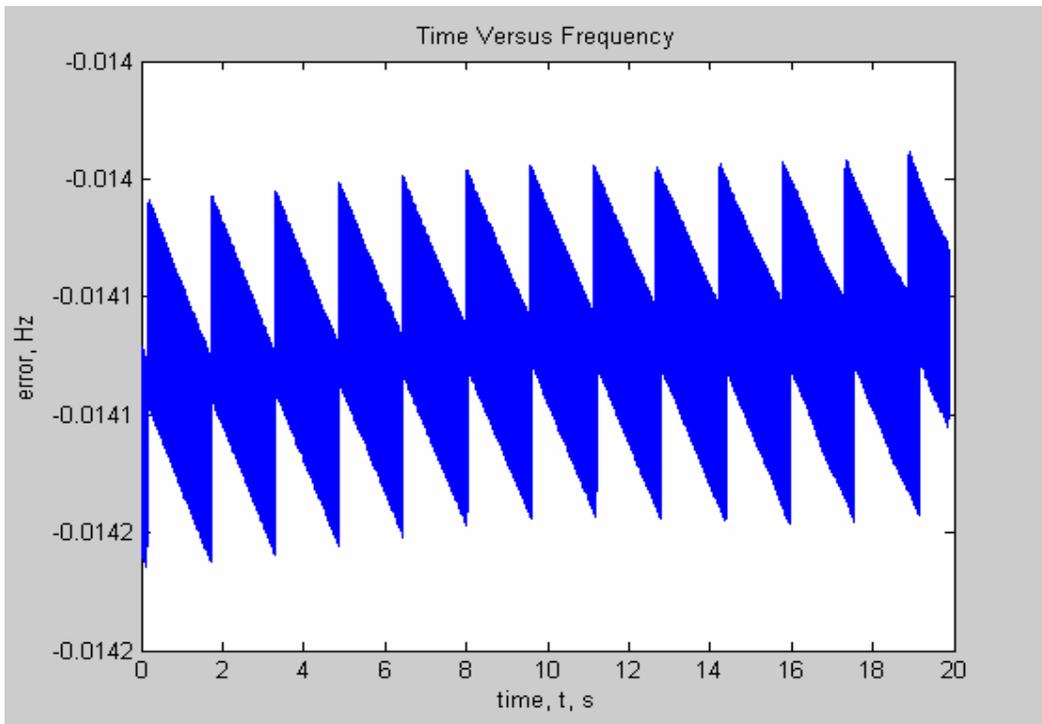


Figure 5-14 the error between the estimated frequency for input waveform with frequency changing as a Ramp function with a rate of .1 Hz/sec and the exact frequency resulted from the formula (original algorithm)

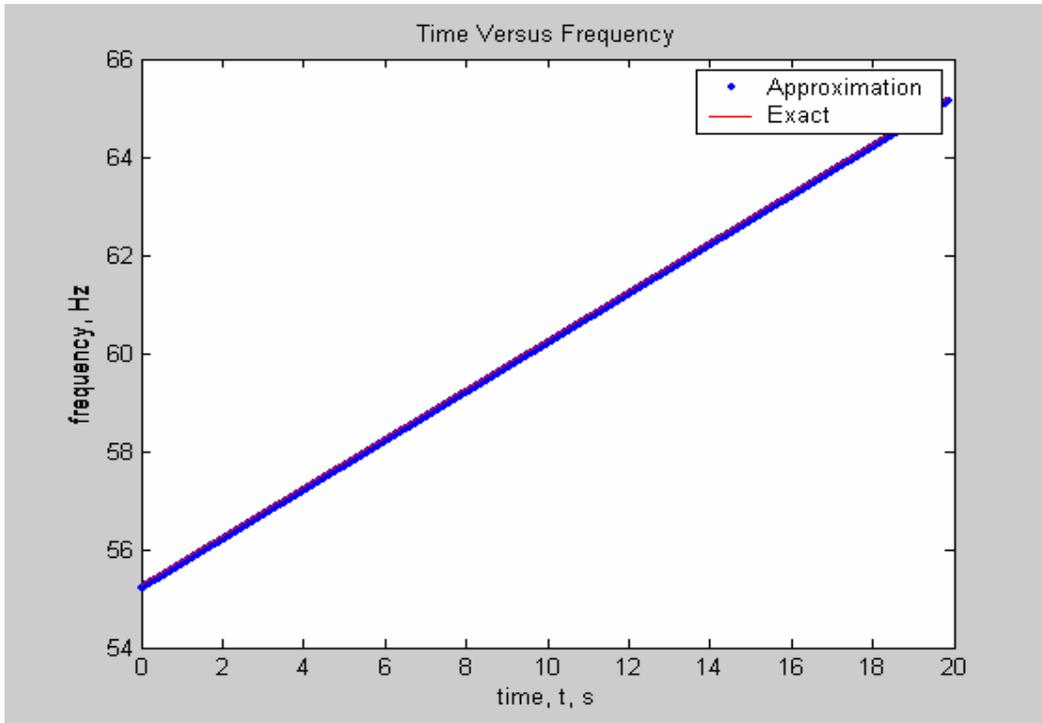


Figure 5-15 the estimated frequency for input waveform with frequency changing as a Ramp function with a rate of .5 Hz/sec (55Hz~65Hz) and the exact frequency resulted from the formula (the updated algorithm with 24-average approach)

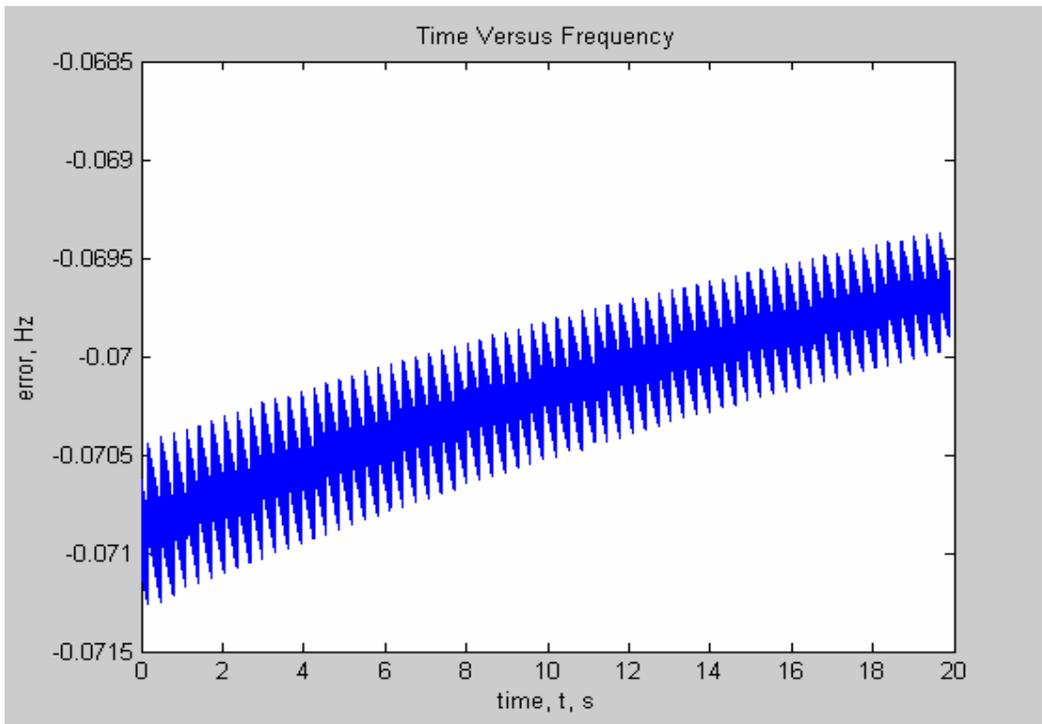


Figure 5-16 the error between the estimated frequency for input waveform with frequency changing as a Ramp function with a rate of .5 Hz/sec and the exact frequency resulted from the formula (the updated algorithm with 24-average approach)

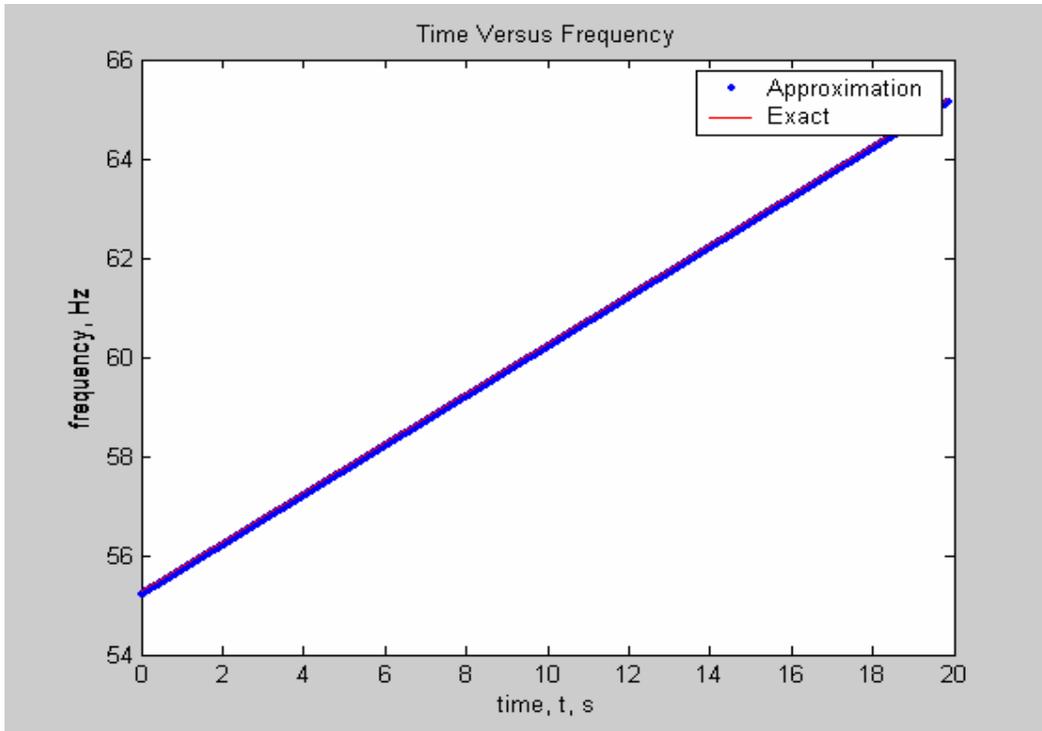


Figure 5-17 the estimated frequency for input waveform with frequency changing as a Ramp function with a rate of .5 Hz/sec (55Hz~65Hz) and the exact frequency resulted from the formula (original algorithm)

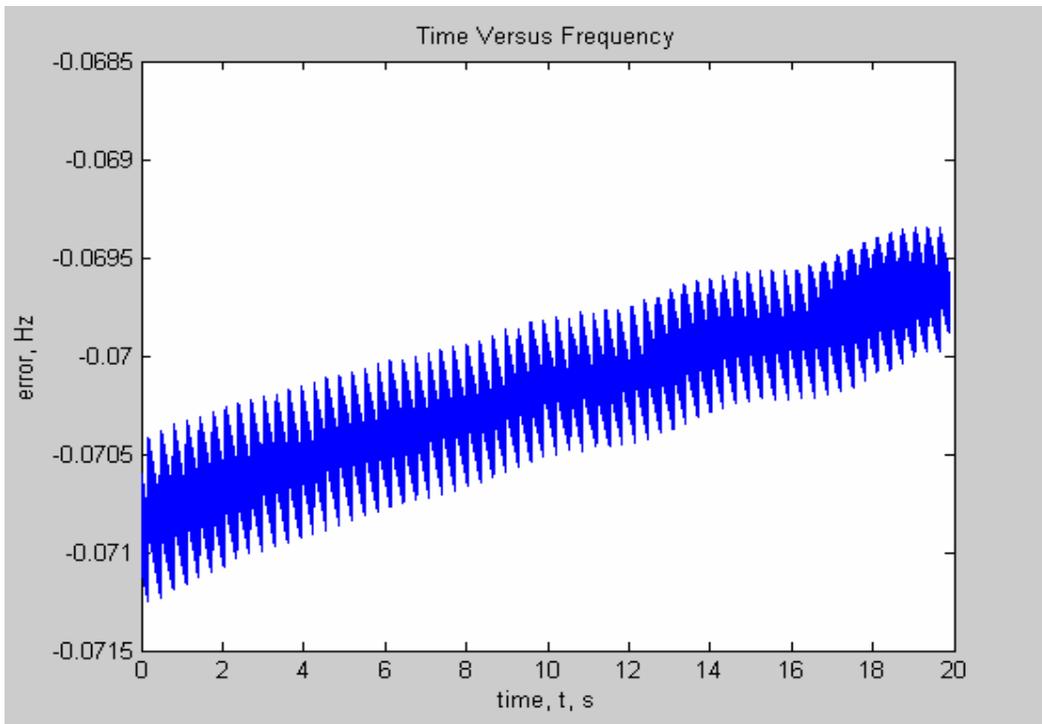


Figure 5-18 the error between the estimated frequency for input waveform with frequency changing as a Ramp function with a rate of .5 Hz/sec and the exact frequency resulted from the formula (original algorithm)

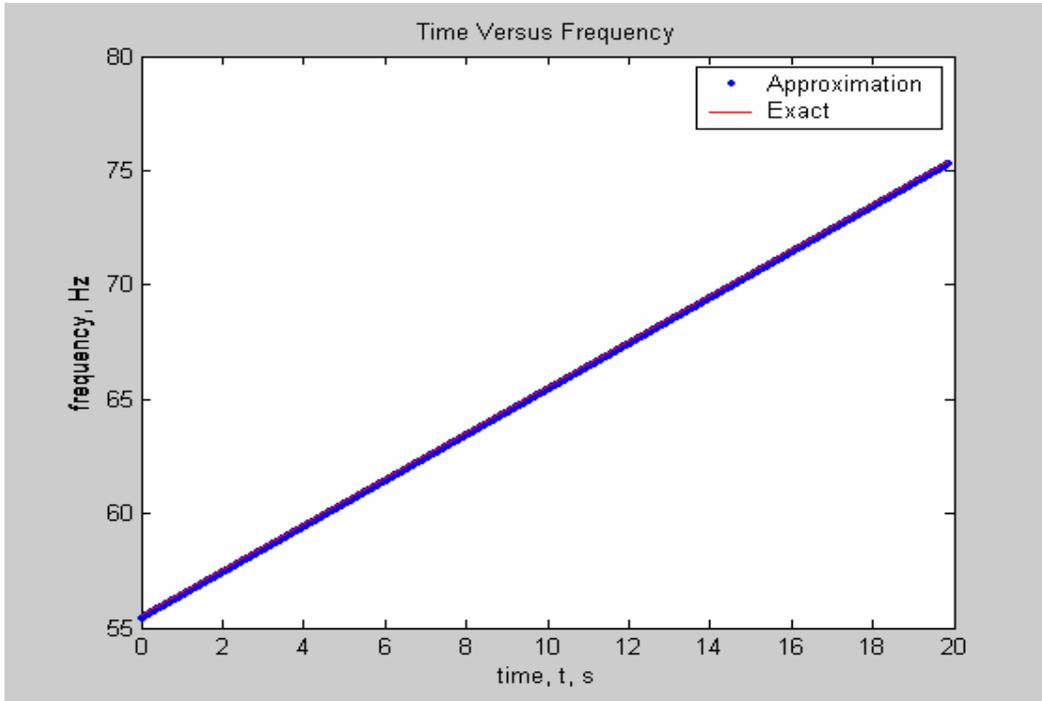


Figure 5-19 the estimated frequency for input waveform with frequency changing as a Ramp function with a rate of 1 Hz/sec (55Hz~65Hz) and the exact frequency resulted from the formula (the updated algorithm with 24-average approach)

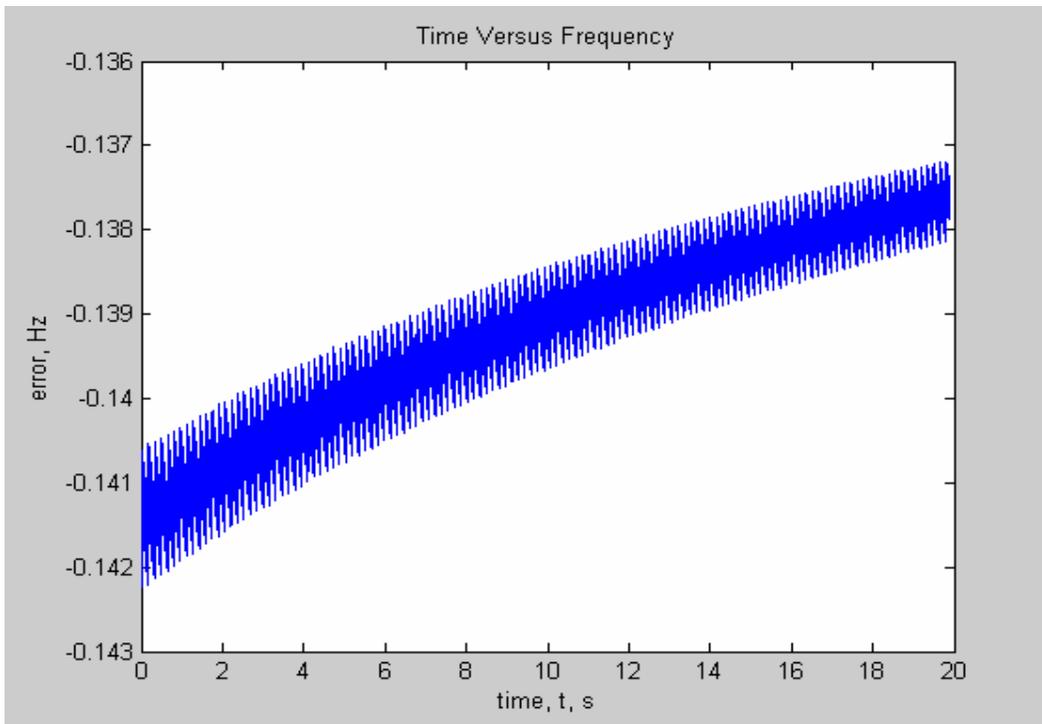


Figure 5-20 the error between the estimated frequency for input waveform with frequency changing as a Ramp function with a rate of 1 Hz/sec and the exact frequency resulted from the formula (the updated algorithm with 24-average approach)

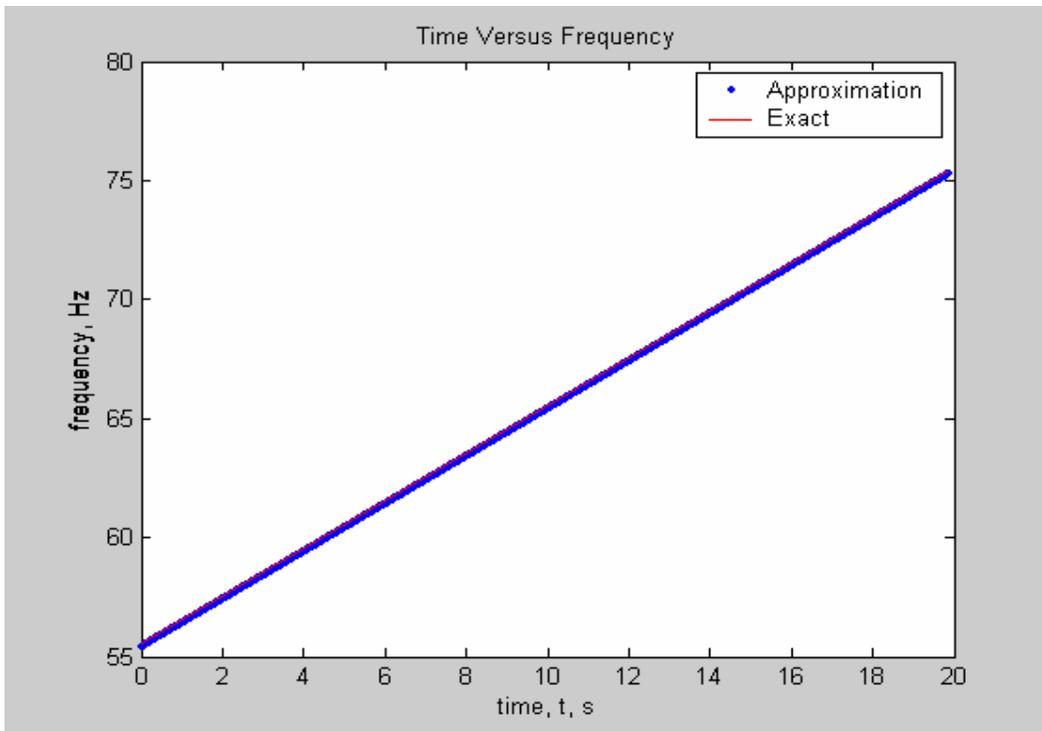


Figure 5-21 the estimated frequency for input waveform with frequency changing as a Ramp function with a rate of 1 Hz/sec (55Hz~75Hz) and the exact frequency resulted from the formula (original algorithm)

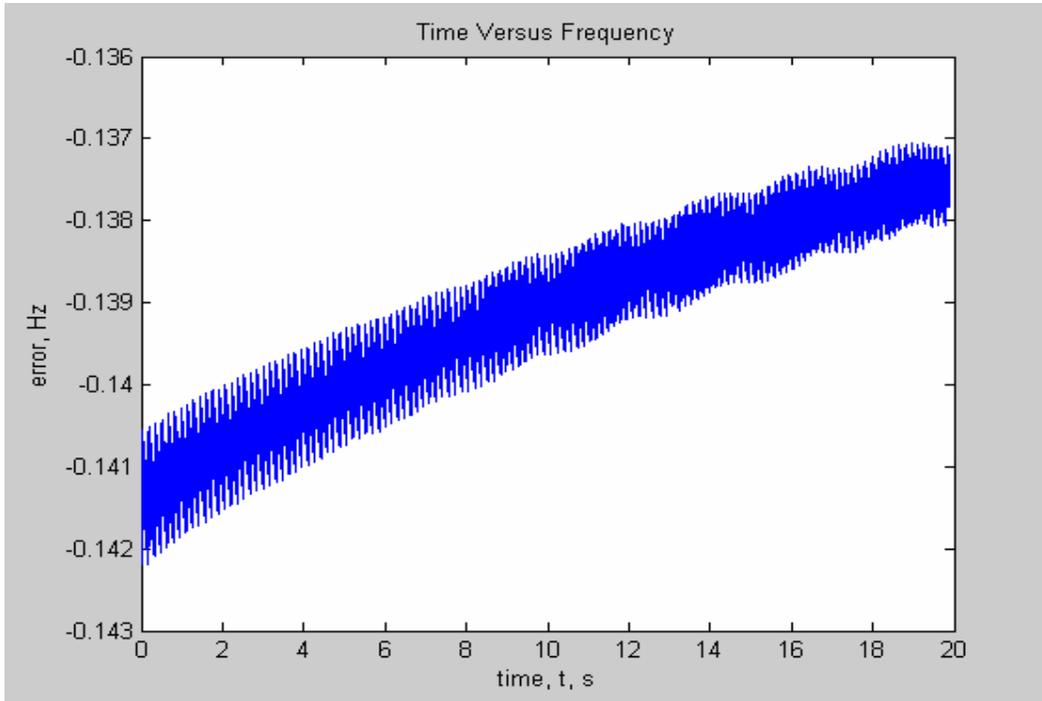


Figure 5-22 the error between the estimated frequency for input waveform with frequency changing as a Ramp function with a rate of 1 Hz/sec and the exact frequency resulted from the formula (original algorithm)

### 5.3.3.2 Testing with Input of Which Frequency Changes as a Sinusoidal

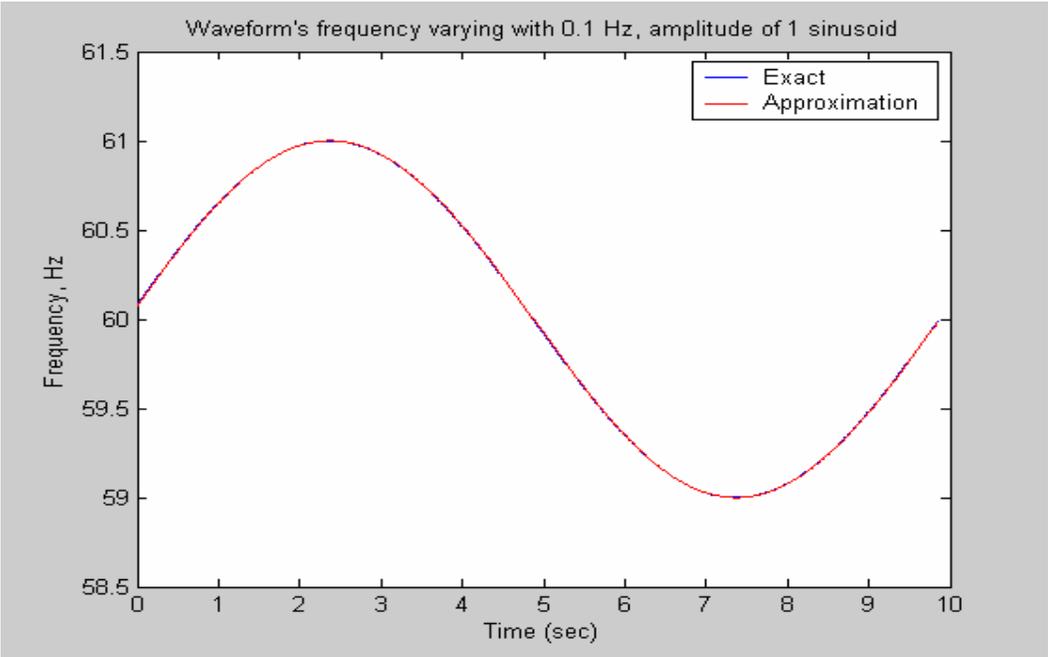


Figure 5-23 the estimated frequency for input waveform with  $f=0.1\text{Hz}$ ,  $\text{Amp}=1$  sinusoidal changing frequency and the exact frequency resulted from the formula (the updated algorithm with 144-average approach)

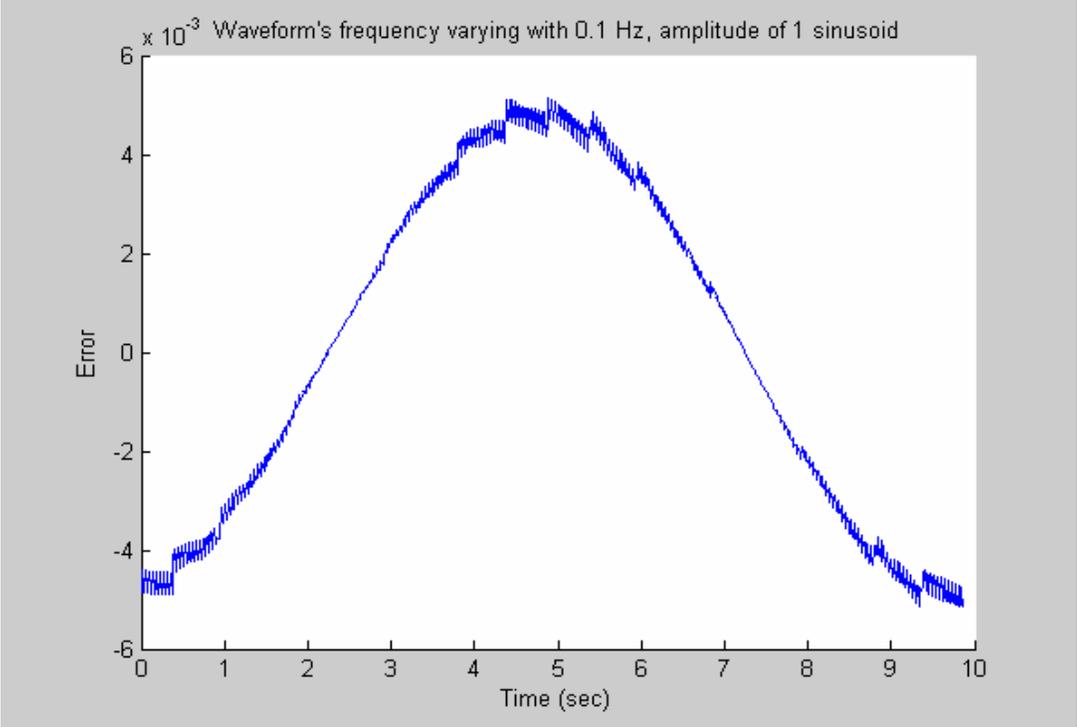


Figure 5-24 the error between the estimated frequency and the exact one for input waveform with  $f=0.1\text{Hz}$ ,  $\text{Amp}=1$  sinusoidal changing frequency (the updated algorithm with 144-average approach)

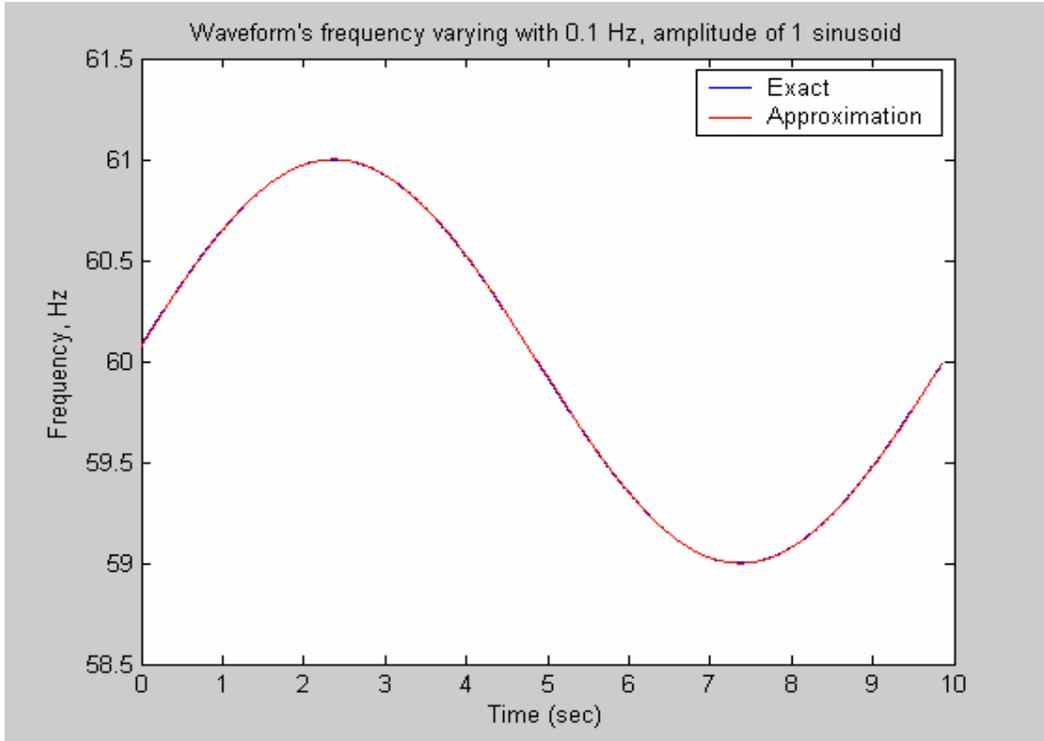


Figure 5-25 the estimated frequency for input waveform with  $f=0.1\text{Hz}$ ,  $\text{Amp}=1$  sinusoidal changing frequency and the exact frequency resulted from the formula (original algorithm)

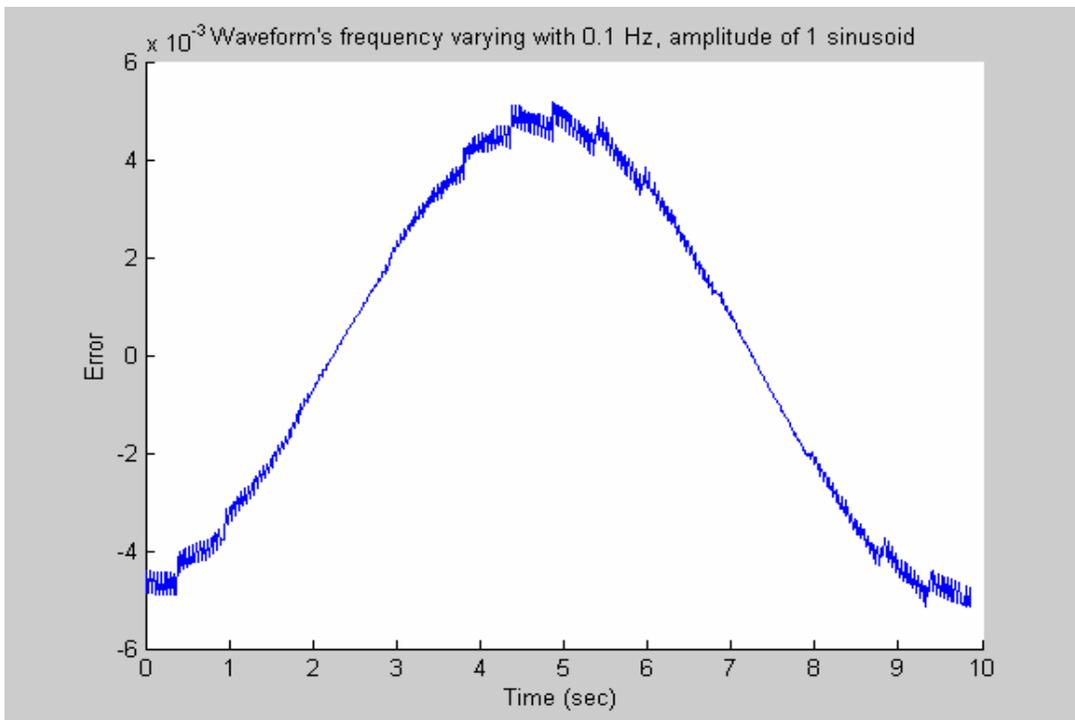


Figure 5-26 the error between the estimated frequency and the exact one for input waveform with  $f=0.1\text{Hz}$ ,  $\text{Amp}=1$  sinusoidal changing frequency (original algorithm)

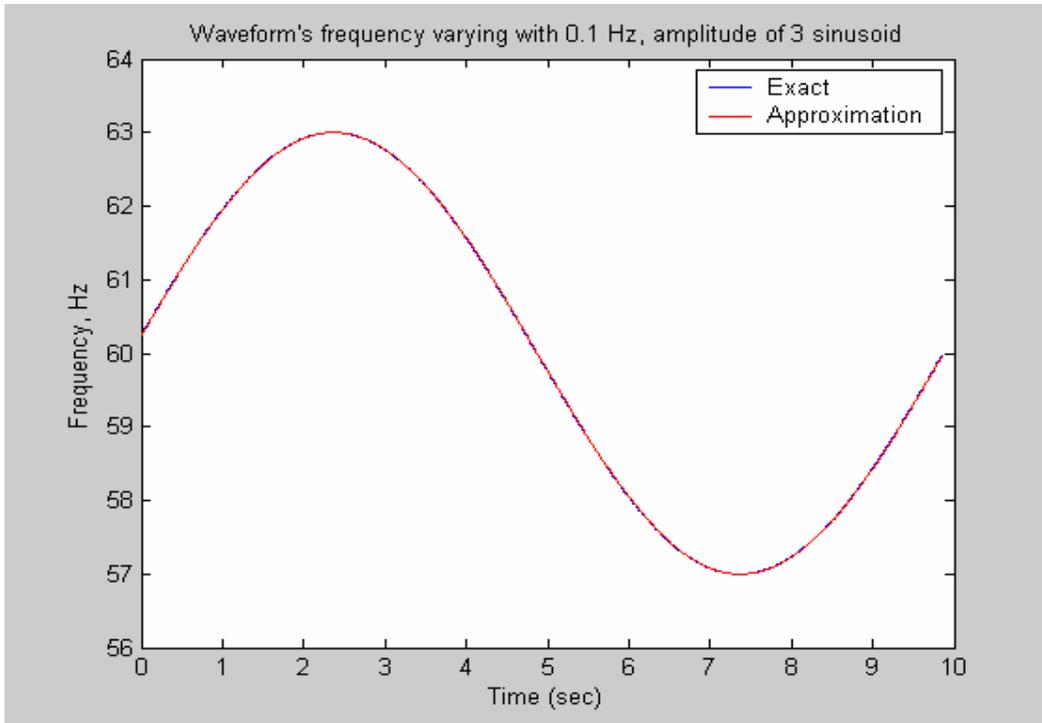


Figure 5-27 the estimated frequency for input waveform with  $f=0.1\text{Hz}$ ,  $\text{Amp}=3$  sinusoidal changing frequency and the exact frequency resulted from the formula (the updated algorithm with 144-average approach)

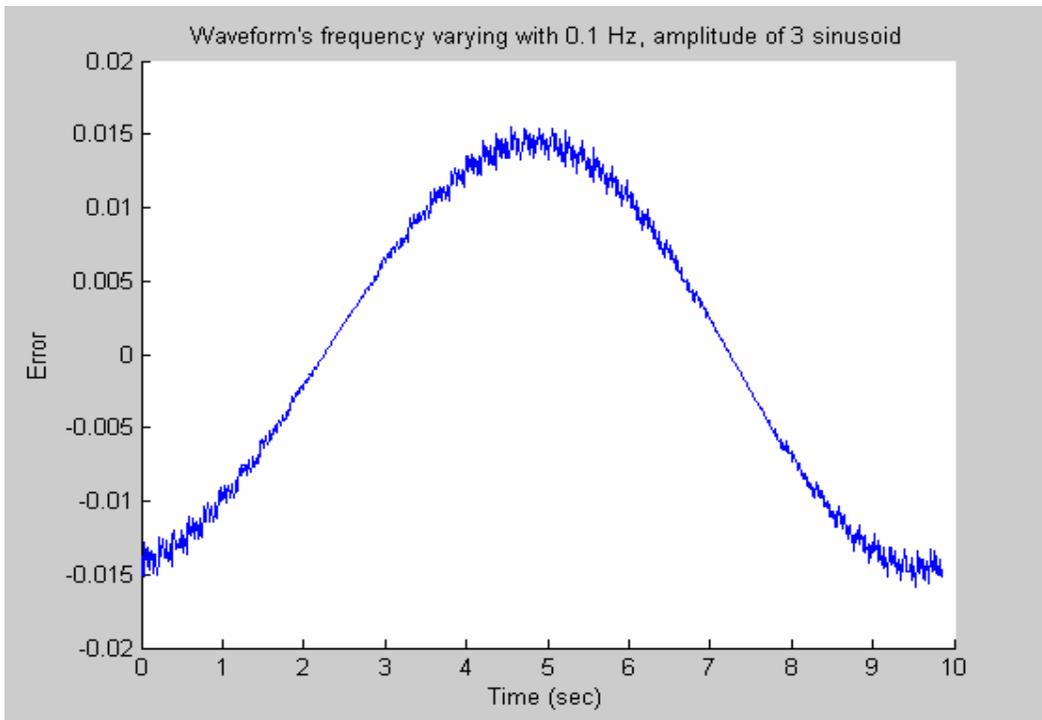


Figure 5-28 the error between the estimated frequency and the exact one for input waveform with  $f=0.1\text{Hz}$ ,  $\text{Amp}=3$  sinusoidal changing frequency (the updated algorithm with 144-average approach)

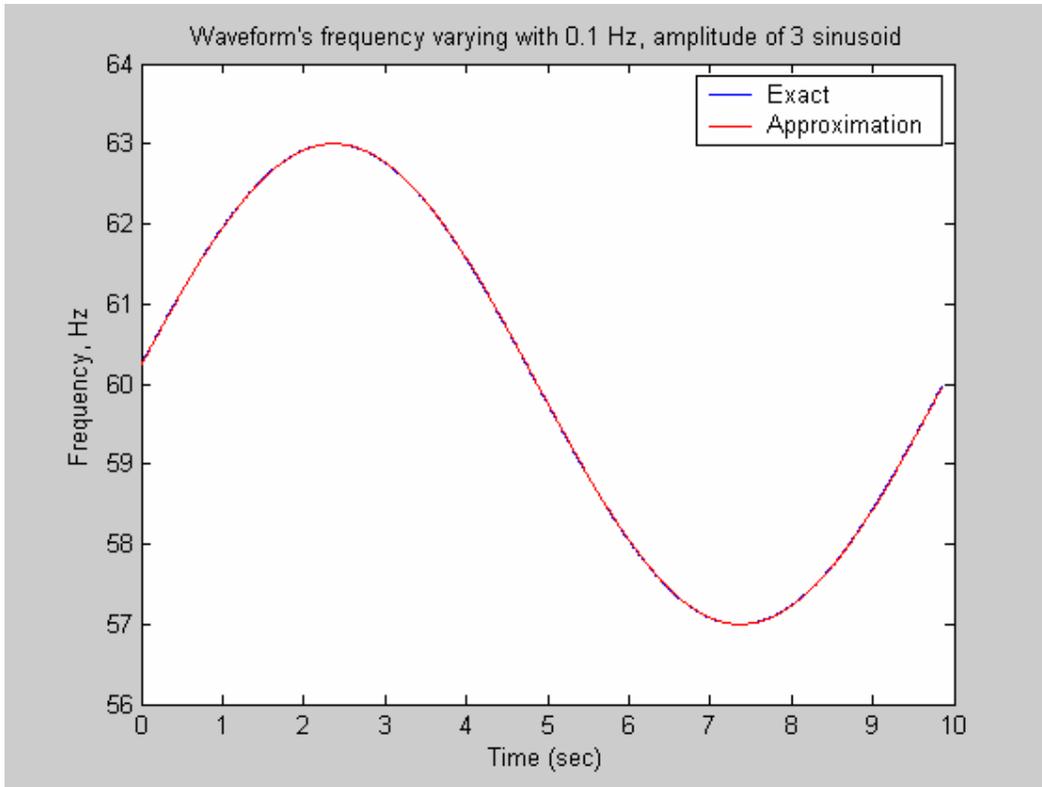


Figure 5-29 the estimated frequency for input waveform with  $f=0.1\text{Hz}$ ,  $\text{Amp}=3$  sinusoidal changing frequency and the exact frequency resulted from the formula (original algorithm)

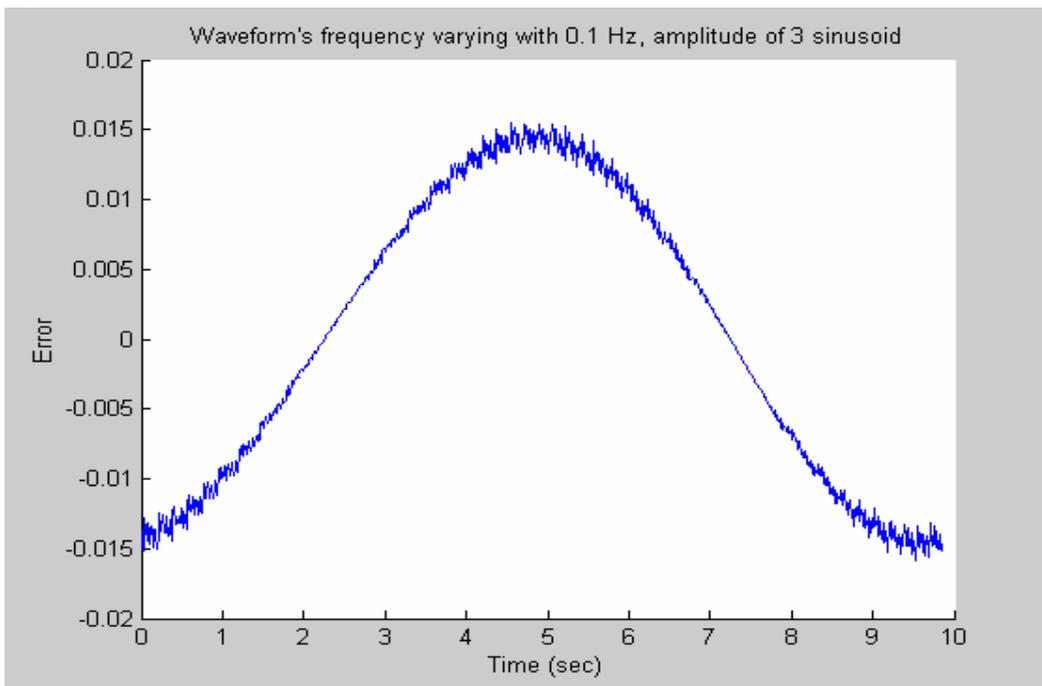


Figure 5-30 the error between the estimated frequency and the exact one for input waveform with  $f=0.1\text{Hz}$ ,  $\text{Amp}=3$  sinusoidal changing frequency (original algorithm)

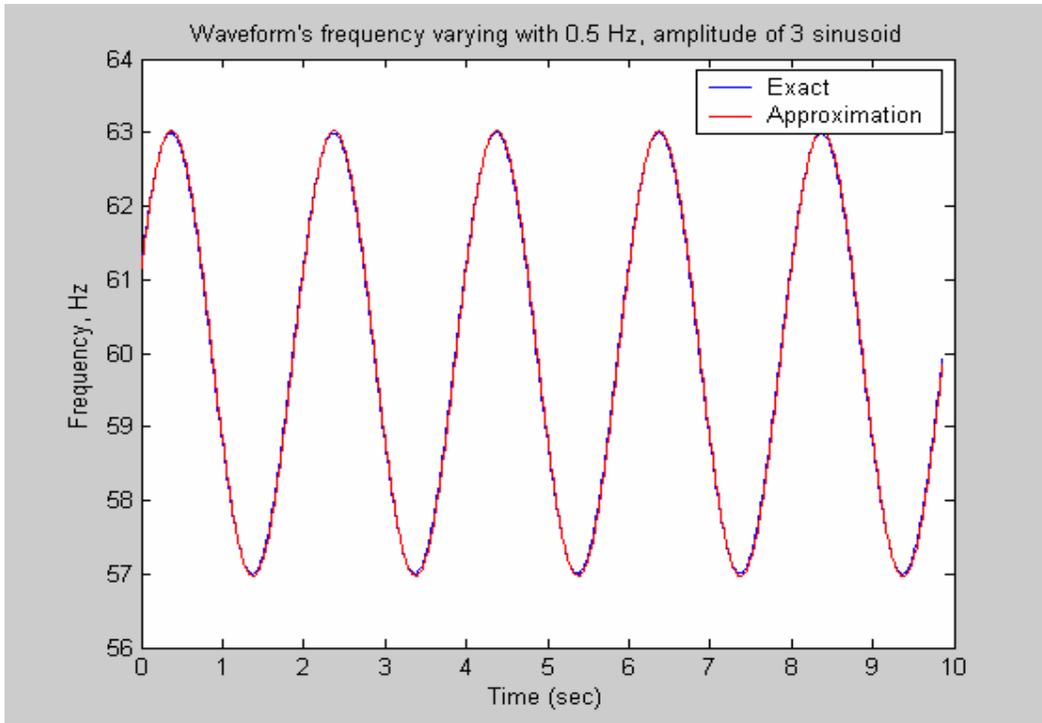


Figure 5-31 the estimated frequency for input waveform with  $f=0.5\text{Hz}$ ,  $\text{Amp}=3$  sinusoidal changing frequency and the exact frequency resulted from the formula (the updated algorithm with 144-average approach)

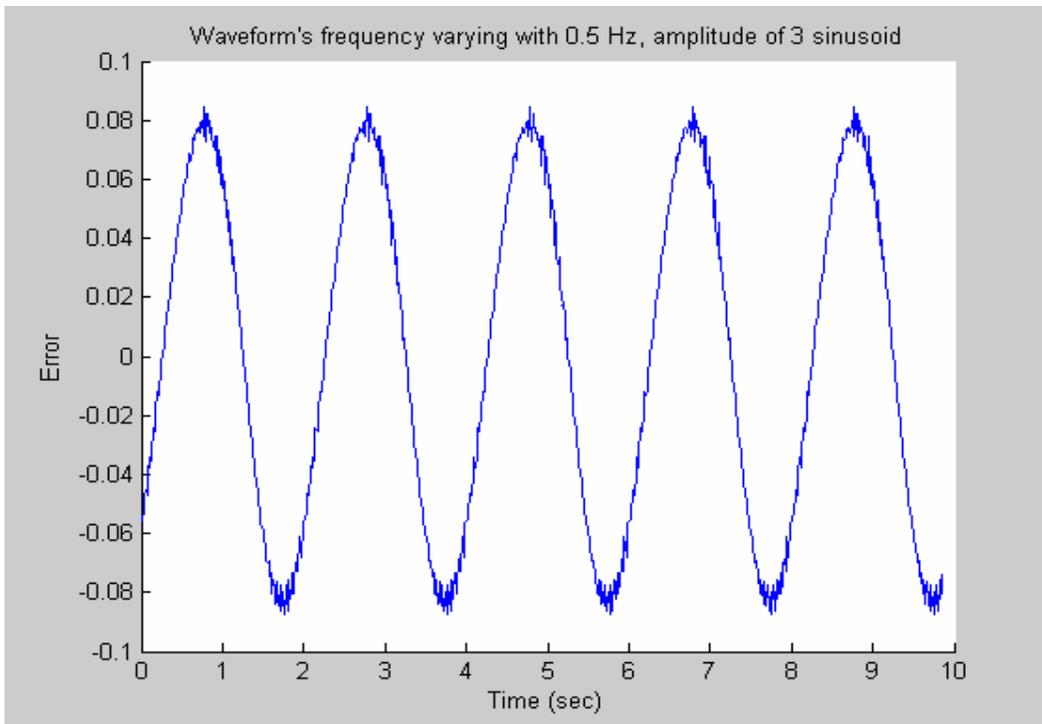


Figure 5-32 the error between the estimated frequency and the exact one for input waveform with  $f=0.5\text{Hz}$ ,  $\text{Amp}=3$  sinusoidal changing frequency (the updated algorithm with 144-average approach)

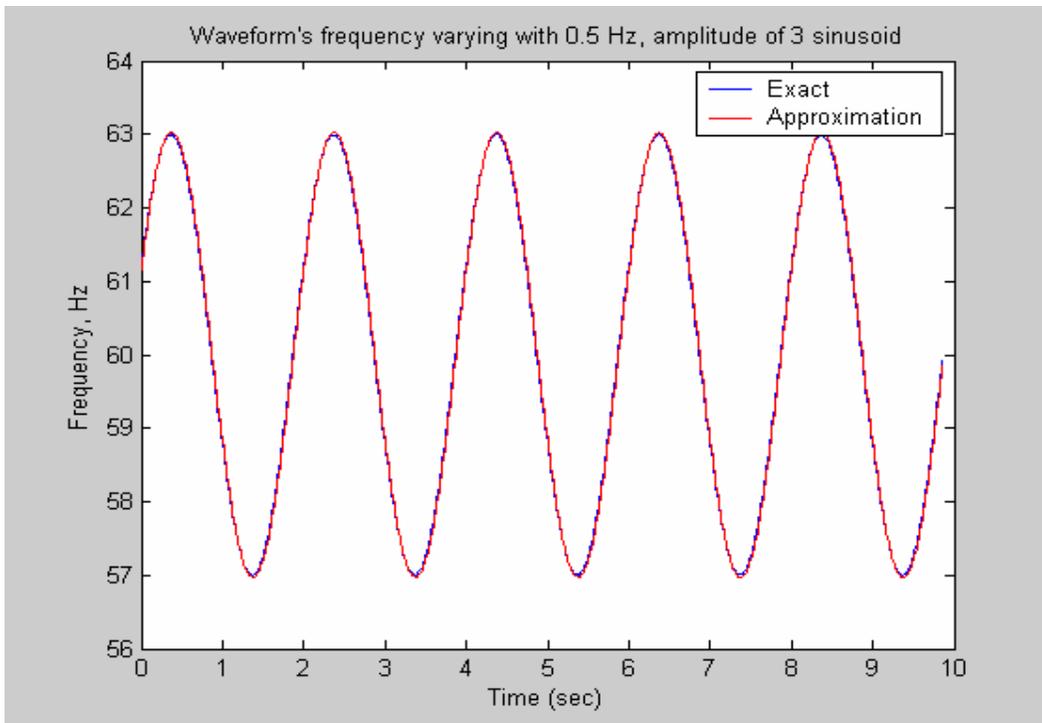


Figure 5-33 the estimated frequency for input waveform with  $f=0.5\text{Hz}$ ,  $\text{Amp}=3$  sinusoidal changing frequency and the exact frequency resulted from the formula (original algorithm)

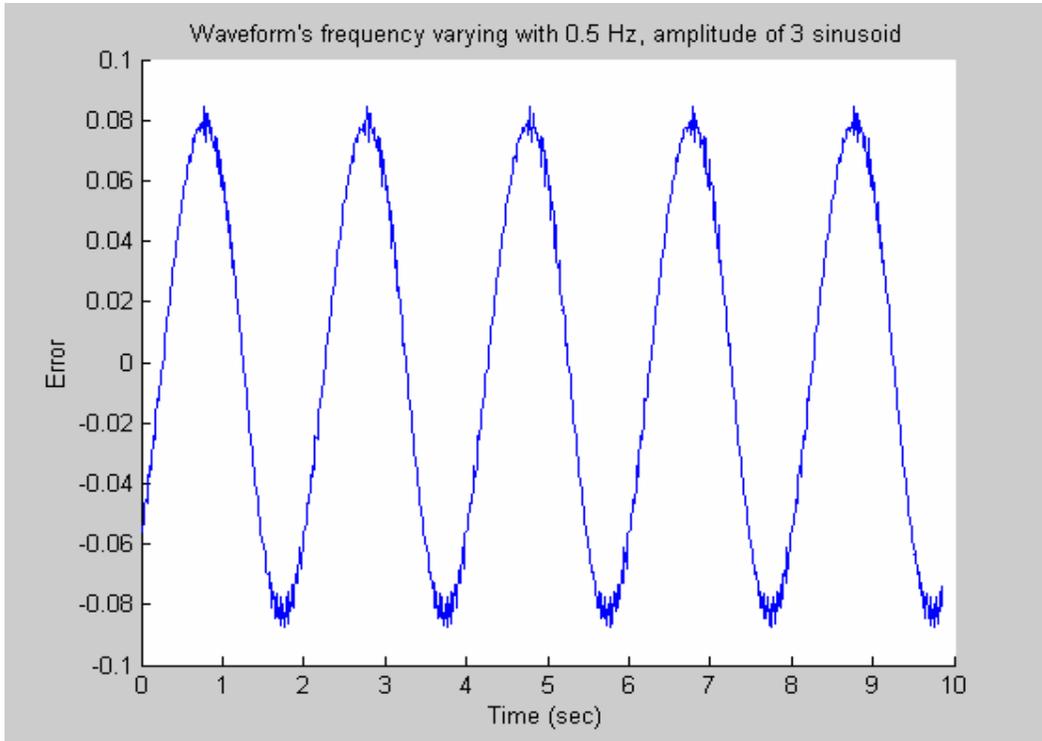


Figure 5-34 the error between the estimated frequency and the exact one for input waveform with  $f=0.5\text{Hz}$ ,  $\text{Amp}=3$  sinusoidal changing frequency (original algorithm)

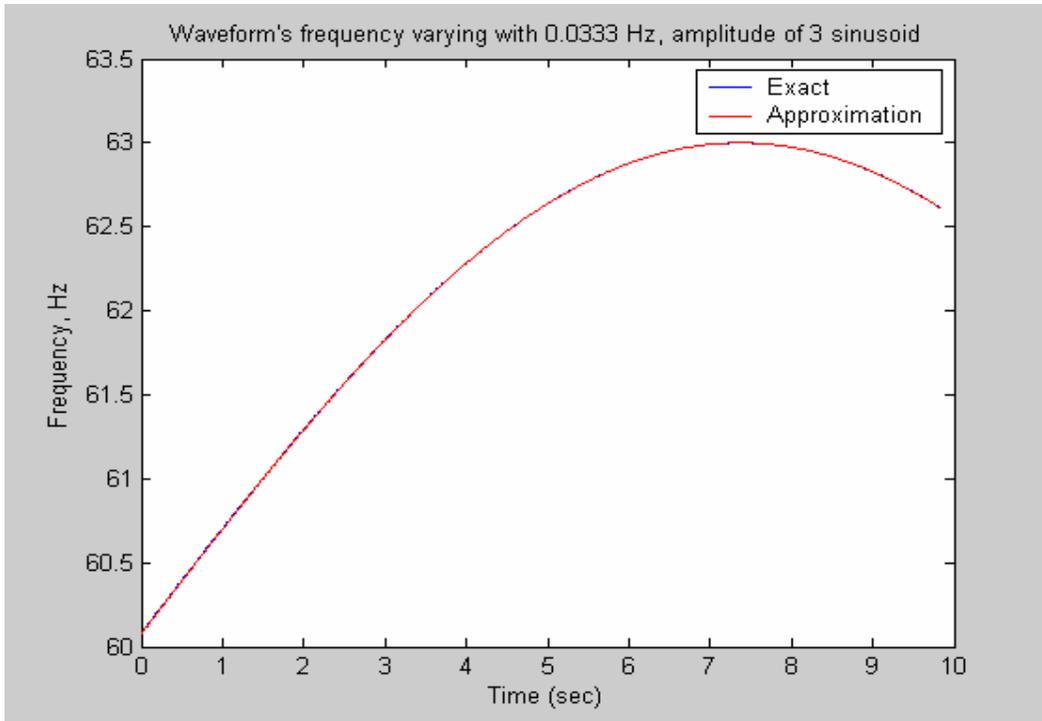


Figure 5-35 the estimated frequency for input waveform with  $f=0.0333\text{Hz}$ ,  $\text{Amp}=3$  sinusoidal changing frequency and the exact frequency resulted from the formula (the updated algorithm with 144-average approach)

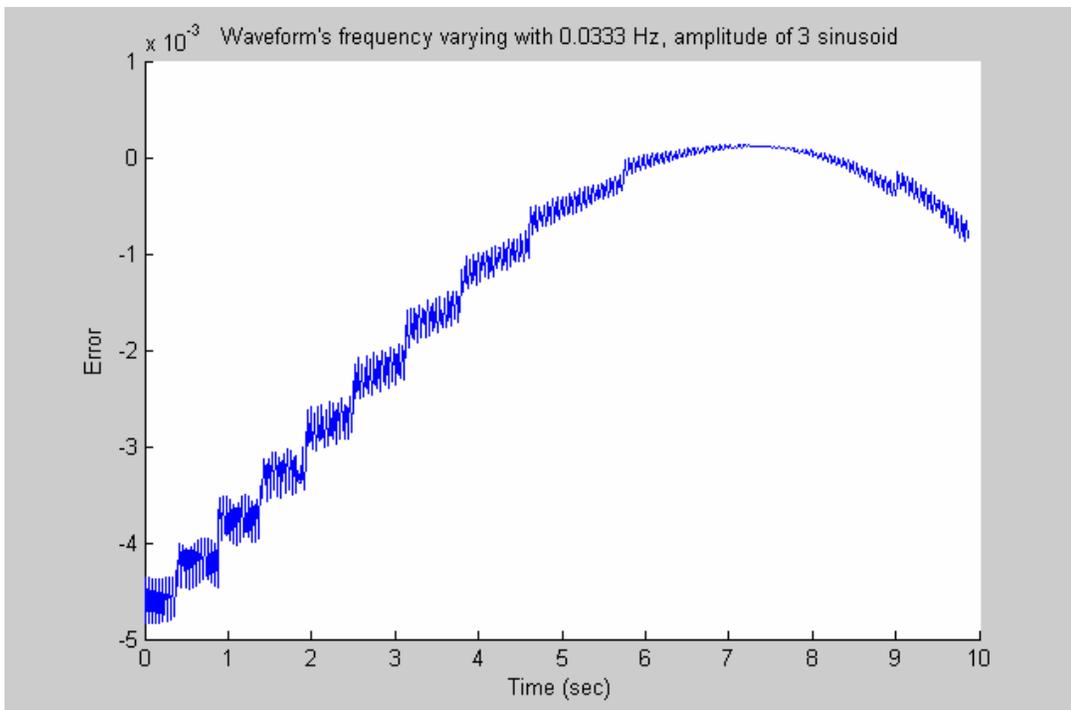


Figure 5-36 the error between the estimated frequency and the exact one for input waveform with  $f=0.0333\text{Hz}$ ,  $\text{Amp}=3$  sinusoidal changing frequency (the updated algorithm with 144-average approach)

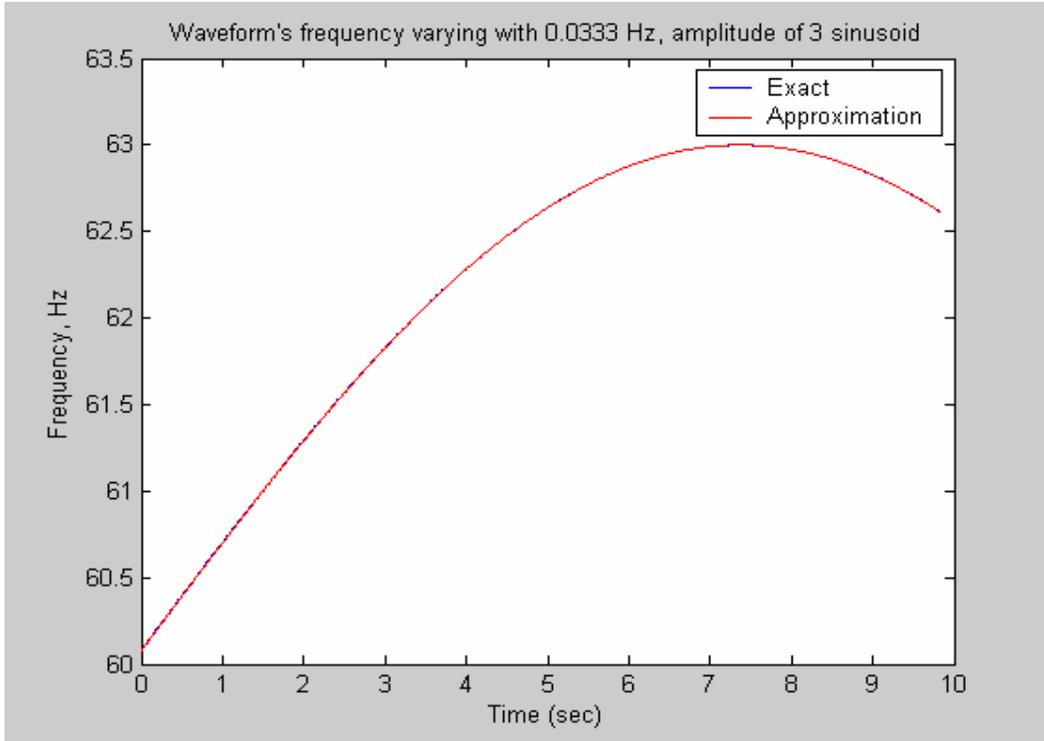


Figure 5-37 the estimated frequency for input waveform with  $f=0.0333\text{Hz}$ ,  $\text{Amp}=3$  sinusoidal changing frequency and the exact frequency resulted from the formula (original algorithm)

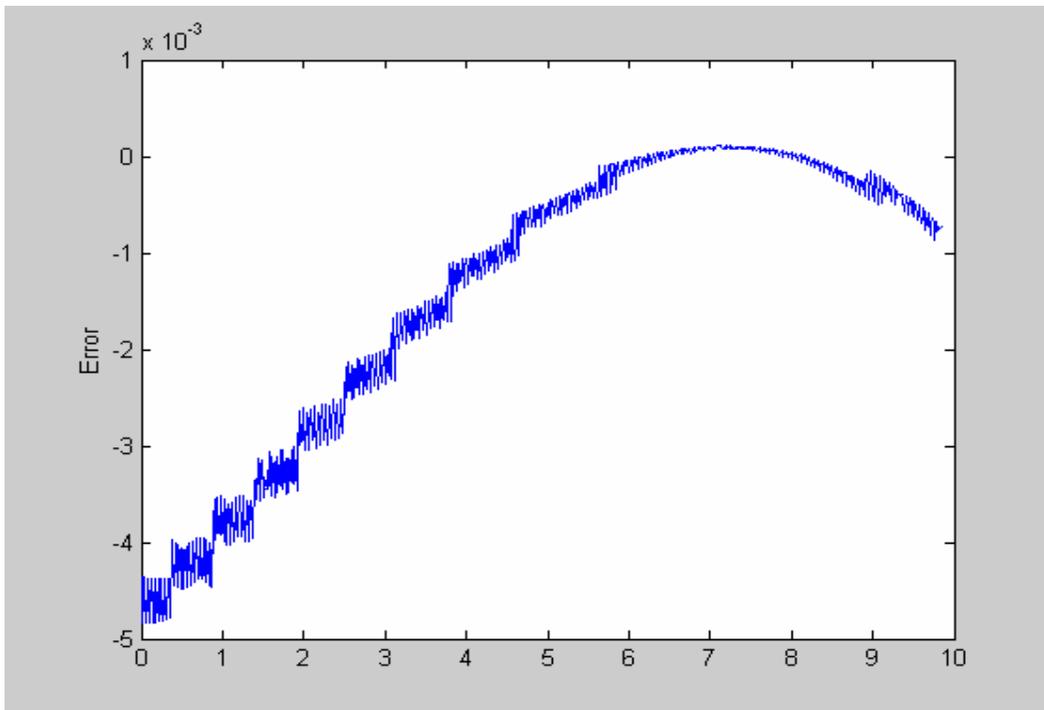


Figure 5-38 the error between the estimated frequency and the exact one for input waveform with  $f=0.0333\text{Hz}$ ,  $\text{Amp}=3$  sinusoidal changing frequency (original algorithm)

### 5.4 Multi-resampling Approach

For original algorithm, resampling greatly improves the accuracy. Resampling is based on the fact that the time-derivative relationship between phasor angle and waveform frequency becomes more accurate as the system frequency approaches the frequency assumed for establishing the sampling rate. Thus, **multiple resampling** may bring about even higher accuracy (as Section 5.4.1 demonstrates.) For multiple resampling, the resampling is done multiple times instead of just once after the initial estimation. More specifically, the details on the multiple resampling are discussed below:

After the phasor angles of the sampled data are computed, Eq.(2-26), Eq.(2-29) and Eq.(2-30) are employed to obtain the first frequency deviation  $\Delta_1 f$  and the first estimated frequency  $f_1 = f_0 + \Delta_1 f$  ( where  $f_0$  is the nominal frequency 60Hz). Then the first estimated frequency  $f_1$  is used to resample the initial sampled input data according to the resampling technique illustrated in Figure 5-7.

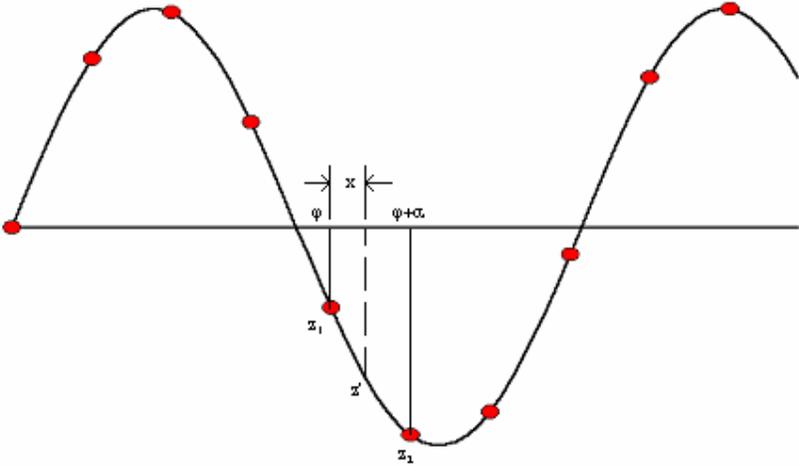


Figure 5-39 Illustration of Resampling Technique

In Figure 5-39 the values of  $z_1$  and  $z_2$  can be represented by the following two equations

$$z_1 = Z_m \sin(\varphi) \quad (5-1)$$

$$z_2 = Z_m \sin(\varphi + \alpha) = Z_m \sin \varphi \cos \alpha + Z_m \cos \varphi \sin \alpha \quad (5-2)$$

where  $Z_m$  is the amplitude of the waveform

$\varphi$  is a sample instant and is an arbitrary known value

$\alpha$  is the interval between two samples at the new frequency and is

$$2\pi f_{new} / (Nf_0)$$

Combining Eq. (5-1) and Eq. (5-2) results in

$$Z_m \cos \varphi = \frac{(z_2 - z_1 \cos \alpha)}{\sin \alpha} \quad (5-3)$$

Let  $x$  be the fractional distance between  $z_1$  and  $z_2$ , the resampled point  $z'$  is then given by

$$\begin{aligned} z' &= Z_m \sin(\varphi + x\alpha) \\ &= Z_m \sin \varphi \cos x\alpha + Z_m \cos \varphi \sin x\alpha \\ &= z_1 \cos x\alpha + (z_2 - z_1 \cos \alpha) \frac{\sin x\alpha}{\sin \alpha} \end{aligned} \quad (5-4)$$

After resampling points have been found, the phasor angles of the newly sampled data are computed and another estimation using Eq.(2-26), Eq.(2-29) and Eq.(2-30) is made to obtain the second estimated frequency deviation  $\Delta_2 f$  after the first resampling, and the second estimated frequency  $f_2$ .

$$f_2 = f_1 + \Delta_2 f = f_0 + \Delta_1 f + \Delta_2 f.$$

Then the second estimated frequency  $f_2$  is used to resample once again the initially sampled input data according to the same resampling technique illustrated in Figure 5-39. After resampling points have been found, the phasor angles of the newly sampled data are computed and another estimation using Eq. (2-26), Eq. (2-29) and Eq. (2-30) is made to obtain the third estimated frequency deviation  $\Delta_3 f$  after the second resampling and the third estimated frequency  $f_3$ :

$$f_3 = f_2 + \Delta_3 f = f_1 + \Delta_2 f + \Delta_3 f = f_0 + \Delta_1 f + \Delta_2 f + \Delta_3 f.$$

If we just do twice resampling, then  $f_3$  will be the final estimated frequency. You can also do

one more time resampling as what has been done in the 3<sup>rd</sup> resampling case. Then what you need to do is to use the third estimated frequency  $f_3$  to resample once again the initial sampled input data according to the same resampling technique illustrated in Figure 5-39. After resampling points have been found, the phasor angles of the new sampled data are computed and another estimation using Eq.(2-26), Eq.(2-29) and Eq.(2-30) is made to obtain the fourth estimated frequency deviation  $\Delta_4 f$  after the third resampling, and the third estimated frequency  $f_4$ :

$$f_4 = f_3 + \Delta_4 f = f_2 + \Delta_3 f + \Delta_4 f = f_1 + \Delta_2 f + \Delta_3 f + \Delta_4 f = f_0 + \Delta_1 f + \Delta_2 f + \Delta_3 f + \Delta_4 f .$$

For the 3<sup>rd</sup> resampling case,  $f_4$  is the final estimated frequency.

Of course, you can do the resampling more times according to the same procedures as what have been taken to do the first three.

#### 5.4.1 Results with Pure Sinusoidal Input

A significant improvement of the frequency estimation accuracy with pure sinusoidal input has been obtained after the multiple resampling has been employed, which can be clearly seen in Table 5-5.

frequency(Hz)	1resampling error (Hz)	2 resampling error (Hz)	3 resampling error (Hz)
51	2.159000E-01	2.728000E-01	2.82900E-01
52	1.420000E-02	1.030000E-02	9.31800E-03
52.1	1.370000E-02	1.015000E-02	9.49100E-03
52.2	8.318000E-03	6.000000E-06	0.00000E+00
52.3	2.246000E-03	5.000000E-06	0.00000E+00
52.4	1.980000E-03	4.000000E-06	0.00000E+00
52.5	2.340000E-04	1.000000E-06	0.00000E+00
52.9	2.260000E-04	1.000000E-06	0.00000E+00
53	2.160000E-04	0.000000E+00	0.00000E+00
54	9.900000E-05	0.000000E+00	0.00000E+00
55	2.800000E-05	0.000000E+00	0.00000E+00
56	7.000000E-05	0.000000E+00	0.00000E+00
57	8.200000E-05	0.000000E+00	0.00000E+00
57.5	7.100000E-05	0.000000E+00	0.00000E+00
58	5.000000E-05	0.000000E+00	0.00000E+00
58.5	2.800000E-05	0.000000E+00	0.00000E+00
59	1.400000E-05	0.000000E+00	0.00000E+00
59.5	4.000000E-06	0.000000E+00	0.00000E+00

60	0.000000E+00	0.000000E+00	0.00000E+00
60.5	5.000000E-06	0.000000E+00	0.00000E+00
61	1.600000E-05	0.000000E+00	0.00000E+00
61.5	3.000000E-05	0.000000E+00	0.00000E+00
62	4.700000E-05	0.000000E+00	0.00000E+00
62.5	5.600000E-05	0.000000E+00	0.00000E+00
63	5.900000E-05	0.000000E+00	0.00000E+00
64	3.900000E-05	0.000000E+00	0.00000E+00
65	2.800000E-05	0.000000E+00	0.00000E+00
66	1.070000E-04	0.000000E+00	0.00000E+00
67	1.380000E-04	0.000000E+00	0.00000E+00
68	1.170000E-04	0.000000E+00	0.00000E+00
69	5.400000E-05	0.000000E+00	0.00000E+00
70	3.900000E-05	0.000000E+00	0.00000E+00
71	1.450000E-04	0.000000E+00	0.00000E+00
72	1.920000E-04	0.000000E+00	0.00000E+00
73	1.610000E-04	0.000000E+00	0.00000E+00
74	1.190000E-04	0.000000E+00	0.00000E+00
75	4.100000E-05	0.000000E+00	0.00000E+00
76	1.510000E-04	0.000000E+00	0.00000E+00
77	1.700000E-04	0.000000E+00	0.00000E+00
78	2.270000E-04	1.000000E-06	0.00000E+00
79	1.870000E-04	0.000000E+00	0.00000E+00
80	3.500000E-05	0.000000E+00	0.00000E+00
81	1.210000E-04	0.000000E+00	0.00000E+00
82	2.860000E-04	1.000000E-06	0.00000E+00
83	3.430000E-04	1.000000E-06	0.00000E+00
84	2.290000E-04	1.000000E-06	0.00000E+00
85	6.900000E-05	0.000000E+00	0.00000E+00
86	2.100000E-04	0.000000E+00	0.00000E+00
87	4.030000E-04	1.000000E-06	0.00000E+00
88	4.300000E-04	1.000000E-06	0.00000E+00
89	2.590000E-04	1.000000E-06	0.00000E+00
90	8.900000E-05	0.000000E+00	0.00000E+00
91	2.930000E-04	1.000000E-06	0.00000E+00
92	4.810000E-04	1.000000E-06	0.00000E+00
93	4.380000E-04	1.000000E-06	0.00000E+00
94	2.530000E-04	0.000000E+00	0.00000E+00
95	9.700000E-05	0.000000E+00	0.00000E+00
96	3.110000E-04	1.000000E-06	0.00000E+00
97	4.550000E-04	1.000000E-06	0.00000E+00
98	3.790000E-04	1.000000E-06	0.00000E+00
99	2.070000E-04	0.000000E+00	0.00000E+00

100	8.600000E-05	0.000000E+00	0.00000E+00
101	2.980000E-04	1.000000E-06	0.00000E+00
102	3.930000E-04	1.000000E-06	0.00000E+00
103	2.720000E-04	1.000000E-06	0.00000E+00
104	1.800000E-04	0.000000E+00	0.00000E+00
105	6.900000E-05	0.000000E+00	0.00000E+00
106	3.020000E-04	1.000000E-06	0.00000E+00
107	3.380000E-04	1.000000E-06	0.00000E+00
108	3.800000E-04	1.000000E-06	0.00000E+00
109	2.620000E-04	0.000000E+00	0.00000E+00
110	8.200000E-05	0.000000E+00	0.00000E+00
111	2.950000E-04	1.000000E-06	0.00000E+00
112	3.720000E-04	1.000000E-06	0.00000E+00
113	5.130000E-04	1.000000E-06	0.00000E+00
114	3.340000E-04	1.000000E-06	0.00000E+00
115	7.800000E-05	0.000000E+00	0.00000E+00
116	2.170000E-04	0.000000E+00	0.00000E+00
117	4.820000E-04	1.000000E-06	0.00000E+00
118	5.290000E-04	1.000000E-06	0.00000E+00
119	3.780000E-04	1.000000E-06	0.00000E+00
121	3.390000E-04	1.000000E-06	0.00000E+00
125	1.240000E-04	0.000000E+00	0.00000E+00
130	1.160000E-04	0.000000E+00	0.00000E+00
135	9.700000E-05	0.000000E+00	0.00000E+00
140	7.800000E-05	0.000000E+00	0.00000E+00
145	1.730000E-04	0.000000E+00	0.00000E+00
150	1.220000E-04	0.000000E+00	0.00000E+00
155	1.400000E-04	0.000000E+00	0.00000E+00
160	1.230000E-04	0.000000E+00	0.00000E+00
165	9.000000E-05	0.000000E+00	0.00000E+00
170	9.900000E-05	0.000000E+00	0.00000E+00
175	6.400000E-05	0.000000E+00	0.00000E+00
185	1.680000E-04	0.000000E+00	0.00000E+00
190	1.370000E-04	0.000000E+00	0.00000E+00
191	2.647000E-01	1.000000E-06	1.00E-06
192	6.280000E-04	1.000000E-06	0.00E+00
193	4.000000E-01	8.920000E-04	2.00E-06
194	2.646000E-01	1.000000E-06	1.00E-06
195	2.500000E-01	1.380000E-04	1.00E-06
196	2.918000E-01	6.050000E-04	1.00E-06
197	2.740000E-01	3.700000E-04	1.00E-06
198	2.790000E-01	4.040000E-04	1.00E-06
199	4.200000E-01	1.090000E-03	3.00E-06

200	3.260000E-01	5.540000E-04	1.00E-06
201	2.720000E-01	5.000000E-04	1.00E-06
202	3.238000E-01	6.900000E-04	1.00E-06
203	3.292000E-01	8.000000E-04	2.00E-06
204	3.130000E-04	1.000000E-06	0.00E+00
205	3.184000E-01	7.820000E-04	2.00E-06
206	3.745000E-01	8.680000E-04	2.00E-06
207	3.849000E-01	8.940000E-04	2.00E-06
208	3.955000E-01	9.910000E-04	2.00E-06
210	1.040000E-04	0.000000E+00	0.00E+00
215	3.856000E-01	9.910000E-04	2.00E-06
220	3.052000E-01	5.950000E-04	1.00E-06
230	1.223000E+02	9.940000E-02	1.14E-04

Table 5-5 frequency estimation error comparison: algorithm with once, twice and three times resamplings

In Table 5-5, the first column is the frequency of the input pure sinusoidal signal. The second column is the estimation error for the algorithm with only once resampling. The second and third columns are respectively the estimation error for the algorithm with twice and three times resampling. Table 5-5 clearly illustrates the improvement in the frequency estimation accuracy when multiple resampling is employed. This improvement can be summarized more specifically in the following aspects.

1) the range of the frequencies with zero estimation error:

The number of resampling	1	2	3
Range of 0-error frequency	Only at 60Hz	53 Hz ~ 77Hz	52.2Hz ~190Hz

Table 5-6 Comparison of the range of frequencies with zero estimation error: algorithm with once, twice and three times resamplings

2) the estimation error for the frequencies between 51Hz ~52.9Hz

frequency(Hz)	1 resampling (Hz)	2 resamlings (Hz)	3 resamlings (Hz)
51	2.159000E-01	2.728000E-01	2.82900E-01
52	1.420000E-02	1.030000E-02	9.31800E-03
52.1	1.370000E-02	1.015000E-02	9.49100E-03
52.2	8.318000E-03	6.000000E-06	0.00000E+00
52.3	2.246000E-03	5.000000E-06	0.00000E+00
52.4	1.980000E-03	4.000000E-06	0.00000E+00
52.5	2.340000E-04	1.000000E-06	0.00000E+00
52.9	2.260000E-04	1.000000E-06	0.00000E+00

Table 5-7 Error Comparison for frequencies between 51Hz and 52.9Hz: algorithm with once, twice and three times resamplings

3) Comparing once resampling and twice resamplings for frequencies between 78Hz and

190 Hz, the error for twice resampling is either zero or  $1.00E-06$  with the expectation of 120 Hz and 180Hz while the error for once resampling is between  $3.5E-5$ (80Hz) and  $5.29E-4$ (118Hz)

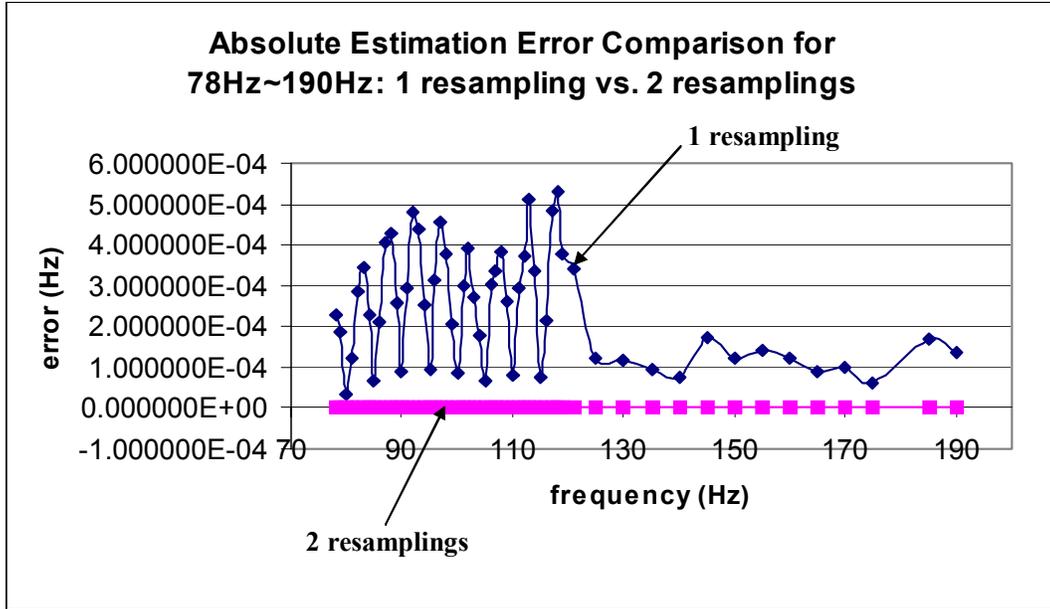


Figure 5-40 comparison of frequency estimation error for frequencies between 78Hz and 190Hz (algorithm with once and twice resamplings)

4) For the frequencies between 191Hz and 220 Hz, we can still see the significant improvement as shown in Figure 5-41 and Figure 5-42.

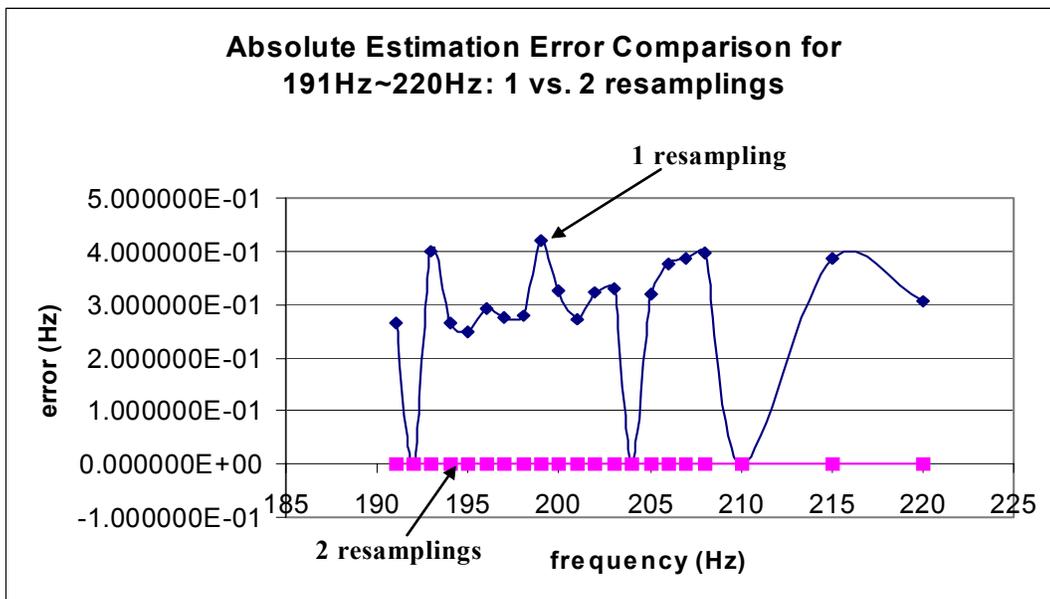


Figure 5-41 comparison of frequency estimation error for frequencies between 191Hz and 220Hz (algorithm with once and twice resamplings)

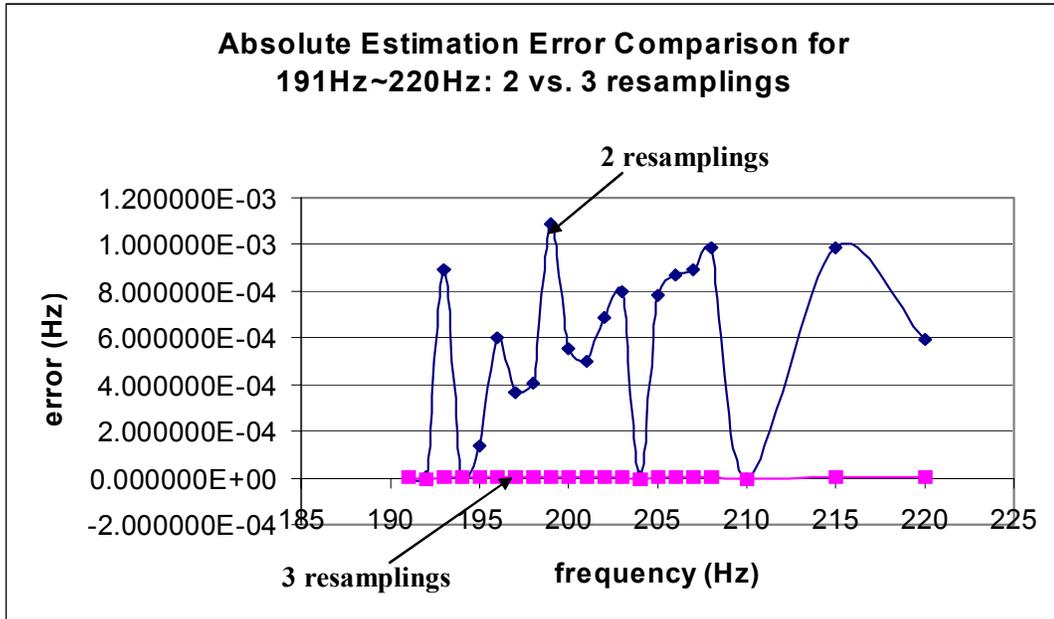


Figure 5-42 Estimation comparison of frequency estimation error for frequencies between 191Hz and 220Hz (algorithm with twice and three times resamplings)

### 5.4.2 Test with Input That Contains Harmonic Noise

Since the multiple resampling improves the frequency estimation accuracy significantly as shown in section 5.4.1, one wonders if the difference will be as significant if the input is not a pure sinusoidal waveform. As shown next the results for input that contains harmonic noise shows no big difference. The results with input with a variable frequency will be displayed in the next section.

For comparison, the base frequencies, the harmonic components and their percentage used to do the test are the same as those used to test the original algorithm (the results shown in Chapter Three).

Harm No.(percentage)	Original (Hz)	2 <sup>nd</sup> resampling (Hz)	3 <sup>rd</sup> resampling (Hz)
DC (10%)	3.05000E-04	3.08000E-04	3.11000E-04
3(10%)	3.44000E-04	3.41000E-04	3.45000E-04
5(5%)	1.61000E-04	1.58000E-04	1.63000E-04
7(5%)	1.42000E-04	1.56000E-04	1.55000E-04
9(5%)	1.24000E-04	1.44000E-04	1.43000E-04
20kHz (2%)	2.88700E-03	2.88800E-03	2.89800E-03

Table 5-8 the frequency estimation error comparison with different harmonics present at the base frequency of 59.5Hz: updated algorithm with twice resampling, updated algorithm with three times resampling and original algorithm

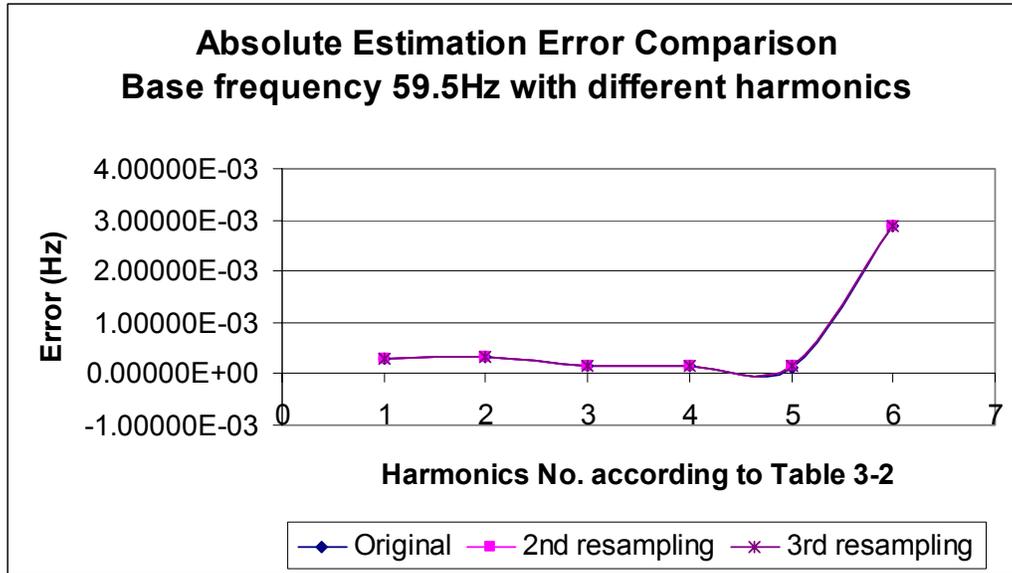


Figure 5-43 the frequency estimation error comparison with different harmonics present at the base frequency of 59.5Hz: updated algorithm with twice resampling, updated algorithm with three times resampling and original algorithm

Harm No.(percentage)	Original (Hz)	2 <sup>nd</sup> resampling (Hz)	3 <sup>rd</sup> resampling (Hz)
DC (10%)	0	0.00000E+00	0.00000E+00
3(10%)	0	0.00000E+00	0.00000E+00
5(5%)	0	0.00000E+00	0.00000E+00
7(5%)	0	0.00000E+00	0.00000E+00
9(5%)	0	0.00000E+00	0.00000E+00
20kHz (2%)	1.33800E-03	1.33800E-03	1.33800E-03

Table 5-9 the frequency estimation error comparison with different harmonics present at the base frequency of 60Hz: updated algorithm with twice resampling, updated algorithm with three times resampling and original algorithm

Harm No.(percentage)	Original (Hz)	2 <sup>nd</sup> resampling (Hz)	3 <sup>rd</sup> resampling (Hz)
DC (10%)	3.15000E-04	3.17000E-04	3.17000E-04
3(10%)	3.35000E-04	3.54000E-04	3.54000E-04
5(5%)	1.55000E-04	1.70000E-04	1.69000E-04
7(5%)	1.66000E-04	1.77000E-04	1.75000E-04
9(5%)	1.89000E-04	1.94000E-04	1.91000E-04
20kHz (2%)	2.35700E-03	2.38700E-03	2.38800E-03

Table 5-10 the frequency estimation error comparison with different harmonics present at the base frequency of 60.5Hz: updated algorithm with twice resampling, updated algorithm with three times resampling and original algorithm

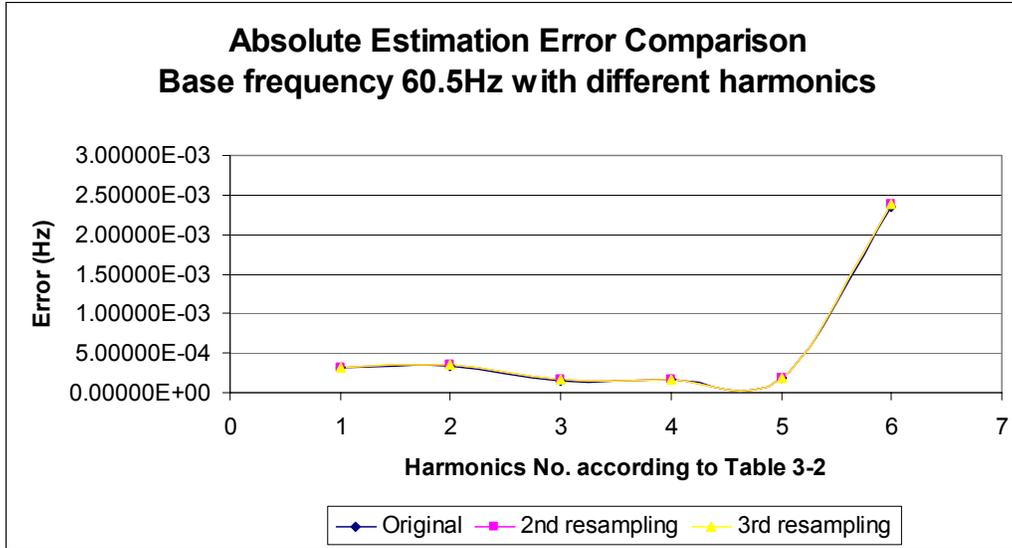


Figure 5-44 the frequency estimation error comparison with different harmonics present at the base frequency of 60.5Hz: updated algorithm with twice resampling, updated algorithm with three times resampling and original algorithm

### 5.4.3 Test with Input That Has a Variable Frequency

This section considers the sensitivity of the updated algorithm with multiple resampling (2<sup>nd</sup> resampling case was tested) to the change of frequency. For comparison, the same two cases of the changing frequency input were studied as those tested with the original algorithm in Chapter Three.

#### 5.4.3.1 Test with input for which frequency changes as a ramp function

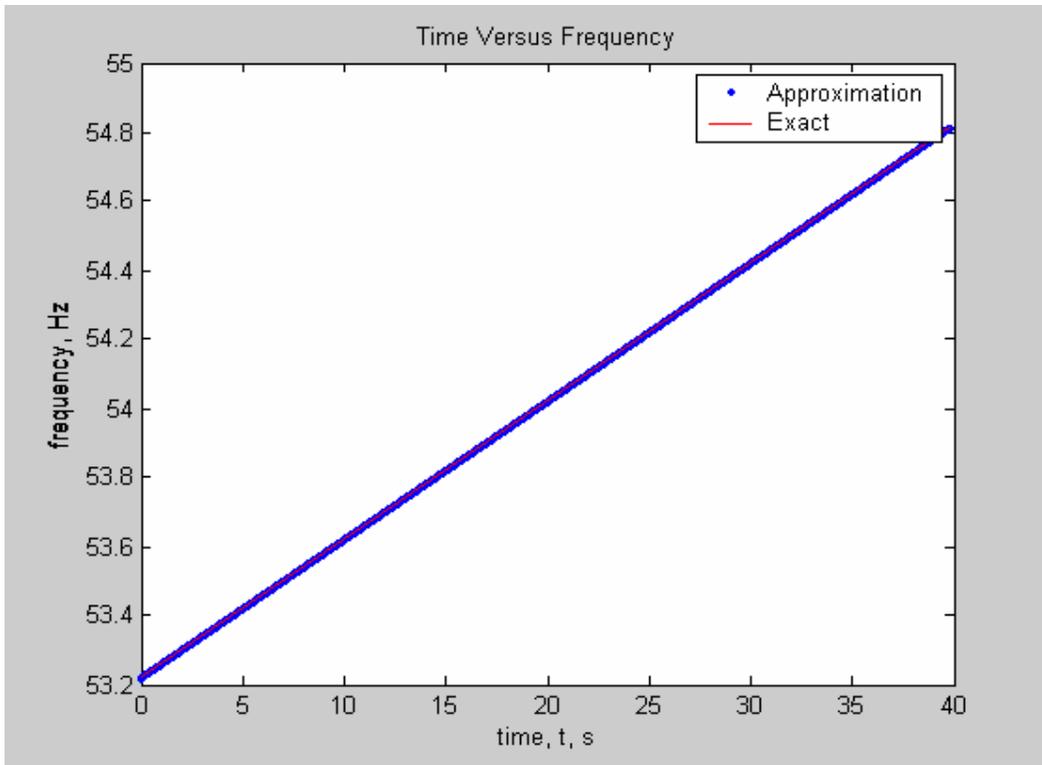


Figure 5-45 the estimated frequency for input waveform with frequency changing as a Ramp function with a rate of .04 Hz/sec (53.2Hz~54.8Hz) and the exact frequency resulted from the formula (the updated algorithm with 2<sup>nd</sup> resampling)

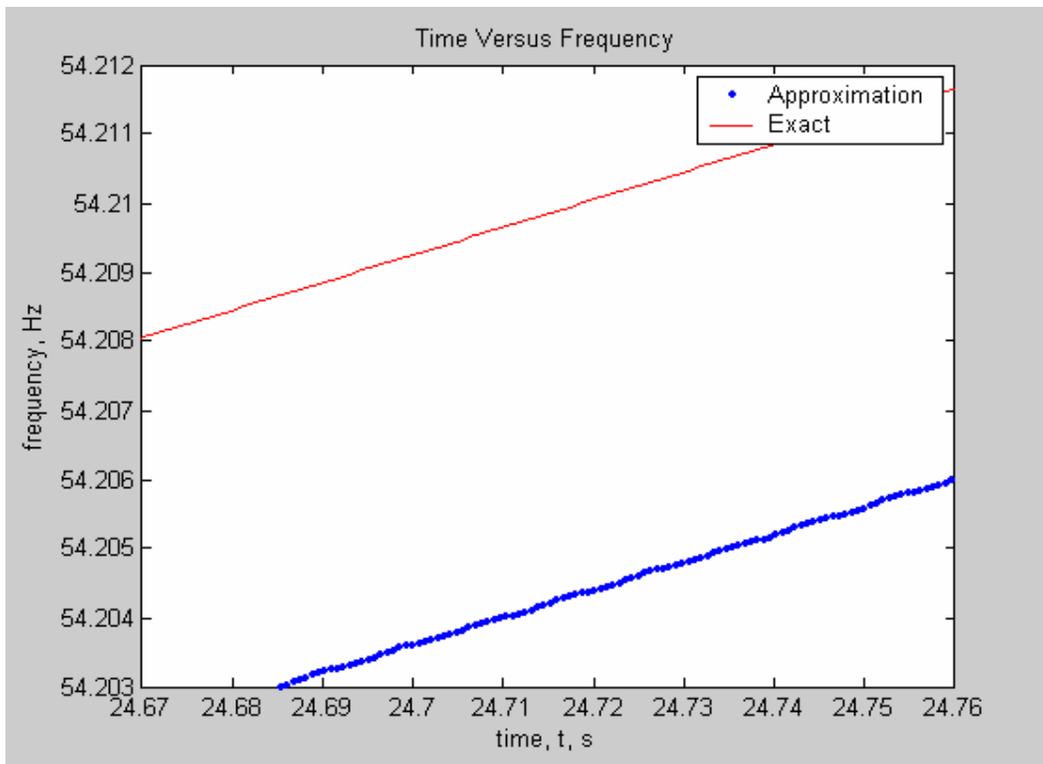


Figure 5-46 a zoomed in part of Figure 5-45

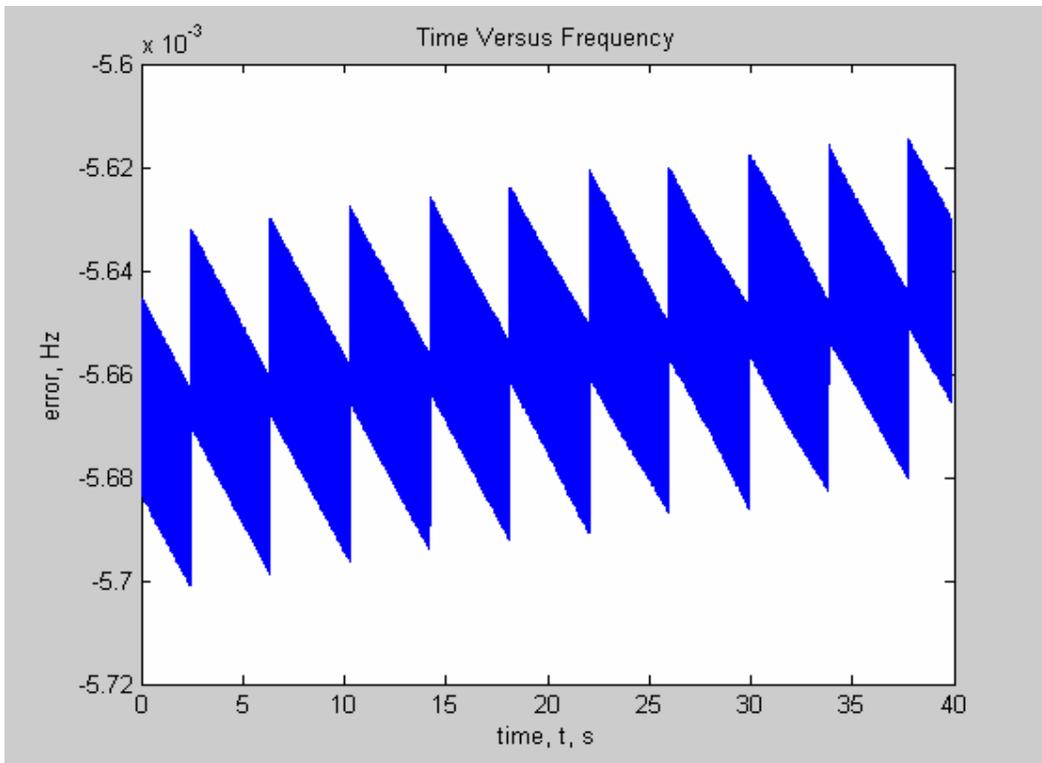


Figure 5-47 the error between the estimated frequency for input waveform with frequency changing as a Ramp function with a rate of .04 Hz/sec and the exact frequency resulted from the formula (the updated algorithm with 2<sup>nd</sup> resampling)

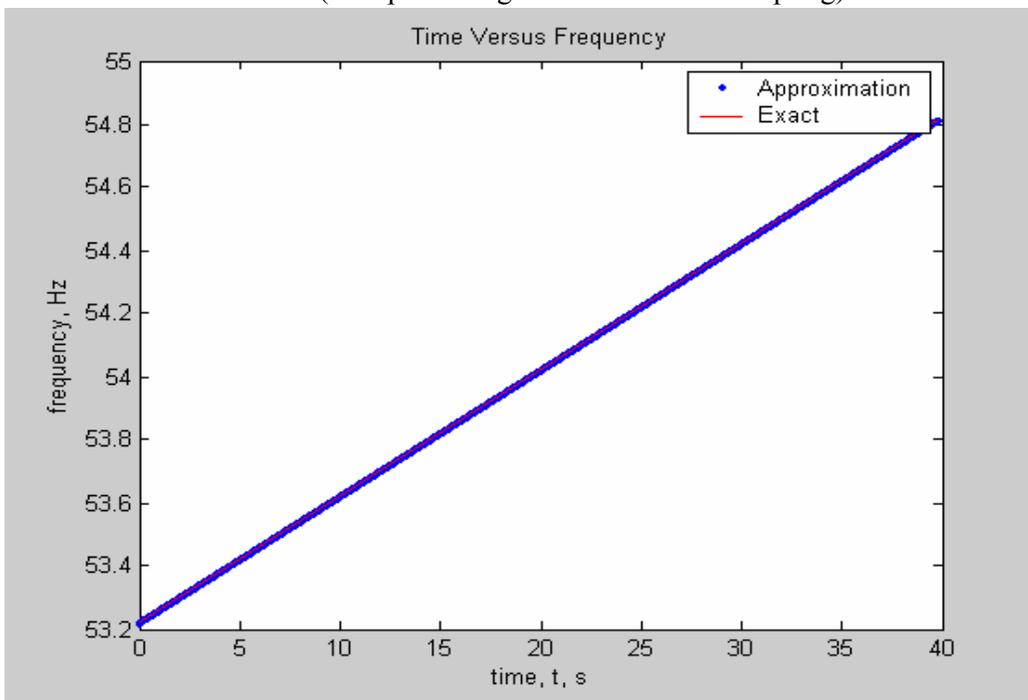


Figure 5-48 the estimated frequency for input waveform with frequency changing as a Ramp function with a rate of .04 Hz/sec (53.2Hz~54.8Hz) and the exact frequency resulted from the formula (original algorithm)

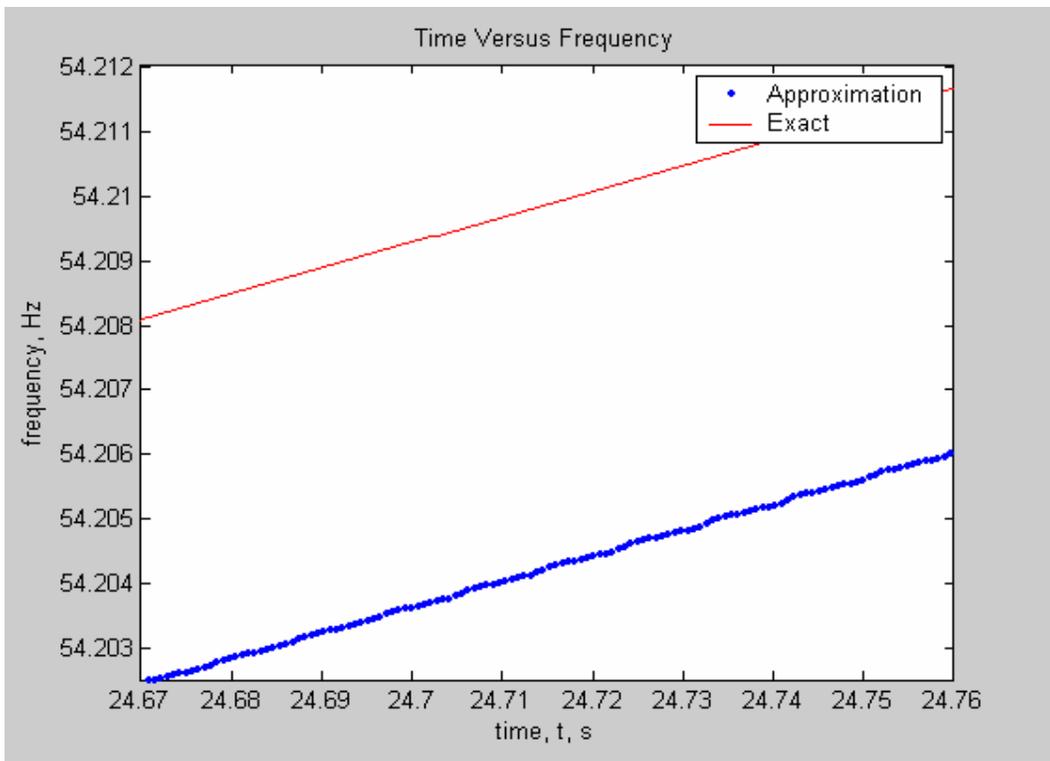


Figure 5-49 a zoomed in part of Figure 5-48

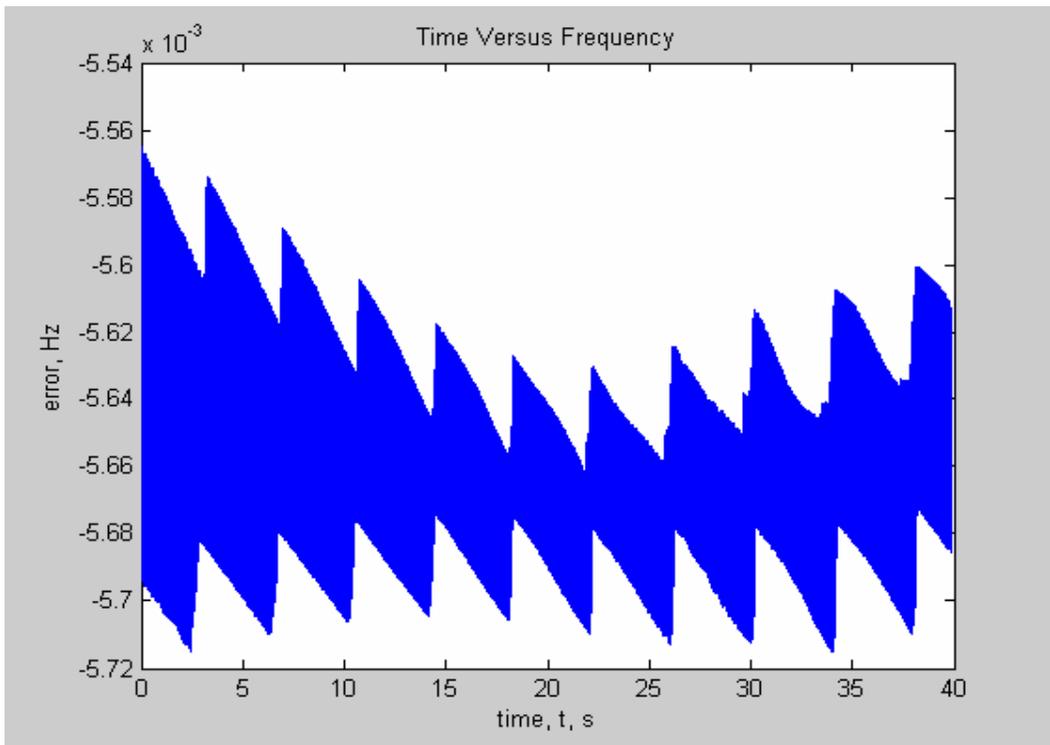


Figure 5-50 the error between the estimated frequency for input waveform with frequency changing as a Ramp function with a rate of .04 Hz/sec and the exact frequency resulted from the formula (original algorithm)

Comparing Figure 5-47 and Figure 5-50 then we can see that for the ramp change rate of 0.04Hz/s the difference between the estimated frequency and the exact frequency decreased only a little bit after the 2nd resampling was used.

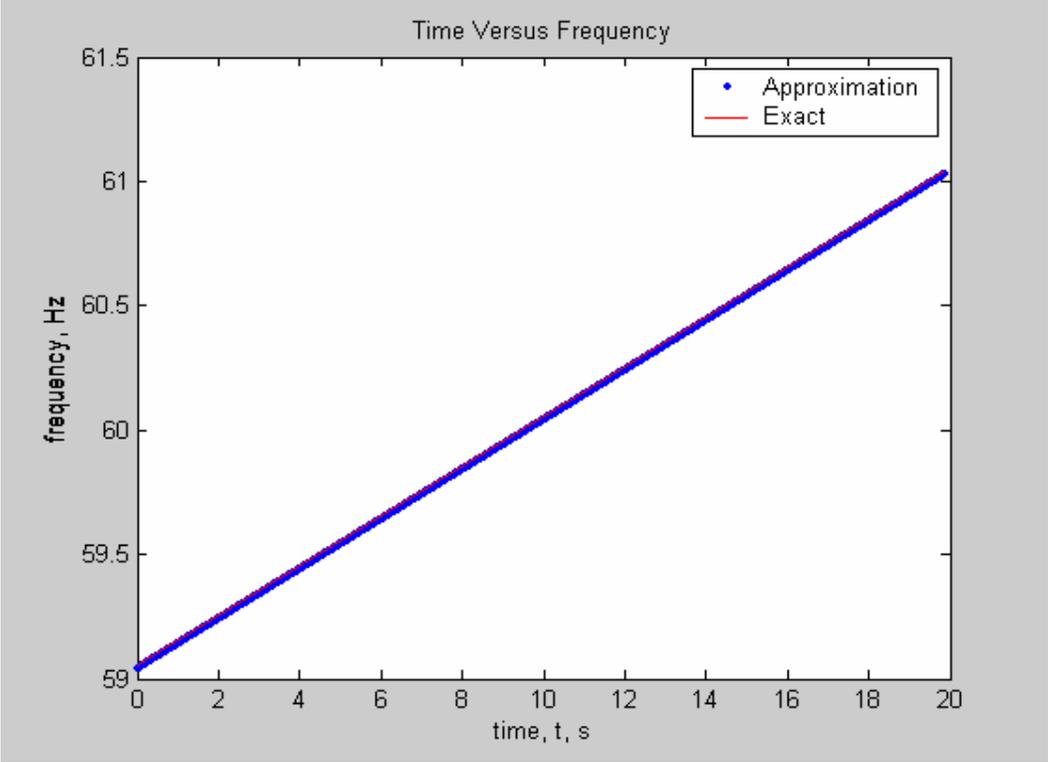


Figure 5-51 the estimated frequency for input waveform with frequency changing as a Ramp function with a rate of .1 Hz/sec (59Hz~61Hz) and the exact frequency resulted from the formula (the updated algorithm with 2nd resampling)

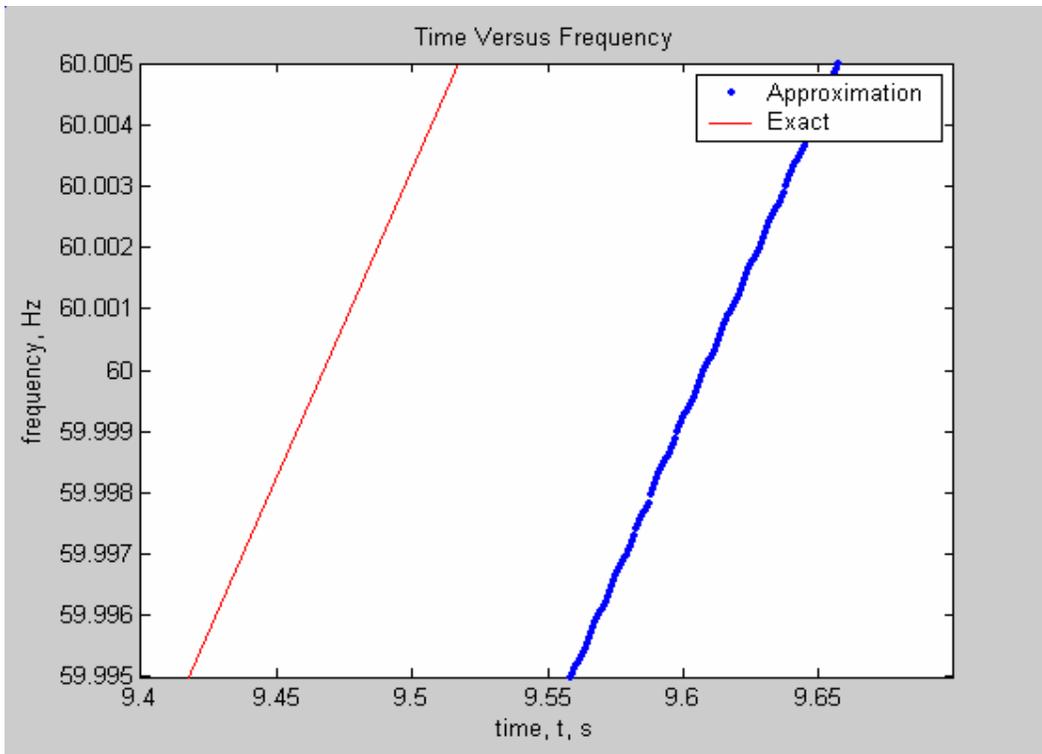


Figure 5-52 a zoomed in part of Figure 5-51

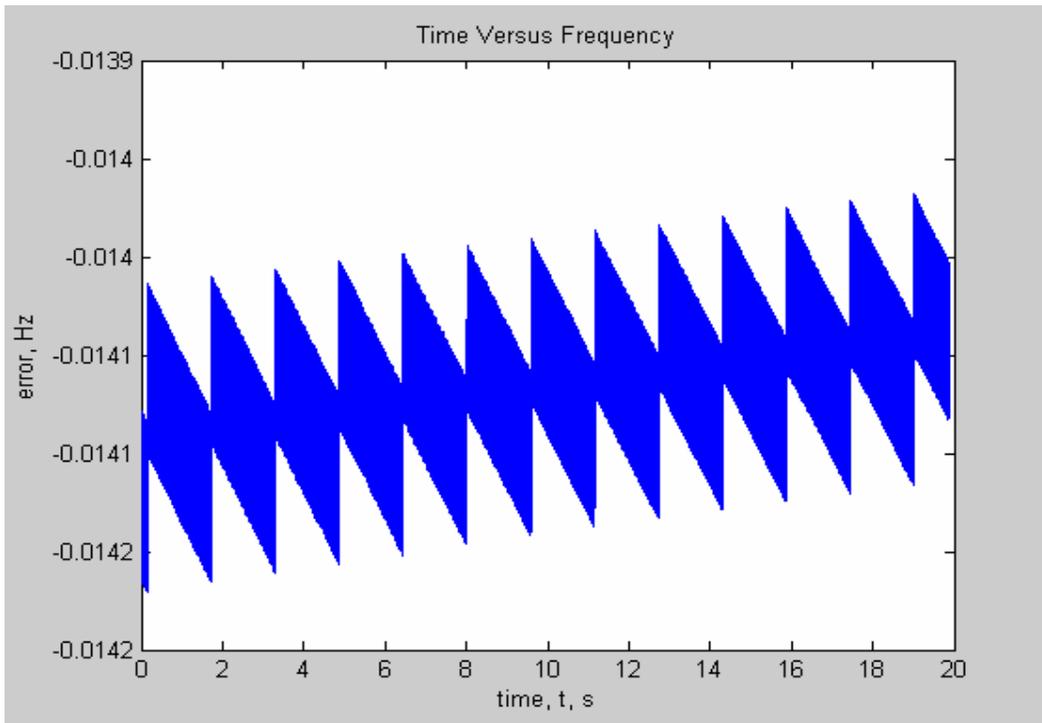


Figure 5-53 the error between the estimated frequency for input waveform with frequency changing as a Ramp function with a rate of .1 Hz/sec and the exact frequency resulted from the formula (the updated algorithm with 2nd resampling)

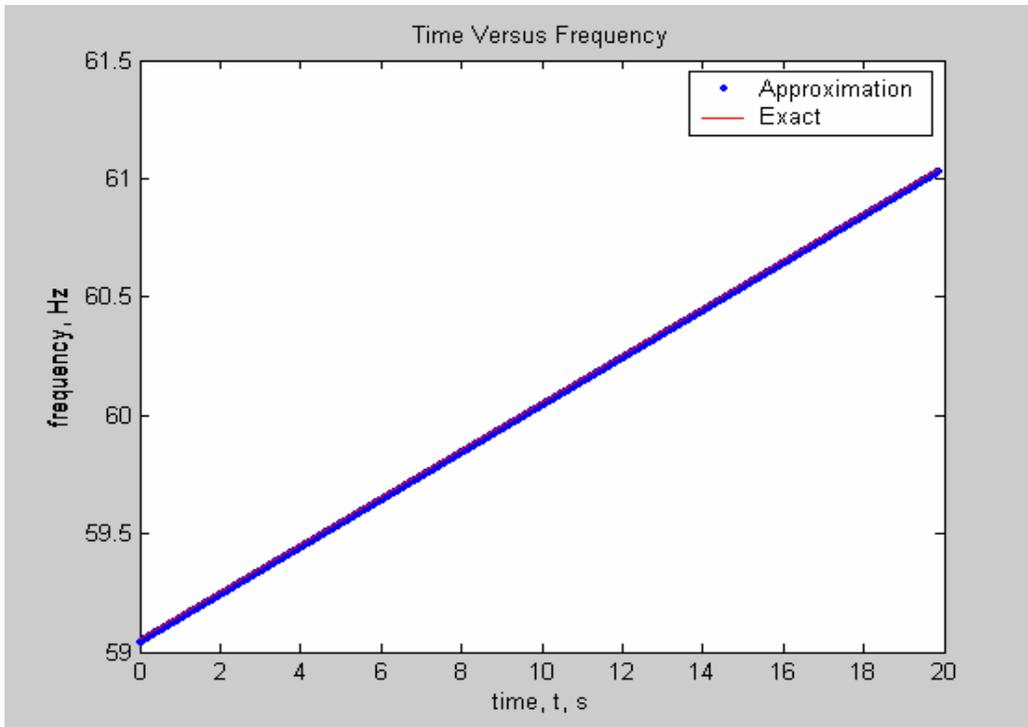


Figure 5-54 the estimated frequency for input waveform with frequency changing as a Ramp function with a rate of .1 Hz/sec (59Hz~61Hz) and the exact frequency resulted from the formula (original algorithm)

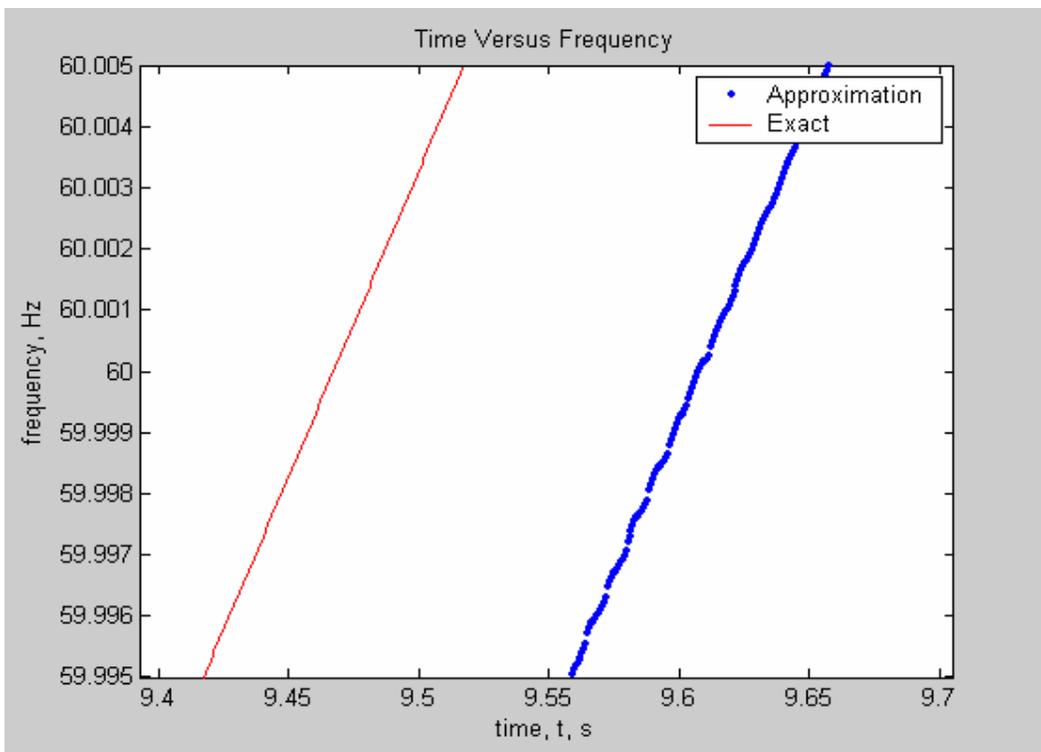


Figure 5-55 a zoomed in part of Figure 5-54

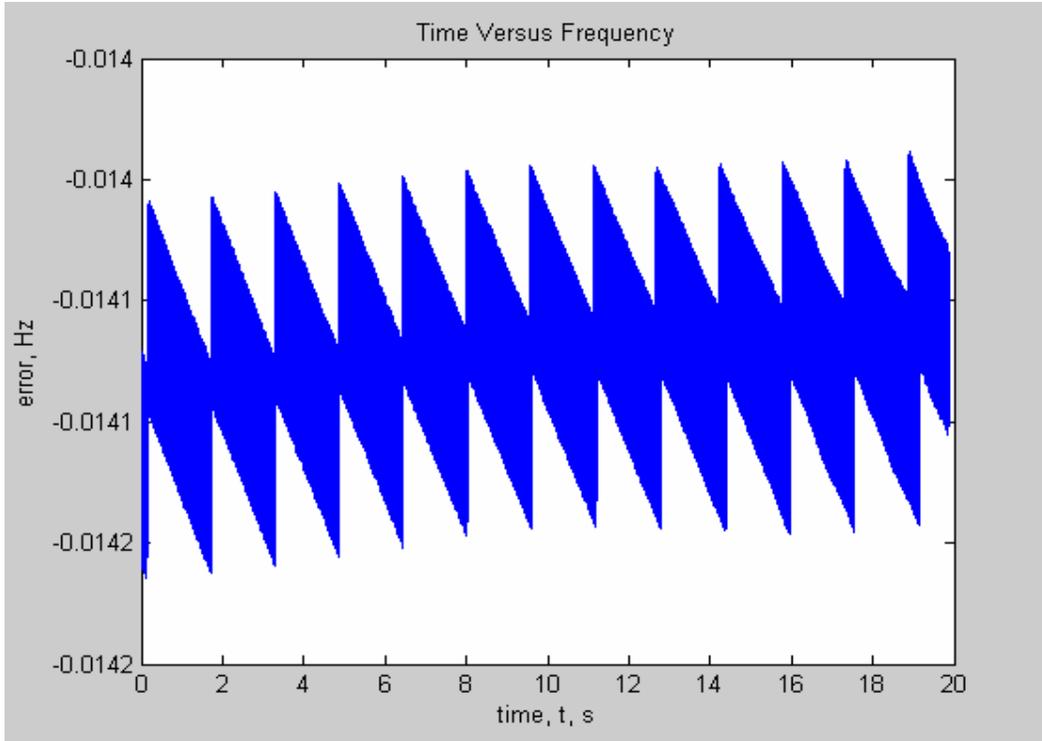


Figure 5-56 the error between the estimated frequency for input waveform with frequency changing as a Ramp function with a rate of .1 Hz/sec and the exact frequency resulted from the formula (original algorithm)

Comparing Figure 5-53 and Figure 5-56 then we can see that for the ramp change of 0.1Hz/s the difference between the estimated frequency and the exact frequency almost remained the same before and after the 2nd resampling was used.

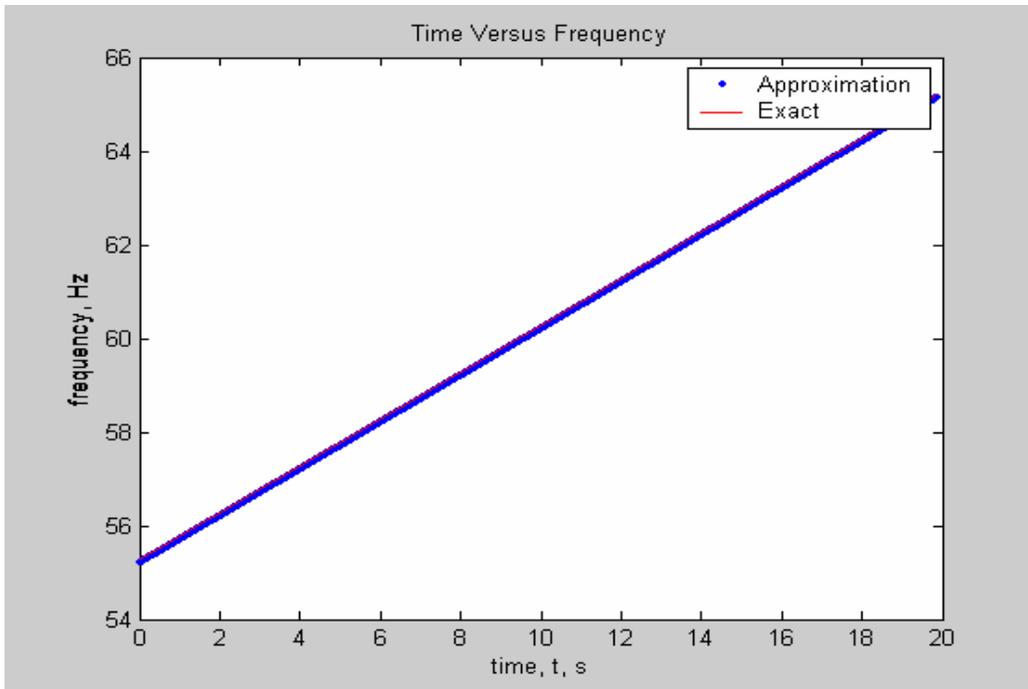


Figure 5-57 the estimated frequency for input waveform with frequency changing as a Ramp function with a rate of .5 Hz/sec (55Hz~65Hz) and the exact frequency resulted from the formula (the updated algorithm with 2<sup>nd</sup> resampling)

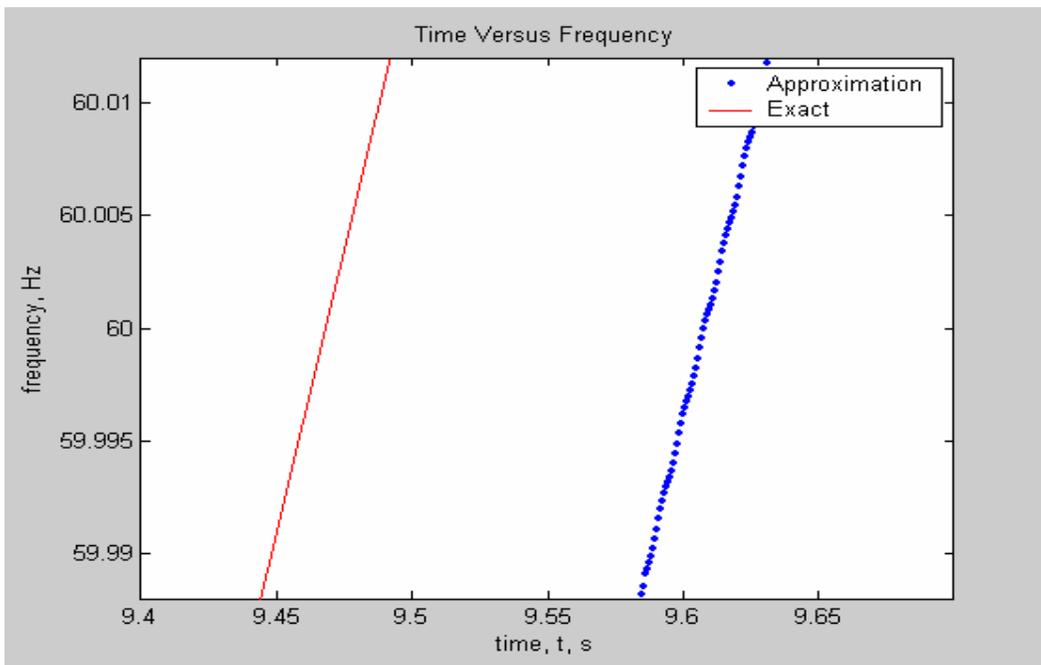


Figure 5-58 a zoomed in part of Figure 5-57

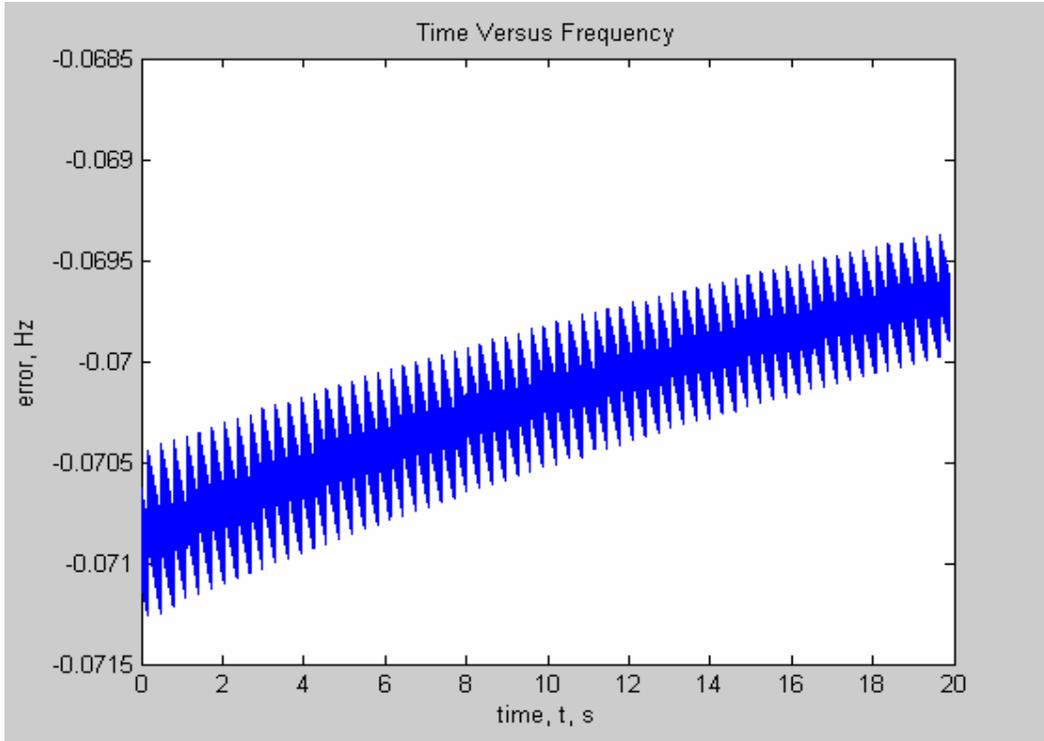


Figure 5-59 the error between the estimated frequency for input waveform with frequency changing as a Ramp function with a rate of .5 Hz/sec and the exact frequency resulted from the formula (the updated algorithm with 2<sup>nd</sup> resampling)

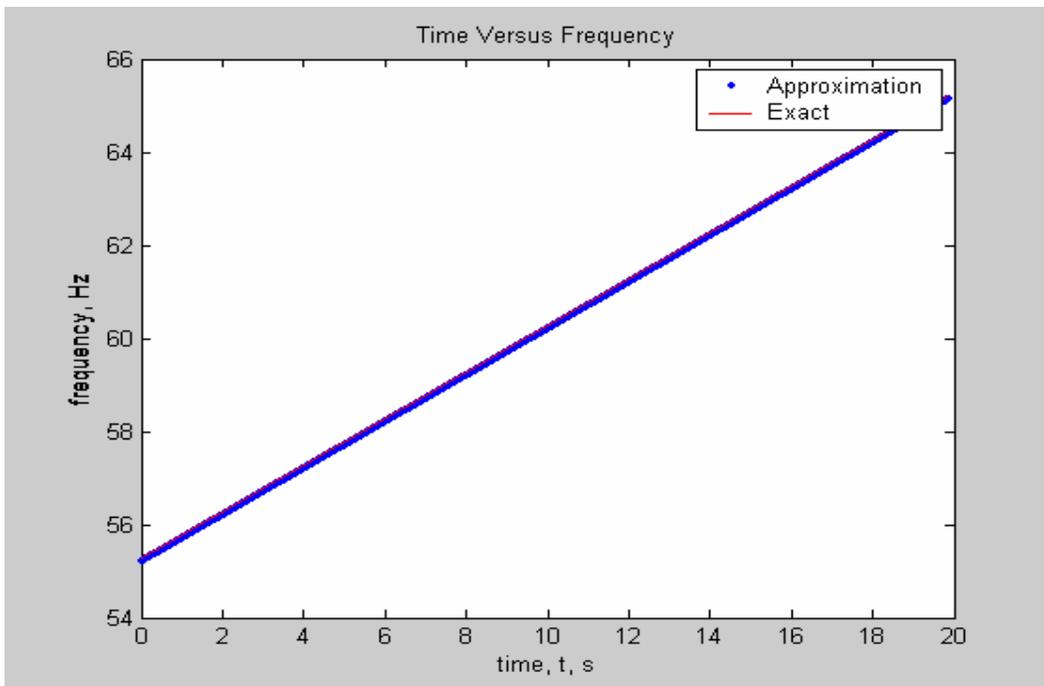


Figure 5-60 the estimated frequency for input waveform with frequency changing as a Ramp function with a rate of .5 Hz/sec (55Hz~65Hz) and the exact frequency resulted from the formula (original algorithm)

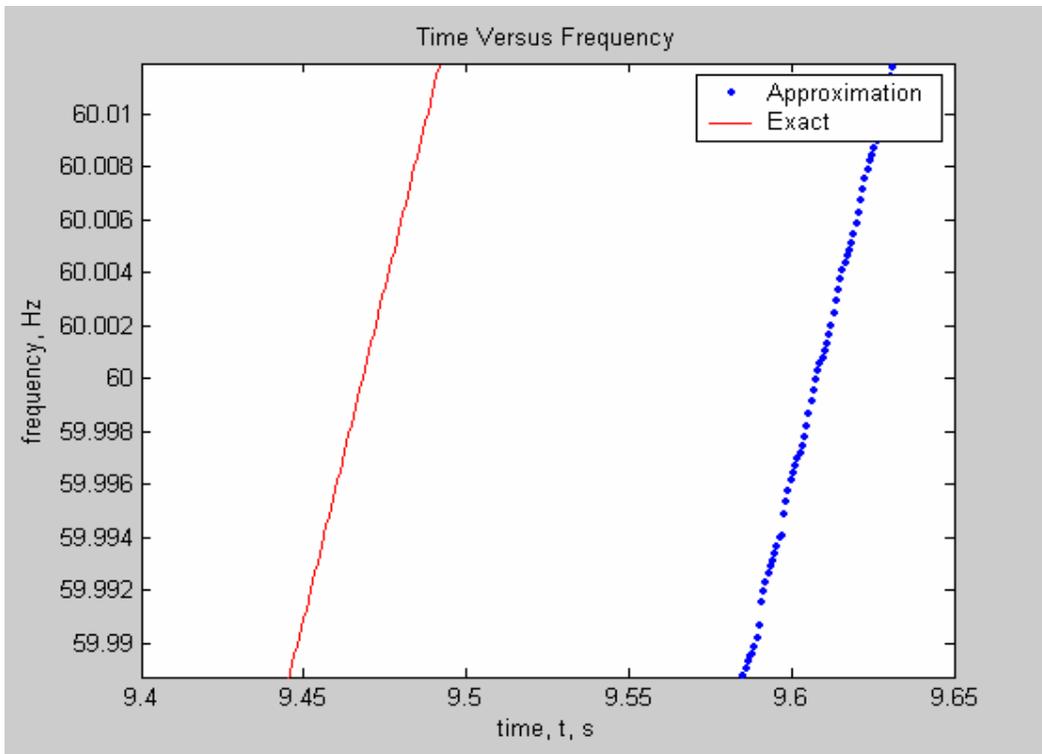


Figure 5-61 a zoomed in part of Figure 5-60

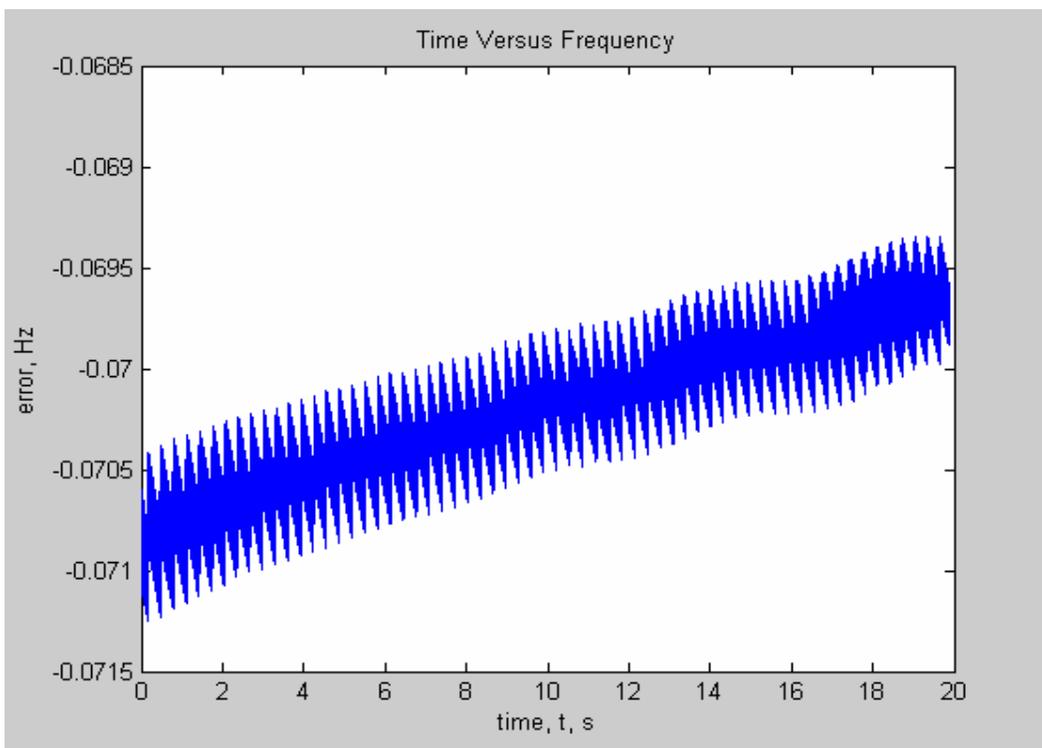


Figure 5-62 the error between the estimated frequency for input waveform with frequency changing as a Ramp function with a rate of .5 Hz/sec and the exact frequency resulted from the formula (original algorithm)

Comparing Figure 5-59 and Figure 5-62 then we can see that for the ramp change of 0.5Hz/s the difference between the estimated frequency and the exact frequency remained almost the same after the 2nd resampling was used.

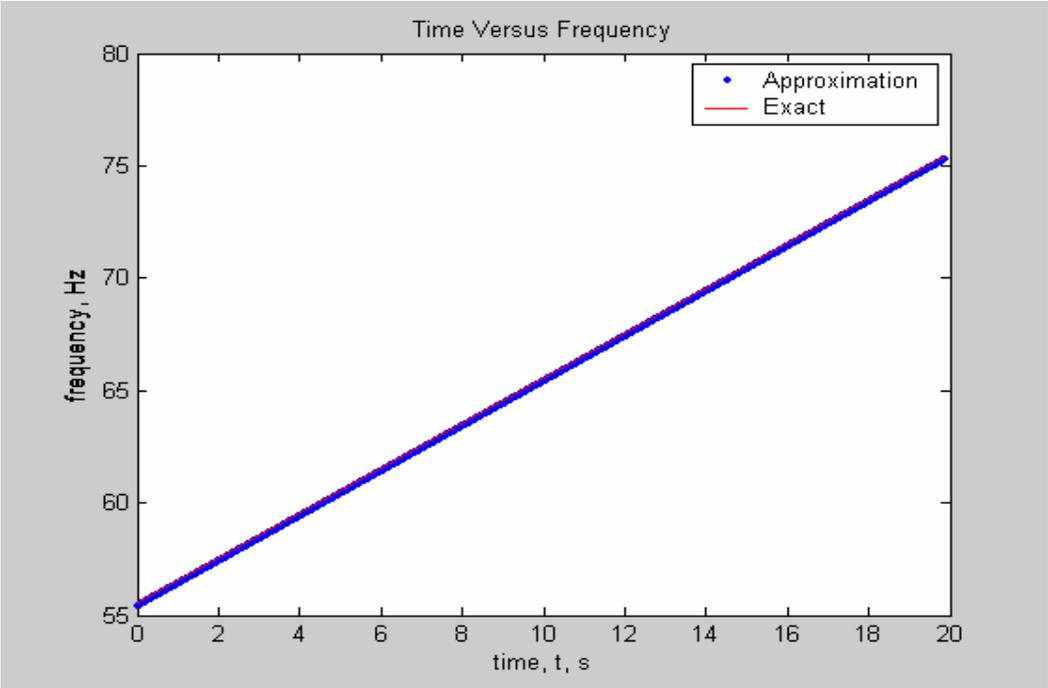


Figure 5-63 the estimated frequency for input waveform with frequency changing as a Ramp function with a rate of 1 Hz/sec (55Hz~75Hz) and the exact frequency resulted from the formula (the updated algorithm with 2<sup>nd</sup> resampling)

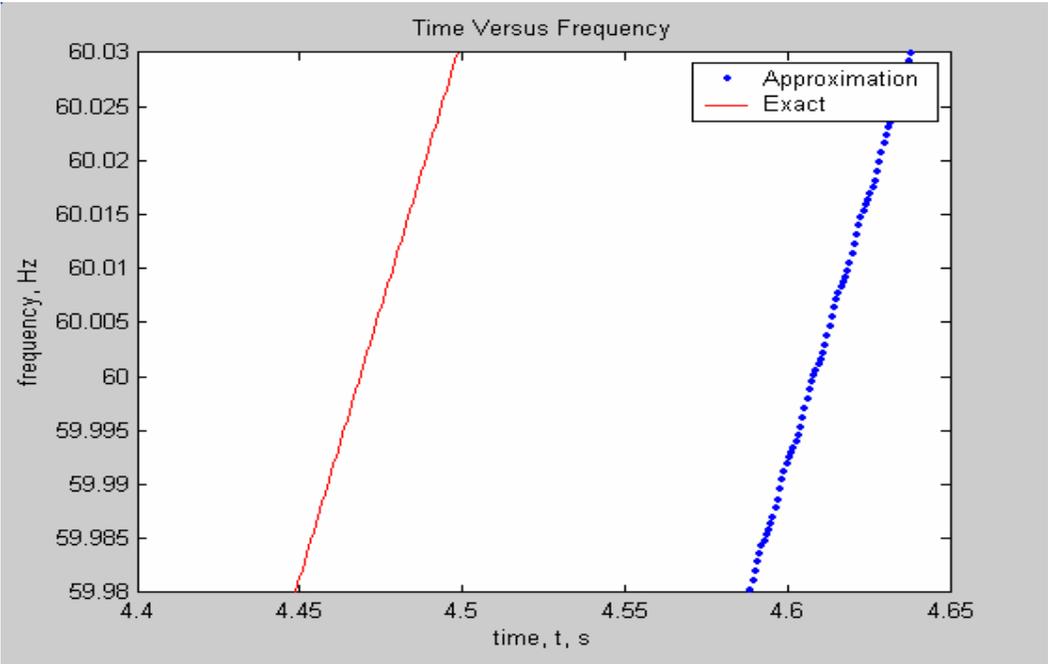


Figure 5-64 a zoomed in part of Figure 5-63

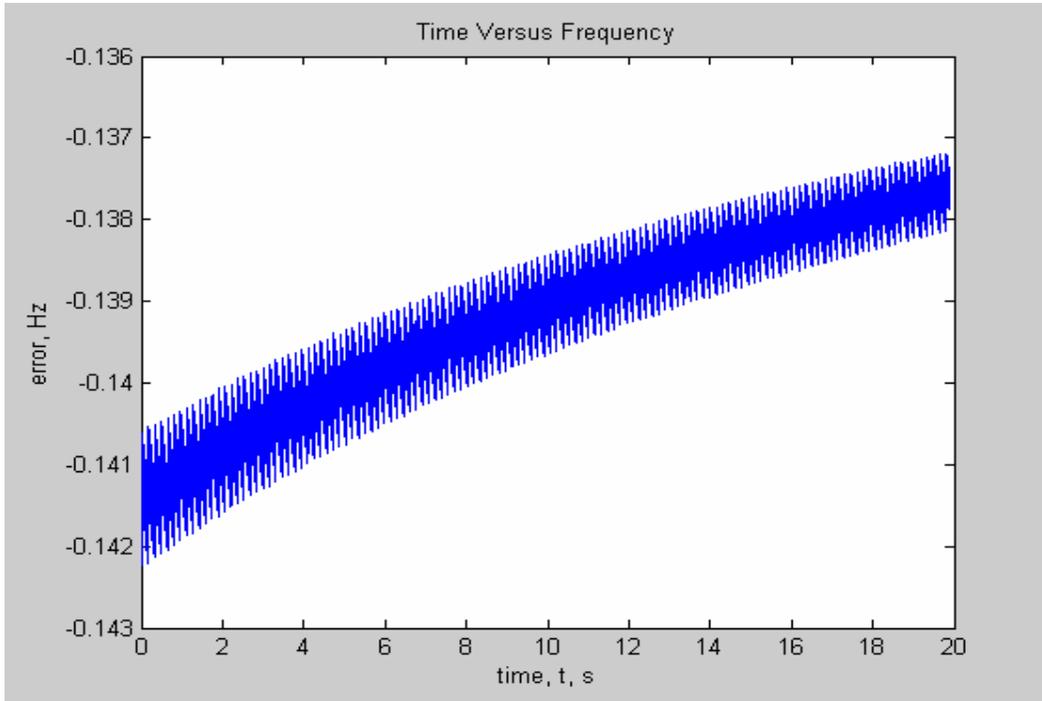


Figure 5-65 the error between the estimated frequency for input waveform with frequency changing as a Ramp function with a rate of 1 Hz/sec and the exact frequency resulted from the formula (the updated algorithm with 2<sup>nd</sup> resampling)

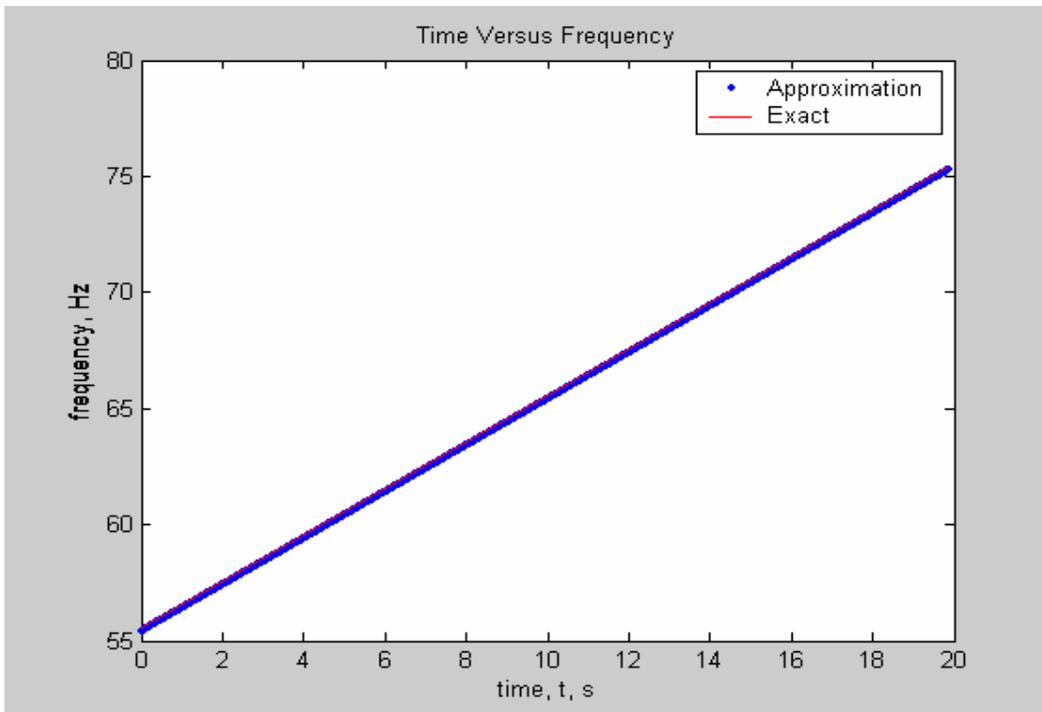


Figure 5-66 the estimated frequency for input waveform with frequency changing as a Ramp function with a rate of 1 Hz/sec (55Hz~75Hz) and the exact frequency resulted from the formula (original algorithm)

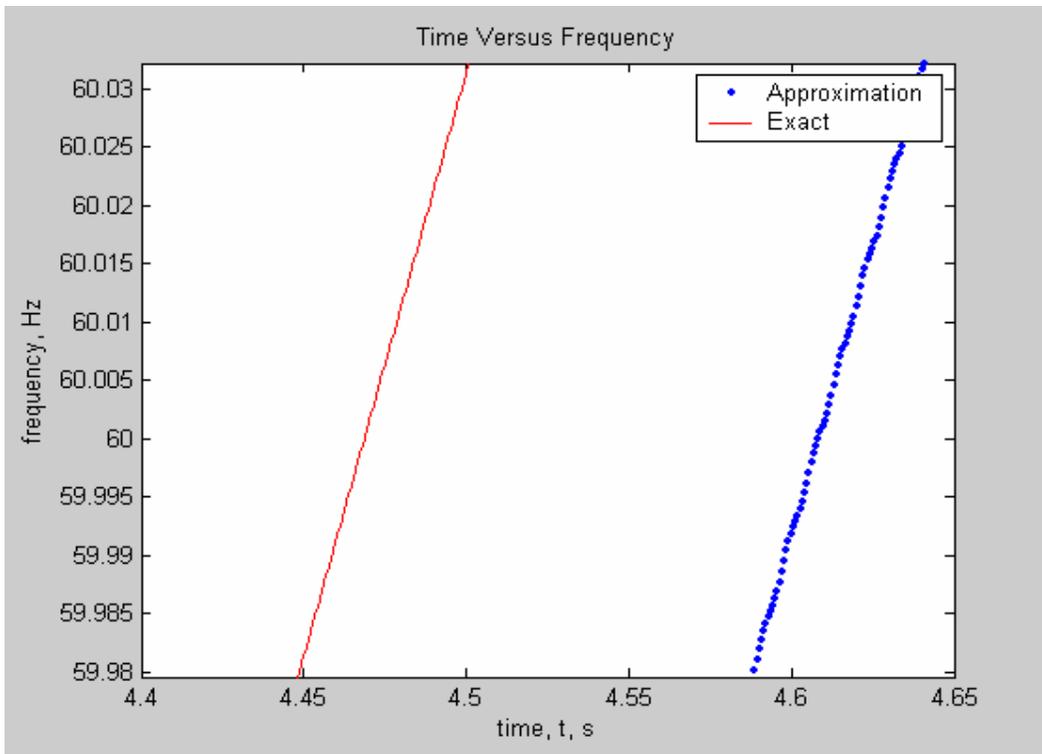


Figure 5-67 a zoomed in part of Figure 5-66

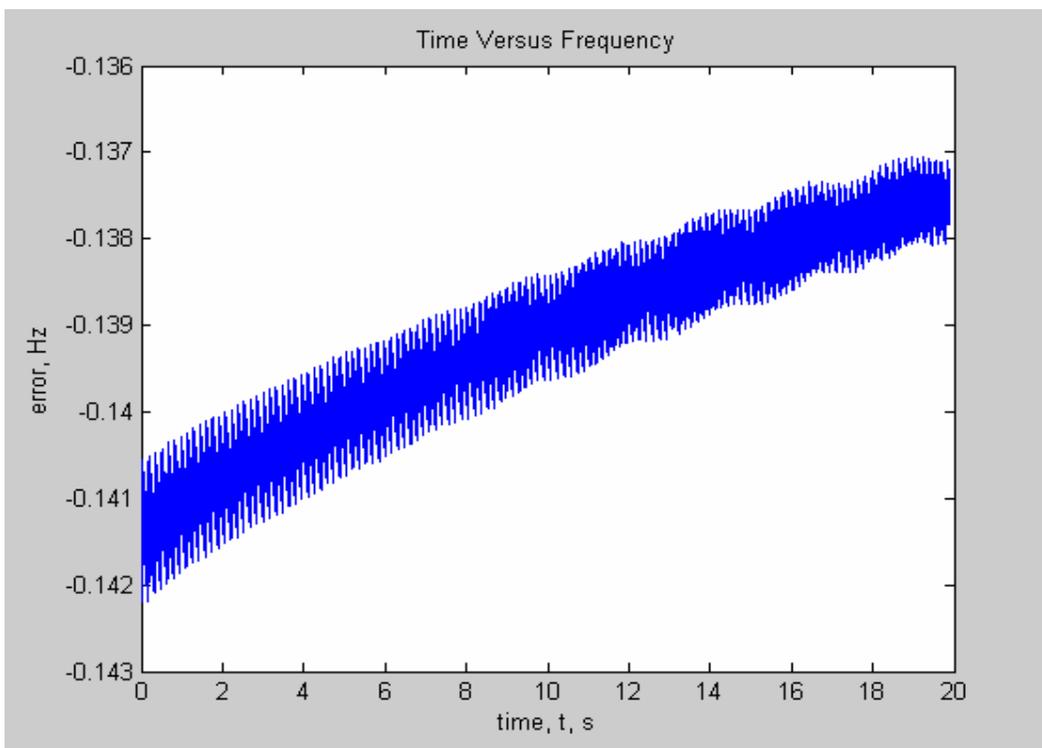


Figure 5-68 the error between the estimated frequency for input waveform with frequency changing as a Ramp function with a rate of 1 Hz/sec and the exact frequency resulted from the formula (original algorithm)

Comparing Figure 5-65 and Figure 5-68 then we can see that for the ramp change of 1Hz/s the difference between the estimated frequency and the exact frequency almost remained the same before and after the 2nd resampling was used.

### 5.4.3.2 Test with Input for Which Frequency Changes as a Sinusoidal

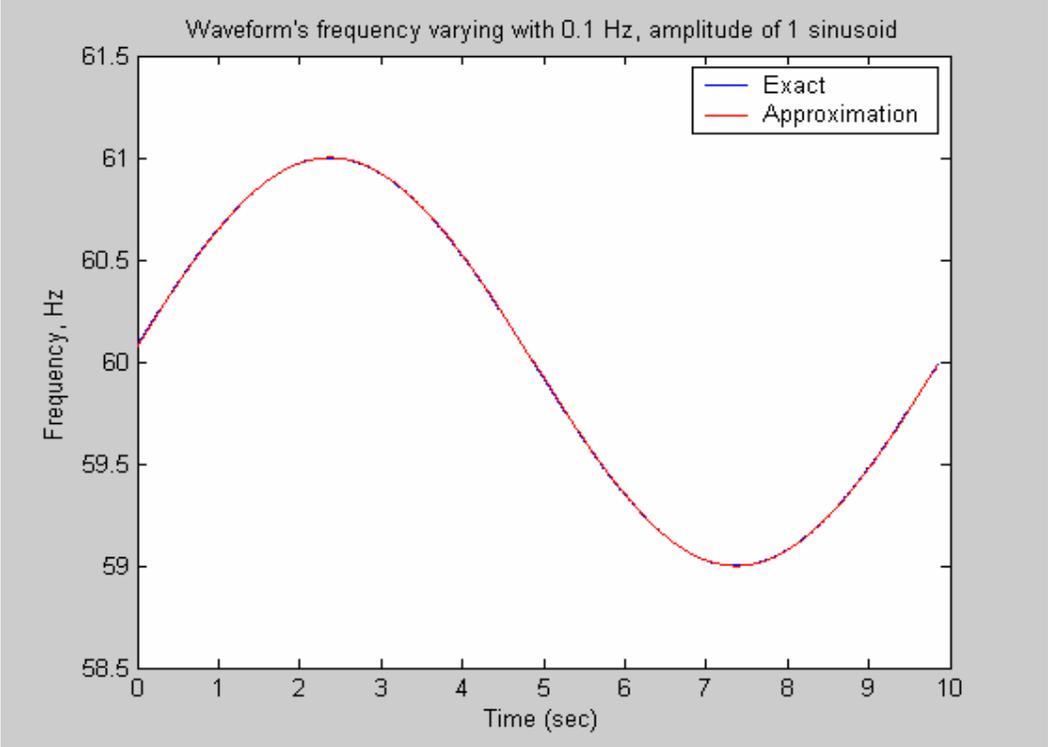


Figure 5-69 the estimated frequency for input waveform with  $f=0.1\text{Hz}$ ,  $\text{Amp}=1$  sinusoidal changing frequency and the exact frequency resulted from the formula (the updated algorithm with 2nd resampling)

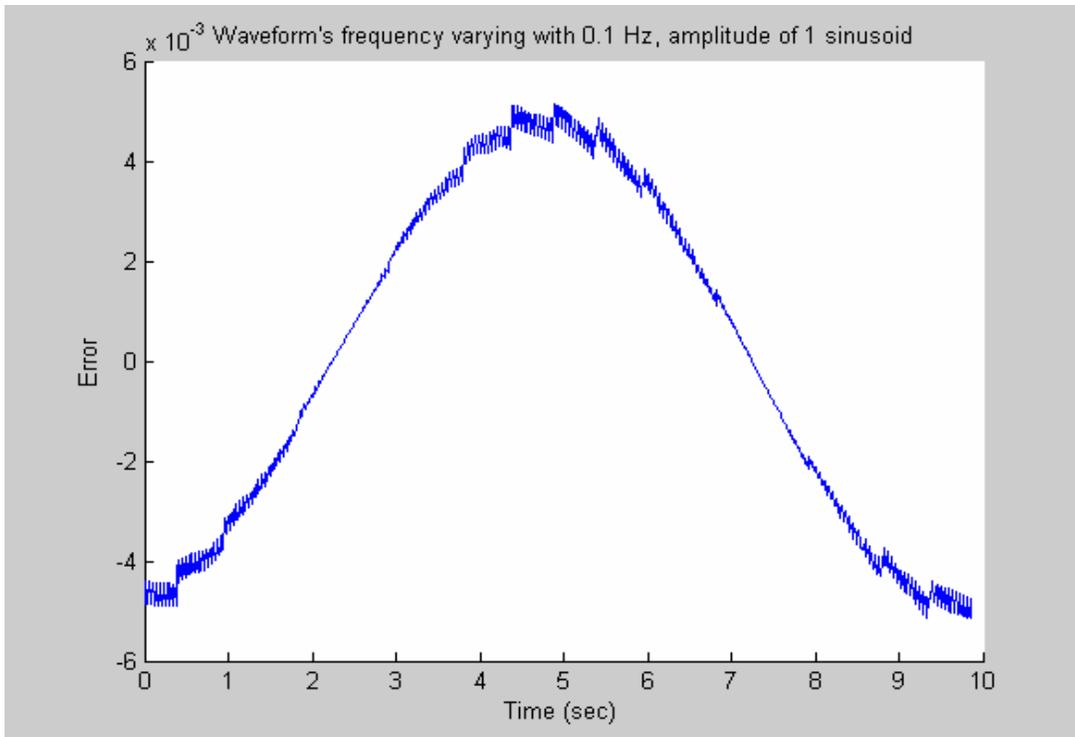


Figure 5-70 the error between the estimated frequency for input waveform with a  $f=0.1\text{Hz}$ ,  $\text{Amp}=1$  sinusoidal changing frequency and the exact frequency resulted from the formula (the updated algorithm with 2nd resampling)

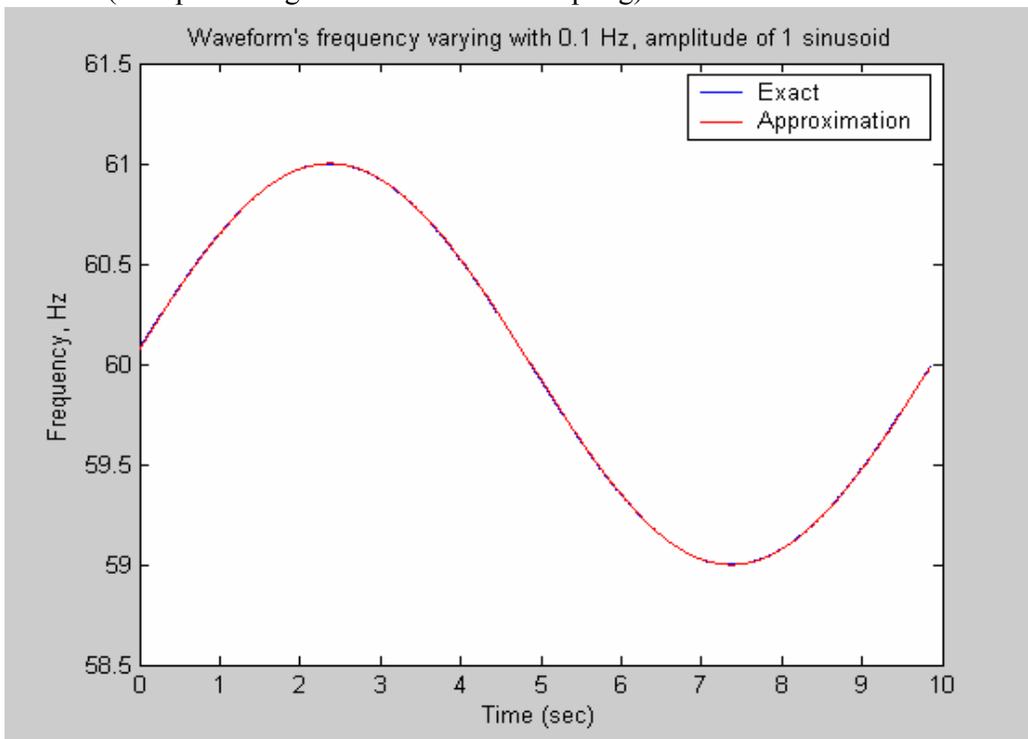


Figure 5-71 the estimated frequency for input waveform with a  $f=0.1\text{Hz}$ ,  $\text{Amp}=1$  sinusoidal changing frequency and the exact frequency resulted from the formula (original algorithm)

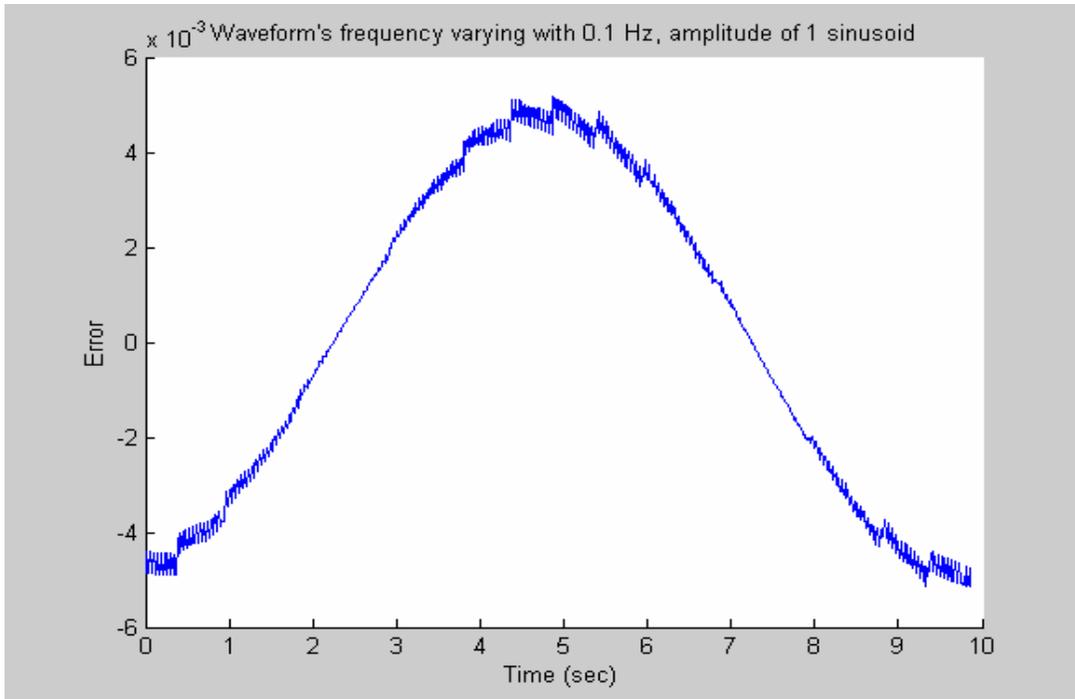


Figure 5-72 the error between the estimated frequency for input waveform with a  $f=0.1\text{Hz}$ ,  $\text{Amp}=1$  sinusoidal changing frequency and the exact frequency resulted from the formula (original algorithm)

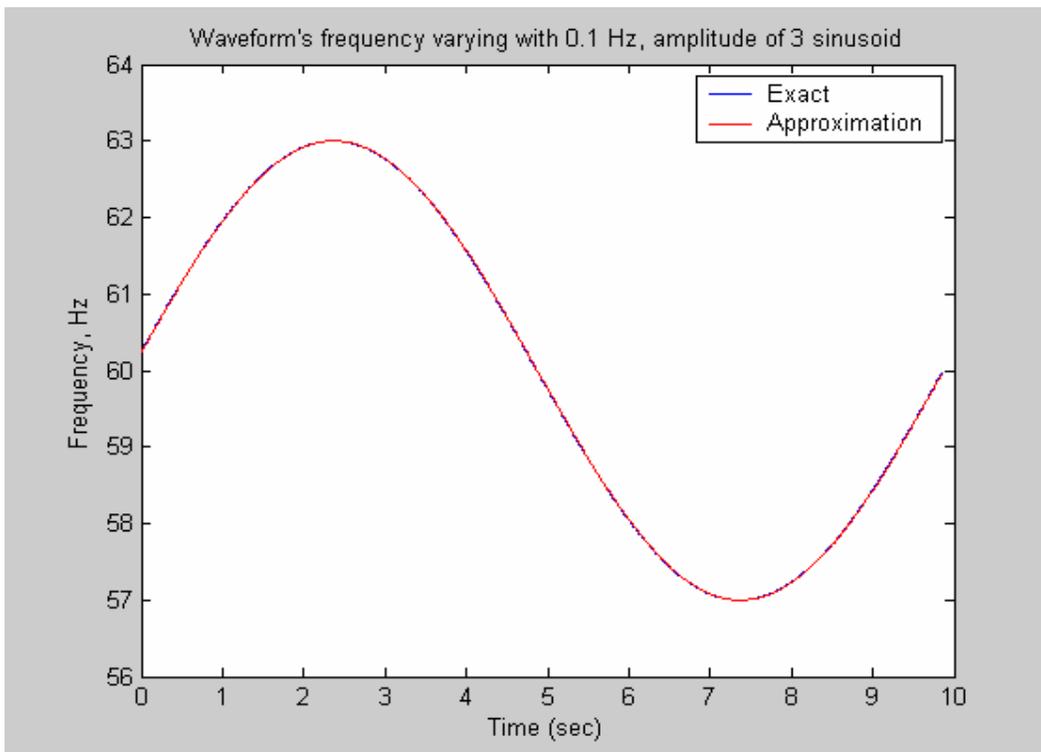


Figure 5-73 the estimated frequency for input waveform with  $f=0.1\text{Hz}$ ,  $\text{Amp}=3$  sinusoidal changing frequency and the exact frequency resulted from the formula (the updated algorithm with 2nd resampling)

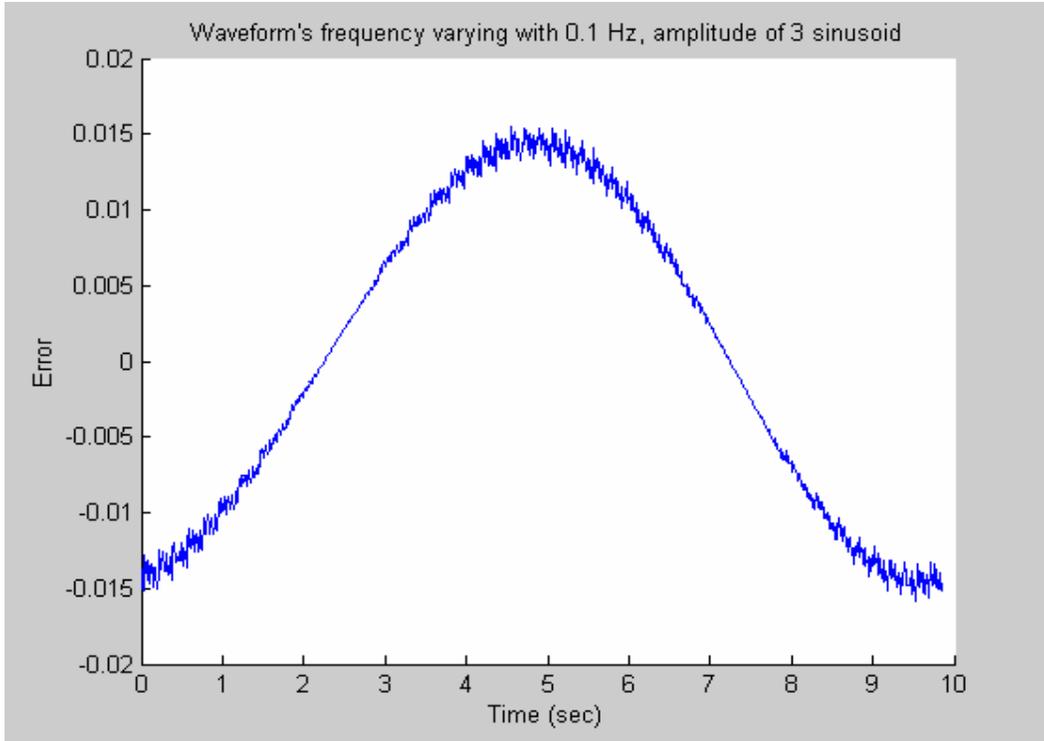


Figure 5-74 the error between the estimated frequency for input waveform with a  $f=0.1$  Hz, Amp=3 sinusoidal changing frequency and the exact frequency resulted from the formula (the updated algorithm with 2nd resampling)

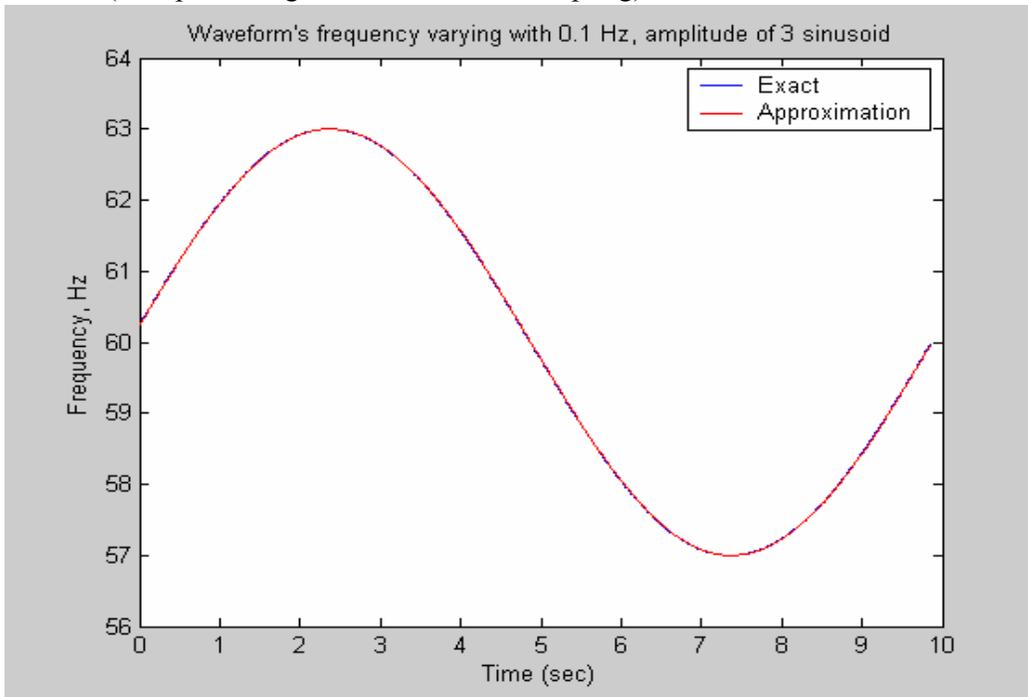


Figure 5-75 the estimated frequency for input waveform with a  $f=0.1$  Hz, Amp=3 sinusoidal changing frequency and the exact frequency resulted from the formula (original algorithm)

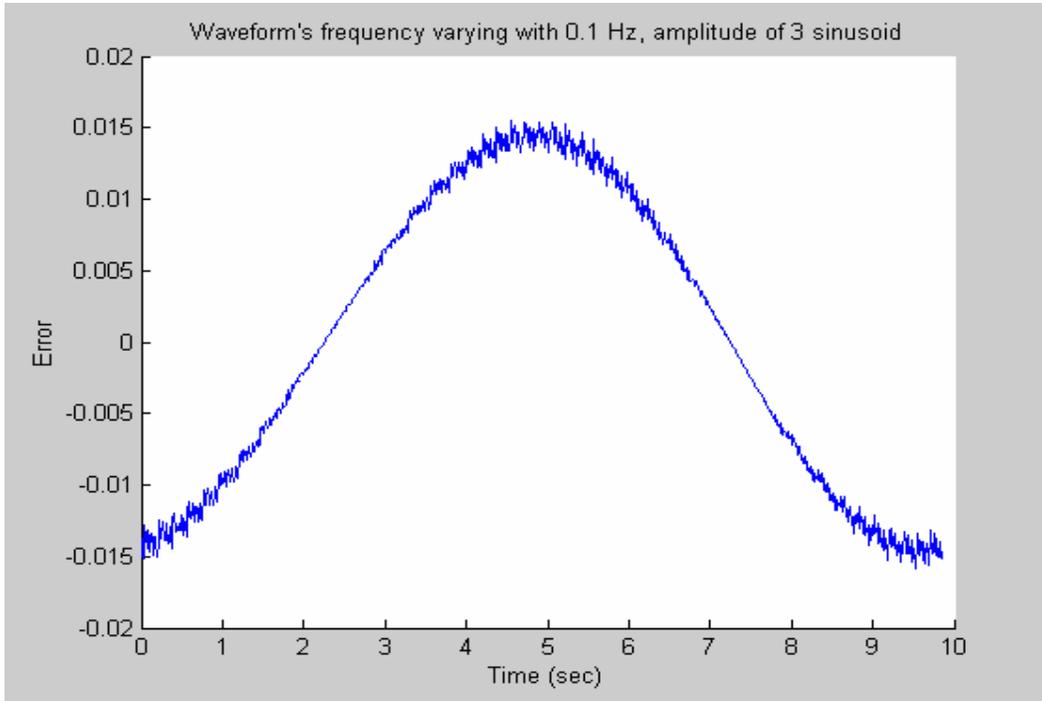


Figure 5-76 the error between the estimated frequency for input waveform with a  $f=0.1\text{Hz}$ ,  $\text{Amp}=3$  sinusoidal changing frequency and the exact frequency resulted from the formula (original algorithm)

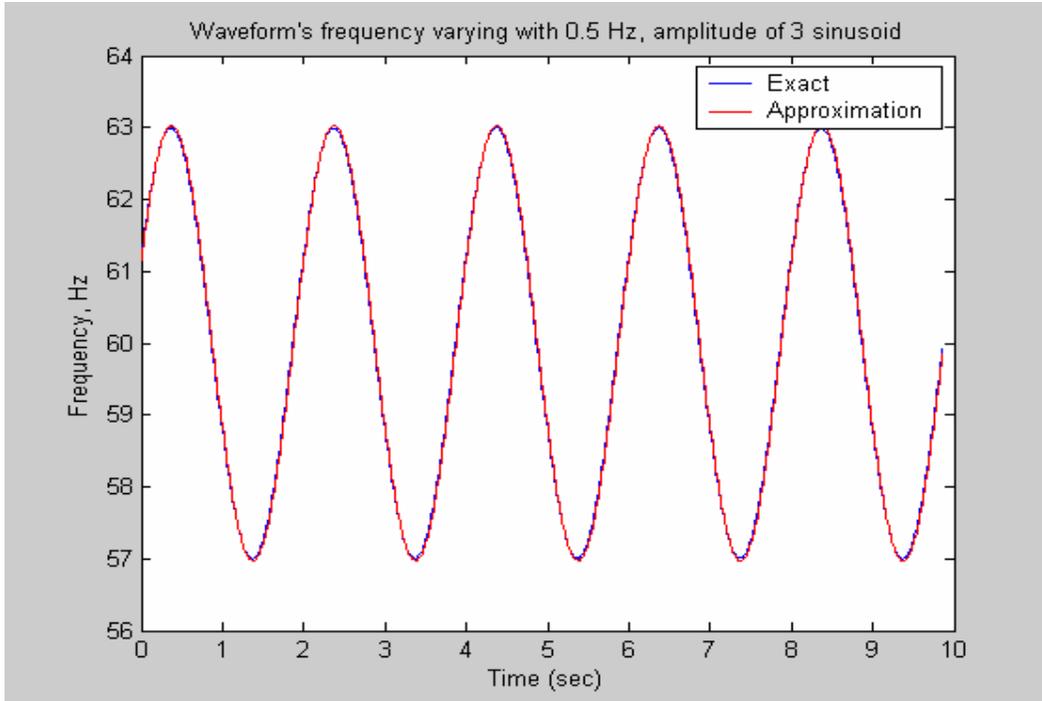


Figure 5-77 the estimated frequency for input waveform with  $f=0.5\text{Hz}$ ,  $\text{Amp}=3$  sinusoidal changing frequency and the exact frequency resulted from the formula (the updated algorithm with 2nd resampling)

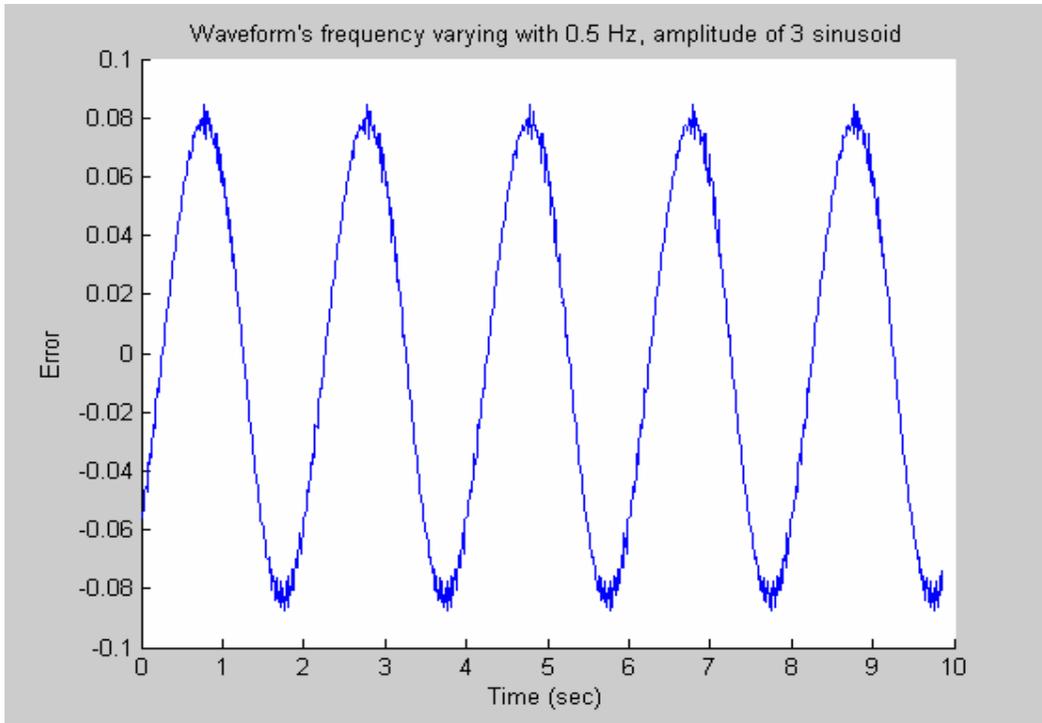


Figure 5-78 the error between the estimated frequency for input waveform with a  $f=0.5\text{Hz}$ ,  $\text{Amp}=3$  sinusoidal changing frequency and the exact frequency resulted from the formula (the updated algorithm with 2nd resampling)

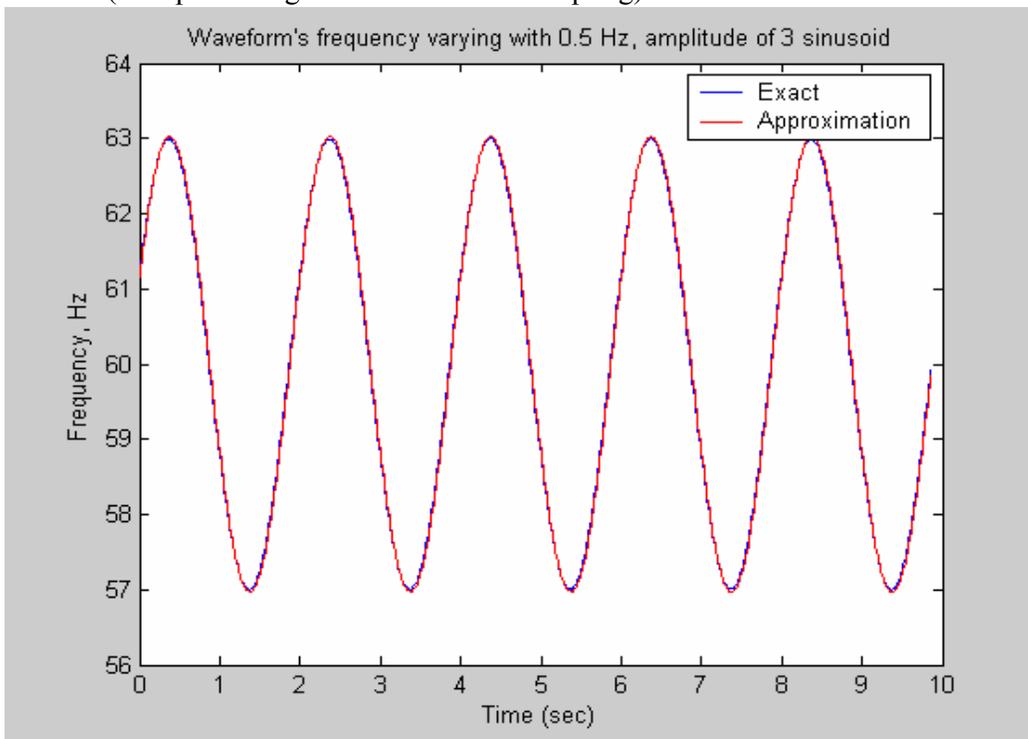


Figure 5-79 the estimated frequency for input waveform with a  $f=0.5\text{Hz}$ ,  $\text{Amp}=3$  sinusoidal changing frequency and the exact frequency resulted from the formula (original algorithm)

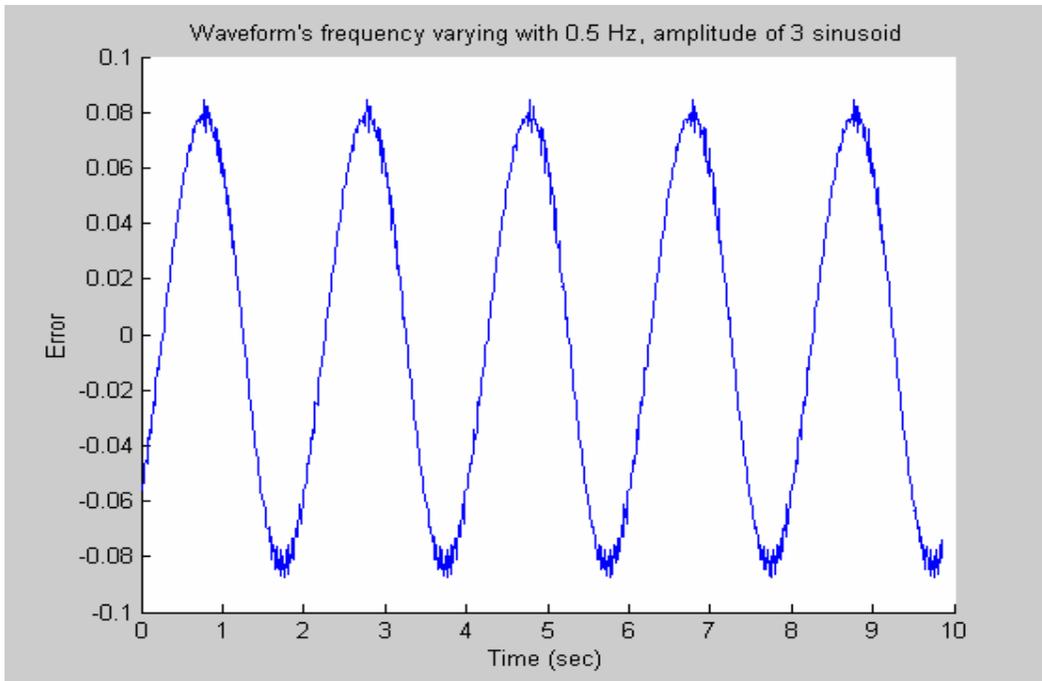


Figure 5-80 the error between the estimated frequency for input waveform with a  $f=0.5\text{Hz}$ ,  $\text{Amp}=3$  sinusoidal changing frequency and the exact frequency resulted from the formula (original algorithm)

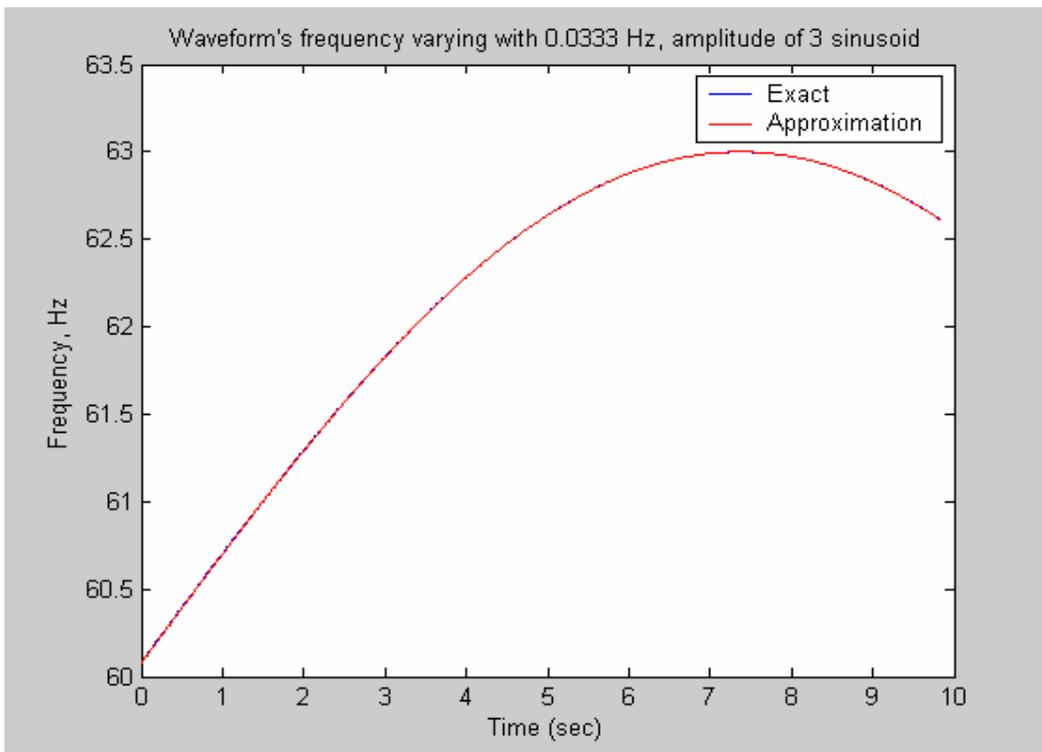


Figure 5-81 the estimated frequency for input waveform with  $f=0.0333\text{Hz}$ ,  $\text{Amp}=3$  sinusoidal changing frequency and the exact frequency resulted from the formula (the updated algorithm with 2nd resampling)

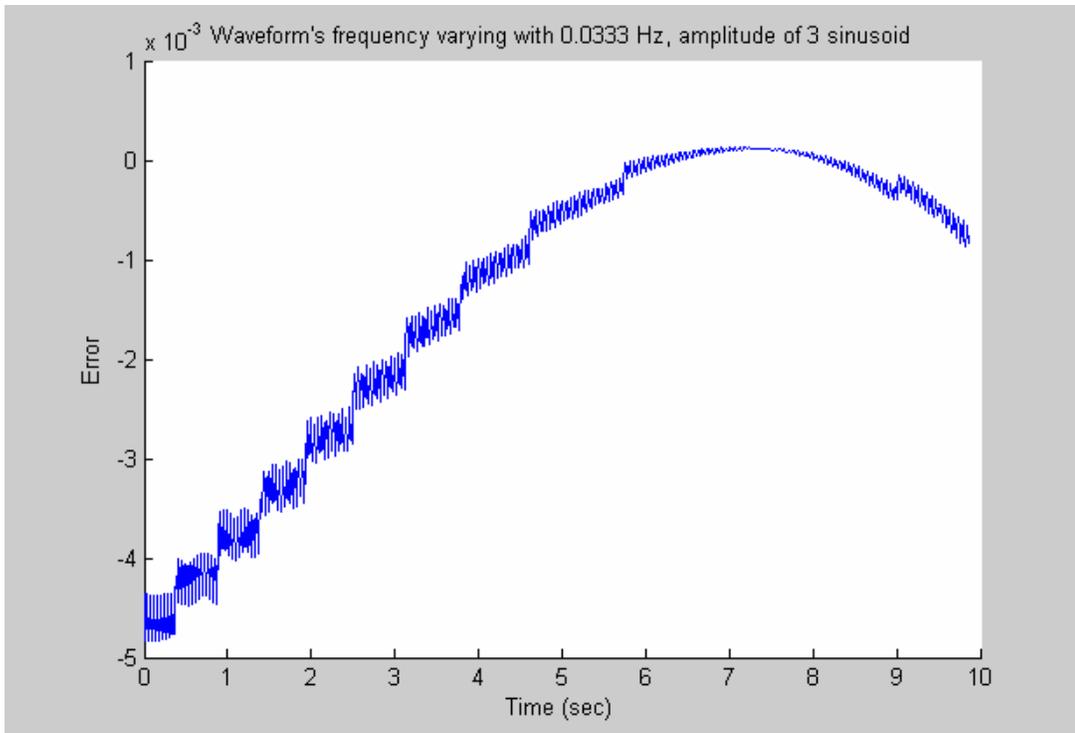


Figure 5-82 the error between the estimated frequency for input waveform with a  $f=0.0333\text{Hz}$ ,  $\text{Amp}=3$  sinusoidal changing frequency and the exact frequency resulted from the formula (the updated algorithm with 2nd resampling)

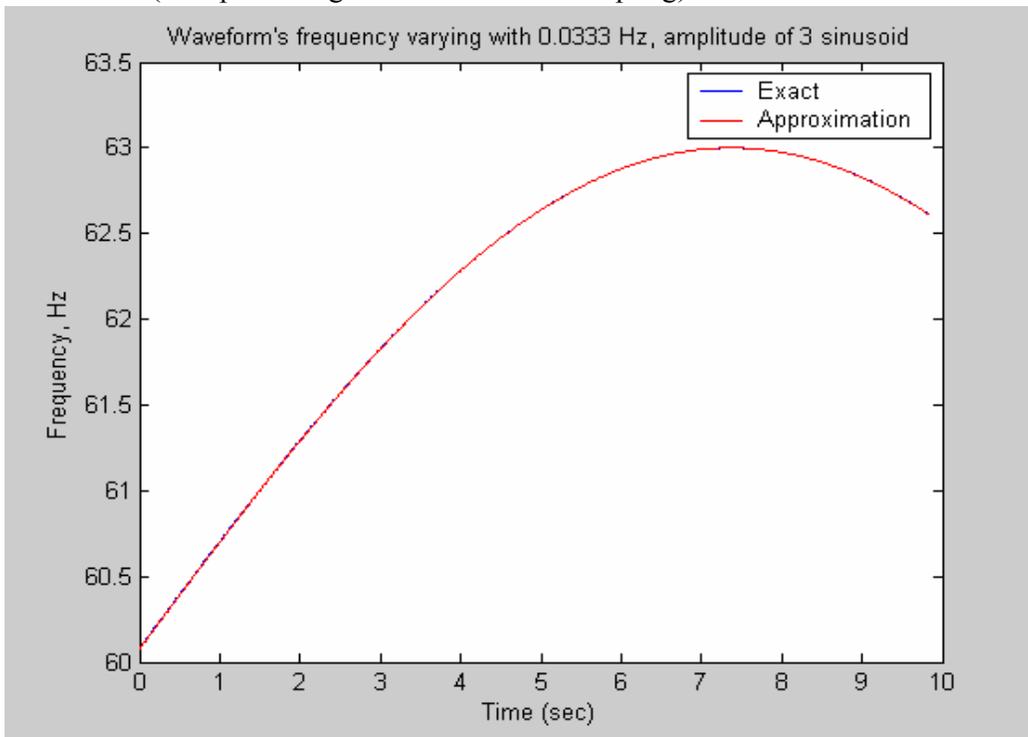


Figure 5-83 the estimated frequency for input waveform with a  $f=0.0333\text{Hz}$ ,  $\text{Amp}=3$  sinusoidal changing frequency and the exact frequency resulted from the formula (original algorithm)

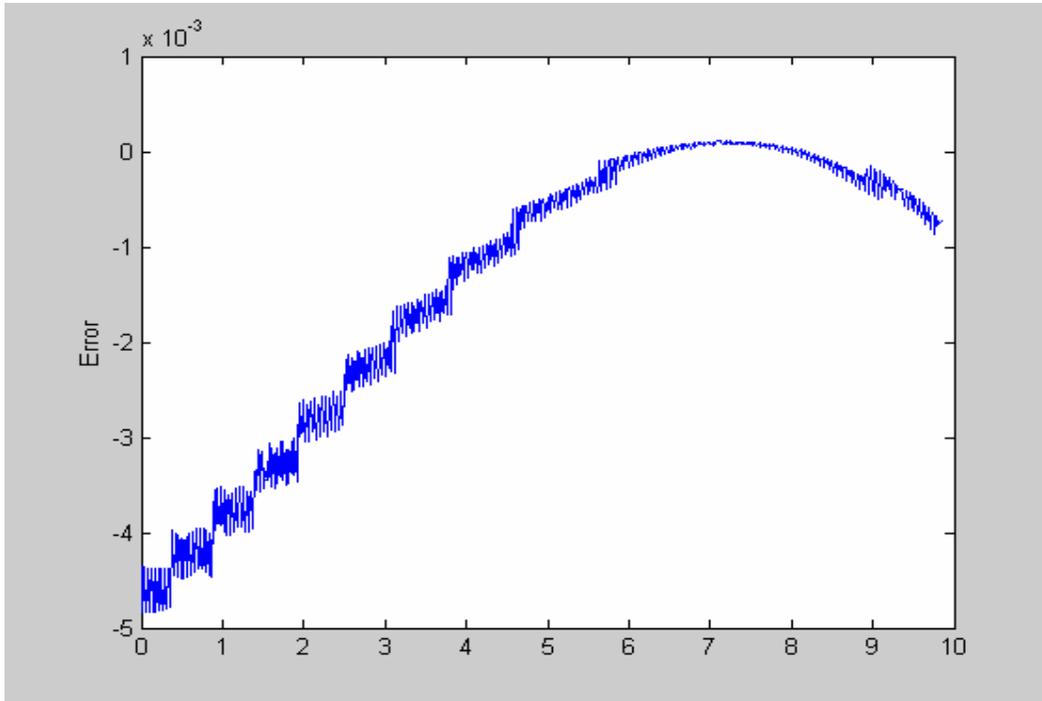


Figure 5-84 the error between the estimated frequency for input waveform with a  $f=0.0333\text{Hz}$ ,  $\text{Amp}=3$  sinusoidal changing frequency and the exact frequency resulted from the formula (original algorithm)

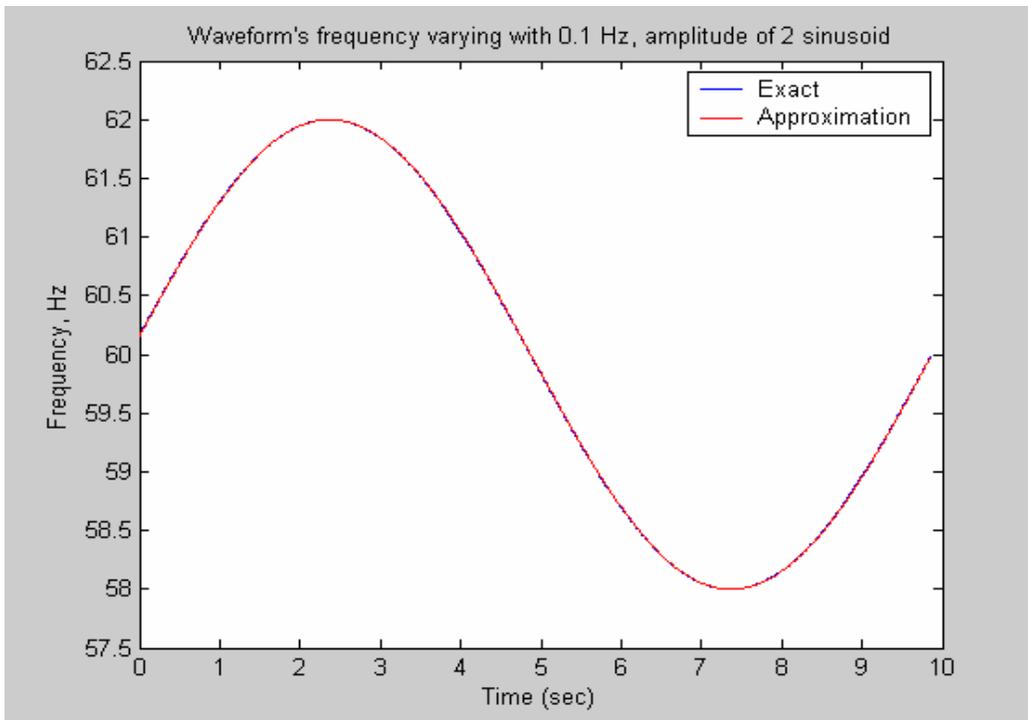


Figure 5-85 the estimated frequency for input waveform with  $f=0.1\text{Hz}$ ,  $\text{Amp}=2$  sinusoidal changing frequency and the exact frequency resulted from the formula (the updated algorithm with 2nd resampling)

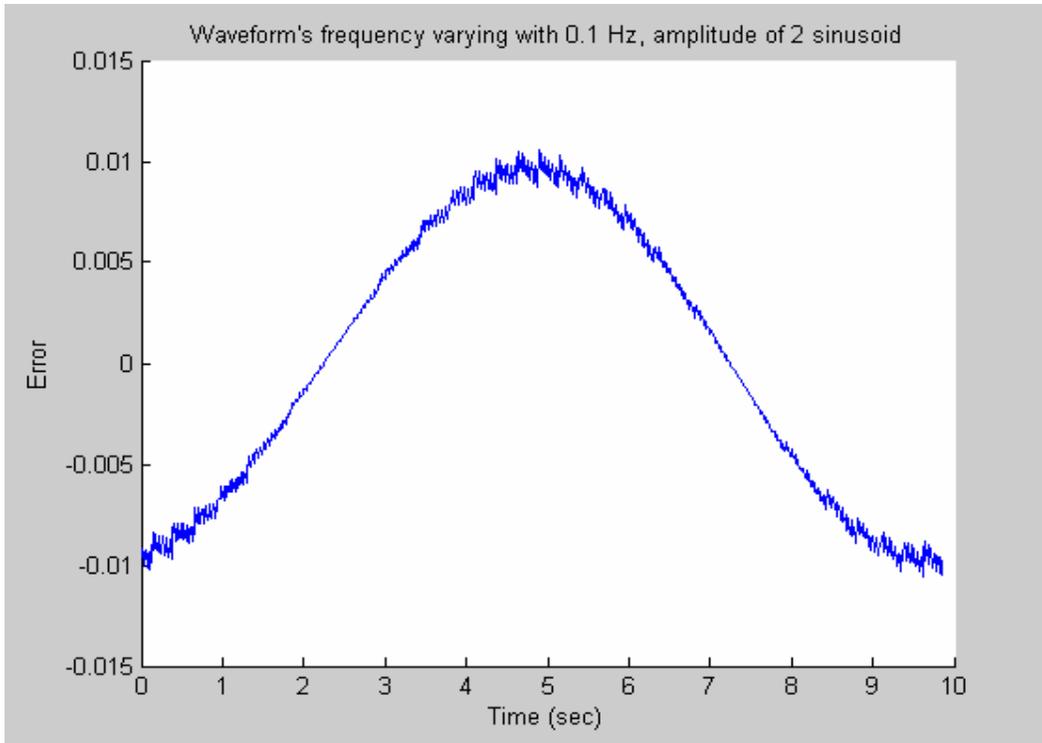


Figure 5-86 the error between the estimated frequency for input waveform with a  $f=0.1$  Hz, Amp=2 sinusoidal changing frequency and the exact frequency resulted from the formula (the updated algorithm with 2nd resampling)

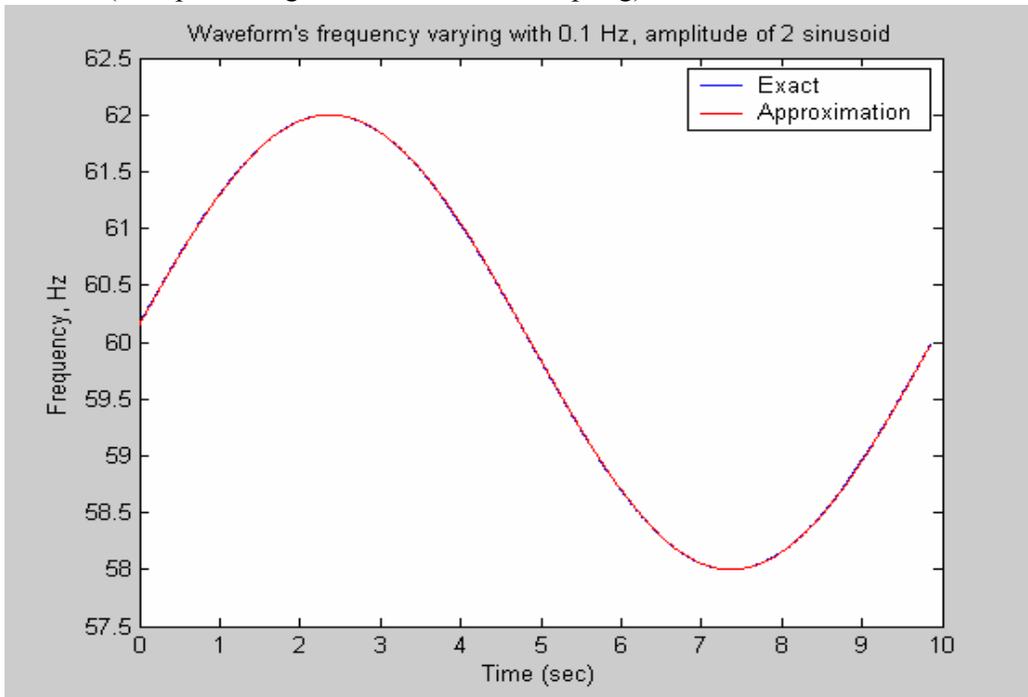


Figure 5-87 the estimated frequency for input waveform with a  $f=0.1$  Hz, Amp=2 sinusoidal changing frequency and the exact frequency resulted from the formula (original algorithm)

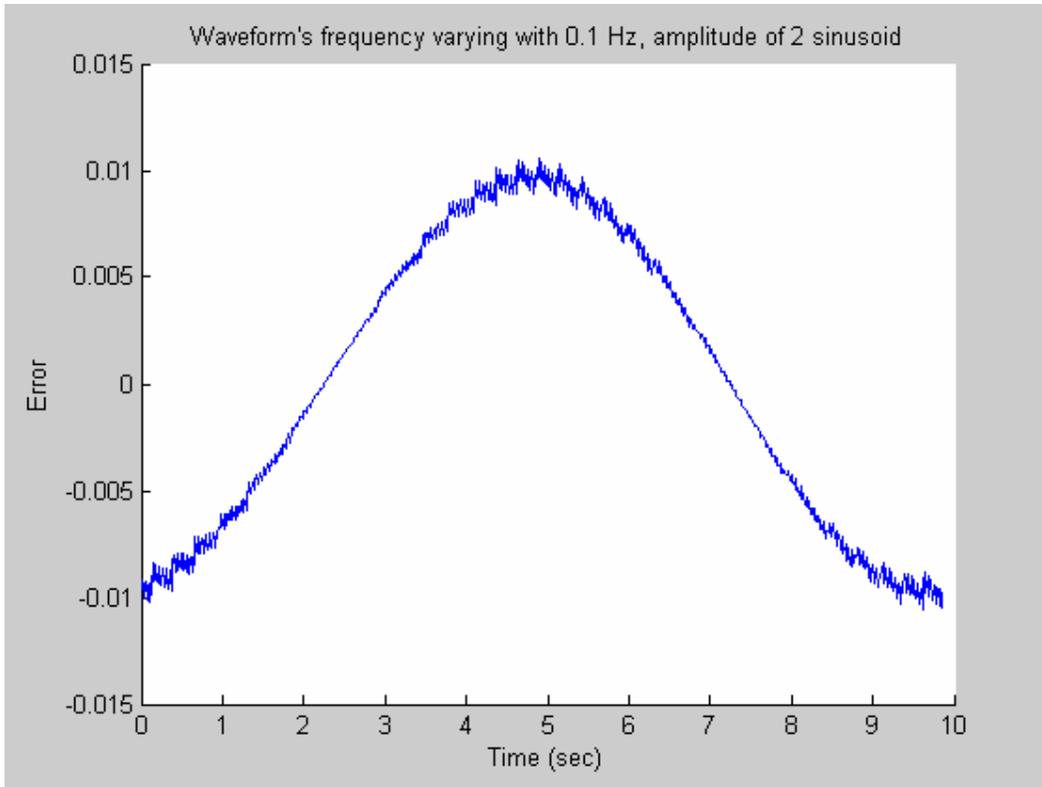


Figure 5-88 the error between the estimated frequency for input waveform with a  $f=0.1\text{Hz}$ ,  $\text{Amp}=1$  sinusoidal changing frequency and the exact frequency resulted from the formula (original algorithm)

From Figure 5-69 to Figure 5-88 we can see that there is no difference in frequency estimation accuracy between with and without 2<sup>nd</sup> resampling when frequency changes in a sinusoidal fashion.

## Chapter Six

### Computation Time Study

In this chapter, the computation time study results of different versions of the algorithm will be presented. All the tests were performed on a 1.8Ghz Intel Pentium CPU computer. The input data for the program is sampled at the frequency of 1440Hz for a 10 second sinusoidal waveform. And the frequencies of the sinusoidal waveform that have been tested are 58Hz, 59Hz, 60Hz, 61Hz and 62Hz. The computation time was obtained by employing two Microsoft Visual C++ functions QueryPerformanceCounter and QueryPerformanceFrequency. The QueryPerformanceCounter function retrieves the current value of the high-resolution performance counter. The QueryPerformanceFrequency function retrieves the frequency of the high-resolution performance counter. The QueryPerformanceCounter function is called twice: one is called before the start of the period of the program that needs to be measured the computation time and the other is called at the end of the same period of the program. The difference of the two returned values of the twice-called QueryPerformanceCounter function is then divided by the returned value of the QueryPerformanceFrequency function, so obtained the computation time.

Figure 6-1 to Figure 6-6 display the total frequency estimation computation time of different versions of algorithm. Figure 6-7 shows how much more time it takes to calculate one estimated frequency for the algorithm with twice resamplings than for the algorithm with only once resampling. Figure 6-8 shows how much more time it takes to calculate one estimated frequency for the algorithm with three resamplings than for the algorithm with only once resampling.

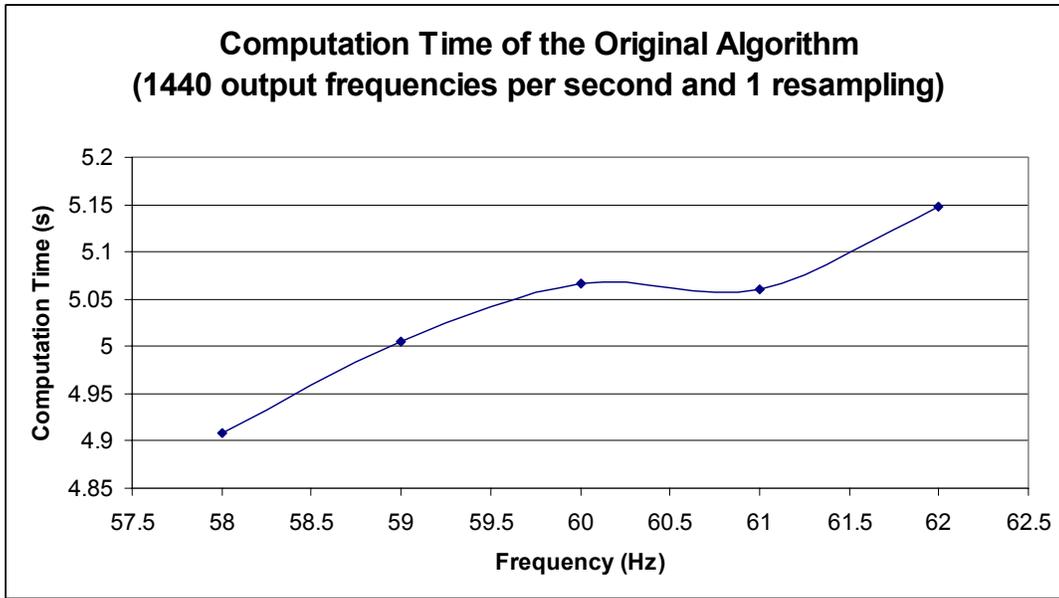


Figure 6-1 Computation time of the original algorithm that outputs 1440 frequencies per second and has only once resampling (for frequencies 58Hz, 59Hz, 60Hz, 61Hz and 62Hz)

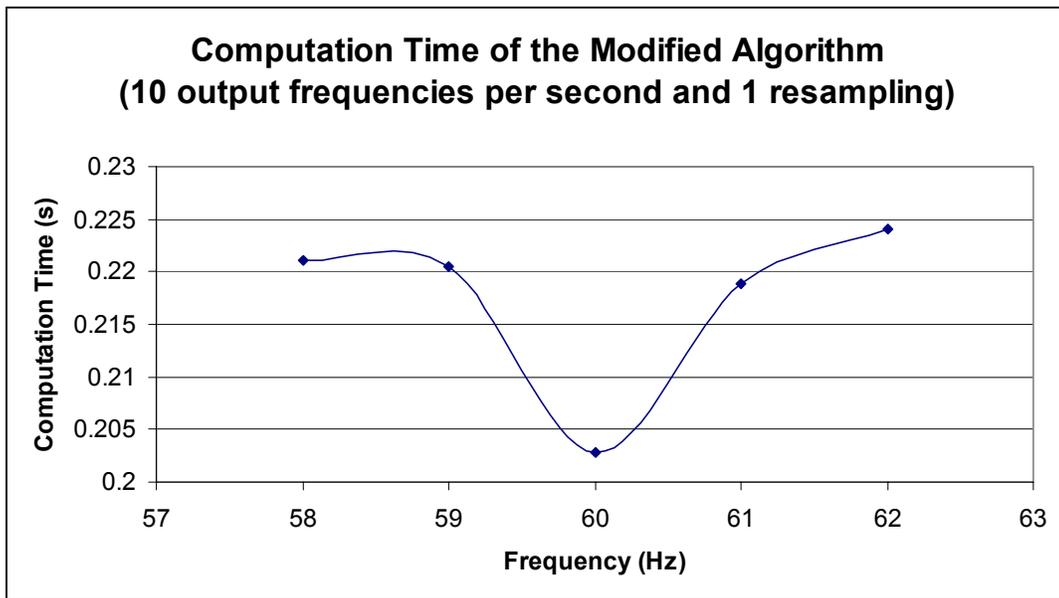


Figure 6-2 Computation time of the modified algorithm that outputs 10 frequencies per second and has only once resampling (for frequencies 58Hz, 59Hz, 60Hz, 61Hz and 62Hz)

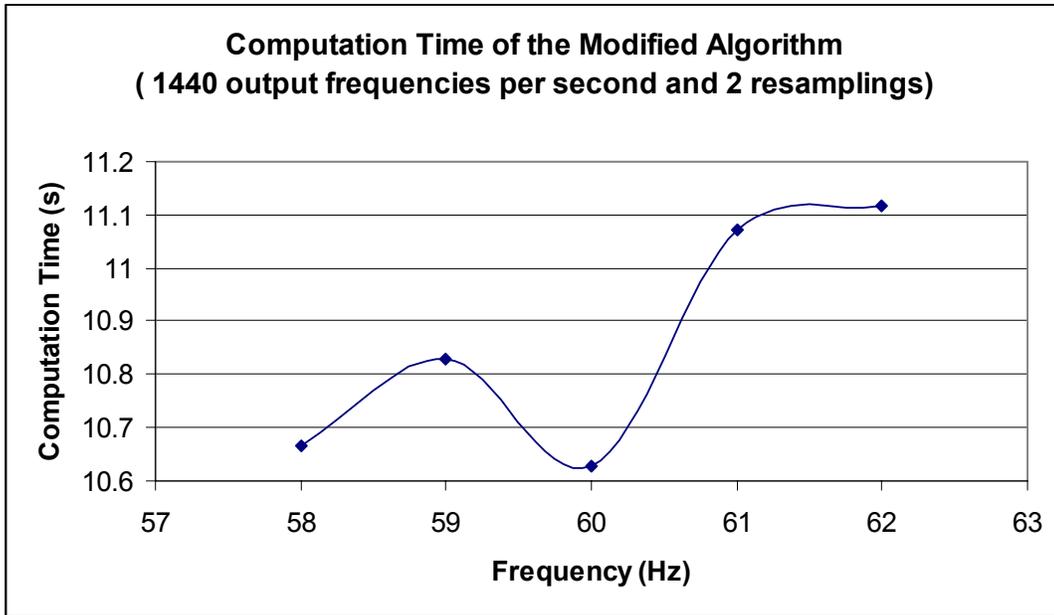


Figure 6-3 Computation time of the modified algorithm that outputs 1440 frequencies per second and has twice resamplings (for frequencies 58Hz, 59Hz, 60Hz, 61Hz and 62Hz)

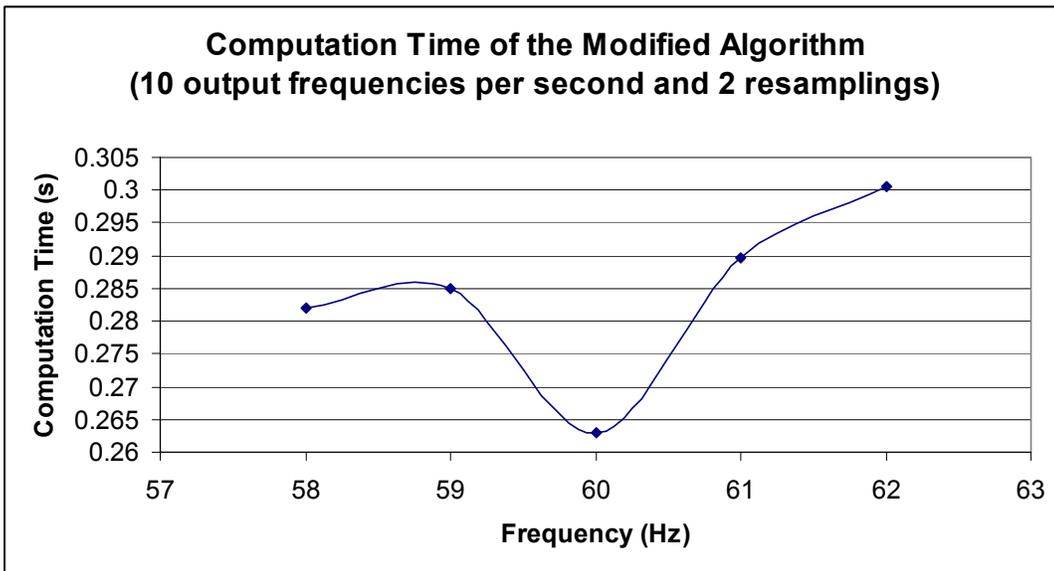


Figure 6-4 Computation time of the modified algorithm that outputs 10 frequencies per second and has twice resamplings (for frequencies 58Hz, 59Hz, 60Hz, 61Hz and 62Hz)

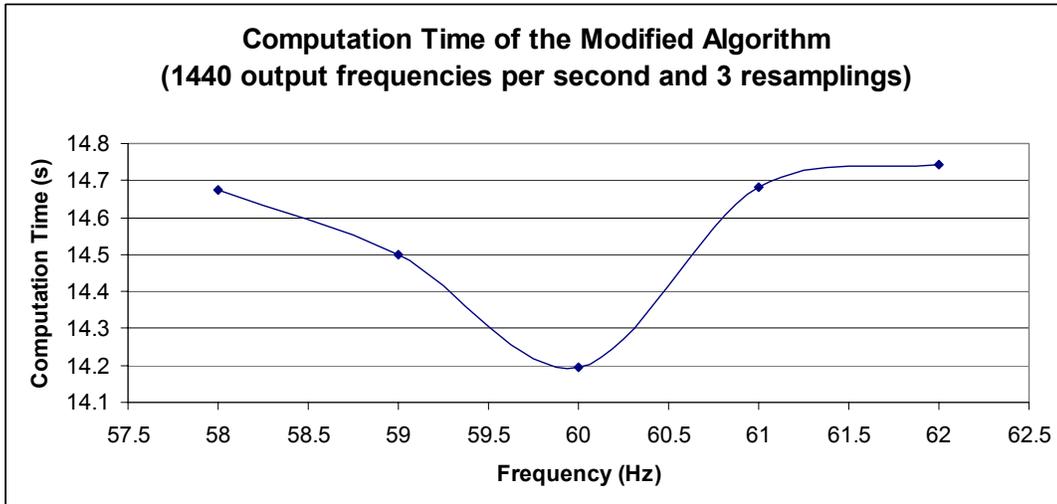


Figure 6-5 Computation time of the modified algorithm that outputs 1440 frequencies per second and has three times resamplings (for frequencies 58Hz, 59Hz, 60Hz, 61Hz and 62Hz)

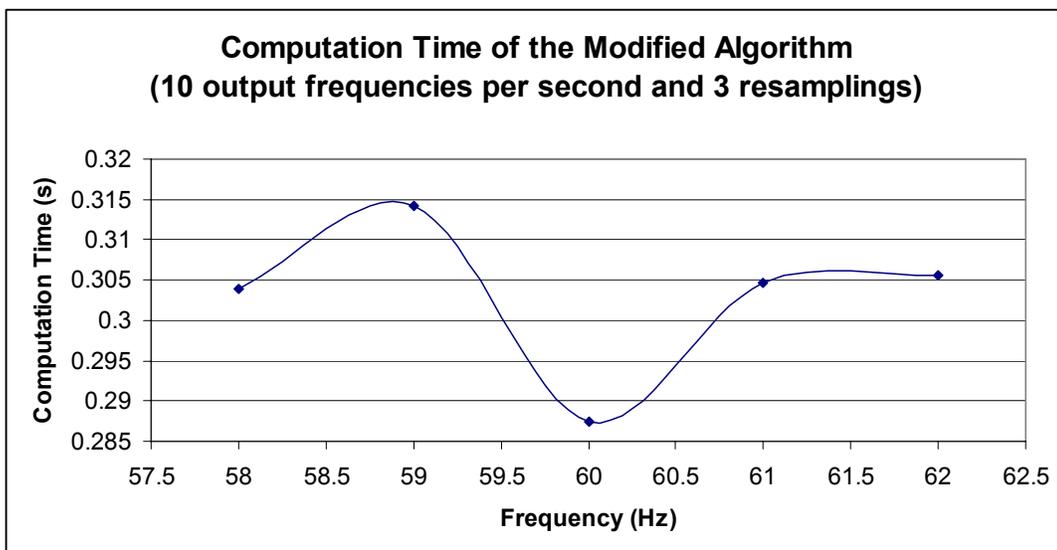


Figure 6-6 Computation time of the modified algorithm that outputs 10 frequencies per second and has three times resamplings (for frequencies 58Hz, 59Hz, 60Hz, 61Hz and 62Hz)

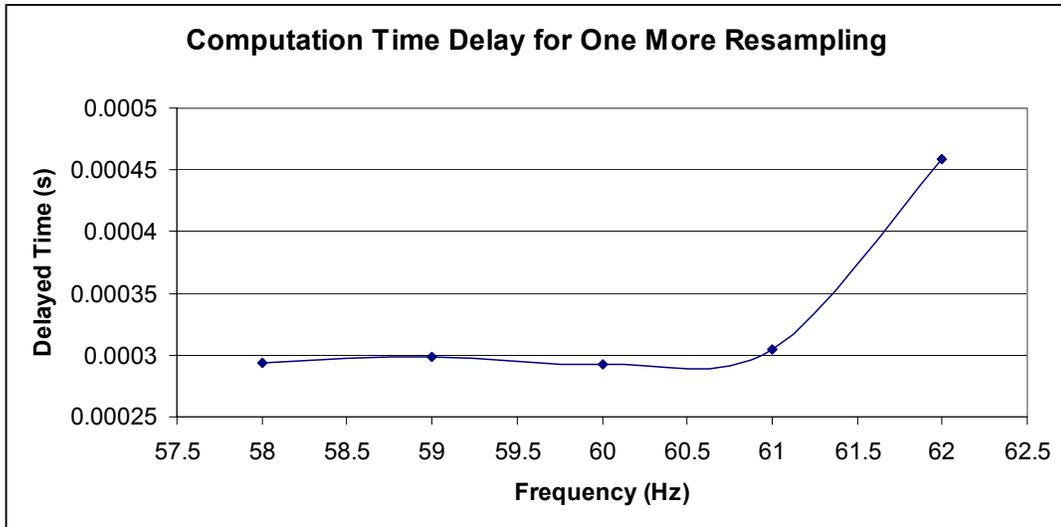


Figure 6-7 Computation time Delay for one more resampling (for frequencies 58Hz, 59Hz, 60Hz, 61Hz and 62Hz)

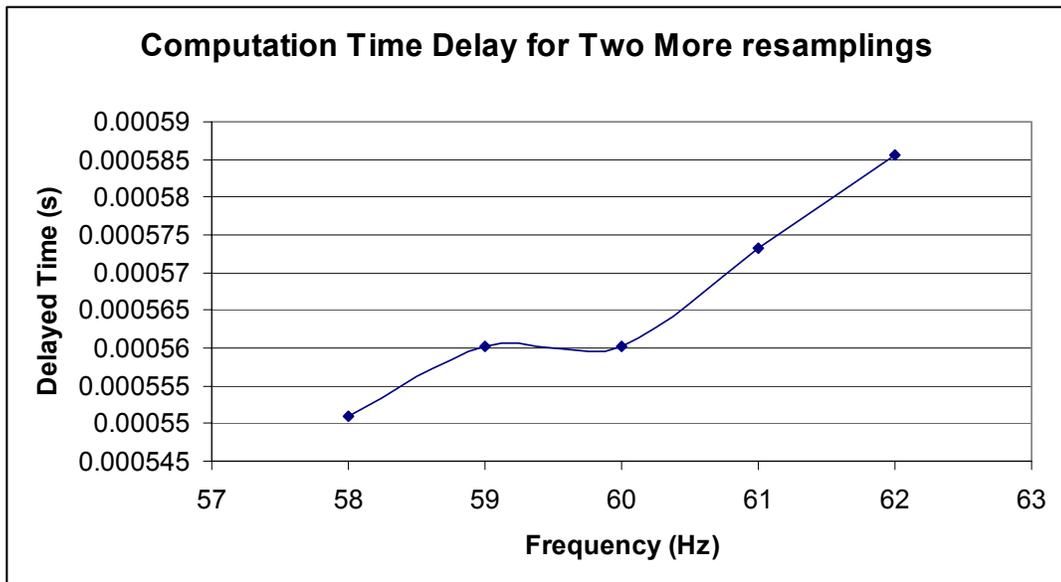


Figure 6-8 Computation time Delay for two more resamplings (for frequencies 58Hz, 59Hz, 60Hz, 61Hz and 62Hz)

## Chapter Seven

### Summary and Future Work

This study of the frequency estimation algorithm used in our FNET system compares three approaches that improve the frequency estimation accuracy. One---multiple resampling---proved significantly superior. Practical problems that have affected the output estimated frequency of our FNET system are analyzed.

First the effect of non-pure sinusoidal input on the frequency estimation accuracy of the algorithm is studied: the frequency estimation accuracy of the algorithm decreases markedly for non pure sinusoidal input compared to pure sinusoidal input. Indeed, the larger the distortion of the input from the pure sinusoid, the worse the frequency estimation accuracy will be. More specifically, for the case of harmonic noise, the high frequency component more adversely affects the estimation accuracy than do the low order harmonics. For the case wherein the frequency changes at a constant rate as a ramp function, the higher the rate of the ramp function, the lower the frequency estimation accuracy will be. And if frequency changes as a sinusoidal function, the higher the sinusoidal frequency and the larger the amplitude of the sinusoidal, the larger will be the frequency estimation error.

Then the practical problems that have affected the estimated frequency of our FNET system are analyzed. The input data directly from the power grid is processed by the means of averaging and moving averaging which got rid of part of the noise and a good result is obtained. When it comes to a spike of the output frequency occurring every 29 or 30 seconds, it is confirmed to be caused by one point being missing in the output data of the ADC in our FNET system. As far as the phase or amplitude shift problem is concerned, significant deviation from the normal output frequency range results whenever a phase or amplitude shift occurs to the input voltage; the bigger the shift, the larger the deviation will be.

Finally three possible approaches improving the frequency estimation accuracy of the algorithm are discussed. The first--- increasing the number of samples per cycle  $N$ --- proves ineffective. The second---using as the resampling frequency the average of the first estimated frequencies instead of the instant first estimated frequency---moderately improves the frequency estimation accuracy. However, it has no effect on the frequency estimation accuracy whenever the input is not a pure

sinusoidal. The third---multiple resampling---makes a really significant difference, as summarized in the following aspects:

- The range of the frequencies with zero estimation error has been expanded greatly after multiple resampling is used. More specifically, the zero-estimation-error frequency range is 53 Hz ~ 77Hz for 2<sup>nd</sup> resampling case and 52.2Hz ~190Hz for 3<sup>rd</sup> resampling case whereas the original algorithm which uses only once-resampling has 100 percent accuracy (zero estimation error) only at 60 Hz.
- Comparing once-resampling and twice-resampling for frequencies between 78Hz and 190 Hz, the error for twice-resampling is either zero or 1.00E-06 with the exception of 120 Hz and 180Hz while the error for once-resampling is between 3.5E-5(80Hz) and 5.29E-4(118Hz).
- For the frequencies between 191Hz and 220Hz, the estimation accuracy also shows a big difference for 1 resampling case, 2<sup>nd</sup> resampling case and 3<sup>rd</sup> resampling case, which can be clearly seen in Table 7-1.

Frequency (Hz)	1 resampling (Hz)	2 <sup>nd</sup> resampling (Hz)	3 <sup>rd</sup> resampling (Hz)
191	2.647000E-01	1.000000E-06	1.00E-06
192	6.280000E-04	1.000000E-06	0.00E+00
193	4.000000E-01	8.920000E-04	2.00E-06
194	2.646000E-01	1.000000E-06	1.00E-06
195	2.500000E-01	1.380000E-04	1.00E-06
196	2.918000E-01	6.050000E-04	1.00E-06
197	2.740000E-01	3.700000E-04	1.00E-06
198	2.790000E-01	4.040000E-04	1.00E-06
199	4.200000E-01	1.090000E-03	3.00E-06
200	3.260000E-01	5.540000E-04	1.00E-06
201	2.720000E-01	5.000000E-04	1.00E-06
202	3.238000E-01	6.900000E-04	1.00E-06
203	3.292000E-01	8.000000E-04	2.00E-06
204	3.130000E-04	1.000000E-06	0.00E+00
205	3.184000E-01	7.820000E-04	2.00E-06
206	3.745000E-01	8.680000E-04	2.00E-06
207	3.849000E-01	8.940000E-04	2.00E-06
208	3.955000E-01	9.910000E-04	2.00E-06
210	1.040000E-04	0.000000E+00	0.00E+00
215	3.856000E-01	9.910000E-04	2.00E-06
220	3.052000E-01	5.950000E-04	1.00E-06

Table 7-1 the comparison of frequency estimation error for 1 resampling case, 2<sup>nd</sup> resampling case and 3<sup>rd</sup> resampling case in the frequency range of 191Hz ~220Hz

- Multiple resampling does not have an effect on the frequency estimation accuracy whenever the input is not a pure sinusoidal

From the summary of the thesis mentioned above, we can see the following possible directions for future work:

- Since the accuracy of the frequency estimation of the algorithm decreases dramatically and even the multiple resampling does not help when the input is not is a pure sinusoidal, attention needs to be focused on how to eliminate the noise of the data directly from the power grid so that the input data finally fed to the algorithm is very close to pure sinusoidal. Although some simple analog filters have been in use in our FNET system and the two simple digital filters tested (averaging and moving-averaging) prove to be effective, cleaner data is to be desired. Therefore, it will be worthwhile to try more sophisticated digital filters to process the input data before feeding it to the algorithm.
- The phase shift or the amplitude shift of the input voltage is not unusual in the real power grid

since the load change happens often. It has been shown in the thesis that big deviation from the normal value range will occur to the output estimated frequency of our algorithm whenever the phase or amplitude shift occurs. Some work can be done with it in the future. One may start by checking whether it matters if the phase or amplitude shift occurs at different locations in one sinusoidal cycle.

- One simple averaging digital filter for the second harmonic component  $2f_0$  in the output frequency can be tried in the future. Basically, it is to average three successive values of the estimated frequency such that relative phase angles are  $60^\circ$  and  $120^\circ$  at the nominal fundamental frequency, which would correspond to  $120^\circ$  and  $240^\circ$  for the second harmonic.

## Reference

- [1] W. Fromm, A. Halinka, “Accurate Measurement of Wide-range Power System Frequency Changes for Generation Protection”, *IEEE Conference Publication* No. 434, 1997, pp53-57.
- [2] A.. Adly, G. William, L. Peterson, “Adaptive Estimation of Power System Frequency Deviation and Its Rate of Change for Calculation Sudden Power System Overload”, *IEEE Transactions on Power Delivery*, Vol. 5, No. 2, April, 1990, pp 585-590.
- [3] N. Jaleeli, D. N. Ewart, “Understanding automatic generation control”. *IEEE Transactions on Power Systems*, Vol. 7, No.3, Aug. 1992, pp1106-1122.
- [4] J.R. Smith, D. A. Pierre, “A supplementary adaptive VAR unit controller for power system dumping”.
- [5] M. Klein, G. J. Roger, “A Fundamental Study of Inter-Area Oscillations In Power System”, *IEEE Transactions on Power Systems*, Vol. 6, No.3, Aug. 1991, pp914-921.
- [6] J. Hauer, D. Trudnowski, “Keeping an eye on Power system Dynamics”, *IEEE Computer Applications in Power*, Vol. 10, No. 4, Oct. 1997, pp 50 – 54.
- [7] W. A. Mittelstadt, P. E. Krause, The DOE wide area measurement system (WAMS) project – Demonstration of dynamic information technology for the future power system, *EPRI conference on the future of power delivery*, April 1996.
- [8] Report of a Panel Discussion, “Power System Disturbance Monitoring Utility Experiences”, *IEEE Transactions on Power Systems*, Vol. 3, No. 1, Feb. 1988, pp 134 -- 147.
- [9] J. F. Hauer, R. L. Cresap, “Measurement and Modeling of Pacific Inter-tie Response to Random Load Switching”, *IEEE Transactions on Power Apparatus and Systems*, Vol. PAS-100, No. 1, Jan. 1981, pp 353 – 357.
- [10] B. Qiu, X. Dong, L. Chen, V. Centeno, Y. Liu, “Internet Based Power System Frequency Monitoring Network (FNET),” *IEEE PES Winter Meeting Proceedings*, Columbus, OH, Feb. 2001.

- [11] Yilu Liu "Internet Based Frequency Monitoring Network," *Proceedings of the CRIS Conference*, Beijing, China, Oct. 2002.
- [12] B. Qiu, Y. Liu, "Information Management System for an Internet Based Power System Frequency Monitoring Network," *IEEE PES Winter Meeting Proceedings*, Columbus, OH, Feb. 2001.
- [13] J. Chen, "Accurate frequency estimation with phasor angles", Virginia Tech M.S. thesis, April, 1994.
- [14] Girgis, A.A., and Ham, F.M., "A New FFT-Based Digital Frequency Relay for Load Shedding", *IEEE Transactions on Power Apparatus and Systems*, Vol. PAS-101, No. 2, February 1982, pp. 433-439.
- [15] David Hart, Damir Novosel, Yi Hu, Bob Smith, Mike Egolf, "A New Frequency Tracking and Phasor Estimation Algorithm For Generator", *IEEE Transactions on Power Delivery*, Vol. 12, No. 3, July, 1997, pp1064-1073.
- [16] Benco, Joseph P., Perfect, Frederick P., Hart, David G., Stoupis, James D. "Generator Protection System and Method for Phasor Estimation and Frequency Tracking during Frequency Ramping", United States Patent 5,832,413, Sep. 29, 1997.
- [17] Hart, David G., Stoupis, James D., Novosel, Damir, "Generator Protection System and Method of Compensating for Errors in Phasor Estimation due to Oscillations in Discrete Fourier Transform", United States Patent 5,832,414, Sep. 29, 1997.
- [18] Hart, David, Yi Hu, Novosel, Damir, Smith, Robert, "System and Method for Phasor Estimation and Frequency Tracking in Digital Protection Systems", United States Patent 5,721,689, Dec. 18, 1995
- [19] Gabriel Benmouyal, "An Adaptive Sampling-interval Generator for Digital Relaying", *IEEE Transactions on Power Delivery*, Vol. 4, No. 3, July, 1989, pp1602-1609
- [20] Phadke, A.G., Thorp, J.S., and Adamiak, M.G., "A New Measurement Technique for Tracking Voltage Phasors, Local System Frequency, and Rate of Change of Frequency", *IEEE Transactions on Power Apparatus and Systems*, Vol. PAS-102, No. 5, May 1983, pp. 1025-1038.
- [21] Phadke, A.G., "Technical Report No. 2 On Frequency Calculation from Phasors With Renormalization Through Resampling For High Accuracy"

- [22] Nguyen, C.T., and Srinivasan, K., "A New Technique for Rapid Tracking of Frequency Deviations Based on Level Crossings", *IEEE Transactions on Power Apparatus and Systems*, Vol. PAS-103, No. 8, August 1984, pp. 2230-2236.
- [23] Sachdev, M.S., and Giray, M.M., "A Least Error Squares Technique for Determining Power System Frequency", *IEEE Transactions on Power Apparatus and Systems*, Vol. PAS-104, No. 2, February 1985, pp. 437-443.
- [24] Girgis, A.A., and Hwang, T.L., "Optimal Estimation of Voltage Phasors and Frequency Deviation Using Linear and Non-Linear Kalman Filtering: Theory and Limitations", *IEEE Transactions on Power Apparatus and Systems*, Vol. PAS-103, No. 10, October 1984, pp. 2943-2951.
- [25] EPRI, "Study of Distribution System Surge and Harmonic Characteristic", EPRI EL-1627, Project 1024-1, Final Report, November 1980.

## **Vita**

Xuan Zhang was born in Chongqing, People's Republic of China. She received her B.S. in Electrical Engineering from Chongqing University in 2002. She is currently pursuing her M.S. in Electrical Engineering at Virginia Polytechnic Institute and State University.